University of Southampton

Faculty of Environmental and Life Sciences

School of Biological Sciences

Phenotyping of *Pseudomonas aeruginosa* Biofilms in Cystic Fibrosis Patients, Biofilm Biomarker Identification, and Understanding the Nitric Oxide Mediated Biofilm Dispersal Response.

by

Declan Matthew Power

ORCID ID 0000-0001-5049-713X

Thesis for the degree of Doctor of Philosophy

February 2025

University of Southampton

Abstract

Colonisation of *Pseudomonas aeruginosa* (PA) in the airways is associated with persistent morbidity, and increased mortality in cystic fibrosis (CF) patients. Treatment strategies include aggressive antibiotic regimes aimed at eradicating or controlling the infection. However, structured biofilm aggregates offer an increased tolerance to antimicrobials, with eradication treatments failing in 10-40% of patients. Biofilms are largely unculturable, are unable to be diagnosed via culture-based methods. A lack of biomarkers for a biofilm infection escalates this diagnostic issue. Previous studies have explored the relationship of novel nitric oxide (NO) donors as biofilm dispersal agents for potential new antibiofilm therapy to be used in CF. Biofilms formed by CF isolates in vitro were found to have varied responses to the NO donor sodium nitroprusside (SNP).
This study focuses both assessing the biofilm status of CF patients chronically infected with *P. aeruginosa* undergoing exacerbation and looks to combine the phenotypic biofilm status and proteomic data to identify potential biomarkers for biofilm infection. Secondly the study also aims to further explore the underlying mechanisms of the varied responses of clinical CF *P. aeruginosa* biofilms to the NO biofilm dispersal signal determining patient suitability for the therapeutic use of NO.

Using series of microbiological techniques including fluorescently labelled via in-situ hybridisation (FISH) microscopy, dispersal assays, biofilm culture models, and multi-omics methods, the biofilm status was determined for 62 patients and further assessed for alterations following antibiotic treatment. Sputum samples were processed for proteomic analysis to identify correlations between biofilm status and disease state to seek out potential human protein biomarkers for the presence of a biofilm infection. Histone H4 was observed positively correlate with the disease state, with a decreased abundance post antibiotics suggesting a potential infection marker. Despite showing no correlation to that of the biofilm biomass, histone H4 remains to be of interest for further analysis.

An extended panel of 10 PA isolates obtained from the sputum of Cystic fibrosis patients at the University hospital Southampton were assessed for their NO response. Interestingly, three distinct phenotypes were identified: dispersing, no change, and growth promotion. Isolates underwent whole genome sequencing, however, no obvious genetic adaptation to the NO signal was discovered suggesting deeper regulatory mechanisms to be responsible. Analysis of the transcriptomes of isolates with differing responses was unable to confidently identify any regulatory mechanism, but has suggested the roles of numerous elements, raising questions on the involvement of the two-component regulatory system, PhoPQ, reported to play a role in virulence and polymyxin resistance, and flagella in the increased biofilm integrity in response to NO.

Overall, this study used biofilm phenotyping to characterise the patient biofilm status by identifying bacterial aggregates in expectorated sputum and highlighted the variability between individual patients, raising questions for personalised approaches to CF treatments. A potential biomarker, histone H4, for the CF disease state and PA biofilm phenotype has been identified as being of interest for further proteomic analysis within an extended patient cohort. Further analysis of the bacterial isolates in the CF culture collection is required for full understanding of the varied NO dispersal response.

Table of Contents

Table of Tables

Table of Figures

Research Thesis: Declaration of Authorship

Print name:	Declan Matthew Power

Title of thesis:	Phenotyping of *Pseudomonas aeruginosa* Biofilms in Cystic Fibrosis Patients, Biofilm Biomarker Identification, and Understanding the Nitric Oxide Mediated Biofilm Dispersal Response.

I declare that this thesis and the work presented in it are my own and has been generated by me as the result of my own original research.

I confirm that:

1. This work was done wholly or mainly while in candidature for a research degree at this University;
2. Where any part of this thesis has previously been submitted for a degree or any other qualification at this University or any other institution, this has been clearly stated;
3. Where I have consulted the published work of others, this is always clearly attributed;
4. Where I have quoted from the work of others, the source is always given. With the exception of such quotations, this thesis is entirely my own work;
5. I have acknowledged all main sources of help;
6. Where the thesis is based on work done by myself jointly with others, I have made clear exactly what was done by others and what I have contributed myself;
7. Parts of this work have been published as:

Power D, Webb J (2022) Nitric Oxide-Mediated Dispersal as an Adjunctive Strategy for the Control of Biofilm-Associated Infection. pp 501–519

Signature:		Date:	30/10/2023

Acknowledgements

Firstly, I would like to thank my supervisors Jeremy Webb, Saul Faust, and Gary Connett for the opportunity to work on such a project. Despite delays and the ever-difficult restrictions caused by COVID-19, supervisory meetings were always constructive and their help and advice throughout have been invaluable. I extend my thanks to the UK CF Trust for funding this project, and to colleagues at Imperial College London, in particular Jane Davies who headed the Strategic Research Centre, and organised valuable meetings to discuss and gain guidance on the project from others in the SRC.

Huge thanks to all members of Webb group lab, and those that worked in the CL2 labs in Southampton. Such a friendly group of people made days in lab much more enjoyable, with particular thanks to Bhavik and Conor, since day one they have provided guidance, endless laughs, and a listening ear for me to vent my frustrations and keep me sane.

Thanks to Liam, Jo, Toby, Kirsty, and Lucy who have provided me food, laughs, fun and always a place to stay when the drunken walk was just that little too far! If nothing else, I am happy to have gained such an amazing group of friends from this process.

A final special thanks to my family, especially my parents for their continued love and support in all my endeavours thus far.

Definitions and Abbreviations

ABC	ATP-binding cassette
AHLs	N-acyl-L-homoserine lactones
AI	Autoinducer
ASL	Airway surface liquid
ATP	Adenosine triphosphate
C3D	Cephalosporin-3'-diazeniumdiolates
cAMP	Cyclic adenosine monophosphate
c-di-GMP	Cyclic dimeric guanosine monophosphate
CF	Cystic Fibrosis
CFTR	Cystic Fibrosis Transmembrane Conductance Regulator
CFU	Colony forming unit
Cif	CFTR inhibitory factor
CV	Crystal Violet
DGC	Diguanylate cyclase
eDNA	Extracellular DNA
ENaC	Sodium epithelial channel
EPS	Extracellular polymeric substance
ESBLs	Extended spectrum β-lactamases
FEV	Forced expiratory volume
FISH	Fluorescence in-situ hybridisation
GSH	Glutathione
H-NOX	Heme-nitric oxide/oxygen domain

iNO	Inhaled NO
IQS	Integrated quorum sensing system
LB	Luria Bertani/ Lysogeny Broth
LPS	Lipopolysaccharide
MFP	Membrane fusion protein
MIC	Minimum inhibitory concentration
NBD	Nucleotide binding domain
NBS	New-born screening
NO	Nitric oxide
Nos-P	Nitric oxide sensing protein
NOSs	Nitric oxide synthases
OD	Optical density
OMF	Outer membrane factor
$OSCN^-$	Hypothiocyanite
PCL	Periciliary layer
PDE	Phosphodiesterase
PEx	Pulmonary exacerbation
PKA	Protein kinase
PML	Polymorphonuclear leukocytes
PMN	Polymorphonuclear neutrophil
PQS	*Pseudomonas* quinolone signal
PYO	Pyocyanin
QS	Quorum sensing
R	Regulatory domain

RND	Resistance-nodulation-division
ROS	Reactive oxygen species
rRNA	Ribosomal RNA
SCN^-	Thiocyanate
SNP	Sodium nitroprusside
TCS	Two component signalling
TLR	Toll like receptor
TMD	Transmembrane spanning domain
UK	United Kingdom
WHO	World Health Organisation
WT	Wild type

Chapter 1 *P. aeruginosa* biofilms in the cystic fibrosis Lung

1.1 Cystic Fibrosis

Cystic fibrosis (CF) is the most common fatal autosomal recessive genetic disorder, with the highest prevalence in Caucasian populations of Europe, North America, and Australia with between 7-8 incidences per 100,000 of the general population (Elborn 2016; Bell et al. 2020). In the United Kingdom (UK) alone, there are over 10,000 patients diagnosed with CF and registered on the CF Trust registry as of 2018 (Cystic Fibrosis Trust 2018).

Cystic fibrosis was first described as a new disorder by Dorothy Andersen in 1938, as 'cystic fibrosis of the pancreas' she identified common features including; bronchitis, bronchiectasis, and pulmonary abscesses in the bronchi that were plugged with mucus (Andersen 1938). Since its first description, the disorder is now recognised as a multifaceted disease that affects multiple organ systems, with particularly increased morbidity and mortality being attributed to recurrent and chronic infections of the lungs and respiratory system, due to a build-up of thick mucus and a subsequent decline in lung function. Infections are seen in early childhood and progress into adult life (Stoltz et al. 2015).

1.1.1 Cystic Fibrosis Transmembrane Conductance Regulator Dysfunction

Cystic fibrosis is caused by a defective Cystic Fibrosis Transmembrane Conductance Regulator (CFTR) gene, it is the most common severe inherited disorder with one in 2500 new-borns in the Caucasian population being affected, indicating a carrier frequency of 1 in 25 (Bertranpetit and Calafell 1996; Vankeerberghen et al. 2002). The CFTR gene was identified in 1989 by positional cloning and is located on the long arm of chromosome 7 (q31.2). It is approximately 250kb in length and contains 27 exons encoding for the CTFR protein (Zielenski et al. 1991; Gadsby et al. 2006).

The CFTR gene encodes for a gated conductance protein containing 1480 amino acids that's primary function is transport of chloride ions across the cell membrane. This protein is a member of the ATP-binding cassette (ABC) transporter superfamily of proteins and is regulated by cAMP dependent phosphorylation and ATP hydrolysis (SHEPPARD and WELSH 1999; Patrick and Thomas 2012). The CFTR protein has two motifs, each including a transmembrane spanning domain (TMD) typically comprised of 6 α-helices, and a cytoplasmic nucleotide binding domain (NBD). The two motifs are adjoined by a regulatory domain (R) (SHEPPARD and WELSH 1999; Gadsby et al. 2006;

Liu et al. 2017). The protein is expressed in many different tissues including the pancreas, sweat glands, gut, and notably it is typically expressed on the apical surface of lung epithelial cells (Carroll et al. 1993; Guo et al. 2009)

The CFTR shares some structural homology with other ABC transporters within the same family of transporters, however, it has unique characteristics with the R domain, and is the only ABC transporter to function as an ion channel with its gating also displaying enzymatic activity in ATP hydrolysis (Gadsby et al. 2006; Kirk and Wang 2011). To fulfil its primary function, the opening and closing of the channel is regulated by activation of the cAMP-dependent protein kinase (PKA). After PKA causes phosphorylation of the R domain, channel gating is controlled by ATP binding and hydrolysis at NBDs causing repeated dimerization and conformation changes in a continuous cycle until protein phosphatases dephosphorylate the R domain and allow the channel to return to an inactive state (Chen et al. 2005; Gadsby et al. 2006; Hwang and Kirk 2013).

The primary function of the CFTR is the transcellular excretion of Cl^-. The increase in salt concentration in the extracellular space creates an osmotic gradient and thus water and fluids follow and maintain the hydration of the luminal airway surface liquid (ASL) (Saint-Criq and Gray 2017). The water content of this layer plays a crucial role in the effective functioning of mucocilliary clearance and the removal of inhaled foreign particulates (Boucher 2007; Ratjen et al. 2015).

In conjunction with Cl- secretion, another function of the CFTR in the lung is the transport of bicarbonate ions (HCO_3^-), enabling the correct pH regulation and formation of a normal mucosal layer optimising the airway defence and mucocilliary clearance. This is a secondary to Cl- transport as CFTR is around 5 times more conductive for Cl^- than HCO_3^- (Ratjen et al. 2015; Saint-Criq and Gray 2017).

Molecules that are shown to have a role in the regulation of the immune response are known to be transported by CFTR. Glutathione (GSH) ensures redox balance in the airway and can inactivate reactive oxygen species (ROS) that in high concentrations from either endogenous or exogenous sources can lead to excessive inflammation and tissue damage (Kogan et al. 2003; Kettle et al. 2014). Thiocyanate (SCN^-) is a secreted precursor into the airway lumen, it undergoes oxidation by lactoperoxidase to produce hypothiocyanite (OSCN−) reducing tissue-damaging by other oxygen species. OSCN− itself also displays potent antimicrobial properties (Moskwa et al. 2007; Lorentzen et al. 2011; Saint-Criq and Gray 2017)

Other functions of the CFTR include the interaction with other transport channels including the sodium epithelial channel (ENaC), this is a major regulator of Na+ reabsorption across epithelial tissue. The inhibition of ENaC by CFTR regulates the flow of ions and fluids maintaining osmotic balance and ASL hydration (Riordan 2008; Butterworth 2010; Ratjen et al. 2015)

1.1.2 Mutations of the CFTR

More than 2000 variants of the mutated CFTR gene have been identified, although fewer than 150 are known to cause disease (Ratjen et al. 2015). Functional consequences of the mutations are not all defined, and around 15% are not associated with disease. Each mutation can be classified into 6 different classes once their effect on protein function is known (Figure 1) (Elborn 2016; Bell et al. 2020). Mutation of the CFTR causes spectrum of disease; Classes I, II, and III are associated with little or no CFTR function and hence linked to a more severe phenotype. Class IV, V, and VI have residual CFTR function and are associated with a milder disease presentation, often with preserved pancreatic function in early childhood (Proesmans et al. 2008; Bell et al. 2020).

The high frequency of mutations and the ability for CF to persist in humans since ancient generations, suggests a selective pressure that conferred an advantage to individuals who carry the mutated gene (Alfonso-Sánchez et al. 2010). It had been suggested that CF heterozygotes were more resistant to diarrhoeal diseases such as cholera and typhoid. However, it has since been shown that neither of these would have provided enough selection pressure to produce the incidence of CF found today, but rather a pandemic of tuberculosis (TB) over centuries beginning in the early 1600s could have provided such pressure. The link between both TB and CF arylsulphatase B deficiency is to be further explored (Poolman and Galvani 2007).

The most frequently identified mutation is the Phe508del (also known as F508del) accounts for almost two thirds of mutations overall, however the remaining one-third of alleles are widely distributed and show great heterogeneity (Schrijver 2011). F508del, is a missense amino acid deletion of a phenylalanine in the 508th position of the protein structure, within the NBD1, resulting in the misfolding of the normal CFTR structure (Okiyoneda et al. 2013). The impaired folding is recognised by numerous quality control systems within the endoplasmic reticulum (ER), namely Hsp70, and is subsequently retained and degraded via the ubiquitin proteasome system and is not trafficked to the plasma membrane resulting in loss of function (Du and Lukacs 2009; Kim and Skach 2012; Mendoza et al. 2012).

The spectrum and frequency of the CFTR mutations varies greatly between ethnic groups and geographical populations (Schrijver 2011). Whilst F508del might be the most common, there are certain alleles with distinct ancestry, some of these include; G551D, W1282X, N1303K (Bobadilla et al. 2002).

G551D is a mutation of single origin and is associated with ancient Celtic tribes, and N130K linked with ancient Mediterranean populations. Geographic spread accounts for high incidences of the mutations in various regions around the world due to the early colonisers and influence of these ancestral founders on the population (Bobadilla et al. 2002). W1282X is a mutation found predominantly in Ashkenazi Jews and allele frequency is almost double that of the F508del within the population. The influences of genetic conservation can be identified with a high prevalence of the W1282X mutation being found within an array of countries that have had a significant Ashkenazi Jewish influence (Bobadilla et al. 2002).

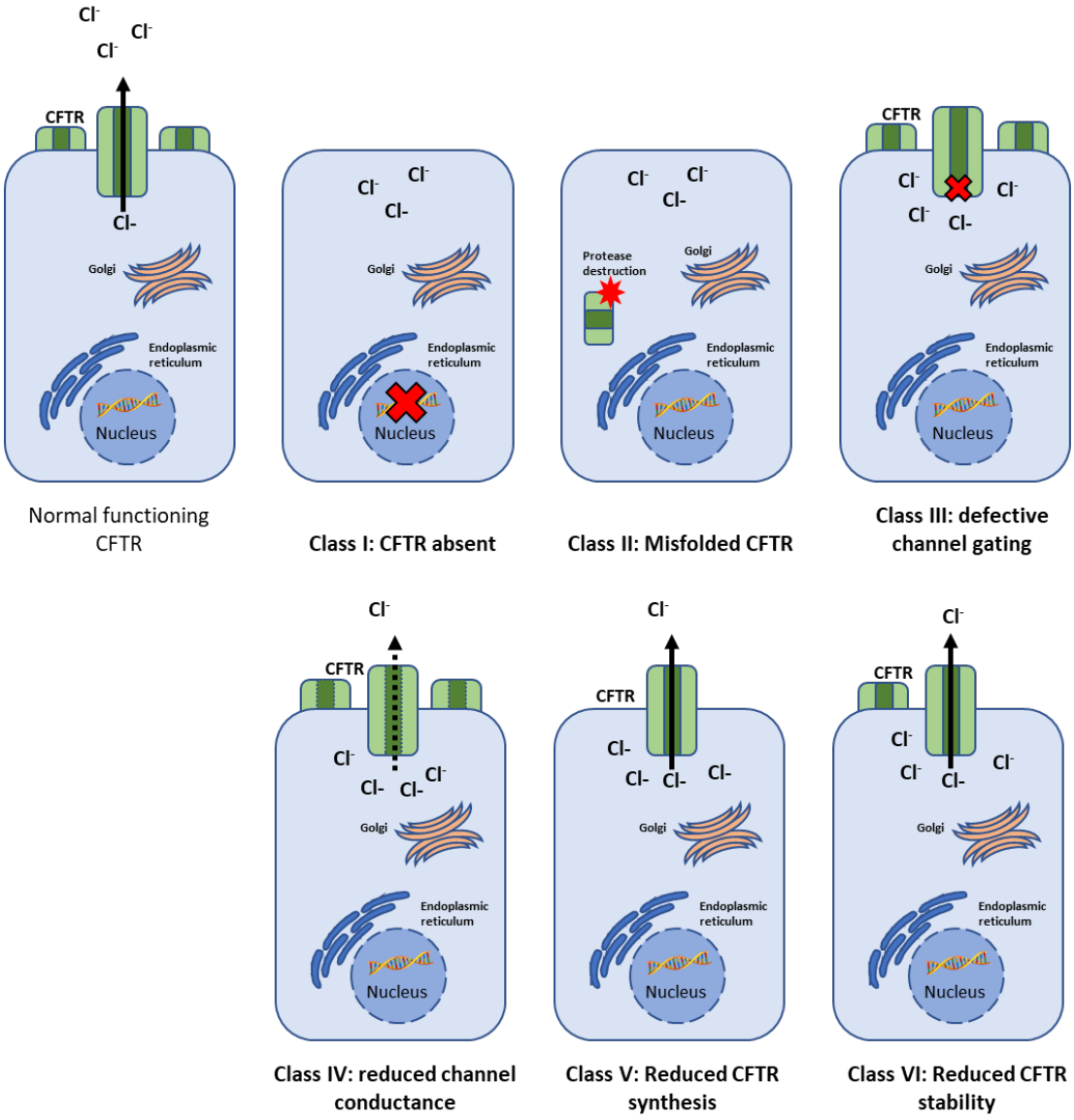

Figure 1. Mutation classes for CFTR protein defects. In a healthy individual, the CFTR is expressed extensively on the apical membrane of the airway epithelium following correct transcription, translation and post-translational modifications and processing. In class I mutations, large deletions, nonsense mutations or frameshift mutations result in either no transcription of the protein or production of unstable, truncated RNA that cannot be translated to a functional protein, thus CFTR is absent at the membrane surface. Missense amino acid deletions cause class II mutations, the protein becomes misfolded and is degraded via protease before Golgi processing resulting in no presentation of the protein at the membrane. The remaining classes (III, IV, V, VI) all CFTR at the membrane surface but with reduced or no functionality due to missense, amino acid change or splicing defect. Class III mutations have defective ion channel regulation as it is no longer able to interact with cAMP. Class IV have a defect in channel conductance, with a reduced chloride ion transport. Class V splicing mutations result in a reduced amount of the correct RNA and thus a functional CFTR is present but scarce. Class VI mutations produce a functioning membrane protein but has decreased stability and is subject to rapid turnover and overall decreased expression on the membrane surface.

1.1.3 Pathophysiological cascade of lung dysfunction in cystic fibrosis.

The identification of the mutated CFTR gene responsible for CF was published by a series of three research papers in 1989. With cloning and DNA characterisation of the gene, the authors of these papers identified the most common F508del mutation (Kerem et al. 1989; Riordan et al. 1989; Rommens et al. 1989). Over the decades since this discovery, there have been multiple investigations into the understanding of the pathogenesis and origins of airway disease in the CF patients. Despite this, there remains a lack of clarity on the exact mechanisms, although several hypotheses have been proposed (Ratjen and Döring 2003). The hindered progress in discovering the pathophysiology have been attributed to the lack of an animal model that mimics the human CF lung (Stoltz et al. 2015). CF models that used mice generated some information as to the origins in a variety of organs most notably in the intestinal tract, however these animals did not develop spontaneous lung disease like that in humans (GRUBB and BOUCHER 1999). In order to overcome the challenges with studying CF in mouse models, recently, studies utilising new animal models including pigs, ferrets, and rats have been undertaken (Stoltz et al. 2015). Porcine models are of focus since their anatomy, biochemistry, physiology, size, lifespan, and genetics are the most similar in relation to humans. Pigs lacking the functional CFTR also manifest classical CF abnormalities and features seen in human patients with CF (Rogers et al. 2008). Most importantly, F508del pigs were reported to display spontaneous development of typical CF airways features of inflammation, remodelling, mucus accumulation, and infection containing multiple bacterial species. The authors concluded that this may provide important insight into the pathogenesis of lung disease and avenues for therapeutics for individuals with CF (Stoltz et al. 2010).

The most widely held hypothesis explaining the establishment of lung infection is the dehydration of the ASL (Boucher 2007). In the cystic fibrosis lung where CFTR would otherwise be highly expressed, there is reduced or no transport of Cl^- anions into the extracellular space. Secondly, in the absence of CFTR, the inhibitory effect of CFTR on ENaC is removed, resulting in an uncontrolled hyperabsorption of Na+ (Clunes and Boucher 2007). Thus, the osmotic gradient needed for water to enter the luminal space and maintain the hydration of the ASL is impaired (Saint-Criq and Gray 2017). The ALS is a thin (~10 μm) liquid layer made up of a lower periciliary layer (PCL) (~7 μm) and an upper mucous layer. The viscoelastic properties and transportability of mucus, and the lubricating periciliary layer separating the mucus from the cell surface rely on appropriate hydration (Boucher 2007; Saint-Criq and Gray 2017). Reduction of the water content of this layer can impair the efficiency of normal mucocilliary clearance (Boucher 2007).

In a healthy individual, the mucus traps particles and inhaled microorganisms and transports them from the lower airways towards the mouth by means of ciliary action and cough (Fahy and Dickey 2010; Kurbatova et al. 2015). The PCL provides a low viscosity layer to facilitate ciliary beating whilst also producing a grafted brush of mucins and polysaccharides suspending the mucus layer, preventing mucins and any trapped particulates from entering the PCL (Button et al. 2012). When the hydration of the PCL and mucus layer is depleted, the mucus becomes a highly viscoelastic, difficult to transport, adhesive material; and the height of the PCL is significantly reduced. This removes both the PCLs lubricant properties ideal for ciliary beating and the separation of the mucus from the epithelial surface, compressing the cilia and allowing mucus adhesion to the airway surfaces obstructing their normal function, as illustrated in Figure 2. Despite the excess not being cleared from the airway, mucus production by goblet cells and submucosal ducts continues creating thick mucus plugs on airway surfaces (Knowles and Boucher 2002; Boucher 2007; Button et al. 2012). This results in microorganisms that have been inhaled becoming trapped within the thick viscous ASL and colonising the lung environment without being cleared, increasing the contact time with airways cells promoting excessive inflammation and irreversible lung damage (Davies 2002).

Additionally, CFTR dysfunction results in a lack of bicarbonate secretion into the ASL and therefore a reduced pH. The ASL contains multiple antimicrobial factors including lysozyme, lactoferrin and secretory leukoproteinase inhibitor (SLPI), that kill bacteria that may be present (Travis et al. 2001). In a porcine model, it was reported the wild-type animals were able to effectively clear *Staphylococcus aureus,* and *Pseudomonas aeruginosa* introduced to the airway. The CF-pigs, however, were reportedly defective in killing the bacteria, with the lack of CFTR reducing the killing effect by around half. The authors noted that this was not due to a reduced concentration of antimicrobial factors but the change in pH of the ASL inhibiting their function (Pezzulo et al. 2012).

The mechanisms mentioned above result in excessive inflammatory response to the same bacterial load in a CF patient than a non-CF patient with a lower respiratory tract infection (Davies et al. 2007). There is evidence to suggest that mutations in the CFTR result in the impairment of the epithelial innate immune function, and even in the absence of a clinically apparent viral or bacterial infection (Cohen and Prince 2012). This effect has even been noted the cystic fibrosis foetus before birth and bacterial exposure, increased inflammation is apparent in the cystic fibrosis airway with increased polymorphonuclear neutrophil (PMN) accumulation (and neutrophil

derived DNA), elevated levels of interleukin-8 (IL-8), free proteases and NF-κB (Verhaeghe et al. 2007). The immune response generates an increase in reactive oxygen species (O2, H2O2), that, as discussed previously, are typically controlled by the antioxidants, SGH and SCN- transported by CFTR. Antioxidant activity is hence impaired with CFTR dysfunction resulting in further impaired antimicrobial action destruction of lung tissue (Moskwa et al. 2007).

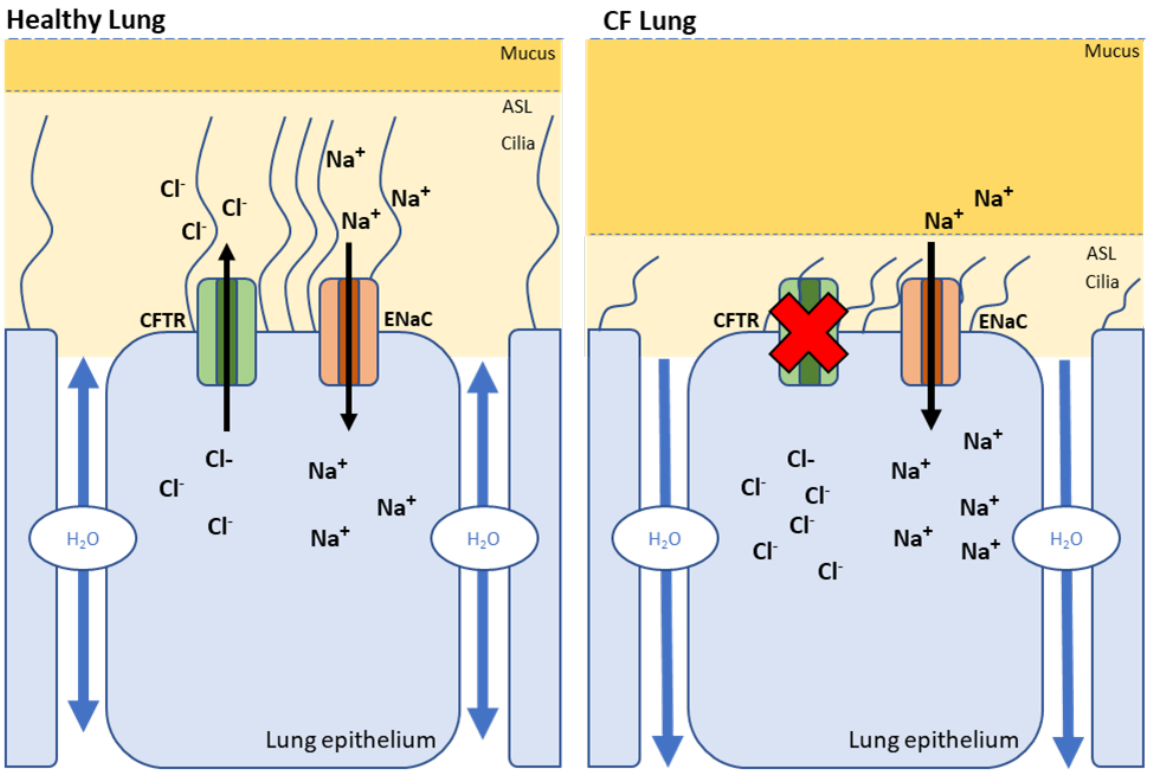

Figure 2. Pathophysiology of the CF lung. In a healthy lung (left) correctly expressed CFTR is presented on the epithelial surface and maintains airway surface liquid (ASL) hydration through ion transport, enabling effective mucocilliary clearance. In the CF lung, the loss of CFTR function as both an ion transport channel and ENaC inhibitor results in an osmotic imbalance and subsequent dehydration of the ASL, compressing cilia and as a consequence of ineffective mucocilliary clearance causing defective clearance of inhaled pathogens and a build-up of mucus.

1.1.4 Diagnosis of Cystic Fibrosis

In the present day, most people in the UK with cystic fibrosis will be diagnosed shortly after birth (5-7 days of age) through the UK New-born Screening (NBS) Programme, introduced nationwide in 2006 (National Institute for Health and Care Excellence 2017; Cystic Fibrosis Trust 2018).

Screening involves a blood spot immunoreactive trypsin test followed by the identification of CFTR variation, if positive. However, the test is not able to screen and detect for all mutations so there remains a cohort of individuals that were not diagnosed by NBS, but by clinical presentation (National Institute for Health and Care Excellence 2017; Bell et al. 2020). The most common non-NBS clinical manifestations used for diagnosis in the UK include; persistent or acute respiratory infection (36.5%); failure to thrive and malnutrition (31.4%); evidence of malabsorption with abnormal/ fatty stool (22.4%) (Cystic Fibrosis Trust 2018). Meconium ileus is also a typical feature observed in CF patients occurring in 15-20% of all patients (18.3%, UK 2018) with up to 10% neonatal presentation (Davies et al. 2007; Ratjen et al. 2015; Cystic Fibrosis Trust 2018). More than 95% of patients presenting any of the classical symptoms of cystic fibrosis can be diagnosed with a chloride sweat test, this often considered the optimal and most conclusive test with an abnormal chloride concentration (≥60 mmol/l) indicative of CF, although molecular confirmation is recommended (Ratjen et al. 2015; Farrell et al. 2017; Simmonds 2019).

1.1.5 Lung disease in Cystic Fibrosis

Lung disease and respiratory failure brought on by chronic infection is the most life-threatening feature of cystic fibrosis disease. A vicious cycle of airway obstruction, and inflammation, and bronchiectasis leads to the progressive decline in lung function with increased severity of coughing and sputum production (Chmiel et al. 2002; Ratjen et al. 2015). Lung function is routinely monitored at visits to CF clinics for all ages capable of performing a spirometry test and is measured using FEV1 (the Forced Expiratory Volume of air in the first second of a forced exhaled breath) and FEV1 % predicted (FEV1 we would expect for a person without CF of the same demographic). For people with CF, an FEV1 % predicted of >85% indicates lung health close to normal (Cystic Fibrosis Trust 2018). Chronic bacterial infection and the associated decline in lung function ultimately results in the respiratory failure and death in 80-95% of cystic fibrosis patients (Lyczak et al. 2002; Szczesniak et al. 2017).

Complications of CF lung disease also contribute to increased morbidity and mortality. Pneumothorax occurs in 3-4% of CF patients, with airway obstruction leading to the trapping of air resulting in chest pain and shortness of breath (Flume et al. 2005a). Haemoptysis (coughing up blood from the lungs) can occur in episodes classed as ‘massive haemoptysis’ (>240ml of blood in 24hrs) and put patients at risk of death by asphyxiation and hypovolemia. Around 5% of patients with experience a haemoptysis event during their lifetime with 25% of these occurring in patients

<18 years of age (Hurley et al. 2011; Turcios 2020). The aetiology of these events remains unknown, but it has been associated with infection with *P. aeruginosa* or *Staphylococcus aureus* causing inflammation and damage of capillary and arterial walls. Decline in lung function has also been implicated, however, episodes have been seen to occur in patients with normal lung function (Flume et al. 2005b; Turcios 2020).

Pulmonary exacerbations (PEx) are of significant importance in monitoring the clinical course of cystic fibrosis disease, despite this there is no consensus diagnostic criteria, nor standard definition (Rosenfeld et al. 2001; Goss and Burns 2007). It has been suggested that PEx represents an intrapulmonary spread of microbial infection by the resident taxa as opposed to a shift in the diversity or microbial density within lung communities (Fodor et al. 2012). PEx are generally associated with acute worsening of symptoms, short term decline in FEV1, malaise and fatigue, and reduced overall quality of life (Goss and Burns 2007; Turcios 2020). Exacerbations vary in severity and may be treated at home with oral antibiotics or may be require hospitalisation and intravenous antibiotics (Turcios 2020). The decline in lung function after PEx is sometimes not restored. A cohort study revealed 75% of patients FEV1 did not return to baseline function within 6 months, and 58% did not recover after 12 months post PEx treatment. Those that did not recover often had a persistent infection with MRSA, *P. aeruginosa* or MDR *P. aeruginosa* (Sanders et al. 2010).

1.1.6 Management and therapy of cystic fibrosis pulmonary disease

Care for cystic fibrosis patients is delivered at specialist CF centres and involves a multi-disciplinary team of specialist healthcare professionals to ensure that all the aspects of the disease and addressed. Visits to clinics are dependent on disease severity, but it is recommended for stable patients to maintain routine appointments every 2-3 months (Cystic Fibrosis Trust 2011; Stern et al. 2014)

Microbiological assessment of respiratory secretions should be taken at each visit to clinic (Cystic Fibrosis Trust 2011). A sputum sample is preferable for culture if the patient is able to expectorate, however in younger patients this is not always the case, and a cough swab can be used to guide antibiotic therapy. A positive cough swab has been shown to be a good predictor of lower airway infection, but infection cannot be ruled out if negative (Equi et al. 2001). Any infection of the respiratory tract calls for intense repetitive treatments with antibiotics to maintain lung function. The antibiotics to be used vary from patient to patient and are dependent

on numerous factors including age, colonising organism and its antimicrobial resistance profile, and the stage of lung disease (Lyczak et al. 2002).

In the initial stages of disease where no pulmonary infection is presented, the main target is preventing infection and maintaining pulmonary function by reducing mucus and inflammation, assisting natural ciliary clearance, and thus keeping the airway clear. A variety of methods exist; devices can generate both intrathoracic and extrathoracic oscillations that create air flow and mobilise mucus; rehydration therapy with inhalation of hypertonic saline; mucolytic dornase alpha to reduce sputum viscosity; non-steroidal anti-inflammatory drugs (NSAIDs) e.g. ibuprofen, and segregation of cohorts at clinic visits to prevent cross infection (Davies et al. 2007; Turcios 2020).

If in the initial stages of the disease, there is intermittent lung infection with *P. aeruginosa* or other infectious agents 'early eradication therapy' can be used to delay the progression of lung disease and onset of chronic infection (Davies et al. 2007). The optimal combination, dosages, delivery, and duration of antibiotic eradication strategy remain unclear. Meta-analysis of various trials indicated trivial difference between oral and nebulised antibiotics administered either alone or in combination, and duration of treatment may be up to two years (Langton Hewer and Smyth 2017). Success of eradication ranges from 81-93% and the median period before reinfection is 18 months. Unfortunately for some, eradication therapy is unsuccessful and the patient will become chronically infected (Taccetti et al. 2005; Jones 2005).

When patients become chronically infected, most typically with *P. aeruginosa*, the infection can no longer be cleared by an antibiotic treatment strategy, with around 10-40% failure rate of eradiation therapies (JACKSON, WATERS 2019). Thus, the focus of therapy shifts to prolonging lung function and reduce the frequency of pulmonary exacerbations improving the quality of remaining life (Ehsan and Clancy 2015). Inhaled antibiotic therapy is the continued standard of care for chronic infection with either a single-agent or alternating antimicrobial therapy. Nebulised tobramycin, aztreonam, and colistin are recommended for chronic *P. aeruginosa* infection. Continuous azithromycin use is also recommended due to its anti-inflammatory properties (Mogayzel et al. 2013; Turcios 2020).

There comes a point in the advanced stages of pulmonary disease in which respiratory failure is inevitable, and a bilateral lung transplant is the only treatment option for survival. A key criterium for lung transplant listing is advanced disease with a FEV1 of <30% predicted, or moderate disease

(50% FEV1) with a rapid decline in lung function (>20% in previous 12 months) (Morrell and Pilewski 2016; Ramos et al. 2019). Unfortunately, donor lungs are a limited resource, and late referral may lead to patient death whilst on a waiting list. In 2018, just 58 transplants were reported in the UK. If successful, patients have an 82% 1-year survival rate and a 51% 10-year survival in the UK (Meachery et al. 2008; Cystic Fibrosis Trust 2018; Ramos et al. 2019).

1.1.6.1 CFTR modulator drugs

CFTR modulator drugs look to restore functionality of the defective protein. Five main groups of modulators exist, categorised by their action with differing CFTR mutations: potentiators – restore channel gating and conductance; correctors - rescue the folding, processing and trafficking of the protein to the membrane; stabilizers – increase protein stability at the membrane; read-through agents – rescue protein synthesis and allow expression of the full-length CFTR; and amplifiers – increasing the abundance of the CFTR protein (Lopes-Pacheco 2020). To date only four drugs belonging to these classes are approved for use for the treatment of CF patients.

Ivacaftor is a CFTR potentiator, allowing for an increase in chloride ion flow with a concomitant increase in channel open probability. Ivacaftor was approved for use in 2012 initially for those with the G551D mutation, a Class III defect with impaired channel gating (Van Goor et al. 2009; Condren and Bradshaw 2013). In clinical trials, patient lung function was seen to improve within 2 weeks of use, and substantial improvement of other factors was also observed (Ramsey et al. 2011; Sermet-Gaudelus 2013). Given the G551D mutation accounts for 5.9% of CF in the UK (Cystic Fibrosis Trust 2018), only a small subset of patients was eligible for treatment. However, with the success of ivacaftor and following subsequent studies, approval has been extended to 38 other CF gating mutations (Lopes-Pacheco 2020).

A first-generation corrector, lumacaftor, showed promise increasing cell surface density of F508del mutations in vitro. Unfortunately, no significant improvement for both lung and CFTR function was seen in phase two trials (Clancy et al. 2012). When given in combination with ivacaftor, modest improvements in lung function were observed in homozygous F508del patients and lumacaftor/ivacaftor (Orkambi®) was approved for use in 2015 (Cholon et al. 2016).

Tezacaftor is a second-generation corrector with similar structure to lumacaftor but presents fewer adverse effects. It is administered as a co-treatment with ivacaftor and demonstrates a preservation of lung function and reduced sweat chloride. Tezacaftor/ivacaftor (Symkevi®) was approved for use in 2018 for patients with the F508del mutation (Lopes-Pacheco 2020).

Kaftrio (Trikafta™) is a triple combination therapy of elexacaftor, tezacaftor, and ivacaftor available on the NHS (NHS England 2020). Following two randomised, controlled, phase 3 clinical trials for safety and efficacy evaluations. Kaftrio was approved suitable for 90% of patients aged 12 or over with an f508del mutation and gave significant improvements in lung function, reduction in sweat chloride, reduction in pulmonary exacerbation rate, and improved quality of life. (Middleton et al. 2019; Heijerman et al. 2019). Working in combination with those mentioned above, the additional next generation CFTR corrector, elexacaftor, works at an alternate binding site to tezacaftor further facilitating the functionality of the protein at the cell surface. The long-term outcomes and benefits are still to be assessed for this promising new therapy but indications that its already more effective than dual therapy treatments (Ridley and Condren 2020).

Whilst these modulators are a promising therapy for restoring CFTR function, the issue of chronic infection with *P. aeruginosa* and its correlated clinical outcome remains (Davies and Martin 2018). Having only been introduced to the market in the past decade, these modulator drugs so far, have limited evidence for the impact on *P. aeruginosa* abundance in chronic infection, or delaying infection. Whilst a few studies have indicated a reduced infection with *P. aeruginosa* (Rowe et al. 2014), a better representation of the impact of these drugs on infection may be apparent with longer term studies involving patients who started modulator therapy from an early age (Davies and Martin 2018). Taking this into consideration, there remains the need for effective treatment strategies, including antimicrobial chemotherapy, for chronic biofilm infections in those patients that may not be suitable for modulator treatment, or are at a stage of irreversible lung damage.

1.1.7 Microbiome of the CF lung

The respiratory tract and airways provide a highly structured environment and varied niches that enables the development of complex microbiota with a range of both Gram-negative and Gram-positive organisms. The bacteria typically associated, and have the most notable impact, in CF patients include *P. aeruginosa, Haemophilus influenzae, S. aureus,* and *Burkholderia cepacia complex* (BCC) (Bhagirath et al. 2016). These 'classical' CF pathogens are often identified using conventional and phenotypic analysis of pure cultures. However, many problems can arise using these methods and may lead to misidentification (Bittar and Rolain 2010), for example, the culture methods that typically determines data on national trends on CF registries does not typically include screening for anaerobic bacteria, hence, these may be missed leading to a distorted picture of the CF lung microbiome (Cuthbertson et al. 2020)

The CF lung environment is not limited to bacterial infection. Yeasts, and filamentous fungi (*Candida,* and *Aspergillus* species respectively), are also frequently isolated from CF patients, and may lead to complications such as Allergic Bronchopulmonary Aspergillosis (ABPA). Respiratory syncytial virus (RSV) whilst thought not to chronically infect the lungs, it has been shown to be a contributing factor in the onset of pulmonary exacerbations (LiPuma 2010; Zemanick and Hoffman 2016).

In children H. influenzae and intermittent *S. aureus* are the most isolated species. However, in adulthood, chronic *P. aeruginosa* infections affect up to 60% of patients (Figure 3) (Cystic Fibrosis Trust 2018). This trend is generally observed on most CF registries worldwide, interestingly, the 2018 CF registry in the US identified *S. aureus* as the most frequently detected pathogen. However, the authors have attributed this to anti-staphylococcal prophylaxis in more routine use outside of the US and thus *S. aureus* is less frequently isolated in other countries (Bernardy et al. 2020).

1.1.7.1 Bacterial evolution and diversity within the CF lung

In recent years, non-culture-based methods have enhanced the understanding of the diversity and polymicrobial environment of the CF lung with many organisms identified that have not previously been recovered (Burns and Rolain 2014). 16S rRNA gene amplicons sequencing, real-time polymerase chain reaction, and matrix assisted laser desorption-time of flight mass spectroscopy (MALDI-TOF MS) have identified organisms such as: *Stenotrophomonas maltophilia*, *Achromobacter xylosoxidans*, *Pandoraea*, *Ralstonia*, and *Streptococcus* species (Salipante et al. 2013; Burns and Rolain 2014; Prior et al. 2017).

Extensive microbiome studies have reported greater bacterial diversity than previously thought from earlier studies and saw correlations between this diversity and lung function. Cuthbertson et al. (2020), via high throughput targeted amplicon screening, identified 598 distinct bacterial operational taxonomic units (OTUs) from 297 CF patient respiratory samples. The authors also discovered that a decrease in diversity of species shared an associated decline in lung function, with the core taxa of 'traditional' pathogens conserved in severe lung disease, including *P. aeruginosa*. Interestingly, the authors reported that patients with better lung function display a high microbiota diversity with anaerobes being the most dominant taxa.

Cystic fibrosis patients ultimately progress to a state of chronic lung infection, most typically colonised by *P. aeruginosa.* Through multiple molecular investigations it is evident that there is a great diversity within *P. aeruginosa* isolates obtained from CF patients, both within geographically

defined populations, and across sub-compartments of the lungs due to localised ecological adaptation to the surrounding milieu (Waters and Goldberg 2019; Kordes et al. 2019; Acosta et al. 2020). Epidemic, clonal strains of *P. aeruginosa* also exist such as Australian epidemic strain 1 (AES-1) appear to have similar traits and are of concern due to their ability to transfer patient-patient, often with a worse clinical prognosis (Acosta et al. 2020). Non-clonal strains however display marked evolved differences in proteomic profiles resulting in variations in nutritional requirements, host-defence and antibiotic resistance, and virulence due to type 3 secretion systems (Jorth et al. 2015). Parallel evolution and adaptation are also observed to occur between initial colonisation to established infection within a biofilm, enabling distinct phenotypic mutations and antibiotic resistance traits facilitating persistence within the CF lung (McElroy et al. 2014; Bartell et al. 2019).

1.1.8 Susceptibility of the CF lung to *P. aeruginosa*

As mentioned above, chronic *P. aeruginosa* infections affect up to 60% of adult patients. The reasons why *P. aeruginosa* is the most prevalent are yet to be fully elucidated, and many proposed hypotheses are debated. It was initially hypothesised that an increased level of asialo-GM1, a non-sialylated glycoprotein, increased the adherence of *P. aeruginosa* to the respiratory epithelial cells though pili interactions (Saiman and Prince 1993; Bryan et al. 1998). However, multiple studies have refuted this hypothesis for numerous reasons, including a high titre of *P. aeruginosa* antibodies and antigens in commercially produced anti-sera to asialo-GM1. The proposed subunit for asialo-GM1 binding was also not found to be surface exposed on the pilus (Pier 2002)

Another proposed reason for high susceptibility to *P. aeruginosa* infection is that CFTR can phagocytose *P. aeruginosa* as part of the innate immune response, acting as a receptor for the bacterial LPS (Pier 2002). Pier et al (1996) suggested that CFTR acts as a receptor for *P. aeruginosa* and correlates with internalization of the bacteria into the lung epithelia. *P. aeruginosa* LPS was identified as the ligand for cell ingestion, and cultured human airway epithelial cells with the F508del mutation were defective at bacterial internalization compared to the wild type, with 10-50 times more *P. aeruginosa* internalisation in the latter and decreased numbers of bacteria in the luminal space. They also demonstrated this effect was specific to *P. aeruginosa* with other pathogens tested equally internalised by both WT and F508del cells.

The persistent colonisation of *P. aeruginosa* in the CF lung can be generally attributed to the ability of the bacterium to produce a wide array of virulence factors, high levels of antimicrobial resistance, and its ability to undergo phenotypic and genotypic changes to better survive different environmental niches and the host defence, most notably the formation of biofilms.

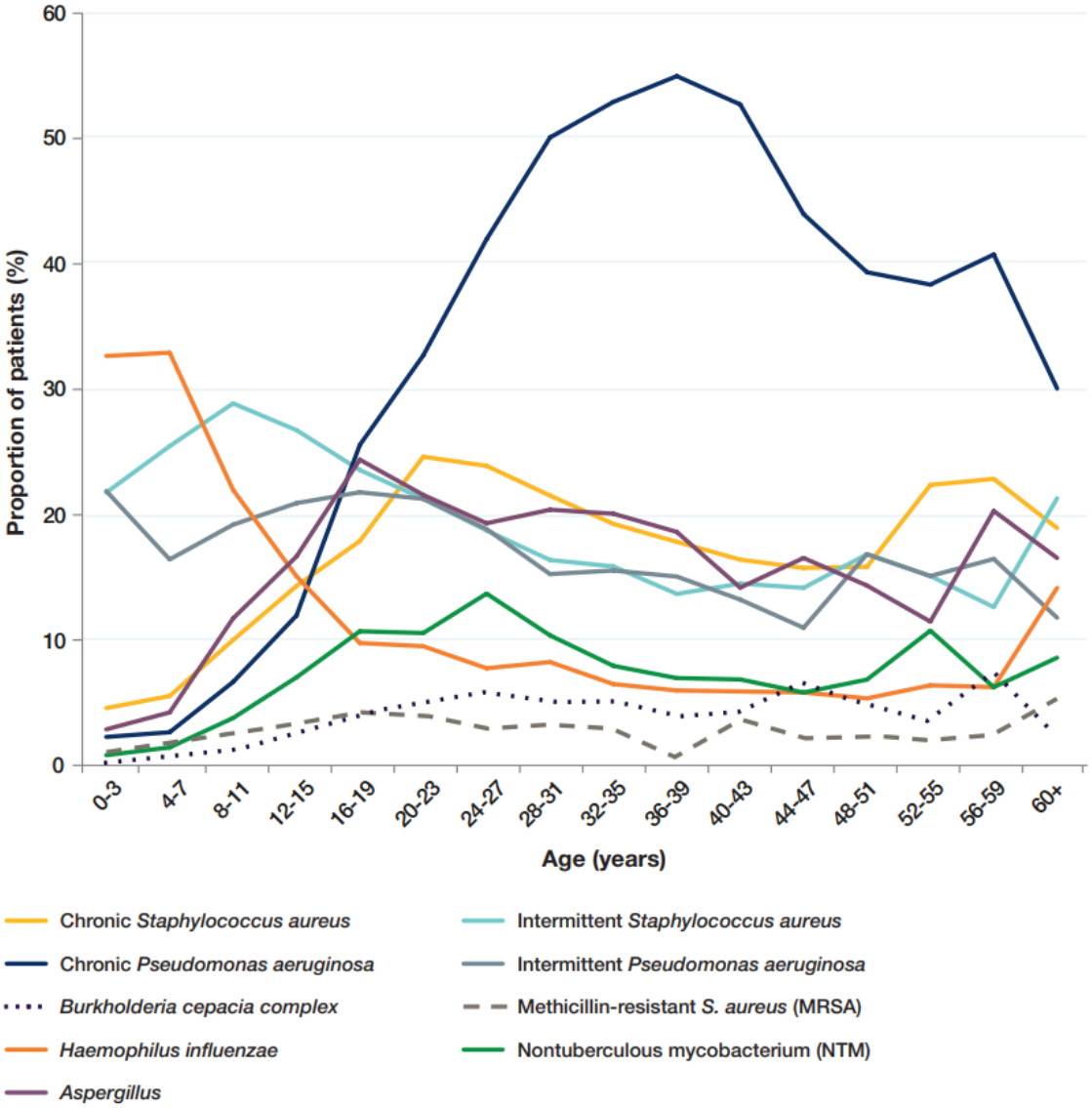

Figure 3. Frequency and diversity of the most common bacterial and fungal infections in CF patients. Graphical representation of the main pathogens that infect the CF lung and the changes in frequency dependant on age. Chronic *P. aeruginosa* infection increases and is the most prevalent organism with progressing age. Chronic infection is defined as three or more culture positive samples taken in one year (n=9847. proportions calculated from 9632 (97.8%) patients who had a culture taken in 2018). (Cystic Fibrosis Trust 2018)

1.2 *P. aeruginosa*: a formidable pathogen

P. aeruginosa is a well-studied, highly versatile, Gram-negative organism. *P. aeruginosa* is rarely pathogenic in healthy individuals but is an important cause of serious opportunistic health care associated infection in patients with HIV, malignancy, or immunosuppression, whereby the normal immune defences are rendered ineffective (Sadikot et al. 2005; Mulcahy et al. 2014)

P. aeruginosa is found abundantly and ubiquitously in a wide variety of environments including, fresh and saltwater sources, soil, and clinical and domestic fresh water and wastewater systems. The bacterium is also an opportunistic plant and insect pathogen (Aujoulat et al. 2012). The success of *P. aeruginosa* to colonise these environmental niches with varying nutrient and oxygen availability lies within the bacterium's large genome and its high metabolic diversity and ability to adapt to nutrient-depleted environments (Frimmersdorf et al. 2010; Klockgether et al. 2010). The *P. aeruginosa* genome ranges from 5.5 to 7 million base pairs; the largest genome seen in any pathogenic Gram-negative bacteria. This genome includes 5570 open reading frames (ORF) with a large repertoire of regulatory genes, genes encoding for transporters, metabolism, and substrate uptake. It also encodes for an array of virulence factors and resistance mechanisms used by the cell to evade both the host immune system and antagonism from antimicrobial agents (Stover et al. 2000; Alhede et al. 2014).

Whilst *P. aeruginosa* is notably associated with a high morbidity and mortality in cystic fibrosis. It is also of major concern in chronic wounds, burns, middle ear infections, and implanted medical devices (Mulcahy et al. 2014).

1.2.1 Virulence factors

The outcomes of an infection are largely dependent on the virulence factors produced/ displayed by the bacteria in conjunction with the host immune response to such factors. A considerable proportion of these factors are tightly regulated with the modulation of gene expression and complexity cell signalling quorum sensing systems in response to environmental stimuli (Sadikot et al. 2005; Chakravarty and Massé 2019). The virulence factors of *P. aeruginosa* can be categorised as either cell associated or secreted/ extracellular products (Strateva and Mitov 2011)

1.2.1.1 Cell Associated factors

P. aeruginosa expresses polar type IV pili and flagella, these are important for both twitching and swimming motility, respectively. Type IV pili play a significant role in the attachment of the

bacterium to the host epithelial cells (binding to glycolipids on the cell surface), and in the formation of biofilms (Sadikot et al. 2005; Strateva and Mitov 2011). Flagella are critically involved in the initial stages of infection providing chemotaxis to suitable environments with sufficient nutrients (Feldman et al. 1998). Both are involved in inciting an innate inflammatory response, binding toll-like receptors 2 and 5 (TLR2/5) and activation of IL-8 production (Sadikot et al. 2005). Lectins, proteins present on the outer membrane, recognise, and adhere to host tissues. Specifically, LecA and LecB bind to receptors of lung epithelial cells (Pang et al. 2019).

Lipopolysaccharide (LPS) is a key component of the outer membrane of Gram-negative bacteria and is composed of three domains: lipid A, a core oligosaccharide, and the O antigen. The latter used for classification and serotyping. Lipid A anchors the LPS to the bacterial outer membrane and is responsible for its toxicity (Ciornei et al. 2010; Lam et al. 2011). TLR4 senses bacterial LPS and initiates TLR-mediated pro-inflammatory signalling within the airway (Hajjar et al. 2002).

LPS of *P. aeruginosa* isolated from chronically infected patients displays a unique LPS structure. Lipid A is typically hexa-acylated in non-CF isolates, whereas chronic CF are penta-acylated and induce a higher inflammatory response within the cystic fibrosis airway via TLR4 recognition with much lower concentrations required to provoke a response. These findings were not however parallel in a murine model, which may indicate the failures of mouse models for the pathogenesis of cystic fibrosis lung disease (Ernst et al. 1999; Hajjar et al. 2002; Ciornei et al. 2010). Loss of the O-antigen and substantially more palmitate and aminoarabinose within the lipid A region of LPS are also characteristics of clinical CF isolates. Increases of palmitate and amino arabinose within lipid A may confer resistance to cationic antimicrobial peptides and may predispose isolates to developing resistance to colistin (Ernst et al. 1999, 2007).

1.2.1.2 Secreted extracellular factors

1.2.1.2.1 Secretion systems

Bacteria have evolved several complex secretion systems directing virulence factors either into the cell cytosol or the extracellular milieu. Of the six secretion systems that have so far been identified in Gram-negative bacteria, *P. aeruginosa* possesses five of them, type one through type six excluding type four (Strateva and Mitov 2011).

Two Type one secretion systems (T1SS) have been identified in *P. aeruginosa*. The Apr system responsible for secreting AprA an alkaline protease, and AprX of unknown function (Bleves et al. 2010). AprA is a zinc-dependent metalloprotease that cleaves various proteins and cytokines belonging to the host immune system including complement protein C2 blocking complement activation and opsonization; and flagellin, inhibiting the activation of TLR5 (Laarman et al. 2012; Bardoel et al. 2012). AprA, can also allow the bacterium avoid phagocytosis by inhibiting chemotaxis functions of neutrophils, and its overexpression has been shown to promote production of another virulence factor, pyocyanin (Iiyama et al. 2017). Another secreted protein via T1SS is HasAp, a heme acquisition protein, is secreted in response to low iron conditions and can scavenge heme-iron from haemoglobin from host erythrocytes ruptured by bacterially produced haemolysins (Alontaga et al. 2009).

Type II secretion systems T2SS are predominately involved in the secretion of hydrolases. LasA, LasB, protease IV, and exotoxin A (ToxA) are considered exoproducts that to play a significant role in the pathogenesis of *P. aeruginosa* (Kida et al. 2008; Bleves et al. 2010). LasA and LasB both degrade elastin, a critical component for the elasticity of lung tissue, can damage epithelial permeability by cleaving tight junction associated proteins, and prevent repair of epithelial injury (De Bentzmann et al. 2000; Bleves et al. 2010). LasB also degrades epithelial surfactant proteins SP-A and SP-D. SP-A and SP-D are involved in innate immune functions, opsonisation and aggregation of bacteria present with the lung. Degrading these components results in the evasion of alveolar macrophages and phagocytosis (Alcorn and Wright 2004; Kuang et al. 2011). Protease IV (PIV) is a serine protease that alters the immune defence by also degrading the surfactant proteins SP-A and SP-D with similar effects to that of LasB (Malloy et al. 2005). PIV has also been shown to degrade cytokines (IL-22) that are key mediators of mucosal immunity at the respiratory epithelial surface (Guillon et al. 2017). Exotoxin A is the most toxic virulence factor belonging to *P. aeruginosa,* it is an ADP-ribosyltransferase and is endocytosed into the cell where it inhibits

protein synthesis by ADP ribosylation of elongation factor 2 resulting in cell death within the host tissue (Morlon-Guyot et al. 2009; Michalska and Wolf 2015)

Four known effector proteins are secreted by type III systems (T3SS) in *P. aeruginosa*, these include ExoS, ExoT, ExoU, and ExoY. These are injected by the bacterium directly into the cytosol of the host cell. All *P. aeruginosa* possess genes required for T3SS but not all have the genes encoding for all of the effectors (Hauser 2009). A study by Feltman et al. showed that clinical and environmental isolates strains have either *exoU* or *exoS* genes, but not both. Suggesting that isolates differ both genotypically and phenotypically dependent on environment and the effectors they produce with *exoS* being favoured in CF isolates (Feltman et al. 2001; Shaver and Hauser 2004). ExoS is a bi-functional enzyme with GTPase activating protein and ADP-ribosyl transferase activity that disrupt the actin cytoskeleton, cellular function, and interferes with host DNA synthesis causing cytotoxicity and cell death. This attributes to an increase in the extent of lung tissue damage (Nicas et al. 1985; Strateva and Mitov 2011). ExoT has 76% amino acid homology with ExoS, and exhibits similar functions with the addition of inhibiting immune cell migration and phagocytosis (Barbieri and Sun 2004). ExoU has been shown to have the most significant effect on virulence as a result of phospholipase A2 activity that can rapidly kill numerous cell types including, macrophages, fibroblasts, and lung epithelial cells (Shaver and Hauser 2004). Little is known about the exact functions of ExoY and its role during infection is yet to be elucidated (Munder et al. 2018). ExoY acts as a nucleotidyl cyclase and it has been proposed that it impairs innate immune response, apoptosis of epithelial cells, and severe lung tissue alterations (Kloth et al. 2018).

Type five secretion systems (T5SS) are responsible for the secretion of EstA, LepA, and CupB5. EstA is an outer membrane bound protein that displays esterase activity and hydrolyses lipids and is also involved in the production of rhamnolipids thought to be essential for bacterial motility and biofilm formation (Wilhelm et al. 2007). LepA activates the NF-κB response by proteolytic cleavage of NF-κB receptors, launching an inflammatory cascade within the host immune system (Kida et al. 2008) resulting in additional lung epithelial damage.

The type six secretion systems (T6SS) have only recently been described and confer a fitness advantage against rival bacteria (both intra- and inter-species) and against the eukaryotic host (Berni et al. 2019). *P. aeruginosa* produces effectors VgrG2b, TplE, PldA, and PldB, these are described as “trans-kingdom effectors” due to the ability to target both prokaryotic and eukaryotic cells the latter two are phospholipases injected directly delivered into target cells and

the former play a role in cell internalisation (Bleves 2016; Wettstadt et al. 2019) Berni et al. identified a novel toxic effector Tle3 secreted by the T6SS which becomes toxic in within the periplasm, the mechanisms of which are still uncharacterised (Berni et al. 2019).

1.2.1.2.2 CFTR inhibitory factor

CFTR inhibitory factor (Cif), is a novel epoxide hydrolase virulence factor of *P. aeruginosa* that reduces chloride secretion by epithelial cells (Ballok and O'Toole 2013). Cif is secreted by the Sec system and packed into outer membrane vesicles which diffuse through the mucus layer and fuse with lipid rafts on the host plasma membrane, releasing Cif into the cytoplasm (Ballok et al. 2014). The enzymatic activity of Cif stabilises the CFTR preventing deubiquitinisation and resulting in lysosomal degradation of the CFTR protein (Ballok and O'Toole 2013). The CFTR function is already compromised in CF patients and the production of Cif by *P. aeruginosa* further reduces CFTR availability and function at the apical membrane surface. With chronic *P. aeruginosa* infection this enhances the airway dehydration through mechanisms discussed previously and facilitates the establishment of additional bacterial infection (Bahl et al. 2010).

1.2.1.2.3 Phenazines

Phenazines are pigmented, redox-reactive, heterocyclic, nitrogen-containing molecules secreted by a considerable number of bacteria, including multiple fluorescent *Pseudomonas* spp. Synthesis of these occurs from modification of chorismic acid to Phenazine-1-carboxylic acid (Phenazine-1-carboxylate, PCA). PCA is further modified into pyocyanin (PYO), 1-hydroxyphenazine (1-HP), or phenazine-1-carboxamide (PCN) (Nadal Jimenez et al. 2012). Pyocyanin (5-*N*-methyl-1-hydroxyphenazine), is a blue-green pigment that gives *P. aeruginosa* its recognisable colour and the most-studied member of the phenazine family and is solely produced by *P. aeruginosa* (Nadal Jimenez et al. 2012; Briard et al. 2015). Pyocyanin is also recognised as both a virulence factor and a small diffusible quorum sensing (QS) molecule, and can promote the biosynthesis of itself and other QS controlled virulence factors such as LasA, and LasB (Jayaseelan et al. 2014)

High concentrations of PYO have been found in CF sputum indicating an active role in lung infection resulting in numerous effects. Pyocyanin modulates redox cycling and generates reactive oxygen species (superoxide and hydrogen peroxide) causing significant oxidative stress on cells, particularly calcium homeostasis in the airway epithelia (Winstanley and Fothergill 2009). Pyocyanin actively inhibits the cellular responses to this oxidative stress by reducing the transcription of, and inhibiting catalase function within the airway, and inactivating glutathione (Lau et al. 2004a). Once pyocyanin has crossed the cell membrane it effects various cellular

functions including respiration, mucin production by goblet cells, ciliary beating, and inhibition of α1 protease inhibitor; reducing clearance of sputum and intensifying neutrophil elastase-mediated damage (Rada and Leto 2013). Pyocyanin has proinflammatory effects and recruits neutrophils to the infection site and induces their apoptosis impairing the host immune response. It has also been shown to inactivate nitric oxide valuable to immune function (Allen et al. 2005; Winstanley and Fothergill 2009). The activity of PYO on cellular respiration leads to reduced intracellular cAMP and ATP concentrations due to the generation of ROS and thus has an adverse effect on the functioning of ATP gated transporters such as CFTR (Rada and Leto 2013).

The role of pyocyanin in the pathogenesis of CF lung infection has been confirmed in murine models. Using PYO-deficient *P. aeruginosa* mutants studies showed that strains unable to synthesise PYO displayed attenuated virulence and reduced interbacterial competition. The authors thus concluded that pyocyanin was an important contributor to the persistence of infection and full virulence of *P. aeruginosa* within the CF lung environment (Lau et al. 2004b; Caldwell et al. 2009).

Anti-bacterial and anti-fungal properties have also been noted. Pyocyanin isolated from *P. aeruginosa* from CF patient's sputum, inhibits the growth of *S. aureus*, *C. albicans*, and *A. fumigatus* (Jayaseelan et al. 2014; Briard et al. 2015). This provides insight into the aggressive, competitive nature of *P. aeruginosa* and may be a contributing factor to the explanation of the persistence and prevalence of the bacterium in chronic CF pulmonary infection.

1.2.1.2.4 Siderophores

Iron availability in the host is typically limited to levels much lower than needed for biological processes. *P. aeruginosa* (as have many bacteria) has developed iron scavenging molecules (siderophores) to obtain the iron that is needed such as pyoverdine and HasAP, as previously mentioned (Alontaga et al. 2009; Kang et al. 2019). Pyoverdine is the main iron uptake system in *P. aeruginosa* seen to be crucial in infection and can both solubilise iron from organic sources and remove bound iron from host factors such as lactoferrin and transferrin (Takase et al. 2000). Pyoverdine gives *P. aeruginosa* a fluorescent, yellow green pigmentation and once iron has been acquired, acts as a signalling molecule for upregulation of its own production and other major virulence factors including the protease Exotoxin A (Minandri et al. 2016; Kang et al. 2019). Reid et al. (2007), found that iron concentrations in the sputum of CF patients were significantly higher

than in healthy individuals, suggesting an increased iron concentration may facilitate and explain the sustained chronic infections in the CF lung.

1.2.2 Resistance mechanisms

Pseudomonas aeruginosa belongs to the WHO (World Health Organisation) ESKAPE (*Enterococcus faecium, Staphylococcus aureus, Klebsiella pneumoniae, Acinetobacter baumannii, Pseudomonas aeruginosa*, and Enterobacter species) list of pathogens that pose a threat to human health with reduced treatment options for serious and chronic infection due to their antimicrobial resistance, ability to 'escape' antibiotic therapy, and associated increased rates of mortality (Marturano and Lowery 2019; De Oliveira et al. 2020). *P. aeruginosa* has many mechanisms which confer resistance to antimicrobials due to its large repertoire of regulatory genes (>8% of the genome), they can be intrinsic, acquired, or adaptive mechanisms (Moradali et al. 2017; De Oliveira et al. 2020).

1.2.2.1 AmpC chromosomal β-lactamase

P. aeruginosa strains possess an inducible ampC gene, which is responsible for the production of AmpC, a chromosomally encoded, inducible β-lactamase able to break the amine bond of the β-lactam ring (Pang et al. 2019). Therefore *P. aeruginosa* intrinsically confers low level resistance to aminopenicillins and most early generation cephalosporins (Yordanov and Strateva 2009). Interestingly, the presence of these antibiotics (particularly imipenem) also strongly induces the overproduction of AmpC (100-1000 times) and thus indirectly bring on their own hydrolysis with subsequent exposures to the antibiotics resulting in mutations conferring a broader spectrum of resistance to other clinically relevant antibiotics such as aminoglycosides and fluoroquinolones (Oliver et al. 2015; Berrazeg et al. 2015; Moradali et al. 2017; Pachori et al. 2019).

1.2.2.2 Efflux pumps

Multi-drug efflux pumps play a significant role in the antimicrobial resistance of *P. aeruginosa*. The large genome of *P. aeruginosa* encodes at least 12 energy dependent efflux pumps belonging to the resistance-nodulation-division (RND) family of secondary active transporters (Lister et al. 2009) The RND pumps typically exist as a tripartite system consisting of a periplasmic membrane fusion protein (MFP) (MexA/C/E/X), an outer membrane factor (OMF) (OprM/J/N), and a cytoplasmic membrane (RND) transporter (MexB/D/F/Y), forming a channel spanning the entire membrane (Lister et al. 2009; Housseini B Issa et al. 2018). Four of the RND transporters have been well characterised: MexAB-OprM, MexXY-OprM, MexCD-OprJ, and MexEF-OprN. The former two with high prevalence in clinical isolates. (Aeschlimann 2003).

MexAB -OprM is produced at basal levels in all *P. aeruginosa* strains and has the broadest spectrum of activity intrinsically offering low level resistance to penicillin's, carbapenems, fluroquinolones and aminoglycosides in all strains (Aeschlimann 2003; Moradali et al. 2017). Acquired resistance via efflux pumps can occur via overexpression of the MexAB -OprM operon. In *nalB,* mutants as a result of mutations in the MexR repressor protein, increased resistance for several antibiotics including most of the β-lactams, quinolones, tetracyclines, chloramphenicol and trimethoprim can be seen (Yordanov and Strateva 2009). MexXY-OprM, may interact with many of the same substrates as MexAB -OprM and can actively remove many clinically useful anti-pseudomonal antibiotics including fluroquinolones. This system is expressed in low levels basally, and confers natural resistance to aminoglycosides, tetracycline, tigecycline, and erythromycin

(Morita et al. 2012). The pump may also be induced in response to antagonism from aminoglycosides (Hancock and Speert 2000; Moradali et al. 2017).

MexCD–OprJ and MexEF–OprN pumps are relevant to acquired resistance (Llanes et al. 2004), detected and overproduced only in *nfxB* and *nfxC* mutants. MexCD-OprJ can expel cefepime, fluroquinolones, macrolides, and tetracycline whereas MexEF-OprN can expel fluroquinolones, imipenem, trimethoprim, and some β-lactamase inhibitors. These two efflux systems also appear to be responsible for adaptive resistance developed towards aminoglycosides, whereby the antibiotic activity decreases with subsequent exposures (Aeschlimann 2003).

1.2.2.3 Outer membrane permeability

The outer membrane (OM) is a unique asymmetrical bilayer of lipopolysaccharide (LPS) and phospholipids which exists as a robust permeability barrier to prevent entry of antibiotics and other toxic molecules into the intracellular space whilst at the same time allowing the selective influx of nutrients via membrane porins (Nikaido 2003; May and Grabowicz 2018). *P. aeruginosa* is intrinsically less susceptible to most antibiotics compared to Enterobacteriaceae with 10 to 100-fold lower permeability attributed to the lack of diffusion porins (Hancock and Speert 2000; Delcour 2009). The outer membrane porin channel, OprD, has a primary role of in the passive uptake of basic amino acids across the outer membrane; however, this also forms pores that are permeable to carbapenems. *P. aeruginosa* has a natural reduction in these proteins and confers a basal resistance to carbapenems (Livermore 2001; Moradali et al. 2017). Acquired, and increased carbapenem resistance can occur driven by the mutational inactivation and complete loss of OprD reducing membrane permeability (Gutiérrez et al. 2007).

1.2.2.4 Transfer of genetic resistance

P. aeruginosa, as with many bacteria can acquire resistance by horizontal gene transfer, whereby mobile genetic elements (plasmids) are transferred between bacterial cells via conjugation. This is a growing threat with the increasing prevalence of transferable resistance determinants, in particular those encoding extended spectrum β-lactamases (ESBLs) and metallo- β-lactamases (MβLs) which can inactivate both penicillin's, cephalosporins and carbapenems (Bennett 2008; Oliver et al. 2015; Moradali et al. 2017). Horizontal gene transfer is also responsible for some enzymatic resistance to aminoglycosides, in particular the ant (4')-IIb gene reported to be of plasmid pMG77 origin in some clinical strains and conferring amikacin resistance in CF patients (Sabtcheva et al. 2003; Poole 2005). However, enzymatic resistance is not the most prevalent mechanism for aminoglycoside resistance. It is reported that fewer than 10% or aminoglycoside

resistance is due to enzymatic mechanisms, and rather an impermeability of *P. aeruginosa* that offered reduced susceptibility in CF patients (MacLeod et al. 2000; Poole 2005). Worryingly, recent reports have shown evidence of plasmid mediated colistin resistance via transmission of *mcr-1* genes. Colistin is a member of the polymyxin class of antibiotics and is considered a last resort of resistant *P. aeruginosa* isolates (Liu et al. 2016; Caselli et al. 2018; Aghapour et al. 2019).

1.3 The biofilm mode of growth

P. aeruginosa can exist either in highly motile non-mucoid planktonic form or can grow in association with a surface and undergo changes to form a sessile community of bacterial within a biofilm. Biofilm-based infections are typically associated with a mucoid phenotype that is highly resistant to antibiotic chemotherapy and many other conventional antimicrobial agents, and has an extreme capacity for evading the host defences (Bjarnsholt 2013).

Biofilms are generally defined as an organised three-dimensional community of bacteria upon either a living or abiotic surface within dense aggregates. These aggregates are encased within a hydrated matrix of extracellular polymeric substance (EPS) made up of polysaccharides and protein that form the characteristic 'slimy' layer (Stewart and William Costerton 2001; López-Causapé et al. 2015). These biofilm structures are associated with increased resistance to antimicrobial chemotherapy, and immune system clearance with some biofilms of the same organism requiring 100 to 1000 times higher concentration of certain antimicrobials to be effective (Ceri et al. 1999). In nature, the biofilm mode of growth dominates in all habitats on the Earth's surface accounting for ~80% of bacterial and archaeal cells, with the exception of the bacterial growth in the oceans where the majority appear to exist as single cells with few (3-4%) in macroaggregates and microaggregates (Flemming and Wuertz 2019). The switch from the planktonic to the biofilm mode of growth is currently recognised as one of the major contributing factors responsible for chronic infections that are notoriously difficult to remove, with 80% of bacterial infections treated in the developed world are claimed to be caused by organisms within biofilms (López-Causapé et al. 2015; Chen et al. 2018).

Since the general definition of a biofilm was first made, the knowledge of the biofilm mode of growth has increased with subsequent research and the definition has been challenged. In the lungs of CF patients, rather than biofilm aggregates adhering to the surface of the lung epithelia. Bjarnsholt, Jensen et al. (2009) demonstrated that the bacterial aggregates were not surface

attached but suspended within the sputum and surrounded by inflammation caused by polymorphonuclear-leukocytes (PMLs). It was further identified that these non-attached aggregates display the same increased tolerance to PML, and antibiotics expected in surface attached biofilms (Alhede et al. 2011). These findings have been extended to many other chronic infections, not just in cystic fibrosis, and thus the definition of a biofilm has shifted to draw focus to the aggregation of sessile bacteria distinct from planktonic cells, rather than their aggregation on a surface.

In order to understand the recalcitrance of biofilms and discover strategies and identify targets that can be used in their control and dispersal, the lifecycle can be studied. The development of a biofilm in *P. aeruginosa* constitutes a sequence of several highly regulated events. Using various approaches, studies have shown significant changes in the regulation of motility, alginate production quorum sensing (QS), and c-di-GMP secondary messenger signalling during development; with an average detectable change in protein regulation of 35% between each stage (Sauer et al. 2002).

The notable stages of development in a motile bacterium are as follows: (i) transient attachment of planktonic cells to a surface or each other; (ii) irreversible surface attachment; (iii) growth and aggregation into microcolonies; (iv) mature structure formation; and (v) detachment and dispersal. These stages are illustrated in Figure 4.

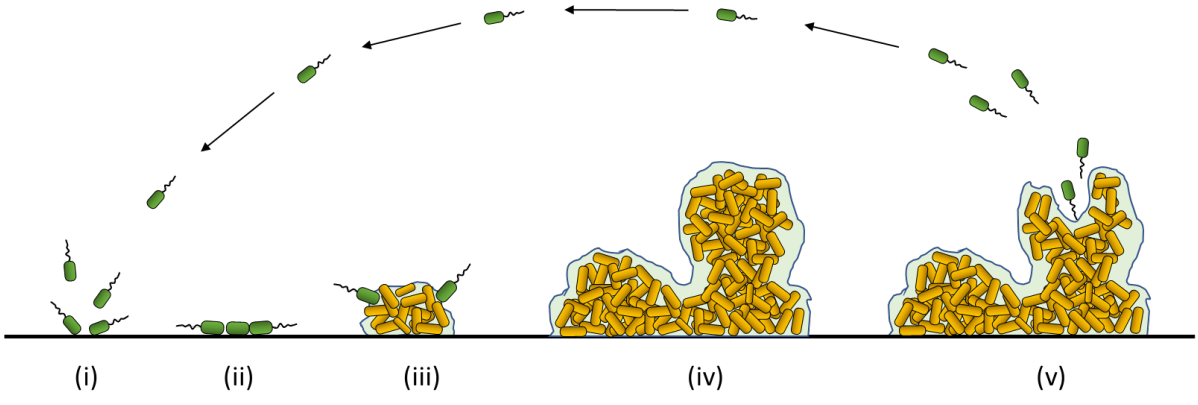

Figure 4. The notable stages of the biofilm lifecycle for a motile bacterium. The aggregation of sessile bacteria is not depicted here. (i) starting with the transient polar attachment of cells to the substratum, (ii) cells then become irreversibly attached and subsequently (iii) proliferate and recruit more cells to form aggregate microcolonies. (iv) with continued growth and production of extracellular matrix components, a mature biofilm structure is formed. (v) cells

are released from the biofilm and dispersed as motile cells, able to restart the cycle of biofilm formation in another location.

1.3.1 Transient attachment of planktonic cells to a surface or each other

Prior to surface colonisation, a surface must be conditioned to allow adhesion, this involves the adsorption of (macro)molecules to the interface. Often referred to as a 'conditioning film' (CF), these molecules can alter the adhesive capabilities and hydrophobicity of an interface and create an area of favourable for bacterial adherence (Lorite et al. 2011). Such molecules may differ depending on the surrounding environmental conditions but may include polysaccharides and other proteinaceous secretions from the host, or by living and dead bacteria (Lorite et al. 2011; Hohmann et al. 2017).

Post surface conditioning, planktonic cells may come into proximity to the surface via diffusive, convective and in some cases active flagellum-driven transport (Tolker-Nielsen 2014). Some weaker interactions such as polar, hydrogen bonding, hydrophilic interactions, and Van der Waals forces on the conditioned surface can also promote adhesion depending on proximity of the bacterial cell (Berne et al. 2015). There is evidence that *P. aeruginosa* biofilm initiation requires flagella and type IV pili, extracellular DNA (eDNA), and Psl polysaccharide (O'Toole and Kolter 1998; Whitchurch et al. 2002; Sauer et al. 2002; Barken et al. 2008; Yang et al. 2018). After initial attachment, the cells can either remain attached, exhibit independent movement across the surface with twitching motility or gliding mediated by type IV pili (O'Toole and Kolter 1998), or may detach from the surface and continue to live in a planktonic manner (Sauer et al. 2002).

1.3.2 Irreversible surface attachment

In order for the biofilm to become established and develop further; cells must irreversibly attach to maintain contact with the substratum. The upregulation of extracellular polymeric substance can result in more stable bonds forming ionic bridges between the cell surface and the biofilm interface. During this stage of development motility ceases as a result of cell-cell signalling and the activation of the Las QS system. The cell clusters formed during this stage remain attached until the final stages of biofilm development (Sauer et al. 2002).

A major component of the biofilm matrix is a galactose and mannose rich exopolysaccharide, Psl (Ma et al. 2007). Psl and is produced in planktonic form and plays a role in the initial attachment

of the bacterium to the surface, and promotion of cell-surface and cell-cell interactions to initiate the biofilm formation. Psl is also involved in maintaining the structure of the developing biofilm post-attachment (Ma et al. 2006; Ghafoor et al. 2011). Psl is anchored on the *P. aeruginosa* cell surface and functions to keep the bacteria attached to the substrata with interactions along the cell body rather than pole-mediated interactions as seen during reversible attachment. (Sauer et al. 2002; Caiazza et al. 2007; Ma et al. 2009).

In *P. aeruginosa*, it has been shown that a protein of unknown function, SadB, is required for the transition from reversible to irreversible attachment during the biofilm formation and that SadB mutants are defective in regulating the permanent attachment to the substrata needed for microcolony formation (Caiazza and O'Toole 2004). SadB is also found to co-regulate swarming motility which may aid in aggregation and its upregulation results in more robust biofilms (Caiazza et al. 2007).

1.3.3 Growth and aggregation into microcolonies

The aggregation of bacteria to form microcolonies may occur in multiple different ways. After becoming irreversibly attached, bacteria in which motility ceases undergo binary division, spreading outwards and upwards from the attachment site to form microcolonies in stalk-like structures (Klausen et al. 2003). When observed microscopically these non-motile microcolonies appear morphologically different with smooth edges compared to a more irregular appearance to the motile phenotype (O'Toole and Kolter 1998)

The formation of bacterial microcolonies at the surface of the substratum can also begin through active cell-cell contact and the redistribution of attached, but motile cells. Aided by type IV pilus mediated twitching, and flagella mediated swarming across the respective surface; the motile cells become entrapped within the EPS expressed by surrounding cells. (O'Toole and Kolter 1998). Zhao *et al.* demonstrated that *P. aeruginosa* deposits a trail of the Psl exopolysaccharide as it moves across a surface, this results in aggregations of small numbers of cells in enriched areas of communally produced Psl. Thus, providing a highly favourable environment for localised exponential growth and the formation of microcolonies (Zhao et al. 2013)

Alternatively, cells may be recruited to the biofilm from the surrounding bulk fluid in a flagellum mediated 'swimming' to favourable chemo-attractants, e.g. high concentration of signalling molecules produced by microcolonies indicating a suitable microenvironment for growth (Tolker-Nielsen et al. 2000; Karimi et al. 2015). The flow rate of the bulk fluid, nature of the surface,

conditioning of the substrata, and the way initial attachment is initiated by *P. aeruginosa* will determine the way in which the cells aggregate in microcolony formation (Chang 2018).

1.3.4 Mature structure formation

Maturation of the *P. aeruginosa biofilm* results in the generation of complex architecture of mushroom-shaped microcolonies of stalk and cap subpopulations; containing pores and fluid filled channels partly regulated and maintained by rhamnolipid biosurfactants; and redistributed bacteria away from the substrata within a structured matrix of extracellular polymeric substance (EPS) (Stoodley et al. 2002b; Rybtke et al. 2015; Moradali et al. 2017). Mature biofilms have notable physiological and metabolic heterogeneity, distinct from free-swimming planktonic cells. This is primarily the result of differing nutrient, oxygen, toxic waste product, and signalling compounds concentrations throughout the biofilm generation multiple microenvironments (Stewart and Franklin 2008).

Sauer *et al.* demonstrated radically different protein profiles between planktonic cells and those within a mature biofilm when grown in chemostats (Sauer et al. 2002) In the mature biofilm, over 800 proteins from the detectable proteome were shown to have a sixfold or greater difference in expression. A large proportion of these were initially undetectable in planktonic bacteria. Difference is regulation include those responsible for metabolism, phospholipid and LPS-biosynthesis, membrane transport and secretion, as well as adaptation and protective mechanisms (Stoodley et al. 2002b).

There are many constituents of mature biofilm matrix, these include three different exopolysaccharides: Psl, Pel, and alginate, along with proteinaceous and DNA components (Ryder et al. 2007). As previously mentioned, the galactose and mannose rich exopolysaccharide, Psl is a major component of the mature biofilm structure and has been found to wrap itself around *P. aeruginosa* cells, increasing effective cross linking and elasticity of the matrix and strengthening the matrix scaffold. When Psl is absent, the matrix becomes more viscous and facilitates the biofilm dispersal and spread (Chew et al. 2014).

Pel is a glucose rich polysaccharide, not typically involved with surface attachment but plays a role in the formation of pellicles (the formation of biofilm at an air-liquid interface) and can be upregulated in the absence of Psl as a redundant exopolysaccharide for the matrix scaffold (Colvin et al. 2012). Pel has also been shown to have an increased role in interspecies S. aureus- *P.*

aeruginosa biofilms and the association of the two bacteria. Conversely to Psl role in the matrix, Pel has been found to reduce the crosslinking in the matrix leading to faster erosion of the biofilm (Flemming and Wingender 2010; Chew et al. 2014).

Alginate is an acylated polymer of non-repetitive monomers consisting of 1-4 linked β-D-mannuronate and α-L-guluronate and is responsible for the mechanical stability of a mature biofilm (Flemming and Wingender 2010). It is somewhat involved in the establishment of biofilm formation, but alone it is not sufficient for microcolony formation, Pel and Psl are also required to be present to have a significant impact on biofilm formation and maturation (Hay et al. 2009; Rybtke et al. 2015). With genetic adaptations within *P. aeruginosa* to an environment of infection, particularly mutations in the gene encoding the σ-factor AlgU negative regulator (MucA), alginate can be overproduced leading to the characteristic mucoid phenotype most commonly associated with chronic infection (Flemming and Wingender 2010; Mann and Wozniak 2012).

EPS was initially referred to as 'extracellular polysaccharides,' but have since been renamed after it was apparent the biofilm matrix also contains proteinaceous and DNA components (Flemming and Wingender 2010)

Extracellular DNA (eDNA), when available, forms an integral part of the matrix, acting as a cell-cell interconnecting component. There is evidence to suggest that eDNA is self-derived from a lysed sub-population of cells (Allesen-Holm et al. 2006) or released into the matrix by DNA containing membrane vesicles (Renelli et al. 2004; Okshevsky and Meyer 2015). eDNA forms grid like structure in *P. aeruginosa* biofilms and can combine with Psl to form a web of eDNA–Psl fibres, resembling a biofilm skeleton to give bacteria structural support and defence against agents targeted on one matrix component. The combined eDNA–Psl offered increased resistance to DNase treatments (Flemming and Wingender 2010; Wang et al. 2015). Psl can interact with DNA from multiple sources, suggesting that *P. aeruginosa* has the ability to use DNA of other organisms which might increase the survival in multispecies biofilms (Wang et al. 2015).

Other protein components of the mature matrix include; type IV pili, which can act as crosslinkers between cells and eDNA; surface adhesin CdrA, involved in the auto-aggregation of *P. aeruginosa*; the lectin LecB, that binds to specific carbohydrate components within the matrix offering a robust biofilm structure; and Fap, a functional amylated protein that when overexpressed form biofilms with increased thickness (Rybtke et al. 2015).

1.3.5 Detachment and dispersal

The growth of a biofilm is limited by certain factors, including the availability of nutrients and oxygen, and the accumulation of toxic waste products. Biofilm detachment and dispersal is also closely related with the biofilm microcolonies reaching critical size, in *P. aeruginosa* biofilms this is a microcolony diameter of 80 μm or greater as the threshold before initiation of detachment (Purevdorj-Gage et al. 2005). Detachment is a generalised term for the release of cells from the biofilm or substratum. It can be caused by external agitation, such as increased fluid shear (Stoodley et al. 2002a), or internal biofilm processes, such as endogenous enzymatic degradation (Hall-Stoodley et al. 2004).

It has been shown that there is physiological heterogeneity with the biofilm dispersal structures with an outer wall of stationary bacteria, and a 'liquified' centre of 'free-swimming' motile (planktonic) cells (Webb et al. 2003; Hall-Stoodley et al. 2004; Stewart and Franklin 2008). Sauer et al. (2002) demonstrated that small cell clusters undergo alterations in their structure due to the dispersal of motile bacteria from within the centre of the biofilm. The motile bacteria were observed to actively 'swim' out of the microcolony and into the bulk liquid leaving behind hollow, shell-like structures with walls of non-motile bacteria (Sauer et al. 2002). These fluid-filled channels may offer better access of nutrients to the cells that remain in the biofilm. The ability of bacteria to swim freely within the centre of the biofilm structure indicated the absence of dense polymer or other gel-like material within these voids (Sauer et al. 2002). It was further demonstrated that organised, prophage mediated cell death and lysis occurs within the centres of the biofilm microcolonies, and the importance of cell lysis in creating hollow structures was identified for the dispersal of subpopulations of the surviving cells (Webb et al. 2003; Kirov et al. 2007).

Alginate lyase has been observed to have a role in the detachment and sloughing of cells from the biofilm. Boyd and Chakrabarty reported that increased expression of alginate lyase in mucoid strains of *P. aeruginosa* led to alginate degradation to those of a lower molecular weight and decreased viscosity. These lower molecular weight alginates corresponded with and increased number of detached cells and thus the authors suggested the role of alginate lyase in the release of, and the dispersal of cells from the biofilm (Boyd and Chakrabarty 1994).

The newly released progeny cells from the biofilm are now able to revert back to the planktonic mode of growth, re-establishing motility, and completing the biofilm growth cycle, colonising new

environmental niches with better access to nutrients compared to those available within the former biofilm structure (Sauer et al. 2002; Hall-Stoodley et al. 2004).

1.4 Recalcitrance of biofilm infection in the CF lung

1.4.1 Restricted penetration

For antimicrobials to be effective in the treatment of biofilm infections, they must be able to penetrate the extracellular biofilm matrix in order to reach the bacteria embedded within (Ciofu and Tolker-Nielsen 2019). Numerous studies have suggested that the matrix alone is not an inhibitor of the diffusion of antimicrobials through the biofilm. It is the interaction of certain antimicrobials with matrix components in the biofilm or cell surfaces that retards the penetration (Ciofu and Tolker-Nielsen 2019). Past studies have shown that aminoglycosides, which are positively charged, bind to sources of alginate with high affinity and are halted in the periphery of the biofilm. On the contrary the neutral fluroquinolone, ciprofloxacin, readily penetrates the biofilm (Gordon et al. 1988; Walters et al. 2003; Tseng et al. 2013). The biofilm matrix may become saturated with bound antimicrobials, progressively allowing penetration further into the biofilm past the periphery; so, tolerance via penetration hindrance may be temporary. It may however, also allow time for bacterial adaptation to counteract the antimicrobial agents (Ciofu and Tolker-Nielsen 2019). Slow penetration is not single-handedly responsible for tolerance, β-lactam antibiotics are often hydrolysed by AmpC β-lactamase that accumulates within in the biofilm matrix produced by *P. aeruginosa* (Hengzhuang et al. 2013). This and other methods of tolerance discussed below are summarised in Figure 5.

1.4.2 Extracellular DNA

eDNA is an integral component of the biofilm matrix; in initial attachment, structure, and antibiotic tolerance and resistance (Hall and Mah 2017). While *in vitro* experiments show self-derived eDNA within the biofilm matrix. In the instance of human infection, it has been shown that eDNA is derived almost entirely from polymorphonuclear leukocytes that are heavily recruited to the area of infection (Wilton et al. 2016) This may increase localised resistance to antimicrobial chemotherapy in chronic infections.

Mulcahy et al. demonstrated that eDNA, was able to induce antibiotic resistance. eDNA as an anionic macromolecule, was able to bind and sequester cations, including magnesium, leading to a decrease of Mg^{2+} in the surrounding environment. This magnesium limitation triggers activation

of two component signalling (TCS) systems in *P. aeruginosa* leading to induction of genes involved in modification of LPS, resulting in physical alterations in the bacterial outer membrane conferring marked increase in resistance to polymyxin B, colistin and aminoglycosides (Mulcahy et al. 2008).

eDNA has also been shown to acidify the biofilm matrix and induce resistance to aminoglycosides in a similar fashion to that mentioned above (Wilton et al. 2016). The authors showed that the accumulation of extracellular DNA was responsible for the acidification of *P. aeruginosa* biofilm cultures resulting in the induction of TCS signalling and subsequently LPS (lipid A) modification and spermidine production, reducing outer membrane permeability and entry of aminoglycosides. eDNA within the microcolonies may also be of bacterial origin and taken up by other bacterial cells, hence sub-populations of bacteria may acquire genetic elements conferring antimicrobial resistance.

1.4.3 Nutrient and oxygen limitation

Biofilm structures display multiple subpopulations characterised by a distribution of metabolic activity and physiological heterogeneity (Figure 5). In the periphery, subpopulations are highly active physiologically, whereas subpopulation from the inner parts of the biofilm have reduced or no physiological activity (Stewart et al. 2016).

The heterogeneity is established through bacterial metabolism and diffusion of solutes into the biofilm (Stewart and Franklin 2008). Oxygen is rapidly taken up and rapidly respired by metabolically active cells in the periphery of the biofilm. Most of the available oxygen is thus taken up from the surrounding bulk fluid leaving little for the bacteria in the inner portions of the biofilm. The same also applies to available nutrients (Stewart et al. 2016; Ciofu and Tolker-Nielsen 2019).

Nutrient and oxygen gradients also occur due to diffusion limitation that readily arises in biofilm structures (Stewart 2003). Fluid flow is reduced in the surrounding environment due to the biofilm structure and its substrata. Within the biofilm matrix, high cell density and EPS retard water flow and transport of nutrients and oxygen into the inner subpopulations of the biofilm (Stewart 2003). Oxygen limitation can result in the reduced metabolic activity of cells in the inner biofilm, altering the effectiveness of antibiotic classes that target active cellular processes (Ciofu and Tolker-Nielsen 2019). This is similar to the tolerance of persister cells discussed below.

The low metabolic activity induces starvation signalling and the stringent response in *P. aeruginosa* regulating the expression of genes *relA* and *spoT* increasing antioxidant capacity. Mutant strains lacking these genes had increased susceptibility to fluroquinolones, gentamycin, meropenem and colistin (Nguyen et al. 2011).

1.4.4 Bacterial persister cells

The chronicity and recalcitrance of biofilm infections is often attributed to the presence of a bacterial subpopulation referred to as 'persisters' that are particularly invulnerable to antimicrobial killing despite increasing concentrations and limit the effectiveness of treatments to eradicate chronic infections (Sultana et al. 2016; Oppezzo and Forte Giacobone 2018).

Persisters are not classed as resistant to antimicrobials, but rather tolerant. In that contrary to previously discussed mechanisms of resistance, the dormancy of the cells prevents target corruption by the antimicrobial agent. The dormant cells will have little or no cellular activity e.g. cell wall synthesis, translation, or topoisomerase activity. Therefore, the antibiotic may bind to its target (e.g. ciprofloxacin to DNA gyrase and topoisomerase) but will not be able to corrupt its function due to inactivity (Lewis 2007).

The persister cells represent only a small subpopulation of the entire biomass of the biofilm, ≤1% (Spoering and Lewis 2001). These cells are not resistant mutants, but merely non-proliferating cells with reduced metabolic activity and sensitivity to antimicrobials and are characterised as phenotypic variants. (Balaban et al. 2004). Evidence to suggest a phenotypic switch rather than mutant strains is displayed when the persister cells are subsequently cultured and do not produce distinct phenotypes from that of the wild type. The MIC of the cultured cells also resembles that of the planktonic wild type, thus have not acquired any additional antimicrobial resistance mechanisms (Spoering and Lewis 2001; Balaban et al. 2004; Orman et al. 2016)

Persister formation, from what is understood, does not follow the typical single regulatory pathway seen in other complex cellular mechanisms, they appear to from through a number of independent parallel mechanisms and hence no single compound i.e. an antibiotic will disable persister formation (Lewis 2010). Persister formation may be linked to numerous type 2 toxin-antitoxin (TA) systems in which dormancy may be selected as a favourable stress response to antimicrobial antagonism (Makarova et al. 2009; Andersen et al. 2017). When the antimicrobial threat is removed, persister cells may revert back to the normal phenotype and can resume growth, 're-seeding' a surface and ensuring the survival of the bacterial population (Defraine et al. 2018).

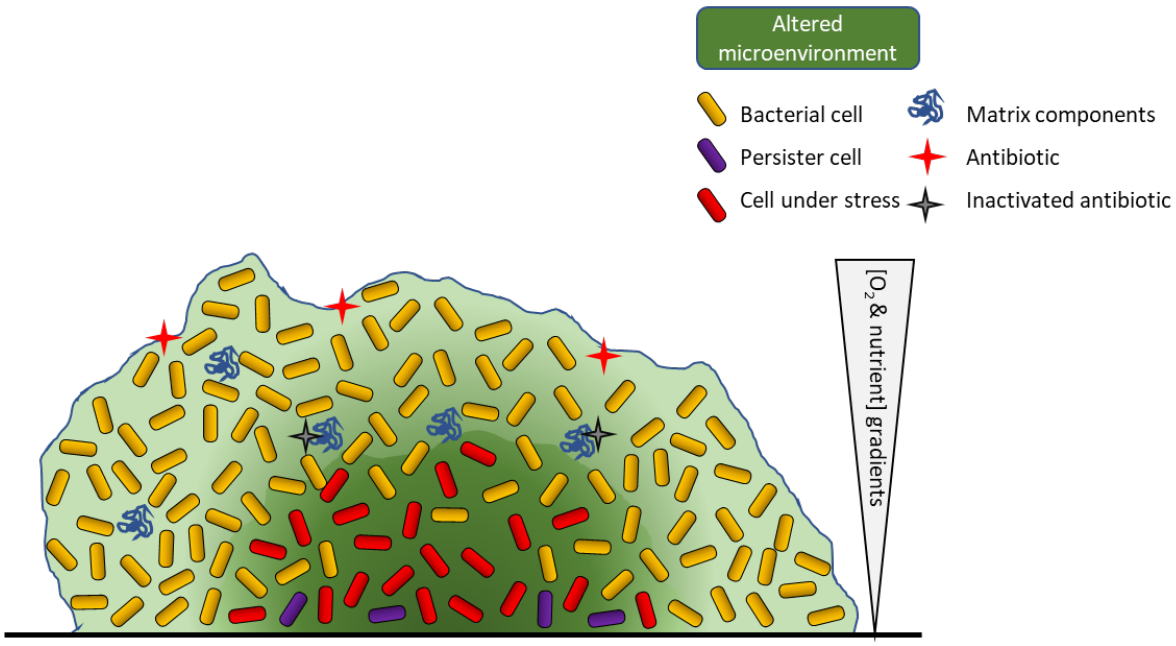

Figure 5. Graphical summary of biofilm recalcitrance. Antimicrobials may be halted from entering the inner biofilm via the physical structure of the extracellular matrix, they may also be inactivated by hydrolysing enzymes or other matrix components (AmpC β-lactamase, eDNA). Restricted distribution of nutrients and oxygen leads to metabolic gradients and altered micro-environments with a build-up of waste products resulting in cells with lower metabolic activity and cells under stress that are more tolerant to antimicrobial activity. Persister cells represent a small, metabolically inactive population of bacterial cells that cannot be eradicated by antimicrobial therapy.

1.5 Regulation of biofilm formation

Biofilm formation is a complex process that requires co-ordinated intercellular and intracellular signalling, to make the transition to the sessile lifestyle within a larger community of bacteria. The two major systems that control biofilm formation and maintenance are QS and c-di-GMP systems (Rinaldo et al. 2018).

1.5.1 Quorum sensing

Many bacterial species are highly coordinated and can control their gene regulation through cell-to-cell signalling in high density populations. This is achieved by the production of small extracellular signalling molecules and specific receptors in a process named quorum-sensing (QS)

(Ciofu et al. 2015). In *P. aeruginosa* QS controls an arsenal of virulence mechanisms including the formation of biofilm and the production of extracellular factors (Lin et al. 2018). *P. aeruginosa*, harbours four QS systems; *las*, *rhl*, PQS, and IQS (Moradali et al. 2017).

The best described systems are *las* and *rhl* involving N-acyl-L-homoserine lactones (AHLs) as the biochemical autoinducer (AI), a small signalling molecule that can readily pass the cell membrane, and a cognate transcriptional activator protein (R-protein). These two systems control up to 10% of virulence expression in *P. aeruginosa*, and share homology with the lux-type QS system as first described in *Vibrio fisheri* and other Gram-negative species (Fuqua et al. 1996; Lazdunski et al. 2004; Williams and Cámara 2009; Strateva and Mitov 2011; Moradali et al. 2017)

The autoinducer synthase LasI is responsible for the synthesis of *N*-3-oxododecanoyl homoserine lactone (3-O-C12-HSL, or PAI-1) in the *las* system. This binds to and activates the transcriptional activator protein LasR. Similarity in the *rhl* system, *N*-butyryl-L-homoserine lactone (C4-HSL, or PAI-2) is synthesised by RhlI and activates the transcriptional activator protein RhlR (Pesci et al. 1999; Lee and Zhang 2014). The AI and R-protein complexes (AI-LasR/AI-RhlR) bind to conserved *las-rhl* boxes in promoter regions of the target genes, activating their expression (Whiteley and Greenberg 2001; Venturi 2006; Williams and Cámara 2009). AI-LasR induces expression of virulence genes *lasB* (elastase)*, lasA* (alkaline protease)*,* and *toxA* (exotoxin A)*,* and *lasI,* creating a positive feedback loop for AI synthesis. The AI-RhlR complex activates transcription of *rhlI* (creating positive feedback) and *rhlAB* genes encoding for a rhamnosyltransferase required for rhamnolipid production (Venturi 2006; Strateva and Mitov 2011)

The above-mentioned systems do not act independently and are interconnected an in hierarchical manner with las affecting activation of the rhl system, with the third *P. aeruginosa* QS system 2-heptyl-3-hydroxy-4-quinolone, also referred to as *Pseudomonas* quinolone signal (PQS) placed between the two, with PQS production induced by LasR, which in turn activates RhlR (Pesci et al. 1999; Gallagher et al. 2002; Ciofu et al. 2015). PQS synthesis depends on pqsABCDE and pqsH, and regulates gene expression through interaction with PqsR, controlling several factors including elastase, rhamnolipid, pyocyanin, and having an influence on the development of structured biofilms (Ciofu et al. 2015)

The final QS system of *P. aeruginosa* is the integrated quorum sensing system (IQS), this is a relatively recent discovery, and its mechanisms and receptors are not fully understood. It is suggested that the 2-2-hydroxylphenyl-thiazole-4-carbaldehyde IQS molecule is produced as a by-product of the pyochelin siderophore synthesis, controlled by AHL-QS. The IQS molecule in turn regulates the PQS network and other virulence factors (Lee et al. 2013; Trottmann et al. 2019). It

has been suggested that IQS acts in a phosphate stress response to maintain regulation of virulence mechanisms, and can interfere with host signalling pathways inducing apoptosis during infection (Lee et al. 2013; Wang et al. 2019).

As mentioned above, QS regulates the expression and synthesis of multiple virulence factors. QS is also found to play a vital role in the formation of structured biofilms. Davies et al. (1998), demonstrated that *lasI* mutants formed flat, undifferentiated biofilms compared to the wild-type and were more vulnerable to the biocide sodium dodecyl sulfate (SDS). Further studies have corroborated these findings with double knockout mutants of both AHL systems (Shih and Huang 2002). As mentioned previously, rhamnolipid production is mediated by QS and is involved in the formation of biofilm structure, by inducing cellular detachment from the internal mushroom cap structures, maintaining fluid filled channels to ensure nutrient flow, oxygen, and removal of waste (Boles et al. 2005; Bjarnsholt et al. 2010; Chrzanowski et al. 2012). Additionally, PQS mutants also demonstrated unstructured, flat, biofilms due to a reduction of the critical component, eDNA. Evidence has suggested PQS can cause the lysis of sub-populations of *P. aeruginosa,* either directly or through the control of pyocyanin production which in turn lyses cells releasing eDNA (Ciofu et al. 2015; Moradali et al. 2017).

1.5.2 Regulation by c-di-GMP

Bis-(3´-5´)-cyclic dimeric guanosine monophosphate (c-di-GMP) is an intracellular secondary messenger that regulates many bacterial behaviours such as motility and virulence though multiple complex signalling pathways. Notably, c-di-GMP is key to the phenotypic switch from a planktonic, free-swimming lifestyle to the sessile biofilm phenotype and vice versa with dispersal (Hengge 2009a; Valentini and Filloux 2016).

The c-di-GMP molecule was first described in 1987 as an allosteric factor to control the activation of cellulose biosynthesis in *Gluconacetobacter xylinus* and has since been implicated in many other bacterial functions across species (Romling et al. 2013) . The effects of c-di-GMP are dependent on the intracellular concentration. This is a tightly regulated dynamic equilibrium controlled by the synthesis and degradation by diguanylate cyclases (DGCs) and phosphodiesterases (PDEs). High intracellular concentrations are favourable for biofilm formation with upregulation of adhesins, exopolysaccharides and inhibition of motility. Whereas low concentrations have the opposite effect and favour the planktonic lifestyle with increased production of acute virulence factors (Hengge 2009a; Wolska et al. 2016; Jenal et al. 2017).

The c-di-GMP is synthesised from two GTP molecules by regulatory proteins DGCs containing catalytic GGDEF domains. Likewise, the degradation of c-di-GMP is by metal dependent PDE proteins carrying either the EAL or HD-GYP catalytic domains (Ha and O'Toole 2015). The degradation of c-di-GMP is a twostep process, it is first split into 5'-phosphoguanylyl-(3'-5')-guanosine (pGpG) by either EAL or HD-GYP catalytic domains; the pGpG is subsequently split into two separate GMP molecules by HD-GYP itself or other non-specific cellular PDEs (Hengge 2009a)

With genomic analysis of *P. aeruginosa*, 41 regulatory proteins with the necessary domains (GGDEF/EAL/HD-GYP) are encoded. This includes 17 with a GGDEF domain, 5 with EAL, 16 containing both GGDEF and EAL, and 3 HD-GYP (Kulasakara et al. 2006; Valentini and Filloux 2016). Of those that contain both GGDEF and EAL, only one of the domains is catalytically active and displays only DGC or PDE activity, with the inactive domain serving a regulatory function (Valentini and Filloux 2016).

The functional output and phenotypic changes due to c-di-GMP signalling comes from the activity of various signal effectors and their associated targets (Valentini and Filloux 2019). This classic example is that of the PilZ domain, suggested by Amikam and Galperin (2006) as the first c-di-GMP binding protein. The authors used sequence analysis to identify a PilZ domain in the Alg44 proteins required for alginate synthesis in *P. aeruginosa*. The location of the domain near the c-

terminus of GGDEF-EAL and HD-GYP lead to the suggestion of c-di-GMP involvement (Ryjenkov et al. 2006). Since this initial finding, multiple other effectors have been found in *P. aeruginosa* that also bind to c-di-GMP e.g., FleQ, a transcriptional regulator for the production of flagellar machinery. Binding of c-di-GMP to FleQ induces a conformational change and thus cannot bind upstream of the *flhA* to activate flagella gene expression, hence swimming motility is repressed (Baraquet and Harwood 2013; Jenal et al. 2017). Interestingly, it was found that FleQ is also repressor for *pel* transcription, and thus when c-di-GMP levels are high, *pel* expression can occur (Hickman and Harwood 2008). FleQ can therefore both repress motility and induce biosynthesis of structural EPS components of the *P. aeruginosa* biofilm matrix.

These already mentioned are but a few of the examples of effectors controlled by c-di-GMP in the formation of biofilm. Briefly, other key c-di-GMP include WspR, contributing to EPS production, and biofilm formation and maturation (Ha and O'Toole 2015); and FimX, regulating twitching motility, biofilm formation, and adherence (Valentini and Filloux 2019).

The intracellular c-di-GMP concentrations are dependent on DGC and PDE activity as previously discussed. Most of the GGDEF, EAL, and HD-GYP domains are linked to sensory input domains, sensory input to these domains can include oxygen and redox conditions, light, nitric oxide, nutrients, cell membrane stress, surface contact, and antibiotics. Thus c-di-GMP signalling can be controlled by a multitude of external environmental stimuli (Hengge 2009a; Wolska et al. 2016; Jenal et al. 2017).

1.6 The significance of biofilms in CF patient care

Biofilms are recognised as an area of serious clinical and public health concern with huge economic impact, it is estimated 80% of bacterial infections are caused by organisms existing in the biofilm phenotype (Chen et al., 2018). Many challenges arise when dealing with biofilm infections. Due to their recalcitrance and complex characteristics as mentioned above, an effective single approach biofilm therapy does not exist, resulting in the need for multi-targeted and combination therapies considering the diversity of infection and the needs of the patient (Koo et al., 2017). In this case, with reference to CF patients and the lung environment colonised with chronic *P. aeruginosa*.

As of yet, there is no direct phenotypic diagnostic available for biofilm infections in the lungs as part of routine clinical care. A method of identifying such infection via imaging or predictive

biomarker from easily attainable airway samples would enable a better planned and more personalised treatment regime for individual patients to reduce the burden of CF lung disease on patient health and wellbeing, indicating the suitability of these patients for certain treatments e.g., early antibiotic intervention or dispersal treatments.

1.7 The role of nitric oxide in the CF lung

Nitric oxide (NO) is small diatomic free radical that has an extremely short half-life (<1s) (Bryan and Grisham 2007). Nitric oxide gained little attention when thought just to be a potent environmental pollutant, however in 1987 it was identified as endothelial-derived relaxing factor and played a role in the pathogenesis of multiple vascular diseases (Katusic et al. 2003; Privett et al. 2010). It is found to be produced endogenously from L-arginine by a family of enzymes aptly named nitric oxide synthases (NOSs) which exist in 3 isoforms and play important roles in vascular endothelial cells, neurone function and host immune defence mechanisms (Bredt 1999; Bryan and Grisham 2007).

Typically, inflammatory lung diseases like asthma and bronchiectasis show an increase in exhaled NO due to stimulation of NOSs in multiple diverse ways. The isoform NOS2, for example, is significantly upregulated in allergic asthma and is expressed by macrophages, neutrophils and bronchial epithelial cells induced by pro-inflammatory cytokines, and can produce large quantities of NO, 100-fold higher than isoforms NOS1/NSO3 (Kharitonov and Barnes 2000; Winter-de Groot and Ent 2005; Ghosh and Erzurum 2011).

In cystic fibrosis patients, however, exhaled NO values remain normal to low, the reasons for which remain unknown (Grasemann et al. 1997; Winter-de Groot and Ent 2005). There remains to be conflicting reports that a lower exhaled NO value correlates positively with bronchial obstruction and a decline in lung function (Grasemann et al. 1997; Texereau et al. 2004; Hubert et al. 2009). Whereas others report no such correlation between exhaled NO (both alveolar and bronchial) and the FEV1 of patients (Hofer et al. 2009; Michl et al. 2013). This conflicting evidence would suggest that exhaled NO is not a good predictor for lung function in cystic fibrosis patients. If NO concentrations of NO are lower in the CF lung and not just undetectable in exhaled air, it could potentially have detrimental effects on lung function with limited bronchodilation effects, increased susceptibility to respiratory viruses, increased adherence of *P. aeruginosa,* and increased oxidative damage (Winter-de Groot and Ent 2005).

Multiple explanations for reduced exhaled NO have been suggested; the thick mucus present in the CF lung may prevent diffusion of NO into gaseous phase and undergoes rapid degradation to its NO_2^- and NO_3^- metabolites, thus it is not able to be exhaled to provide accurate values. This idea is supported by the higher concentrations of these metabolites seen in CF sputum (Morrissey et al. 2002). Other explanations include lack of L-arginine for NOS synthesis; reduced activity of NOS (particularly NOS2) in CF patients; or the consumption of NO within the sputum by *P. aeruginosa* denitrification (Gaston et al. 2002; Zheng et al. 2004; Grasemann et al. 2005).

1.7.1 *P. aeruginosa* denitrification

The cystic fibrosis lung has been demonstrated to have extreme hypoxic gradients within thick mucus zones of the airway. It was highlighted that *P. aeruginosa* was able to thrive and form biofilms under these strict anaerobic conditions, with motile bacterium actively penetrating deep into the mucus plaques (Worlitzsch et al. 2002; Yoon et al. 2002). Under environmental conditions of low oxygen where NO_2^- and NO_3^- are available, *P. aeruginosa* can switch from aerobic respiration to anaerobic denitrification utilising Nitrate (NO_3^-), nitrite (NO_2^-), and nitrous oxide (N_2O) as terminal electron receptors (Yoon et al. 2002). The denitrification pathway is the main source of endogenous NO production.

The denitrification pathway comprises four steps, where NO_3^- is sequentially reduced to NO_2^-, NO, N_2O, and N_2 aided by the enzymes nitrate reductase (NarGHI), nitrite reductase (NirS), nitric oxide reductase (NorCB), and nitrous oxide reductase (NosZ) respectively as shown in Figure 6. NarGHI and NorCB are located at the inner membrane, whereas NirS and NosZ are found in the periplasm (Schreiber et al. 2007; Arai 2011; Arat et al. 2015; Toyofuku and Yoon 2018).

The expression of the denitrification enzymes is under the control of the transcriptional regulators Anr and Dnr, and the two-component regulatory system NarXL (Schreiber et al. 2007). Low oxygen levels are detected by Anr attached to iron-sulfur (Fe-S) clusters that are able to detect iron, environmental oxidants, or nitric oxide (Miller and Auerbuch 2015). Anr, once activated can induce the transcription of *narXL,* and NarGHI. The nitrate sensing NarX activates its response regulator NarL which upregulates NarGHI, and cooperatively activates Dnr in conjunction with Anr. Dnr, responsive to NO, can upregulate all four reductase enzymes, and works with NarL to upregulate the transcription of *nirQ,* in turn modulating the activity of NirS ans NorCB (Arai 2003; Schreiber et al. 2007; Arat et al. 2015).

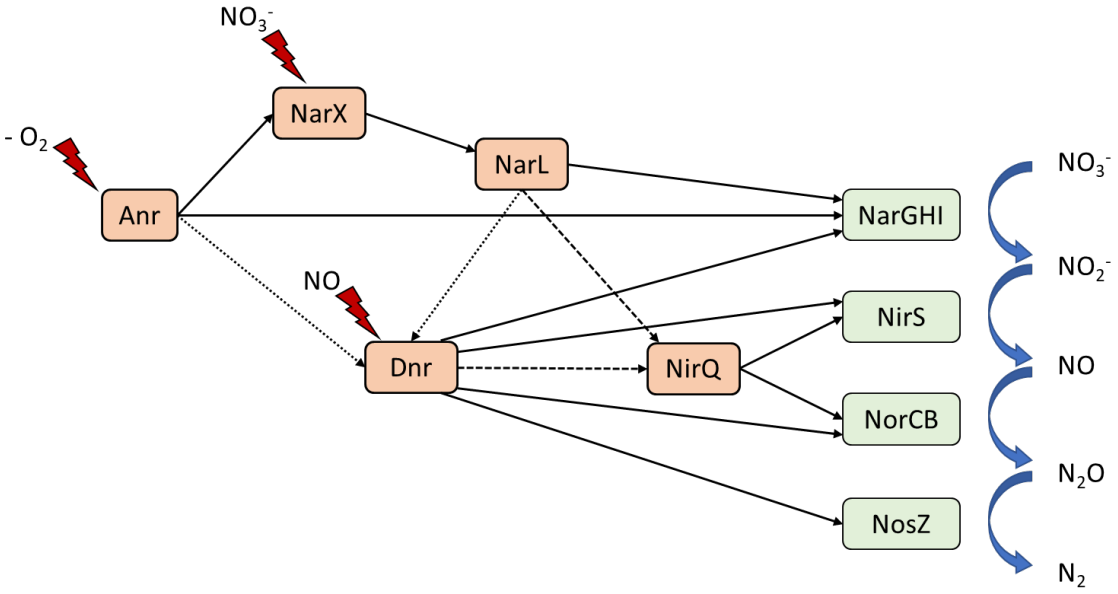

Figure 6. Denitrification pathway in *P. aeruginosa*. Activity of the four reductase enzmes: nitrate reductase (NarGHI); nitrite reductase (NirS); nitric oxide reductase (NorCB); and nitrous oxide reductase (NosZ) is controlled by the major regulator Anr. Anr senses low oxygen conditions in the environment and upregulates the nitrate sensing two component system NarXL, NarGHI reductase and Dnr. Dnr, in response to NO, modulates the expression of the regulator NirQ, subesqently controlling NirS and NorCB reduatses. Dnr can promote expression of all four reductases. Dashed lines represent co-operative activation of regulators.

Yoon et al. (2002) demonstrated that the *rhl* QS system is a key component of denitrification regulation. RhlR mutants we found to die from metabolic NO accumulation, with dysregulated Nar and Nir activity. They therefore suggested the elements of the anaerobic respiration pathway could provide targets for the killing of *P. aeruginosa* biofilms in CF.

Given the high concentrations of nitrogen metabolites found in the CF sputum, and the ability of *P. aeruginosa* to utilise the denitrification pathway and exploit these and their intermediates in anaerobic respiration, enforces the hypothesis that *P. aeruginosa* reduces the levels of exhaled NO in the CF lung via increased consumption, and that chronic *P. aeruginosa* isolates do so to reduce the toxic effects of NO accumulation.

1.7.2 Nitric oxide mediated dispersal of *P. aeruginosa* biofilms

The *P. aeruginosa* biofilm dispersal effect of low-dose NO was first described by Barraud et al. (2006). Investigating the role of endogenous NO in biofilm dispersal, reductase deficient mutants

(Δ*nirS*/Δ*norCB*) were shown to have significant differences in dispersal compared to the wild type. Δ*nirS* mutants (unable to produce NO) did not show dispersal after 6 days and formed thicker and more confluent biofilms. On the other hand, Δ*norCB* mutants (unable to reduce NO) showed an increased number of dispersed cells, with multiple hollow voids in biofilm structures. Thus, implicating the role of NO in biofilm dispersal.

Using an optimised concentration (500nM) of the NO donor sodium nitroprusside (SNP) at a sub-lethal concentration (in the nanomolar range) resulted in a dispersal response of preestablished biofilms, and a 10-fold reduction in the biofilm to planktonic ratio. Further to dispersal, the authors combined NO with antimicrobial treatment with tobramycin. Combination treatment saw an enhanced efficacy of the antimicrobials, with the removal of 80% of cells from the biofilm surface. The dispersal effect was linked to increases of cellular motility, with 25% increase of swimming, and 77% swarming motilities with SNP treatment at the same concentration. These findings suggested a novel therapeutic use for NO in the control of *P. aeruginosa* biofilms.

1.7.2.1 Mechanism of nitric oxide mediated biofilm dispersal

Following microarray analysis, it was reported that exposure to low levels of NO incurred several bacterial responses, mostly associated with regulation of c-di-GMP and the transition from a biofilm to planktonic phenotype (Barraud et al. 2009). Linking the existing literature in which changes in intracellular c-di-GMP concentrations, are regulated by the activities of DGC and PDE in response to external stimuli, BdlA (biofilm dispersal locus A) was identified as the first putative chemotaxis regulator of biofilm dispersal (Barraud et al. 2009). The BdlA protein is expressed constitutively in *P. aeruginosa*, with its expression elevated in dispersing cells. It possesses an TarH/MCP (methyl-accepting chemotaxis protein) domain, and two PAS (Per-Arnt-Sint) domains, ubiquitous regulatory domains involved with environmental signalling cues (Morgan et al. 2006; Barraud et al. 2009; Roy et al. 2012; Petrova and Sauer 2012).

Knockout mutant studies of *P. aeruginosa* strains lacking *bdlA* showed increased levels of c-di-GMP and an impaired dispersal response when treated with NO. However, BdlA itself lacks both GGDEF and EAL domains and thus no PDE activity, it was suggested it may instead present a greater regulatory role of other protein effectors (Morgan et al. 2006; Barraud et al. 2009).

Further proteins capable of reducing the c-di-GMP pool were later identified. These include: RbdA, with highly conserved GGDEF, EAL, and PAS domains; and DipA harbouring two EAL

domains for the PDE activity. Mutational knockout experiments for *rbdA and dipA* by Roy et al. (2012) highlighted the impaired dispersal response to NO as well as other dispersal agents e.g. glutamate, implicating their important roles in biofilm dispersal (An et al. 2010; Roy et al. 2012).

In 2013, Li et al. investigated two membrane bound proteins, MucR and NbdA (NO-induced biofilm dispersion locus A). These two proteins each harboured GGDEF, EAL and MHYT domains, the latter a transmembrane domain purported to sense oxygen, CO, or NO through copper binding motifs (Galperin et al. 2001; Li et al. 2013). Mutant *ΔmucR P. aeruginosa* strains were impaired in biofilm dispersal in response to NO and glutamate, whereas *ΔnbdA* only impaired dispersal with NO exposure. Both MucR and NbdA were shown to be active PDEs, with MucR also having DGC activity, therefore, NbdA is so far the only described PDE to be directly regulated by NO (Pestrak and Wozniak 2020).

In several bacterial species, proteins containing known NO sensors, H-NOX (heme-nitric oxide/oxygen) domains, have been shown to directly bind NO and regulate c-di-GMP levels and thus biofilm formation (Liu et al. 2012; Plate and Marletta 2012). However, *P. aeruginosa* does not encode for H-NOX proteins, yet still display a biofilm dispersal response to NO, suggesting the existence of a different NO sensing protein.

More recently, a novel NO-sensing protein (NosP), comparable to that of H-NOX has been characterised in *P. aeruginosa*, and found widely conversed (more so than H-NOX) across multiple bacterial species (Hossain and Boon 2017; Hossain et al. 2017). NosP is found on the same operon as the NosP associated histidine kinase (NahK) which has previously been implicated in biofilm regulation (Hossain and Boon 2017). With NO bound, NosP has a slow (NO) dissociation rate and is able to control the phosphorelay activity of NahK (Hossain and Boon 2017). *P. aeruginosa* histidine-containing phosphotransfer protein (HptB) is known to accept phosphate from NahK, however signalling downstream of this is has not be implicated in c-di-GMP regulation; rather modulation of flagella-related gene expression and histidine kinase associated PilZ (Hossain and Boon 2017). The exact mechanisms underlying NO/NosP biofilm dispersal in *P. aeruginosa* are yet to be elucidated.

1.7.3 Therapeutic use of nitric oxide for the treatment of biofilm infections in CF

Following the discovery of the NO biofilm dispersal effects; the potential of NO as a therapeutic for *P. aeruginosa* biofilms was identified. A small proof-of-concept clinical trial involving ex vivo CF sputum samples and a cohort of 12 patients in a randomised double-blind clinical trial was undertaken (Howlin et al. 2017). *Ex vivo* experiments with fluorescence in-situ hybridisation (FISH)

of sputum samples showed significant reduction in mean *P. aeruginosa* biofilm thickness when treated with SNP, and again in adjunctive therapy with antibiotics when compared to untreated controls. Twelve patients were randomised to receive either low dose NO inhalation or a placebo in conjunction with antibiotics. Analysis reported a significant reduction of *P. aeruginosa* biofilm aggregates (10 and 20 cells in size). Unfortunately, complete eradication was not observed and *P. aeruginosa* was detected in the sputum following cessation of NO treatment.

1.7.3.1 Cephalosporin-3'-diazeniumdiolates (C3Ds)

Various impracticalities exist with the use of inhaled NO (iNO) gas. NO gas is only available in large, heavy, pressurised cylinders that are required to be handled and stored appropriately with complete exclusion of oxygen to limit production of toxic nitrogen dioxide. Thus, patients undergoing iNO therapy is required to stay in a hospital or clinic for the duration. This is less than ideal for CF patients at risk of cross-infection. Inhaled NO is also extremely expensive and is not a viable option for routine patient care within the CF clinic or therapy at home (Yang et al. 2015; Yu et al. 2019). Based upon these problems, a more practical NO delivery method is required.

Soren et al, (2020) demonstrated the efficacy of a recently produced NO-donor prodrug, cephalosporin-3'-diazeniumdiolates (C3Ds). These prodrugs release NO locally following cleavage of the β-lactam ring by bacterial β-lactamases (Figure 7), thus, triggering biofilm dispersion at the site of chronic infection with maximised NO delivery. The prototype compound used in this study, DEA-C3D ('DiEthylAmin-Cephalosporin-3'- Diazeniumdiolate') synthesised by Kelso et al. has been shown to disperse PA01 laboratory isolate biofilms (Yepuri et al. 2013), whereas Soren et al investigated the dispersal effect on clinical *P. aeruginosa* isolates. It was reported that DEA-C3D alone was able to significantly reduce the biofilm biomass by 50.2% compared with the untreated control but had no direct antibacterial activity. The authors also demonstrated that when DEA-C3D was administered in conjunction with colistin, mean average biofilm biomass was reduced 97.8% compared to the untreated control. The mean biofilm thickness was also reduced with a colistin combination, and a decrease in number of large living cell clusters reported. Thus, it was concluded that DEA-C3D was an effective biofilm dispersal agent particularly when given in combination with colistin and would be favourable over antibiotic alone, albeit with differing responses dependent on clinical isolate (Soren et al. 2020).

The research group lead by Kelso, subsequently looked to synthesise a next generation 'all-in-one" C3D compound with direct antibiofilm effects and antibacterial killing of dispensed

planktonic cells (Rineh et al. 2020). They identified and tested a highly active C3D AMINOPIP2-ceftazidime (compound 12) which produced reduction in biofilm biomass suggesting NO release was responsible for the observed effect, supporting the 'all-in-one' hypothesis. However further experimentation is required to confirm these findings. As mentioned previously, these compounds also saw an isolate dependent response to dispersal.

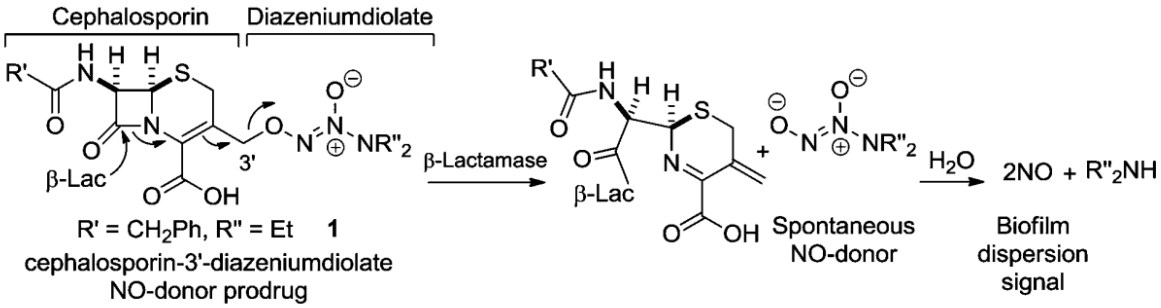

Figure 7. Proposed mechanism of first-generation cephalosporin-3'-diazeniumdiolates (C3Ds). β-lactamase cleavage of the β-lactam moiety releases nitric oxide locally at the site of infection to mediate *P. aeruginosa* biofilm dispersal (Yepuri et al. 2013).

1.8 Aims

1.8.1 Understanding the differing responses of clinical isolates to dispersal agents

Cystic fibrosis patients harbour not only a diverse microbiota in relation to that of a healthy individual that comprises largely of oropharyngeal taxa e.g., *Prevotella*, *Veillonella*, and *Streptococcus* species (Lipinksi et al. 2024), but also broad variation between *P. aeruginosa* isolates. This diversity needs to be considered when investigating the dispersal effects of NO donor chemistries. As has been shown previously, variation exists in the biofilm dispersal response between laboratory reference strain PA01 and clinical isolates, and between clinical isolates themselves (Howlin et al. 2017; Soren et al. 2020).

Varying dispersal responses to NO may be coupled to the numerous effectors produced by the bacterium in response to the environmental stimuli and underlying genomics. Understanding this variation and how it arises is important and may ultimately lead to predicting whether certain

patients may or may not be suitable for therapy with biofilm dispersal agents, based upon the *P. aeruginosa* isolates they are colonised by.

Hypothesis: Genotypic factors and transcriptomic regulation of bacterial cell effectors and virulence factors predispose clinical isolates to a distinct NO dispersal phenotype.

1.8.2 Understanding the role of *P. aeruginosa* biofilms in the CF lung

To apply the therapeutics mentioned above, the role that the biofilm plays within CF lung disease needs to be addressed. To better understand the interactions between biofilm and antimicrobials during therapy, fluorescent in-situ hybridisation (FISH) and proteomic techniques have been utilised at differing stages in the management of pulmonary exacerbations in CF patients (before, after, and following exacerbation). Changes in biofilm phenotype in conjunction with changes in protein expression protein may identify potential biomarkers for the biofilm infection and predictors of pulmonary exacerbation. A better understanding of the behaviour of *P aeruginosa* biofilms in the CF lung may guide personalised therapeutic approaches indicating the suitability for C3D biofilm dispersal.

This aims to analyse available FISH data to identify changes to the biofilm phenotype in response to antibiotic therapy, and correlate this with proteomic analysis already undertaken, with subsequent validation of a protein of interest via western blot analysis.

Hypothesis: The CF sputum proteome can act as predictor of biofilm phenotype within the cystic fibrosis lung and predict disease progression and overall lung fitness of the patient.

Chapter 2 Materials and Methods

2.1 Strains and growth conditions

Laboratory strain PAO1 was obtained from the University of Washington, USA. Twenty clinical isolates of *P. aeruginosa* were obtained from the University of Southampton's culture collection (NHS Research Ethics Committee 08/H0502/126). The 20 isolates have previously been profiled by Soren, 2018, details of these strains are listed in Table 1. For this study, samples from the culture collection were streaked onto selective cetrimide agar (Sigma Aldrich) to confirm isolation of *P. aeruginosa* and single colonies selected to prepare fresh bacterial stocks in 25% glycerol to be stored at -80˚C.

Overnight cultures were prepared by inoculating a single sterile loop of the frozen stock into 10 ml of Luria Bertani (LB) broth (Formedium) and incubated at 37˚C with shaking at 180 rpm. Unless otherwise stated, biofilms were cultivated in 1X M9 minimal media (pH 7; Formedium) containing 48 mM Na_2HPO_4, 22 mM KH_2PO_4, 9 mM NaCl, 19 mM NH_4Cl, and supplemented with 2 mM $MgSO_4$ (Sigma Aldrich), 100 µM CaCl2 (Sigma Aldrich) and 20 mM glucose (Sigma Aldrich). Non-selective LB agar plates (Formedium) were used for general purposes such as colony forming unit (CFU) counting.

2.2 Nitric oxide donor, sodium nitroprusside

Unless otherwise stated, sodium nitroprusside (SNP, Sigma Aldrich) was prepared fresh in sterile millipore water and filter sterilised (0.22µm PES filter, Merck) before use. Due to the light sensitive release of NO by SNP, care was taken during preparation to limit light exposure until the treatment period, upon which a constant light source was used.

2.3 Microtitre plate assay to investigate the NO mediated dispersal response of *P. aeruginosa* biofilms.

The NO mediated dispersal response of *P. aeruginosa* biofilms was analysed using a microtitre plate system. Overnight cultures were diluted 1 in 100 in freshly prepared M9 minimal media and added to a flat-bottomed tissue culture treated 96-well microtitre plates (Costar, Thermo Fisher), perimeter wells were filled with sterile water to prevent evaporation effects on biofilm growth, plates were incubated at 37°C with slow shaking (50rpm) for 24 h. Isolates previously determined

as slow growing or poor biofilm formers were allowed 48 h to establish a robust enough biofilm to be dispersed. Uninoculated M9 media represented the negative control. Post incubation, the planktonic cell suspension was aspirated and discarded, the biofilm containing wells were subsequently washed once with fresh M9 media to remove non-adherent cells. SNP concentrations were prepared fresh in M9 media, serially diluted and added to biofilm containing wells. Six technical repeats were performed for each treatment concentration with 3 placed near the perimeter wells, and 3 near the centre to remove any effects of well location. Plates were incubated at 37°C, with illumination, for 24 h. Following SNP treatment, the planktonic cell densities were recorded via absorbance at 584nm. Biofilms were washed twice with PBS, stained with 0.1% crystal violet for 20 mins, resolubilised in 30% acetic acid and absorbance measured at 584nm. Statistical analyses were performed using GraphPad Prism, one-way ANOVA with Dunnett's multiple comparisons were performed using GraphPad Prism version 8.4.3 (GraphPad Software, La Jolla California USA, www.graphpad.com).

Table 1 Bacterial isolates to be used in this study. Reproduced with permission from Soren.

Strain	Isolate	Morphology[a]	Mucoidy[b]	Pigmentation[c]	Planktonic growth[d]	Biofilm formation[e]	Susceptibility[f]			Reference
							TOB	CAZ	COL	
PA01	Laboratory	Smooth, round	-	PCN	Fast	Good	S	S	S	Soren, 2018
PA05	Clinical	Smooth, round	+	PCN, PRN	Slow	Poor	S	S	S	
PA08	Clinical	SC	-	PRN	V. Slow	Poor	S	R	S	
PA10	Clinical	Smooth, round	+	PCN	Slow	Moderate	S	S	S	
PA15	Clinical	SC	-	-	Slow	Poor	S	R	S	
PA20	Clinical	SC	-	PCN	Slow	Moderate	S	S	S	
PA21	Clinical	Rough, flat, round	-	PCN	Fast	Good	S	R	S	
PA26	Clinical	SC	-	PCN, PVD	Fast	Good	S	R	S	
PA30	Clinical	SC	-	PVD, PRN	Fast	Good	S	S	S	
PA31	Clinical	SC	-	PCN	Slow	Poor	R	S	R	
PA37	Clinical	SC	-	PVD	Fast	Moderate	S	R	S	
PA39	Clinical	Rough, wrinkled	-	-	Slow	Moderate	S	S	S	
PA44	Clinical	SC	-	-	Slow	Good	S	S	R	
PA47	Clinical	SC	-	PVD	Slow	Poor	S	S	R	
PA49	Clinical	Rough, round	-	-	Slow	Moderate	S	S	S	
PA55	Clinical	SC	-	PCN	Slow	Poor	R	S	R	

PA56	Clinical	Smooth, round	-	PVD	Slow	Poor	S	S	S	
PA57	Clinical	Smooth, round	++	PCN, PRN	Slow	Poor	S	S	S	
PA66	Clinical	SC	-	PCN	Slow	Good (M)	S	R	S	
PA68	Clinical	Smooth, round	-	PCN	Fast	Good	S	S	S	

[a] Growth on LB agar. [b] growth on PIA between 24-48h; -, non-mucoid; +, mucoid; ++, hyper mucoid. [c] PCN, pyocyanin; PVD, pyoverdine; PRN, pyorubin. [d] in LB broth, determined spectrophotometrically. [e] biofilms grown for 48h in 96 well plates, stained with crystal violet and analysed spectrophotometrically for total biomass, Poor = OD value of less than 0.5; Moderate = OD value between 0.5 and 1; Good = OD value of above 1. [f] Antimicrobial susceptibility as determined by EUCAST breakpoint standard MIC assay S, sensitive; R, resistant; TOB, tobramycin (S ≤ 4mg/L, R > 4mg/L); CAZ, ceftazidime (S ≤ 8mg/L, R > 8mg/L); COL, colistin (S ≤ 2mg/L, R > 2mg/L)

2.4 Inclusion and exclusion criteria for CF PaCiFy study.

Adults and adolescents with cystic fibrosis were eligible for inclusion when aged 12 or above and colonized with *P. aeruginosa*, confirmed by microbiological assessment of sputum samples (>50% culture positive samples in the preceding 12 months), who are judged by the respiratory consultant to be; clinically stable and free from acute infection; normal oxygen saturations; no complications from previous bronchoscopies. Patients were excluded where; they did not provide informed consent; adolescents not Gillick-competent (and therefore not able to give their own assent in addition to parental consent); patients undergoing treatment with an interventional drug or device prior to enrolment; the clinical consultant does not consider participation to be appropriate.

2.5 CF sputum collection

Sputum samples from CF patients known to be chronically infected with *P. aeruginosa*; United Kingdom National Health Service [NHS] Research Ethics Reference 08/H0502/126) were obtained via unassisted expectoration. To evaluate the changes in the sputum proteome and biofilm phenotype, samples were obtained at three individual timepoints: pre-antibiotics - taken on the day of hospital admission following a pulmonary exacerbation diagnosis, and before the first dose of antibiotics; post-antibiotics - taken on the last day of the antibiotic course (14 days); follow up - sample was taken at a undetermined period of time after patient discharge, at the next clinic appointment when the patient was clinically well. Samples were processed for proteomic and microscopic analysis within 1 hour of expectoration.

2.6 Sampling for proteomic analysis

Sputum samples were processed for proteomic analysis using a Bligh-Dyer extraction methodology as standardised in the PaCiFy Study Laboratory Manual, version SCBR/LAB/V2 (Appendix 1) In short, sputum samples were mixed with 6.3 mM dithioerythritol in HEPES buffered saline, filtered, and centrifuged at 400 x g for 10 minutes. The supernatant was isolated and centrifuged at 12,000 x g for 10 minutes at 4oC. The now separated cell pellets and the supernatant were snap frozen in isopropanol. UHPLC separations were performed using a nanoAcquity UPLC system (Waters).

The raw mass spectra were processed using ProteinLynx Global Server Ver 3.0 (Waters, Manchester, UK) and the data processed to generate reduced charge state and de-isotoped precursor and associated production mass lists. Comparisons were drawn against UniProt Homo sapiens reference proteome protein sequence (December 2019) (UniProt 2019). A maximum of one-missed cleavage was allowed for tryptic digestion and the variable modification was set to

contain oxidation of methionine, carboxyamidomethylation of cysteine and hydroxylation of aspartic acid, lysine, asparagine, and proline.

2.7 Western Blotting

Prior to Western blot analysis for the detection of Histone H4, the total protein concentration of each sputum supernatant sample was determined via a DC protein assay according to the manufacturer's instructions (Bio-Rad Laboratories). The protein concentration of the sample was used to calculate and normalise the total protein to be loaded (20µg), previously determined by assay optimisation.

Western blotting was performed on 16 available clinical sputum samples (Table 2) from archive freezers at the University of Southampton, these included only patients from the Southampton cohort. Samples were mixed with reducing Laemmli buffer (Alfa Aesar, Thermo Fisher Scientific) and PBS, and boiled at 100°C for 10 minutes. Sodium dodecyl sulphate–polyacrylamide gel electrophoresis (SDS-Page) was carried out using NuPAGE™ MES SDS Running Buffer. NuPAGE™ 4-12% Bis-Tris Protein Gels (Invitrogen) were loaded with 20µg/lane total protein in triplicate. Positive sample and in-gel linearity controls included dilutions of recombinant Histone H4 (Abcam UK, ab198115). Sterile filtered water acted as a negative control. Gel migration was carried out at 200V for 50 minutes.

Table 2. Available clinical sputum samples for Western blotting from archive freezers at the University of Southampton. Tick denotes sample availability.

	UOS001	**UOS002**	**UOS007**	**UOS010**	**UOS011**	**UOS014A**	**UOS022**
Pre-Abx	✓	✓	✓	✓	✓	✓	✓
Post-Abx	N/A	✓	✓	✓	✓	N/A	✓
Follow up	✓	N/A	✓	N/A	✓	✓	N/A

A Bio-Rad Mini-PROTEAN Tetra cell western blot transfer system was used to carry out a wet transfer at 5V (4°C) overnight, to a 0.45µm nitrocellulose membrane (Bio-Rad Laboratories) in the presence of transfer buffer. Following protein transfer, the membranes were stained with REVERT total protein stain (LI-COR Biosciences) and imaged on the LI-COR Odyssey Classic Imager, before blocking at room temperature for 1 hour.

Primary antibody incubation was performed overnight at 4°C with 0.4µg/ml primary Rabbit Anti-Histone H4 (Abcam UK, ab222763). Secondary antibody incubation utilised LI-COR IRDye® 800CW Goat anti-Rabbit IgG at a 1:15000 concentration (LI-COR Biosciences). Membranes were again imaged using the LI-COR Odyssey Classic Imager to detect the presence of Histone H4. Image Studio Lite Ver 5.2 and Empiria Studio 1.3 (LI-COR Biosciences) were used to analyse images.

2.8 Fluorescence *in situ* hybridisation and Microscopy

Microscopic analysis with Fluorescence *in situ* hybridisation (FISH) identification of microbial biofilms was performed as previously described by Howlin et al., 2017, and again, standardised in the laboratory manual (A1). Briefly, expectorated sputum samples were fixed in freshly prepared 4% paraformaldehyde in PBS at 4°C for 24-hrs. Samples were washed with PBS and PBS-ethanol (1:1 v/v) and 100-µL drops of sputum were spotted onto poly-L-lysine (PLL)-coated slides and left to dry overnight. *P. aeruginosa* detection was performed using FISH with the following 16S ribosomal probe sequences: PseaerA, 50 -GGTAACCGTCCCCCTTGC-30, specific for *P. aeruginosa*, labelled with Cy3 (Hogardt et al. 2000; Tajbakhsh et al. 2008); EUB338, 50-GCTGCCTCCC GTAG GAGT-30 (domain bacteria), labelled with Cy5 (Integrated DNA Technologies) (Amann et al. 1990). Hybridization with the sample was carried out using 20% formamide, and a 2-hr incubation at 46°C was followed by washing for 15 min at 48°C in pre-warmed wash buffer. Samples were imaged using an inverted DMI 600 SP5 confocal laser scanning microscope with a 63x oil immersion objective (CLSM, Leica Microsystems).

2.9 Image analysis

For FISH image samples, DAIME (Digital Image Analysis in Microbial Ecology) (Daims et al. 2006) an image analysis and visualisation program and 3D object counter software was used to analyse and quantify *P. aeruginosa* clusters and biovolume from the confocal stacks. Using the average volumes of a single *P. aeruginosa* cell from the literature 0.13– 3.67 mm3) (Iglewski 1996; Palleroni 2015; Ghanbari et al. 2016) fluorescently labelled objects were filtered to remove noise and objects determined to be smaller than single cells. Subsequently, the automatic 3D segmentation of objects was used to measure and record all objects in each sample. The segmentation parameters were determined experimentally, with 200 voxels and 75 voxels being used to segment and quantify biofilm clusters and planktonic cells, respectively. The results for each of the eight image stacks per sample were collated into databases and grouped for analysis. A Wilcoxon matched pairs signed rank test was performed for statistical comparison between each time point (Pre-Abx, Post-Abx, Follow Up).

2.10 Inoculation of the microfluidic device

For the microfluid device only, mPA01 will be used as a reference control rather than PA01. The mPA01 strain is the parent strain of the *P. aeruginosa* transposon mutant library from University of Washington (Jacobs et al. 2003). This parental strain has a complete mapped genome, and may facilitate the downstream transcriptomic profiling and the discovery of essential condition-specific genes in the presence of NO (Jacobs et al. 2003; Varadarajan et al. 2020)

Unless otherwise stated, bacterial isolates were first inoculated in liquid LB media and grown as previously described for an overnight culture. Overnight cultures were centrifuged (4000 x *g*), the supernatant was discarded and the pellet resuspended PBS. Minimal M9 medium was prepared with a 0.1% final glucose concentration, all other supplementations remained at the same concentrations as previously used. The M9 media was inoculated 1:100 with the bacterial PBS suspension and incubated as an overnight culture. Post incubation, the culture was centrifuged and resuspended in PBS as described above. A further 1:5 dilution in PBS was performed to achieve the starting inoculum for the microfluidic device approx. 1x 10e5 cells/ml.

2.11 Microfluidic device

The microfluidic chamber used to grow biofilms is a standardised, publicly available design as previously described (Varadarajan et al. 2020), with a straight channel (30 x 2 x 0.02 mm, L x W x D) in a polydimethylsiloxane (PDMS) chip naturally adhered to a glass coverslip (25 x 60 mm, thickness no.1, SLS), representative 3D render in Figure 8 (left).

Negative moulds for the microfluid device were modelled using the 3D design software Autodesk Fusion 360 (Autodesk Inc., USA) using the specifications mentioned above. The moulds were subsequently printed in engineering photopolymer resin (3DFilaPrint, UK) on a Creality Halot One 3D printer (Shenzhen Creality 3D Technology Co, Ltd., China). The produced moulds were washed twice in isopropyl alcohol to remove the excess resin and exposed to a UV light source for 30mins to fully cure. The cured mould was then baked in an oven at 70C for a minimum of 4 hours to 'burn off' any residual photopolymers that may inhibit PDMS curing as previously mentioned (Venzac et al. 2021).

Sylgard 188 (Dow, UK) silicone elastomer PDMS was prepared to the manufacturer's instructions. Parts A and B were mixed 10: 1 (w/w) poured into the mould and incubated at 60°C for 4 hours to

accelerate the curing time. The PDMS chips were carefully removed from mould and immediately placed onto a clean glass coverslip.

The inlet and outlets of the channels were connected to a F100X syringe pump (Chemyx Inc. USA) with a 23 G needle and a waste container respectively, using PTFE microtubing (0.6mm ID/ 0.8mm OD). The device was placed in the lid of petri dish to contain any potential leakage of bacterial inoculum, the petri dish lid was placed in direct contact with a hot plate set at 37°C. Full device setup is in pictured Figure 8 .

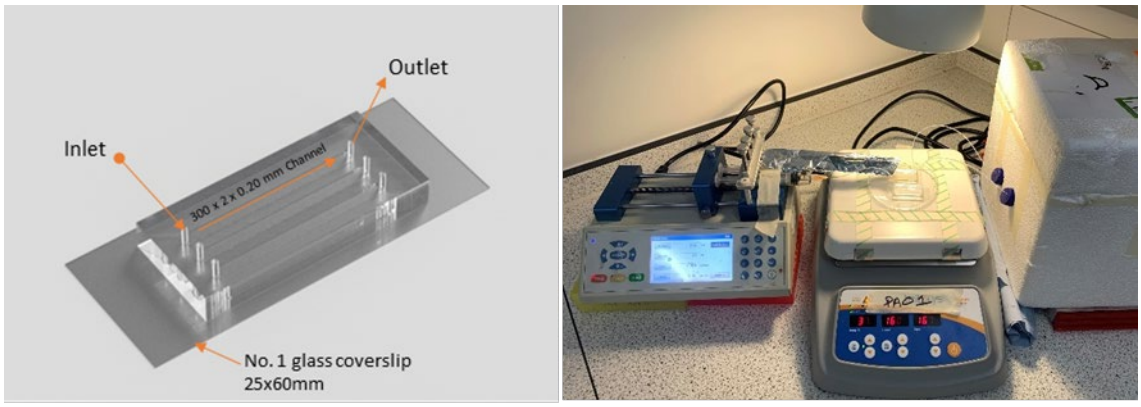

Figure 8. (Left) 3D rendering of the PDMS chip containing 3, 300 x 2 x 0.20 mm (LxWxD) microfluidic channels with inlet and outlet points for 1mm outer diameter PTFE tubing. The PDMS chip is adhered to a no.1 thickness 25 x 60mm glass coverslip. 3D rendering produced in Autodesk Fusion 360 (Autodesk Inc., USA). (Right) Example laboratory setup of microfluidic biofilm experiment, a syringe pump (left) pushes media at the desired flow rate through PTFE tubing into the PDMS chip in contact with a hot plate set to 37°C (middle), tubing from the outlet flows into waste containers or into falcon tubes (for cell collection) contained in an insulated box filled with wet ice (right). A light is kept on constantly to enable NO release from SNP, foil covers the syringe containing the SNP dilution to restrict NO release to within the microfluidic channel and minimise NO release within the syringe.

Prior to inoculation, the PDMS chip was sterilised by flowing 70% ethanol at a rate of 20ul/min for 10 mins followed by M9 media for the same period. The channels in the PDMS chip were inoculated by flowing the suspension prepared above at a rate of 5ul/min for 1h. Following this, M9 media was flowed through the device at the same rate for 48 hrs to allow for appropriate biofilm growth.

After the required growth period, the NO donor SNP was run through the device maintaining the same flow speed, control channels received further flow of M9 minimal media. A concentration of 8µM SNP was flowed through the dispersal channels, as this is a concentration has previous demonstrated to induce biofilm dispersal in a 96 well crystal violet assay. Outflow from the

system from the treatment period was retained on ice for further processing, RNA extraction, and CFU enumeration.

2.12 Confocal Imaging

Following the growth and treatment period ~72hrs total, CLSM images were taken. The biofilm was first washed with PBS at a flow rate of 5µl/min for 10 mins to remove any excess planktonic cells. The biofilms were stained by flowing 300µl of Live/Dead (Life Technologies, Oregon, USA) staining solution (1.5 µl Syto9 + 1.5 µl propidium iodide in 1 ml of sterile PBS) through the PDMS chip at 5 µl/min. Once the channel was filled, the flow was paused, and the biofilm incubated in the dark for 20min min to allow dye penetration. Subsequently, PBS was flown through the system at 5 µl/min for 15 min to remove the excess staining solution. Samples were imaged using an inverted Leica SP8 confocal laser scanning microscope with a 63x oil immersion objective (CLSM, Leica Microsystems). IMARIS (v 10.0.1, Oxford instruments) analysis of confocal data was performed to provide live: dead cell quantification.

2.13 Genomics

Genomic data analyses were performed on the University of Southampton's' high performance computing cluster, Iridis 5.

2.13.1 Genomic DNA extraction

Genomic DNA was extracted from overnight cultures using the DNeasy® PowerBiofilm Kit (QIAGEN®, Germany) according to the manufacturer's instructions. The sequencing library was prepared utilising NBD112.24 ligation barcoding kit to multiplex all genomes (Oxford Nanopore Technologies, Oxford, UK). The prepared library was subsequently loaded onto the Oxford Nanopore Minion sequencer with R10.4 flow cell chemistries.

2.13.2 Genome assembly and sequence analysis

The strain PA01 used as a reference in this study was reannotated in the same way to avoid any potential annotation bias. Base calling and barcode sequence trimming was performed using Guppy (Oxford Nanopore Technologies). Base called sequences were compared to the Kraken 2 database for metagenomic analysis and taxonomic classification (Wood et al. 2019). Genome assemblie were carrries out with Flye (Kolmogorov et al. 2019) and assembled circular contigs for

each isolate were annotated with Prokka (Seemann 2014) using Uniprot PA01 as a reference (https://www.uniprot.org/proteomes/UP000002438) Parsnp was employed to align core microbial genomes of the strains used for phylogenetic analysis and construct maximum likelihood tree (Treangen et al. 2014). The tree was annotated and visualised with iTOL (interactive Tree of Life, v8.8.1 (Letunic and Bork 2021).

For determining the MLTS of isolates the mlst software (https://github.com/tseemann/mlst) made use of the PubMLST database (Jolley et al. 2018). Gene presence/absence matrices were created by blasting a custom database of gene sequences against the isolate genomes using Abricate (https://github.com/tseemann/abricate).

2.14 RNA extraction

The extraction of RNA from the flow cell requires the removal of the glass coverslip adhered to the PDMS chip. Once removed the biofilms were scraped from channel using a sterile p1000 pipette tip and suspended in sterile PBS. A total of three microfluidic channels were pooled together to achieve the starting material for extraction. The bacterial suspension was centrifuged at 13000 x g and the supernatant discarded. The planktonic/ dispersed populations collected in the outflow were pooled and centrifuged at maximum speed (4000 x g) for 10mins and the supernatant discarded. The pellets were resuspended in 250ul DNA/RNA Shield™ (Zymo Research Corp., USA) to protect and stabilise the cellular RNA and prevent regulatory changes. Samples were incubated overnight at 4°C to allow appropriate penetration into the cells.

Following the overnight incubation, samples were stored at -20°C until extractions were performed. The stabilised RNA samples were mixed 1:1 RNA lysis buffer, and on-column RNA extraction was continued using a Quick-RNA™ Microprep Kit (Zymo Research Corp., USA) following the manufacturer's instructions.

In addition to the on-column DNA digestion, to remove any residual genomic DNA, a Turbo DNA-free (Invitrogen, Thermo Fisher) treatment was carried out according to the manufacturer's instructions. Briefly, 20µl of RNA sample was incubated for 1h in a solution containing 4µl TurboDNase, and 2.5µl DNase buffer. Following incubation, 2.5µl DNase inactivation reagent was added and incubated for 2 mins at room temperature with periodic mixing. The samples were then centrifuged at full speed (21,000 x g) for 2 mins to remove deactivation reagent. The supernatant was carefully transferred to a clean microcentrifuge tube and stored at -80°C.

Extracted RNA was tested for quality and quantity using a Nanodrop 1000 spectrophotometer and Qubit 2 fluorometer (Thermo Fisher). A 2% agarose gel was run at 180v for 30 mins to check for

RNA integrity. The gel was stained using SYBR Gold nucleic acid stain (1:10000 dilution) (Invitrogen, Thermo Fisher) with a high range RNA ladder (Thermo Scientific) for reference. Bands were visualised on a G: BOX EF imaging system (Syngene, UK).

2.15 RNA sequencing

In-house RNA sequencing was not possible; therefore, an external Novogene UK prokaryotic RNA sequencing service was used. Library preparation included the removal of rRNA before sequencing on an Illumina NovaSeq system, full details of which were not provided. Raw sequencing data was delivered electronically.

2.15.1 RNA sequence analysis

Genomic data analyses were performed on the University of Southampton's high performance computing cluster, Iridis 5.

Fastqc 0.12 (github.com/s-andrews/FastQC) was used to assess the quality of the raw sequencing data both before and after the trimming of the Illumina adapter sequences with Trimmomatic v0.39 (Bolger et al. 2014). Alignment of the sequencing data to the reference genomes indices of the respective isolates used was performed using Hisat2 (Kim et al. 2019). Featurecounts (Liao et al. 2014) was used created count tables from the aligned sequencing reads.

For differential gene expression analysis, the DESeq2 package in R 4.3.1 was used. Estimated size factors calculated for count matrices from both PA10 and mPA01 were used to normalise and log transform the data sets to allow calculation of correlation between samples and further differential expression analysis. Differentially expressed genes were identified as significant based on an adjusted p value of <- 0.05 and a log2fold change > 1 and <-1. Volcano plots were producing in R using ggplot2.

Chapter 3 Phenotyping of *P. aeruginosa* and identification of biofilm biomarkers in the cystic fibrosis lung – PaCiFy Study.

3.1 Contributions

The work presented in this section represents the integration and analysis of several data sets including those acquired from a multi-centre clinical study (PaCiFy, NIHR Rare diseases Respiratory Translational Research Centre). There are a number of contributions from others as follows: 1) Collection and initial preparation / processing of sputum samples at multiple hospital sites, (Robert Howlin, Caroline Duigan, University of Southampton). 2) Proteomic differential expression analysis was undertaken by Thomas Garfield for a piece of work towards a medical report. 3) Western blot analysis was carried out by both Ellie McNamee (MSc student, University of Southampton) and I together and under my day-to-day laboratory guidance, with part of the data generated included in McNamee's masters thesis.

3.2 Introduction

Establishment of *P. aeruginosa* biofilms within the CF airway increases the tolerance to antibiotics and contributes to chronic infection. Current CF treatment strategies aim to eradicate or control infection using aggressive antibiotic regimes but are rarely capable of clearing the underlying chronic infection. The field urgently needs the ability to diagnose and treat chronic, biofilm-associated infections in cystic fibrosis. This has been hampered historically because bacteria in biofilms are largely unculturable, and therefore unsuited to standard clinical diagnostic testing involving bacterial culture. A lack of biomarkers escalates this diagnostic issue.

Current diagnostics reply on the repeated isolation of *P. aeruginosa* from expectorated sputum, a positive culture is indicative of a bacterial infection; although, this does not allow for the distinction between planktonic and biofilm phenotypes and the status within the patient airways. Alternative methods of biofilm detection are greatly needed to enable identification and diagnosis of a chronic biofilm infection where conventional culture methods have previously failed.

One such method to be explored outside of traditional microbiological culture is fluorescence in situ hybridization (FISH). This method enables visualisation of bacteria with fluorescence microscopy through the annealing of a specific fluorescently tagged probes to bacterial 16S rRNA region of interest. This allows for the detection of multiple specific bacterial targets within the

same sample. Coupled with 3D confocal microscopy, spatial localisation of the labelled bacteria can be determined (Moter and Göbel 2000; Chrzanowska et al. 2020). This may be used to visualise components of the biofilm in situ expectorated sputum allowing the presence of microbial aggregates to be assessed (Høiby et al. 2017). FISH may be a useful diagnostic tool for *P. aeruginosa* biofilm infection of the CF lung; however, it is not routinely employed in the clinic.

Colleagues at the University of Southampton have identified a low throughput microscopic biofilm assay in which *P. aeruginosa* in expectorated sputum samples are fluorescently labelled via FISH and assessed for planktonic or biofilm status based upon the size and volume of bacterial aggregates. This assay has previously been used in a BRU-funded proof-of-concept trial (Howlin et al. 2017) and requires further validation for scaling up for high throughput biofilm phenotyping.

Alternative molecular methods exploit the use of proteomics. Proteomics can study both single proteins and complex samples, with modern techniques now taking mass spectrometry (MS)-based analysis approaches to allow quantification of proteins within a specimen at a fixed point in time. This provides label-free detection of proteins with high sensitivity and specificity enabling the identification of changes between different conditions and has wide applications within medicine and implications in disease-related biomarker discovery (Roxo-Rosa et al. 2006; Rozanova et al. 2021).

The use of proteomics has been used in numerous studies to identify novel biomarkers of CF lung disease (Roxo-Rosa et al. 2006; MacGregor et al. 2008). These studies identify individual markers of airway inflammation (IL-8) (Mayer-Hamblett et al. 2007), but no disease-specific makers for chronic bacterial infection caused by *P. aeruginosa* biofilms. A quantifiable indicator of *P. aeruginosa* required to improve the diagnosis of chronic infection which, in turn, this could guide a personalised and stratified approach to the treatment of CF patients.

In this chapter, fluorescence microscopy data of expectorated sputum samples from CF patients undergoing exacerbation will be analysed to assess the feasibility of using FISH as a clinical diagnostic tool to determine the biofilm phenotype. In particular, how the biofilm status changes with antibiotic treatment over a specified time course, and if this change can be utilised to predict patient outcomes following an exacerbation. This chapter will also consider the microscopy findings alongside the proteomic data sets obtained from the same sputum samples with the potential to identify a 'biofilm specific biomarker' that could be used to screen CF patients and again assess the biofilm status.

3.3 Results

3.3.1 Patient Demographics

The study cohort comprised 32 cystic fibrosis patients. Of these, 12 (38%) were male and 20 (63%) were female. Patients were aged 14 to 73 at the time of the study with a median age of 30 years. The age of diagnosis varied from birth to 54 years old, with the median 3 months and 17 days. 100% of the patients had *P. aeruginosa* at some point throughout their life with 75% being diagnosed with chronic *P. aeruginosa* infection. The median age of 1st known *P. aeruginosa* isolation was 15.5 years old whilst the median age of chronic *P. aeruginosa* diagnosis was 22 years. Cystic fibrosis genotypes varied with 69% homozygous for class II mutations, 9% heterozygous for class I and II mutations, 9% heterozygous for class II and IV mutations, 3% heterozygous for class II and III mutations, 3% having unidentified mutation and 6% unrecorded.

Unassisted expectorated sputum samples were fluorescently labelled via *in situ* hybridisation (FISH) for *P. aeruginosa* and assessed microscopically for biofilm status; the PA phenotype was determined for 27 patients from the University Hospital Southampton (UHS) undergoing an antibiotic-requiring exacerbation, and further assessed for alterations to the biofilm status following antibiotic treatment. The sputum from 22 patients was processed for proteomic analysis across the entire patient cohort, of these 18 were from UHS. Patient and sample timepoint identifiers for the UHS patients are shown in Table 3.

Table 3. Patient ID and sample available from each time point; Pre-Abx, Post-Abx, and Follow Up. The hash represents an available sample that was processed for FISH analysis. Purple highlighted cells represents those that were processed for proteomic analysis.

Patient ID	Sample 1 (Pre-Abx)	Sample 2 (Post-Abx)	Sample 3 (Follow Up)
UOS001		#	#
UOS002	#	#	#
UOS003	#	#	
UOS004	#	#	#
UOS005	#		#
UOS006	#	#	#
UOS007	#	#	#
UOS008	#	#	#
UOS009	#		
UOS010	#	#	
UOS011	#	#	#
UOS013	#		
UOS014A	#		#
UOS014B	#	#	
UOS015	#		#
UOS016	#		
UOS017	#		
UOS018	#		
UOS019	#		#
UOS020	#		
UOS021	#		
UOS022	#	#	#
UOS023	#		
UOS024	#	#	
UOS025	#	#	
UOS026	#	#	#
UOS027	#		

3.3.2 The total biofilm volume in CF patient sputum is unaffected by antibiotic therapy across the cohort.

The patient wide biofilm phenotype remains constant, when collated for the whole cohort, statistical analysis shows no significant change in total average biofilm volume between the three sampling timepoints. The mean average biofilm volume ranges from 1648.31 μm^3 at the pre-antibiotic timepoint to 1215.8 μm^3 in the follow up (Figure 9). The post antibiotic samples, that would be expected to have a lower overall volume due to killing activity of the antimicrobials sits in-between with a mean average of 1609.61 μm^3. The average biofilm biomass was calculated

using DAIME and consisted of 8 separate confocal stacks for each patient, a Wilcoxon matched pair signed rank test used for statistical analysis in GraphPad (v9.2.0). The individual points plotted in Figure 9. Average sum of total biofilm biomass comparing each of the three timepoints, pre-abx, post-abx, and follow up samples from a total of 62 patients. Individual data points represent the mean average of the total biofilm volume for a single patient (n=8). Not all patients are represented in each of the sample timepoints, unpaired data points were ignored in the statistical analysis. A Wilcoxon matched pairs signed rank test was performed for statistical comparison between each time point. No significant difference is observed between the sample points (P= >0.05)identify some outlier that appear to differ from the mean, this can be attributed to patient specific trends as discussed in the next section.

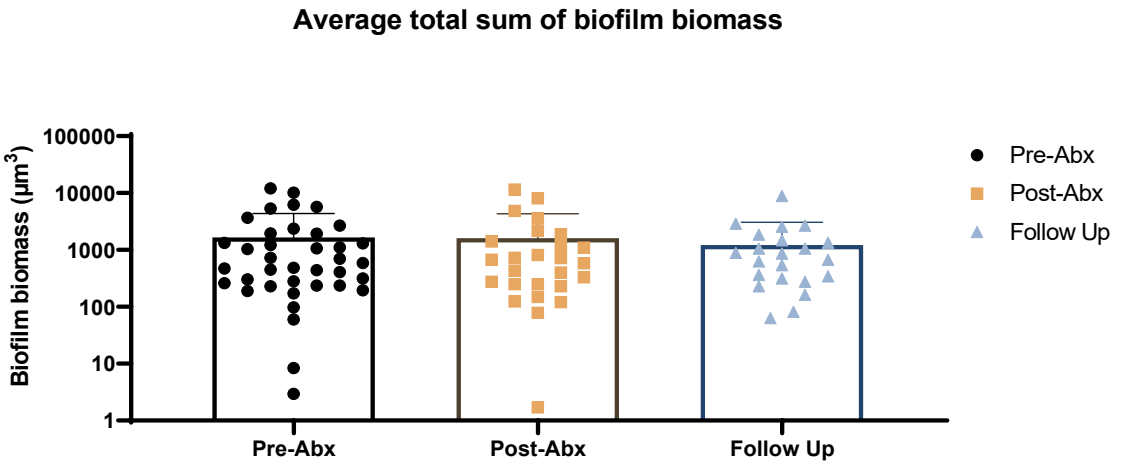

Figure 9. Average sum of total biofilm biomass comparing each of the three timepoints, pre-abx, post-abx, and follow up samples from a total of 62 patients. Individual data points represent the mean average of the total biofilm volume for a single patient (n=8). Not all patients are represented in each of the sample timepoints, unpaired data points were ignored in the statistical analysis. A Wilcoxon matched pairs signed rank test was performed for statistical comparison between each time point. No significant difference is observed between the sample points (P= >0.05)

3.3.3 The average number of biofilm aggregates in the CF sputum remains unaffected despite antibiotic intervention throughout the cohort.

The same observation can be made for the average number of biofilm aggregates, with no significant difference seen between any of the sampling time points. The average number of aggregates pre antibiotics (28.7) is seen to rise slightly following antibiotic intervention (33.7) before again falling a little to a mean average of 23.98 aggregates per sample (Figure 10). The average number of biofilm aggregates were also calculated using DAIME and again consisted of 8

separate confocal stacks for each patient, the same statistical test as for the average biofilm volume was used here.

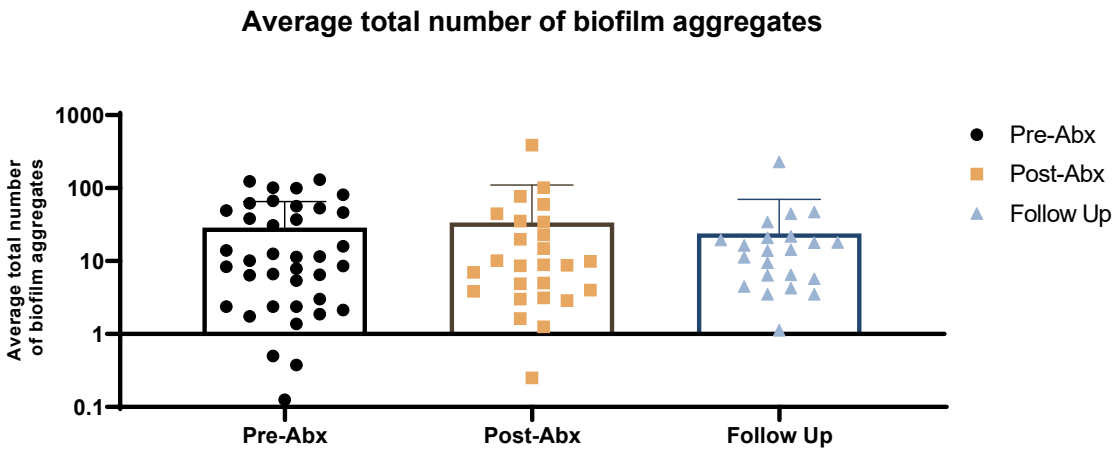

Figure 10 Average total number of biofilm aggregates comparing each of the three timepoints, pre-abx, post-abx, and follow up samples. Individual data points represent the mean average of the total number of biofilm aggregates for a single patient (n=8). Not all patients are represented in each of the sample timepoints, unpaired data points were ignored in the statistical analysis. A Wilcoxon matched pairs signed rank test was performed for statistical comparison between each time point. No significant difference is observed between the sample points (P= >0.05)

These results taken as an entire cohort would suggest that the colonising P aeruginosa in the lung is existing in a robust biofilm that is offering a substantially increased tolerance to antimicrobial intervention and thus having no significant impact on the reduction of the infectious burden as is typically expected for chronic biofilm infections, despite antibiotic therapy. Due to the lack of patient data, it is not possible to state which antibiotics were given, but it can be assumed from general practise that antibiotics were prescribed based up previous microbiological findings and resistance profiling for each patient. This introduces variation across the cohort as some antibiotics may be more effective than others, hence it would be more meaningful to discuss the effects of anti-biofilm therapies on a patient-to-patient basis.

3.3.4 Individual patients show differing trends in biofilm volume in response to antibiotic therapy.

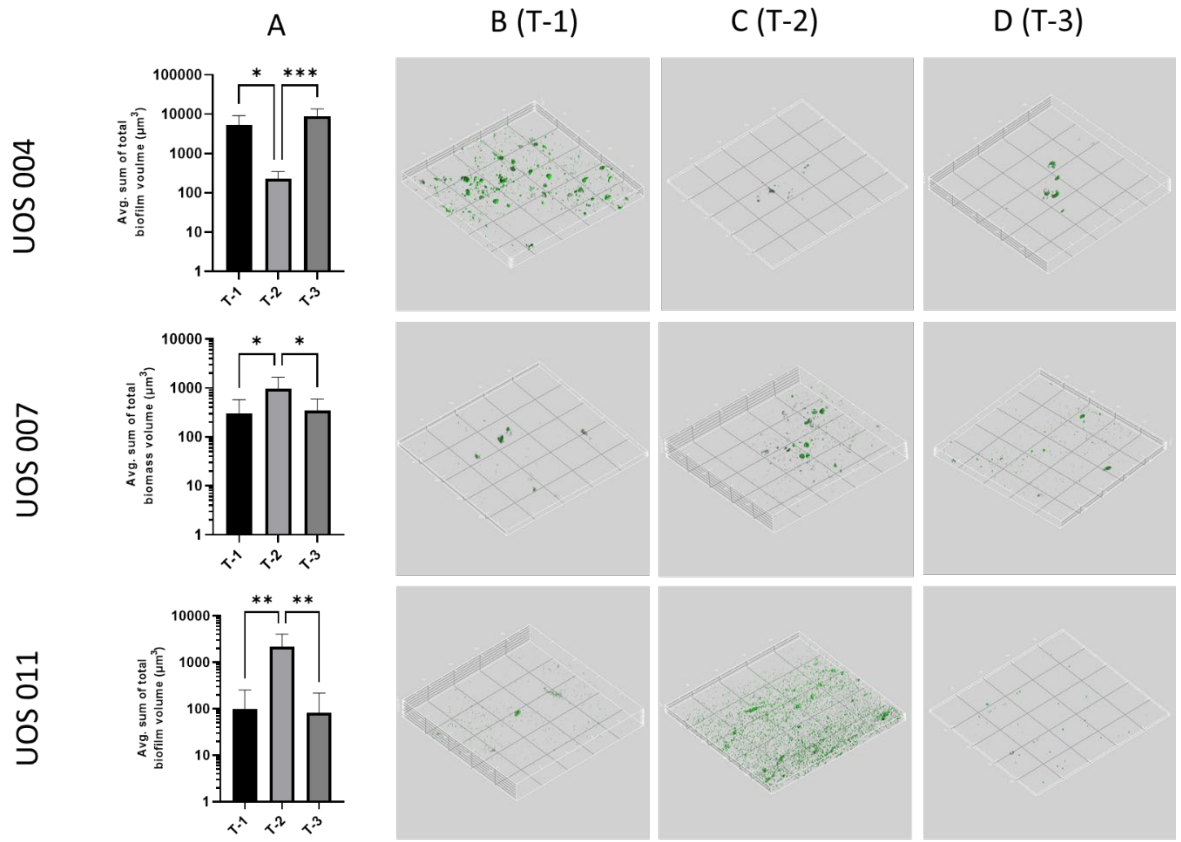

Figure 11. Observed changes in average total biofilm biomass in expectorated sputum samples for individual patients from the cohort. Each row represents data from a single patient (patient numbers UOS004, UOS007, and UOS011). Column A displays a bar graph illustrating the change in average total biofilm biomass between treatment points (T-1; pre-abx, T-2; post-abx, T-3; follow up). Error bars represent the standard deviation from the mean n=8. Asterisks represent the significance values from a one-way ANOVA with Tukey's multiple comparisons (*- P= 0.0332, **- P= 0.0021, ***- P=0.0002). Columns B, C, and D are representative confocal laser-scanning microscopy (CLSM) images showing *P. aeruginosa* identified using fluorescence in situ hybridization (FISH) with Cy3-labeled *P. aeruginosa*-specific 16S rRNA probe. Each image is X'246.03µm, Y'246.03µm, Z' height varies with biofilm thickness. Images were analysed and acquired utilising DAIME (digital image analysis in microbial ecology, V2.2, (Daims et al. 2006)).

More interesting observations are highlighted when looking at individual patients, rather than the whole cohort. Different patients show varying trends in total biofilm volume, shown in Figure 11. The trend seen in patient UOS004 (Figure 11 A) is as would typically be expected following antibiotic therapy, with a significant reduction (P= 0.003) in total biovolume from 5331.09 µm 3 to 229.185 µm 3 seen post antibiotics. This would indicate the antibiotics are performing as

expected and are effectively killing and aiding in the reduction of biofilm biomass within the lung. Once the antibiotic pressure is removed, the growth of the bacteria is re-established, and the biofilm volume increases significantly (P= 0.0002) to 8869.62 μm^3, similar to the volume first observed pre-antibiotics, with no significant difference between the two. A visual representation of this data is also displayed in Figure 11 with 3D confocal images showing the reduction in visible green aggregates. The opposite can be said about patients UOS007 and UOS011 (Figure 11 B/C/D), with the average biofilm biomass increasing at the post antibiotic timepoint, suggesting that the applied treatment is in fact promoting the growth of the biofilm and the bacteria within, rather than the anticipated result of bacterial killing. Whilst both UOS007 and UOS011 both show a significant increase after receiving antibiotics, the degree of significance differs with UOS011 displaying a more significant increase in volume than that of UOS007 (P=0.0031 and P=0.0197 respectively). Both patients returned to basal levels with no significant difference observed between antibiotics and follow up samples.

3.3.5 The biofilm: planktonic ratios suggest biofilm disruption, but not eradication.

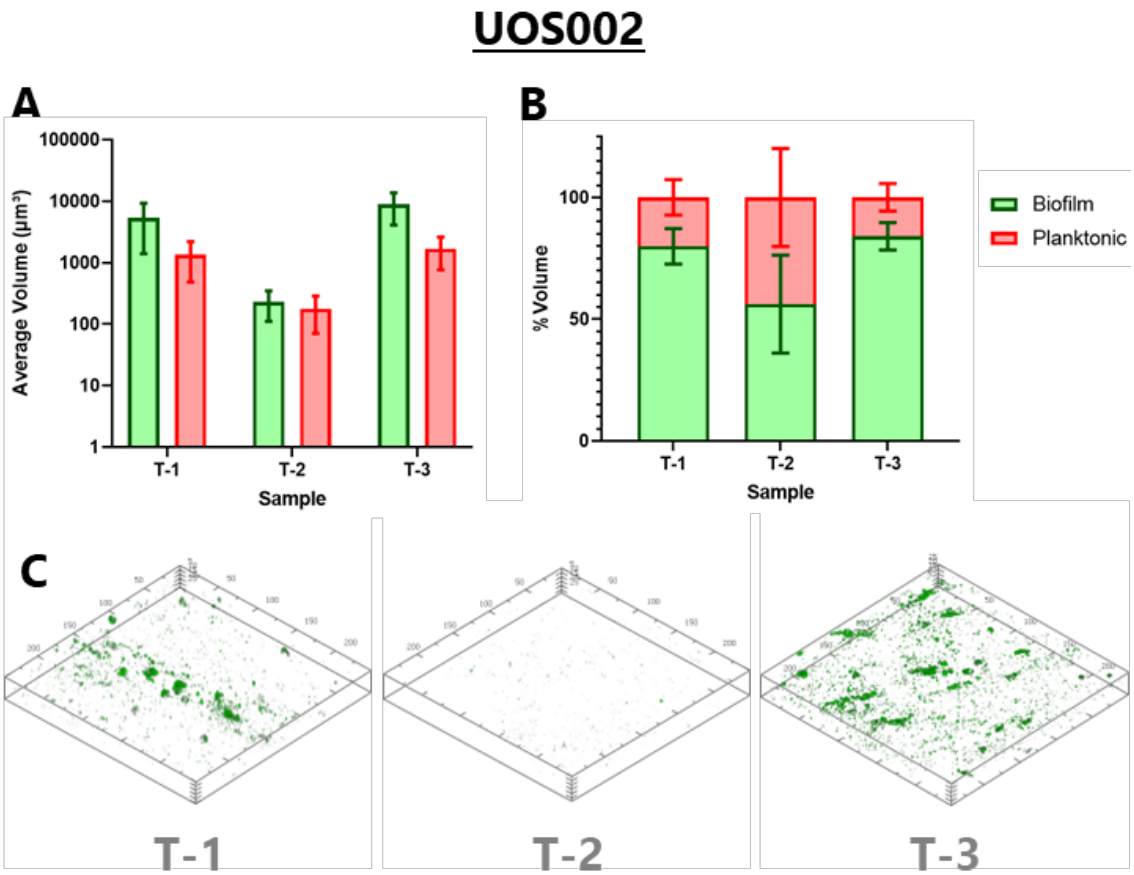

Figure 12. Observed changes in average total biofilm biomass and planktonic cell biomass in expectorated sputum samples for the patient UOS002. (A) displays a bar graph illustrating the change in average total biofilm biomass and planktonic cell volume between treatment points (T-1; pre-abx, T-2; post-abx, T-3; follow up). Error bars represent the standard deviation from the mean n=8. (B) bar chart showing the percentage proportion of biofilm:planktonic biomass for each of the time points. (C) representative confocal laser-scanning microscopy (CLSM) images showing *P. aeruginosa* identified using fluorescence in situ hybridization (FISH) with Cy3-labeled *P. aeruginosa*-specific 16S rRNA probe. Images were analysed and acquired utilising DAIME (digital image analysis in microbial ecology, V2.2, (Daims et al. 2006)).

The entire patient cohort again demonstrated no significant changes in average biofilm and planktonic measurements, however, individual patients showed varying trends between each sample timepoint.

In UOS002, the average total volume of biofilm biomass was greater than that of the average planktonic cell volume at each time point (Figure 12A). The biofilm volume significantly decreased from T-1 to T-2 ($p=0.0243$) and increased from T-2 to T-3 ($p=0.0002$). No significant difference was observed between T-1 and T-3 ($p=0.1408$).

Similarly, the average total planktonic cell volume followed the same trend from pre-antibiotic to post-antibiotic samples (p=0.0121) and post-antibiotic to follow-up samples (p=0.0013) again showing no significant change between pre-antibiotic and follow-up samples (P=0.6122). Changes in biofilm: planktonic cell proportions were observed between samples. For UOS002 planktonic cells accounting for ~20% of the total cell volume at pre-antibiotics (T-1) (Figure 12B). Whereas following antibiotics in T-2, the percentage volume of planktonic cells significantly increases (p=0.0034), to equate to almost half of the total cell volume. In T-3, once the antibiotic pressure is removed, the volumetric proportion of planktonic cells significantly decreases from T-2 returning close to basal levels seen in T-1 (p=0.0008), with the biofilm volume constituting ~85% of the total bacterial population. Representative confocal images from patient UOS002 are shown to support this, demonstrating visible biofilm clusters in T-1 and T-3, with more single-celled bacteria present in T-2 (Figure 12C).

Highlighting the patient-to-patient variability, opposing trends were observed in patient UOS01. Biofilm volume significantly increased from T-1 to T-2 (p=0.0031) and decreased from T-2 to T-3 (p=0.0029), but with no significant change between T-1 and T-3 (p=0.9996) (Figure 13A). Likewise, planktonic cell volumes exhibited the same trend.

In UOS011, the total volume of cellular biomass constituted mainly of biofilm aggregates. At T-1, approximately three quarters of the total bacterial population were present in biofilm aggregate (Figure 13B). Despite an increase in both biofilm and planktonic cell volume from T-1 to T-2 (Figure 13A), the percentage volume of biofilm cells in T-2 decreased, now with planktonic cells accounting for ~55% of the total cell volume, although this change was not observed to be significant. In T-3, the volumetric proportion of biofilm aggregates significantly increases on average to be higher than that observed in T-1 (p=0.0014) with the biofilm aggregates totalling approximately 90% of the total cell volume. Figure 13C provides representative confocal images demonstrating a small number of biofilm clusters and planktonic cells in T-1 and T-3, alongside an equal distribution of larger biofilm aggregates and planktonic bacteria in T-2.

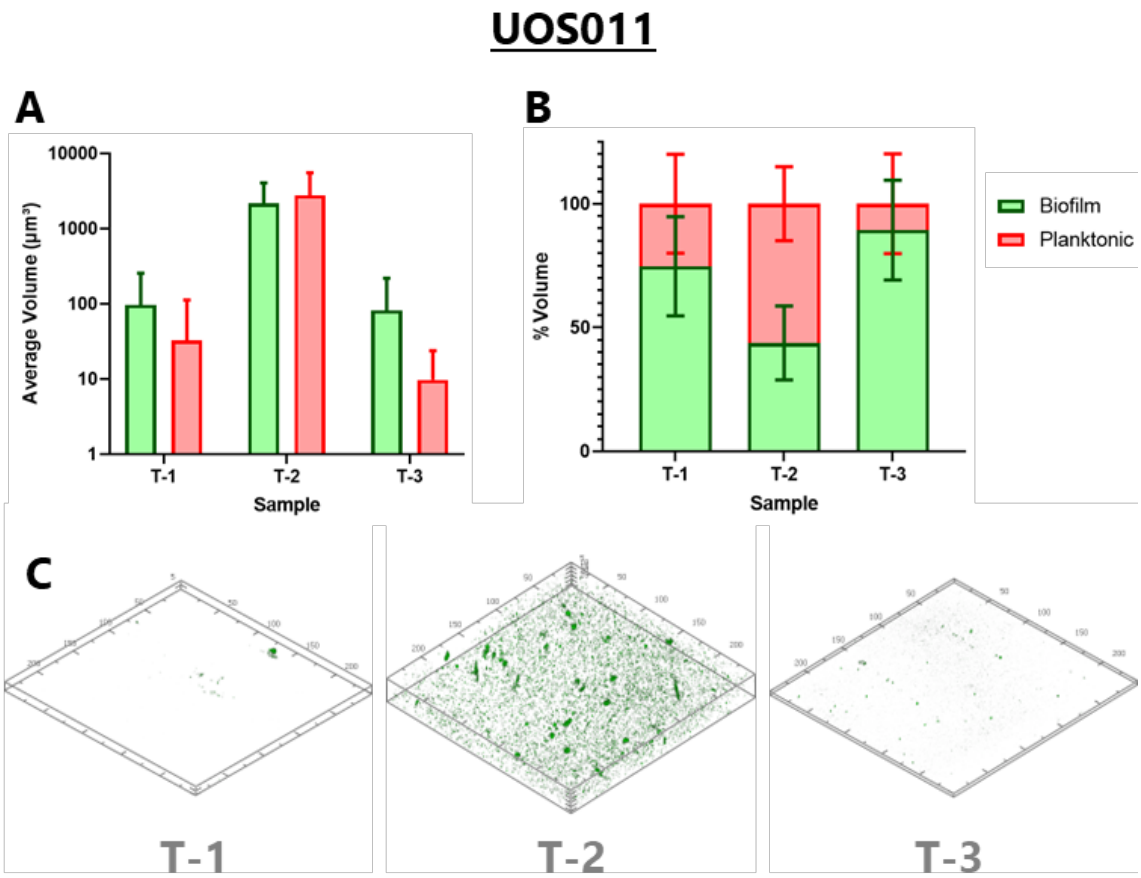

Figure 13. Observed changes in average total biofilm biomass and planktonic cell biomass in expectorated sputum samples for the patient UOS011. (A) displays a bar graph illustrating the change in average total biofilm biomass and planktonic cell volume between treatment points (T-1; pre-abx, T-2; post-abx, T-3; follow up). Error bars represent the standard deviation from the mean n=8. (B) bar chart showing the percentage proportion of biofilm: planktonic biomass for each of the time points. (C) representative confocal laser-scanning microscopy (CLSM) images showing *P. aeruginosa* identified using fluorescence in situ hybridization (FISH) with Cy3-labeled *P. aeruginosa*-specific 16S rRNA probe. Images were analysed and acquired utilising DAIME (digital image analysis in microbial ecology, V2.2, (Daims et al. 2006)).

3.3.6 Mass spectrometry reveals the differential abundance of proteins in the CF sputum in response to antibiotics.

Mass spectrometry was performed in two duplicate sets of the available sputum samples. These sample sets were named PACIFY1 and PACIFY2, containing 17 and 30 sputum samples, respectively. From both sets, a total of 1319 proteins were detected. PACIFY1 and PACIFY2 both contained 929 of the same proteins. One hundred and three proteins were found to be unique to PACIFY1 and 287 proteins were unique to PACIFY2. The differences in the unique proteins may be attributed to the additional three samples included in PACIFY2. Statistical analysis (t-tests) was performed on the relative protein abundances to identify notable changes in protein expression between sample timepoints. From PACIFY1, only 1 protein, Immunoglobulin heavy chain constant α-2, was found to be significantly different ($P<0.0167$) between pre-antibiotics and follow-up samples Table 4. In the PACIFY2 duplicate sample set, 8 total proteins were identified as being significantly different ($p<0.0167$).

Table 4. T-test results of PACIFY 1 identifying proteins of interest with significant changes between pre-antibiotics and post-antibiotic samples (*significance value set at 0.0167). Reproduced with permission from Tom Garfield.

Difference (Follow Up – Pre)			
Protein	*Mean (±SD)*	*95% CI*	*P-value**
Immunoglobulin heavy constant alpha 2	-0.00369 (0.00141)	(-0.0044, -0.00299)	0.0137

3.3.7 Proteins with significant changes between sampling timepoints include the protein of interest, Histone H4

When analysing the differences between timepoints from PACIFY2, pre-antibiotics v. post-antibiotics returned 3 proteins: Protein S100-A9, Histone H4 and Annexin A3. Pre-antibiotics v. follow up found 2 proteins: Histone H4 and α-1-antichymotrpysin. The t-test comparing post-antibiotics v. follow up returned 3 proteins: α-1-antitrypsin, immunoglobulin heavy constant gamma 1 and immunoglobulin heavy constant α-2 (Table 6/Table 7/Table 7 respectively).

Table 5. T-test results of PACIFY 2 identifying proteins of interest with significant changes between pre-antibiotics and post-antibiotic samples (*significance value set at 0.0167). Reproduced with permission from Tom Garfield.

Difference (Post-Pre)			
Protein	*Mean (±SD)*	*95% CI*	*P-value**
Protein S100-A9	-0.0094 (0.00736)	(-0.0118, -0.00694)	0.00501
Histone H4	-0.00241 (0.00203)	(-0.00308, -0.00173)	0.00748
Annexin A3	-0.00211 (0.00193)	(-0.00275, -0.00147)	0.0112

Table 6. T-test results of PACIFY 2 identifying proteins of interest with significant changes between pre-antibiotics and follow-up samples (*significance value set at 0.0167). Reproduced with permission from Tom Garfield.

Difference (Follow Up – Pre)			
Protein	*Mean (±SD)*	*95% CI*	*P-value**
Histone H4	-0.00194 (0.00117)	(-0.00241, -0.00146)	0.00983
α-1-antichymotrypsin	-0.00296 (0.00201)	(-0.00378, -0.00214)	0.0153

Table 7. T-test results of PACIFY 2 identifying proteins of interest with significant changes between post-antibiotics and follow-up samples (*significance value set at 0.0167). Reproduced with permission from Tom Garfield.

Difference (Follow Up – Post)			
Protein	*Mean (±SD)*	*95% CI*	*P-value**
α-1-antitrypsin	0.00272 (0.000736)	(0.00235, 0.00309)	0.00513
Immunoglobulin heavy constant gamma 1	0.0052 (0.00171)	(0.00434, 0.00605)	0.00895
Immunoglobulin heavy constant alpha 2	0.00437 (0.00178)	(0.00348, 0.00526)	0.0163

It was noted that of the proteins detected and calculated to have a higher than 1.5-fold change in abundance, histone H4 was of most interest since it shows a significant change between both pre-antibiotics and post-antibiotics, and pre-antibiotics to follow up samples. It also demonstrated a greater than 1.5-fold increase from post-antibiotics to follow up, although this change was not seen to be significant. It was hypothesised that histone H4 could therefore track with disease state, and the decrease in protein abundance might indicate a subsidence in infection with antibiotic treatment. Therefore, histone H4 was chosen for further protein validation via western blotting and to assess the association with patient biofilm biomass.

3.3.8 Validation of histone H4 biomarker potential with Western blotting

Only 16 samples were available for analysis and validation via western blotting. Histone h4 could only be detected in eight. Four pre-antibiotic samples, and four-post antibiotic samples were shown to contain histone H4. There were no detectable levels of H4 in any of the 4 samples tested from the follow up sample timepoint.

Due to low band intensity, accurate quantification of the visible bands was not possible. In the four incidences where matched pairs from pre- and post-antibiotic samples displayed histone H4 presence, a comparative analysis was carried out on the relative band intensity. Fold change calculations for individual patients showed two increases and two decreases in relative band intensity as seen in Table 8. Of these comparisons, a significant fold decrease ($P<0.01$) was

observed in UOS010 between pre antibiotics and post-antibiotics. In contrast, a significant fold increase (P<0.05) was noted in UOS022 between the pre and post antibiotic sample timepoints. Changes in the relative intensity for patient samples UOS002 and UOS007 were found to be non-significant.

Table 8. Fold-change in relative band intensity of histone H4 pre-antibiotic to post-antibiotic samples detected via western blotting. (* P<0.05, ** P<0.01, ns: P>0.05)

Patient	Fold Change	P Value	Significance (P=0.05)
UOS002	1.309	0.1894	ns
UOS007	-0.335	0.2773	ns
UOS010	-0.789	0.0010	**
UOS022	1.111	0.0206	*

The low intensities and small data set produced from the western blotting is not sufficient to validate the mass spectrometry findings mentioned above as the protein abundance cannot be accurately quantified with this current method.

3.3.9 The association of Histone H4 abundance with total biofilm biomass within the CF sputum

To assess the biofilm biomarker potential of the histone H4 protein within the CF sputum, the nanogram proportions were plotted against the average total sum of biofilm biomass for the patient samples that had the data available for comparison. This totalled 4 patient samples with the associated values for the proportion of histone H4 (Figure 14). The histone H4 proportion can be seen to decrease in all patient samples at the post antibiotic timepoint, and increase can also be seen in patients UOS001 and UOS011, however due to data unavailability, the same trend cannot be observed in the remaining two patients. In addition to this, UOS002 displays a decrease in both volume and H4 proportion, contrary to that seen in UOS011 and UOS022. Again, due to the unavailability of the appropriate data the biofilm volume cannot be displayed for the pre-antibiotics timepoint in UOS001, therefore, no conclusions can be confidently drawn between the association of average biofilm volume and the proportion of H4.

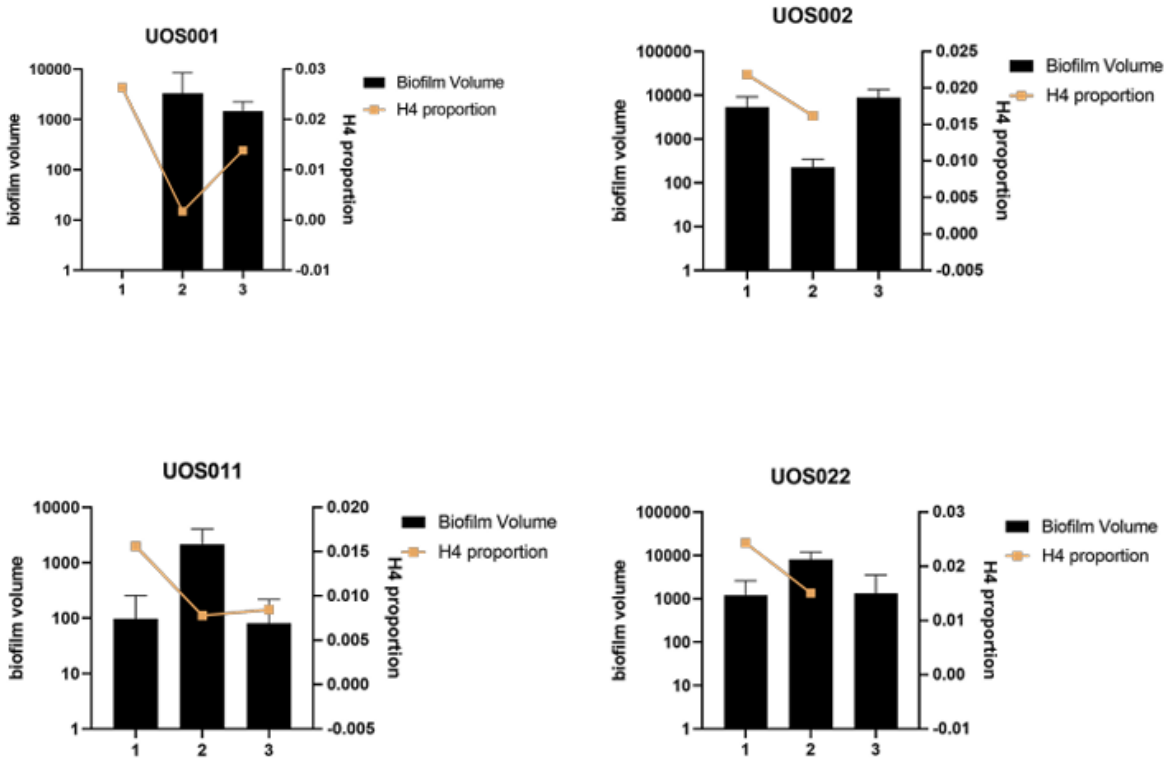

Figure 14. Association of average sum of biofilm volume with the relative proportion of histone H4 detected in CF sputum via mass spectrometry. Patients UOS001, UOS002, UOS011 and UOS022 are represented here.

3.3.9.1 Histone H4 shows no correlation with the total biofilm biomass.

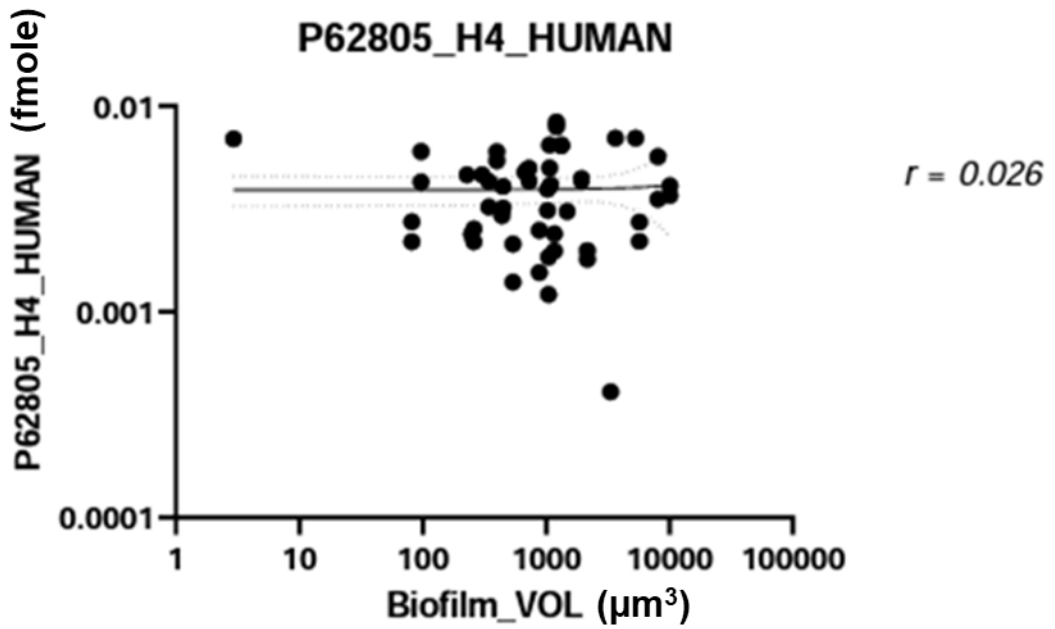

Figure 15 Correlation plot of all patients average total sum of biofilm volumes against the data available for the proportions of histone H4. Using Pearson's correlation coefficient, assuming normal distribution, the relationship between the two variables was assessed. Statistical analysis performed using GraphPad Prism (v9.0)

Using Pearson's correlation coefficient, the relationship between histone H4 and biofilm volume was assessed across the whole patient cohort (Figure 15). A total of 52 pairs were analysed, but no linear correlation was found (r = 0.0268), highlighting an in H4 abundance does not equal an increase in biofilm volume or vice versa. This casts doubt on the biomarker potential of histone H4 for tracking the biofilm phenotype and CF lung disease state.

3.4 Discussion

3.4.1 The use of FISH was successful in the characterisation of biofilm status but highlights patient variability.

Image analysis showed no global change in the biofilm biomass across the whole cohort of patients included within the study. However, the patient specific observations are of great interest in that some individuals responded well to antibiotic intervention with a reduction in biofilm volume, whereas on the contrary, an observed increase in biomass occurred in others. This chapter highlights the need for personalised approaches to the treatment strategies to implicated in the clinic as not all patients will respond to the same treatments, and in the perfect

scenario each patient would have an in-depth analysis of microbiological findings and the antimicrobial susceptibility profiles assessed before their administration. Although, in the case of exacerbation, and in many cases of routine clinical practise it would not be beneficial to the patient health to delay antibiotics whilst awaiting culture results. A more rapid methods for the determination of bacterial species and antimicrobial susceptibility would be required.

The biofilm phenotyping of sputum from CF patients with FISH has been successful in characterising the biofilm status. In patients where biomass is reduced as expected e.g., UOS004, the fall in biomass at the post-abx timepoint suggests the treatment used was effective at disturbing the established biofilm and successful in bacterial killing. However, it would appear that total eradication of the biofilm was not achieved, therefore, it could be suggested that the remaining *P. aeruginosa* cells were able to proliferate and establish a new infection once the antibiotic pressure had been removed, as might be expected of the biofilm lifecycle. The increase observed in biofilm biomass in patients UOS007 and UOS011, could be indicative that a sub-inhibitory concentration of antibiotic agent was administered, and multiple studies have elucidated that low concentrations could be detrimental to patient health (Olivares et al. 2020). Sub-inhibitory concentrations of ciprofloxacin lead to the selection of mutants that display high level resistance, and low levels of fluroquinolones showed induced phenotypic changes and decreased protease activity and swimming motility, favouring a sessile state with increased quorum sensing signalling (Jørgensen et al. 2013; Wassermann et al. 2016). Patient records identifying which antibiotics were specifically used were not available, however, future analyses into this may point towards an explanation as to why the biofilm biomass did not behave as expected.

A limitation of this study may also arise from the nature of the sputum sample given, an unassisted expectoration for sputum is not fully representative of the whole lung microbiota and may reflect different microbiological profiles (Aridgides et al. 2021; Meskini et al. 2021). However, it would not be feasible to elect to perform BAL when patient is already admitted to hospital undergoing exacerbation solely to provide a sample that may be more representative of the whole lung if a patient is unable to produce sputum. Another limitation of the FISH imaging in this study is the lack of a “non-sense” negative control to identify any non-specific binding of the target probes of interest and adjust the experimental conditions as necessary to reduce unwanted background noise (Batani et al. 2019).

3.4.2 Biomarker potential of histone H4

The potential association of the proteomics data to that of the observed biofilm biomass shows promise, histone H4 has previously been reported in acute lung injury primarily associated with chromatin remodelling and DNA replication in conjunction with others in the histone family (Ruan et al. 2015) but has also been implicated in other inflammatory and infection roles. Histone H4 expression has be illustrated to indicate chronic lung infections such as smoking-induced chronic obstructive pulmonary disorder (Sundar et al. 2014). The biomarker potential of histone H4 is also supported by additional research that similarly investigates the proteomic profiles of CF patient sputum, Pattison et al., profiled the proteome of sputum collected from 12 CF patients chronically infected with *P. aeruginosa* found a high abundance of H4 (Pattison et al. 2017) and thus, could have potential as a biomarker if found to accumulate in the presence of a biofilm infection.

Despite optimisation of the western blot protocol, the necessary sensitivity was not achieved for such a low abundance protein. Histone H4 is also a protein of small size ~11kDa that could potentially pass through the nitrocellulose membrane and result in protein loss. To avoid this, a slower transfer from the gel to the membrane could be used, or the transfer step could be avoided completely by performing immunostaining of the polyacrylamide gel itself to reduce any loss of protein. Alternatively, and enzyme-linked immunosorbent assay (ELISA) can be used. Commercial histone H4 ELISA kits are readily available (Abcam, UK) with sensitivity advertised as low as 0.5ng/well, this assay may also be more financially viable, and faster than western blotting should more samples need processing in the future.

3.4.3 Conclusions

The findings of this chapter are, unfortunately, limited. The presence of histone H4 was only identified by mass spectrometry in one of the duplicate sample sets, PACIFY2. This may be due to the fact the sample size of PACIFY2 was larger and gives a better representation of the proteome. Not all samples that were received were processed for certain experiments thus samples could not be properly paired across timepoints for accurate comparison e.g., histone proportions missing in follow up samples. Further analysis in a new subset of patients, and potentially a larger cohort would be required to remedy these limitations along with more meticulous sample collection and record keeping, however due to the nature of the samples required, this may come at a significant cost in both monetary and time. Based upon this, conclusions cannot confidently be drawn about the associations of biofilm volume and the CF sputum proteome ability to predict the biofilm phenotype within the cystic fibrosis lung and the original hypothesis can be rejected.

In the individual patients where total eradication of the biofilm was not achieved, a combination therapy with a dispersal agent may result in increased bacterial clearance. With the dispersal of larger *P. aeruginosa* aggregates, the planktonic cells are rendered more susceptible to the antibiotics used. Nitric oxide donor drugs with dual action of both biofilm dispersal and bactericidal activity i.e., C3D compounds as previously discussed, may be appropriate in this situation. Thus, the role of NO in dispersing these biofilms formed by clinical isolates must be explored.

Chapter 4 Characterisation of the NO dispersal response in clinical *P. aeruginosa* CF isolates.

4.1 Introduction

As reported in the previous chapter, antibiotics may not always be capable of clearing a biofilm infection, and small biofilm aggregates remain. The utilization of an adjunctive therapy to aid in the removal of these persistent aggregates would be beneficial. Nitric oxide (NO) has previously been shown to induce a biofilm dispersal response in laboratory strains of PAO1 and is a promising therapeutic for the treatment of bacterial biofilms. However, the patient variability emphasized in the previous chapter is not exclusive to the use of antibiotics; previous observations note differing response to the NO dispersal signal from NO donor prodrugs (cephalosporin-3'-diazeniumdiolates), and SNP in clinical isolates when tested in vitro (Soren 2018). Isolates were shown to vary with some showing the expected dispersal, and other conversely showing an increase in biofilm biomass.

Soren (2018), elucidated that there was an apparent correlation between the response of the isolate to NO and the biofilm forming ability, and moderate correlation with the planktonic growth rate. Of the isolates tested, those that successfully dispersed in response to NO produced better biofilms and had a faster planktonic growth rate, and those that were not dispersed presented poor or moderate biofilm formation and a slower planktonic growth rate.

Soren performed dispersal experiments on predominantly 'good biofilm formers' with moderate planktonic growth rates. Building on this observation, here we assess an extended panel totalling 10 *P. aeruginosa* isolates obtained from the sputum of Cystic fibrosis patients at the University hospital Southampton that were determined to be poor biofilm formers with a slow planktonic growth rate. These additional isolates were assessed for their NO dispersal response utilizing the

classical crystal violet biofilm assay with the aim of further identifying the growth rate and biofilm forming capability of clinical isolates is responsible for the varied NO response.

4.2 Results

4.2.1 Several isolates display the expected, dispersing phenotype with the low-dose dispersal trigger, NO

To investigate the varied effects of NO mediated dispersal, a CV staining method was used to quantify the biofilm biomass. Forty-eight-hour biofilms were treated with differing concentrations (0.25-64μM) of the NO donor SNP, to produce a dose response curve. The laboratory strain control, PA01, can be seen to disperse in a dose dependant manner starting at a 500nM concentration (Figure 16A), corresponding planktonic values (Figure 16A Left) are also increased at these concentrations indicating a release of cells from the biofilm into the surrounding media. A similar trend to the control can be seen in isolates PA55 and 57 (Figure 16 B and C left) with significant reductions in biofilm biomass and concomitant increase in planktonic values (Figure 16 B and C right).

4.2.2 Several patient Isolates show an increase in biofilm biomass with the low-dose dispersal trigger, NO

Interestingly, increased biofilm biomass was observed in several isolates. PA15, PA37, and PA49 (Figure 17 ABC) all show an increase in biomass after SNP treatment, though this again varies between strains with the highest increases seen at differing concentrations.

4.2.3 A number of patient Isolates show no response to the low-dose dispersal trigger, NO

Isolates PA31, PA39, and PA44 (Figure 18 ABC), when treated with SNP display minimal changes to the biofilm biomass, however PA39 CV values show a large amount of error, and its associated planktonic values (Figure 18B right) show a significant increase in the concentration range between 250nM and 8μM. This suggests that bacterial cells are in fact being dispersed from the biofilm after NO treatment.

4.2.4 Some patient isolates display atypical response to NO

PA05 (Figure 19A) at first glance appears to disperse and have significantly reduced biomass at the 250nM concentrations, however when compared to the planktonic values at the same concentrations, the planktonic value is observed to also decrease, indicating a cytotoxic, rather

than dispersal effect. PA08, is described as having very slow growth in planktonic culture, this may also be reflected in the biofilm culture. Planktonic values shown in Figure 19B left, display no growth within the media in the control group. The significant increase in value at 4µM may be attributed to contamination with another organism forming biofilm, this would also correlate to the increase in biofilm biomass at 4µM (Figure 19B right).

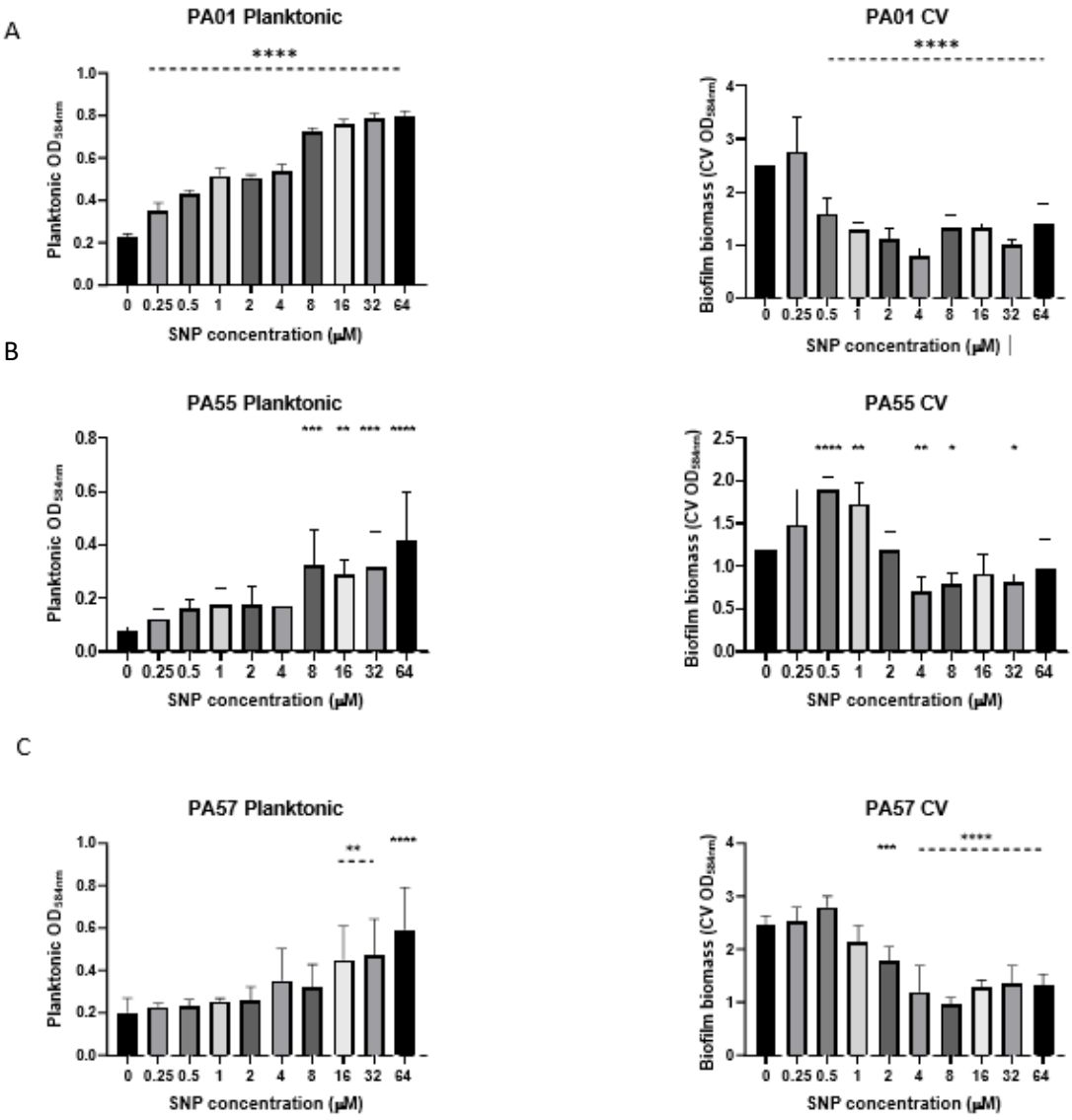

Figure 16. Biofilm dispersal profile of bacterial isolates that respond to the dispersal inducing signal, NO. Strains shown include the laboratory isolate PA01 (A), and clinical isolates PA55 (B), and PA57 (C). Mean planktonic cellular density (left) and biofilm biomass quantified by crystal violet staining (right) are represented by n=6 technical replicates with a 0.25- 64μM concentration range of NO donor, SNP. Asterisks represent the significance values from a one-way ANOVA with Tukey's multiple comparisons to the control group (0 μM SNP) (*- P= 0.0332, **- P= 0.0021, ***- P=0.0002, ****- P=<0.0001) Dashed lines represent the significance value of those concentrations encompassed beneath. Statistical analysis was performed in GraphPad Prism (v9.0 GraphPad Software Inc.). Experiments were repeated three times with similar results.

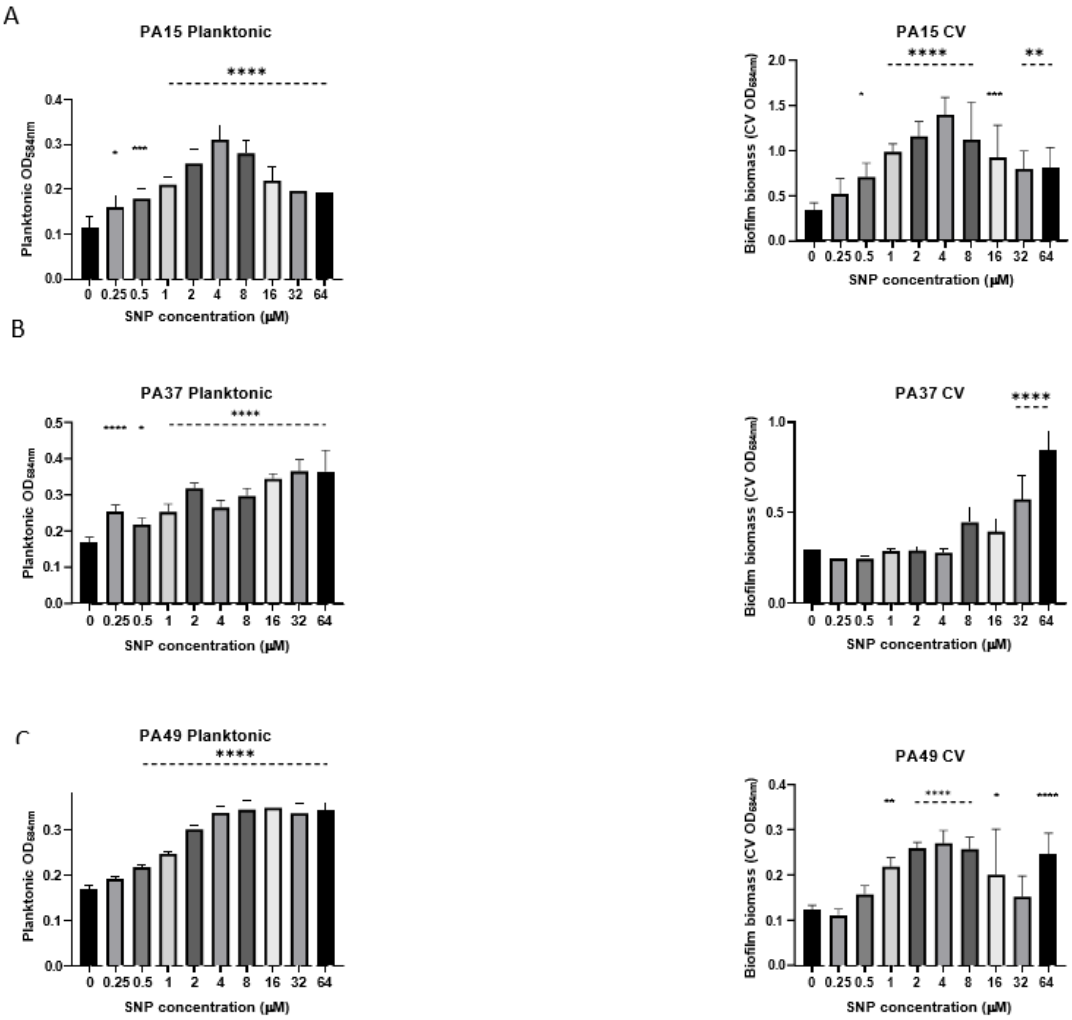

Figure 17. Biofilm dispersal profile of bacterial isolates that show an increase in biofilm biomass when exposed to the dispersal inducing signal, NO. Strains shown include the clinical isolates PA15 (A), PA37 (B), and PA49 (C). Mean planktonic cellular density (left) and biofilm biomass quantified by crystal violet staining (right) are represented by n=6 technical replicates with a 0.25-64μM concentration range of NO donor, SNP. Asterisks represent the significance values from a one- way ANOVA with Tukey's multiple comparisons to the control group (0 μM SNP) (*- P= 0.0332, **- P= 0.0021, ***- P=0.0002, ****- P=<0.0001) Dashed lines represent the significance value of those concentrations encompassed beneath. Statistical analysis was performed in GraphPad Prism (v9.0 GraphPad Software Inc.). Experiments were repeated three times with similar results.

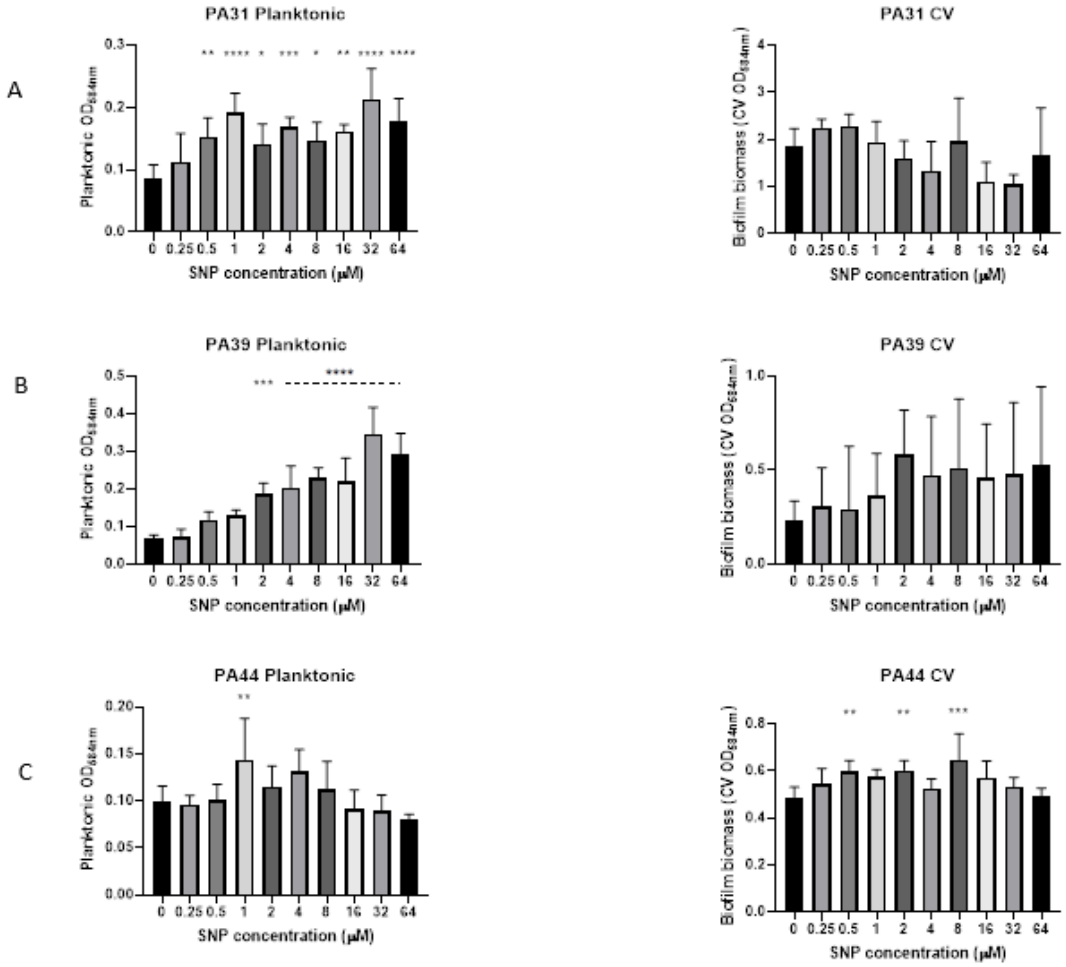

Figure 18. Biofilm dispersal profile of bacterial isolates that do not respond to the dispersal inducing signal, NO and show little to no change in biofilm biomass. Strains shown include the clinical isolates (A), and clinical isolates PA55 (B), and PA57 (C). Mean planktonic cellular density (left) and biofilm biomass quantified by crystal violet staining (right) are represented by n=6 technical replicates with a 0.25-64µM concentration range of NO donor, SNP. Asterisks represent the significance values from a one-way ANOVA with Tukey's multiple comparisons to the control group (0 µM SNP) (*- P= 0.0332, **- P= 0.0021, ***- P=0.0002, ****- P=<0.0001) Dashed lines represent the significance value of those concentrations encompassed beneath. Statistical analysis was performed in GraphPad Prism (v9.0 GraphPad Software Inc.). Experiments were repeated three times with similar results.

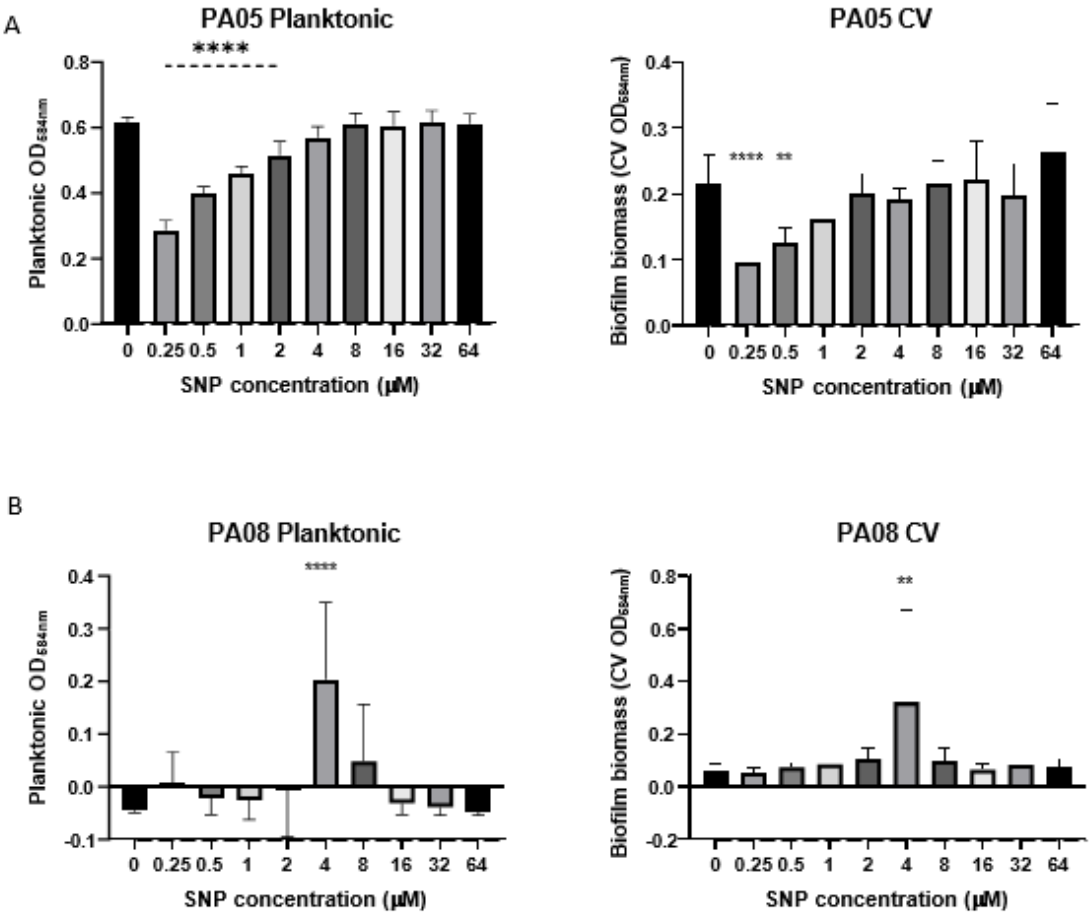

Figure 19. Biofilm dispersal profile of bacterial isolates that showed atypical responses when exposed to the dispersal inducing signal, NO. Strains shown include the clinical isolates PA05 (A), and PA08 (B). Mean planktonic cellular density (left) and biofilm biomass quantified by crystal violet staining (right) are represented by n=6 technical replicates with a 0.25-64µM concentration range of NO donor, SNP. Asterisks represent the significance values from a one-way ANOVA with Tukey's multiple comparisons to the control group (0 µM SNP) (*- P= 0.0332, **- P= 0.0021, ***- P=0.0002, ****- P=<0.0001) Dashed lines represent the significance value of those concentrations encompassed beneath. Statistical analysis was performed in GraphPad Prism (v9.0 GraphPad Software Inc.) Experiments were repeated three times with similar results.

4.3 Discussion

In this chapter, we further explored and built upon the previously observed effects of NO on biofilms formed by CF isolates of *P. aeruginosa*. A classical crystal violet assay identical to that used by Soren, 2018 was used to determine the dispersal phenotype in an extended panel of clinical isolates. Soren had previously characterised the dispersal response in nine *P. aeruginosa* isolates that predominantly showed fast planktonic growth rates, and hypothesised a slower growth rate may be associated with a varied NO response. Therefore, we characterise a further ten isolates determined to be slow growing.

4.3.1 Isolates with slow growth rates show varied responses to NO

Interestingly, despite the isolates tested in this study being of slow planktonic growth rate and poor biofilm forming ability, they did not share the expected dispersal response to NO. It may have been expected from previous findings that all the isolates would have resisted the NO dispersal signal, however this subset of isolates again showed varied responses. Three distinct phenotypes were identified:

- Dispersing with biofilm biomass reduction in response to low dose NO.
- No change in biofilm biomass in response to low dose NO.
- Growth promotion and biofilm biomass increase in response to the NO dispersal signal.

These findings are of great interest, and the mechanisms of which still need to be fully elucidated. (Barraud et al. 2006), demonstrated that there is an optimal concentration range of SNP within PA01 for biofilm dispersal, whereby if outside of this range, promotion of biofilm can occur. Some preliminary experiments were performed with an extended range of SNP concentration for selected isolates (data not shown), but an optimal dispersal concentration was unable to be identified. Due to the labour intensity of the dispersal assay, this was not performed for all isolates.

A possible explanation of the varied response to NO may come from the ability of *P. aeruginosa* to adapt to its environmental niche. It is noted that the mucus in the CF lung creates hypoxic regions in which *P. aeruginosa* can grow due to its ability to grow in anaerobic environments (Worlitzsch et al. 2002). Line et al. 2014 , demonstrated that *P. aeruginosa* isolates from CF sputum acquired energy for growth in anoxic sputum by use of the anaerobic denitrification pathway. This pathway as described previously is both induced by the detection of NO by DNR and is also a constituent

metabolite of the same pathway, being reduced to N_2O by NorCB (Arai 2003; Schreiber et al. 2007; Arat et al. 2015).

This theory may explain the varied response to NO, if the isolates are adapted to hypoxia, and favour the denitrification pathway, they may utilise the NO as a metabolite to support growth, rather than recognising NO as a dispersal signal. It has been shown that in the CF sputum there are physiological levels of nitrate that can support the anoxic growth of *P. aeruginosa* with a slower growth rate (Line et al. 2014). This corroborates the theory that the non-dispersing isolates are using NO as a nutrient source and for upregulation of denitrification.

The findings in this chapter give an extended insight to the variation observed between clinical isolates in response to NO biofilm treatment. Only two out of the ten clinical isolates tested displayed NO mediated biofilm dispersal, with five isolates (to varying degrees), showing increases in biofilm biomass. The results shown above, illustrate that the optimal range may differ greatly depending on the isolate, this opens the question as to why this might be the case and the mechanisms involved which will be further explored throughout this study.

Chapter 5 Comparative Genomics of *P. aeruginosa* isolates from CF patients

5.1 Introduction

With the increasing accessibility and affordability of next generation sequencing in the past couple of decades, whole genome sequencing (WGS) has become a pivotal tool for the study of bacterial genomics. Modern day long read sequencing in conjunction with advanced bioinformatics tools can achieve high depth and resolution required to characterize the genomic features of bacterial isolates quickly and easily.

The complete set of genes that are present in a bacterial species is often referred to as the pangenome. This pangenome can be further divided into the core genome that includes those genes that are present in all isolates, and the cloud/ accessory genome containing genes that are only present in select isolates (Costa et al. 2020). The relatedness of bacterial isolates from the same or distinct species can be accessed via phylogenetics, that can be based upon the alignment of single nucleotide polymorphisms found within the core genome (Shakya et al. 2020).

Study of the genome allows in depth genotype identification and phenotypic predictions for isolates and may be useful in determining antimicrobial resistance profiles, biofilm formation ability, quorum sensing systems, and virulence factors. *P. aeruginosa* has a large and diverse dynamic genome composition ranging from 5.5 to 7 Mbp enabling survival in wide range of conditions, not just in cystic fibrosis patients (Stover et al. 2000; Aujoulat et al. 2012; Alhede et al. 2014).

Aside from the biofilm structures, the prevalence of infections of *P. aeruginosa* in cystic fibrosis can partly be attributed to the native genes present in the core genome that result in intrinsic resistance to antibiotics, this is further enhanced buy the ability of *P. aeruginosa* to acquire resistance through transferable resistance determinants and genomic mutational selection (Moradali et al. 2017; De Oliveira et al. 2020). The transfer of these resistance determinants can be seen to be increased within a close-knit community such as a biofilm (Madsen et al. 2012). This leads to both highly resistant planktonic bacteria alongside the increased tolerance provided from the biofilm, further exacerbating the complexities with complete biofilm eradication. The ability to use NO as a dispersal agent for *P. aeruginosa* biofilm aggregates within the CF lung would be beneficial for the effective treatment of chronic infection and better patient response to antibiotic therapies as has previously been demonstrated (Howlin et al. 2017).

As discussed in the previous chapter, the dispersal response differs between the clinical isolates that have been profiled. Elucidating the underlying mechanisms behind the observed in their dispersal response to NO is important for clinical CF diagnostics. Genomic diversity within *P. aeruginosa* isolates obtained from CF patients can be distinct across sub-compartments of the lungs due to localised adaptations (Caballero et al. 2015; Jorth et al. 2015; Kordes et al. 2019). These adaptations may provide insight as to the dispersing or non-dispersing phenotypes observed. Key genes responsible for NO signal transduction and downstream effects, particularly phosphodiesterase's and diguanylate cyclase for the turnover of c-di-GMP, may be absent or altered in the atypical non-dispersing phenotype. With the advancements and increasing accessibility of next generation sequencing, the potential for non-invasive diagnostics and characterisation is being realised (Feigelman et al. 2017). The results of this chapter may benefit future patients, with further advances in next generation sequencing, gene identifiers and rapid genomic diagnostics may predict whether a patient would be suited to a low dose NO-based therapy.

This chapter aims to explore the genomic variability in the whole genomes of 15 clinical CF *P. aeruginosa* isolates from UHS that have a range of responses to low dose nitric oxide treatment to established biofilms and identify any gene adaptations that may indicate why an atypical response to the NO dispersal signal occurs. The bacterial isolates were sequenced, and comparative genomic analyses was conducted to identify the multi locus sequence type, genomic divergence relationships, antibiotic resistance profiles, and other factors that may influence the NO dose response.

5.2 Results

The panel of 17 clinical CF isolates were sequenced utilising long read sequencing on an Oxford Nanopore sequencing device as previously described. Here the features of the sequencing dataset are explored, including phylogeny, MLST, and gene presence/ absence for those identified to be involved in both the P aeruginosa denitrification pathway, and NO dispersal induction pathways.

5.2.1 Genomic features of 15 clinical *P. aeruginosa* strains

The genomic features of the isolates sequenced are displayed in Table 9. Isolates PA05, PA08, and PA39 are excluded from these analyses as there was insufficient quantity/ quality of DNA required for the sequencing library preparation. All genomes are shown to have a coverage depth of greater than 29x. A sequencing coverage depth of >30x is recommended for increased accuracy in

the downstream genome assembly (Wang et al. 2021). All genomes are circular and can be assumed to be complete in their assembly with no unmapped regions of the chromosome. Genomes are also of the expected size for *P. aeruginosa*.

5.2.2 Metagenomic analysis of isolates identifies species other than *P. aeruginosa*.

The isolates PA44 and PA56 are not the species expected, Kraken2 database report for metagenomic classification revealed these isolates to be *Achrombacter xylosoxidans,* rather than *P. aeruginosa.* A representative Sankey plot was produced using the metagenomics visualiser, Pavian (Breitwieser and Salzberg 2020). Figure 20 shows the metagenomic classification of reads from the isolate, PA44. Given that PA44 and PA56 are not the target species for this study, they have been excluded from further analysis.

Table 9. General features of the *P. aeruginosa* clinical isolates sequenced in this study; table shows the individual isolates sequencing coverage, and genome length. All genomes were assembled into a single circular contig Sequences were compared against a Kraken 2 database for species identification. All isolates were identified as *P. aeruginosa* except for PA44 and PA56 that were identified as *A. xylosoxidans.*

Isolate	Coverage (x)	Length(bp)
PA05	104	6344833
PA10	62	6357454
PA15	85	6542181
PA20	169	6542012
PA21	54	6845339
PA26	112	6384810
PA30	69	6846781
PA31	92	6545497
PA37	94	6198265
PA44	55	6968452
PA47	92	6500040
PA49	68	6262477
PA55	151	6542061
PA56	29	6852559
PA57	108	6319234
PA66	91	6707157
PA68	83	6763763

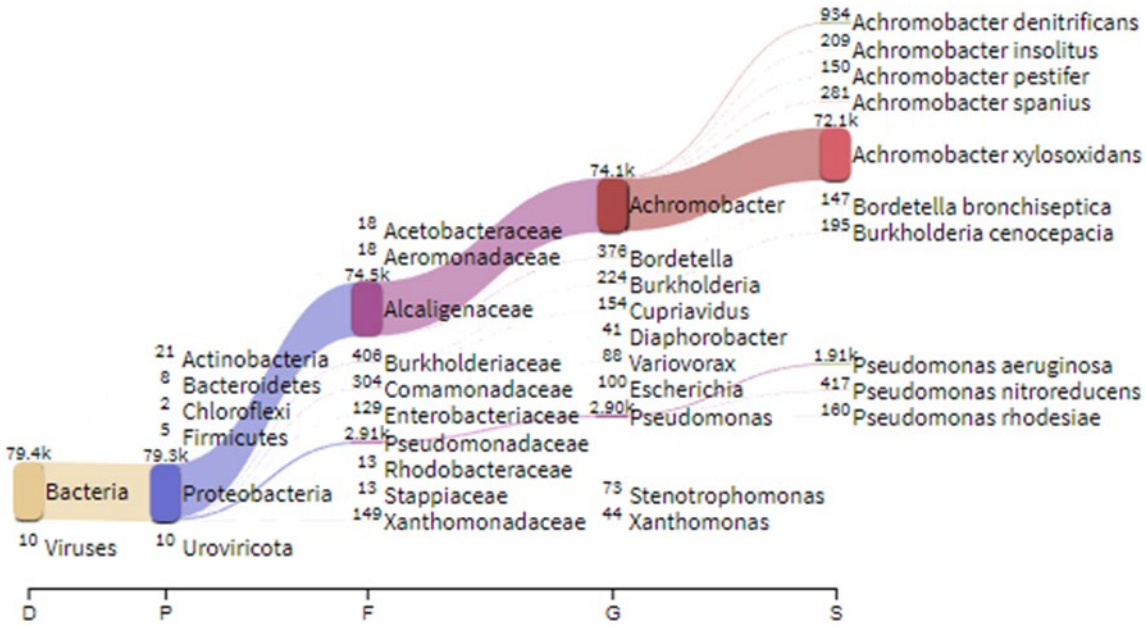

Figure 20. Sankey plot of isolate 'PA44' created from Kraken2 database reports of metagenomic classification. Plot shows the isolate originally thought to be *P. aeruginosa* to contain reads predominantly from the species, *Achromobacter xylosoxidans*. Sankey plot produced using Pavian.

5.2.3 Phylogeny and MLST of 13 *P. aeruginosa* clinical isolates in relation to the NO dispersal phenotype

A maximum likelihood phylogenetic tree was constructed using a core genome alignment with Parsnp. The multifasta alignment output from Parsnp was visualised visualised using iTOL (Interactive Tree of Life). The phylogenetic tree in Figure 21 shows clustering of the isolates into multiple different clades of relatedness, the numbers on each branch represent the isolate age whereby the most distantly related to the reference, PA01, is equal to 0. The value of the age increases the more closely related. It can be seen in Figure 21 that PA05 is very distantly related to that of the reference and all other isolates analysed here. The isolate PA68 is the mostly closely related to the reference genome with an age of 1.385, followed by the clade of 5 isolates PA31, PA47, PA15, PA55, and PA20 with an age of 1.371.

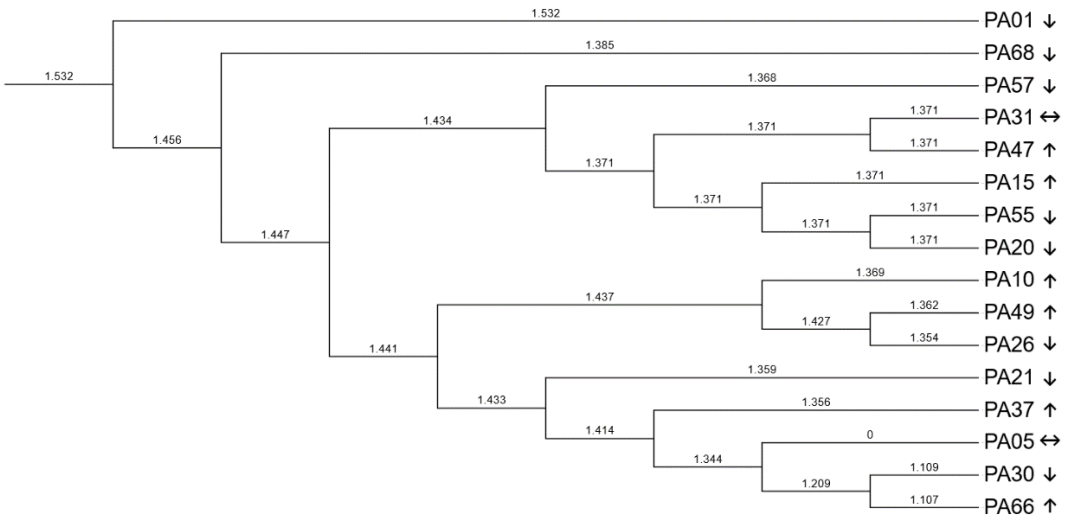

Figure 21. Phylogenetic tree showing the evolutionary history and relatedness of 15 *P. aeruginosa* clinical isolates rooted to the reference genome PA01 (NC_002516.2). Branch labels are displayed as age, with the farthest related leaf from the reference has the age, 0 (PA05). The age is seen to increase as the isolates are more closely related to the comparator PA01. The dispersal phenotype is denoted by arrows (↓ = dispersing, ↔ = no change, ↑ = growth promotion). Tree created using Parsnp core SNP maximum likelihood, and view and annotated with iTOL (Interactive Tree of Life).

The sequence types STs listed in Table 10 are generated by blasting the genome sequences against the PubMLST database to identify the alle numbers for the house keeping genes acsA, aroE, guaA, mutL, nuoD, ppsA, and trpE. Some of the isolates, namely PA10, PA26, PA57, and PA68, have multiple exact matches for the trpeE gene. Following a manual search of the alle numbers in the PubMLST database, only the first mentioned allele number returns a ST match, therefore, here we accept the first allele number e.g., PA68 trpE *n*321 does not equal a known ST, thus we use *n*7 to return the known ST17. Similarly, in PA26, mutL identifies a novel full-length allele similar to the exact known allele (>80% match), here we can presume the identity to be *n*2 resulting in ST399.

The clade containing the 5 clustered isolates as mentioned above, can be seen to share the same ST146 in Table 10, unsurprising given they also share the same age. All other isolates harbour unique STs despite close relatedness, for example, PA30 and PA66 are closely related by age, but do not share sequence types (1.109, 1.107, and ST253, ST532 respectively).

Table 10. Multi Locus Sequence Type of 13 *P. aeruginosa* clinical isolates. The sequence type (ST) displayed are generated from the alle number for the house keeping genes acsA, aroE, guaA, mutL, nuoD, ppsA, and trpE. Sequence types were generated using the mlst packsack (Tseemann) by BLASTing the isolates nucleotide sequences against the PubMLST database. A novel identified full-length allele similar to the exact allele is indicated by '~n', and multiple alleles or ST by '/'. The dispersal phenotype is denoted by arrows (↓ = dispersing, ↔ = no change, ↑ = growth promotion)

Isolate	**Dispersal Phenotype**	**Sequence Type**	**acsA**	**aroE**	**guaA**	**mutL**	**nuoD**	**ppsA**	**trpE**
PA05	↔	1716	68	106	85	92	72	54	72
PA10	↑	262/-	17	5	1	3	4	15	7/321
PA15	↑	146	6	5	11	3	4	23	1
PA20	↓	146	6	5	11	3	4	23	1
PA21	↓	1858	17	2	11	3	81	38	3
PA26	↓	399/-	11	5	1	~2	2	15	2
PA30	↓	253	4	4	16	12	1	6	3
PA31	↔	146	6	5	11	3	4	23	1
PA37	↑	443	15	5	5	5	50	4	1
PA47	↑	146	6	5	11	3	4	23	1
PA49	↑	217	28	5	11	18	4	13	3
PA55	↓	146	6	5	11	3	4	23	1
PA57	↓	274/-	23	5	11	7	1	12	7/ 321
PA66	↑	532	5	4	5	5	5	20	4
PA68	↓	17/-	11	5	1	7	9	4	7/ 321

Curiously, there appears to be no clustering of either related isolates or those that share STs with the response to the NO dispersal signal. The ST146 isolates are noted to still have varied responses to NO despite being so closely related. These isolates do however share same SCV morphology, planktonic growth rate and biofilm forming ability as determined by Soren 2018 (Table 1). Other isolates do not share these characteristics.

5.2.4 Relationship between NO dispersal response and the presence of genes within the nitrate metabolic pathway.

To identify if genomic features in specific pathways were responsible for the varied NO response a gene presence/absence matrix for genes known to play a role in the denitrification pathway of *P. aeruginosa*. A custom database was created for blasting against genome sequences with ABRicate, the database included the following genes: nitrate reductase (NarGHI); nitrite reductase (NirS); nitric oxide reductase (NorCB); nitrous oxide reductase (NosZ); the major regulator Anr; the nitrate sensing two component system NarXL; and Dnr as identified in Figure 6, Chapter 1. In addition to this fhp, a flavohaemoprotein that shows detoxification of NO was included (Arai et al. 2005; Koskenkorva-Frank and Kallio 2009) Genes were identified as present if the sequences possessed ≥80% coverage of the gene sequence identity. As can be seen in Figure 22, all genes are present in each isolate regardless of the observed NO dispersal response with a ≥99.7% coverage of all present genes.

5.2.5 Relationship between NO dispersal response and the presence of genes known to be involved with the NO dispersal induction pathway.

To identify if genomic gain or loss was responsible for the varied NO response a gene presence/absence matrix for genes known to be involved with the turnover of c-di-GMP and the NO dispersal induction pathway in *P. aeruginosa*. A custom database of encoding proteins capable of reducing the c-di-GMP with known activities of DGC and PDE, and those with response to the NO signal was created to blast against genome sequences. This database includes bdlA; dipA; mucR; nbdA; pilZ; fimX; and fleQ as discussed in section 1.5.2 and 1.7.2.1. The database also includes PA0575, PA1181, PA1930, PA2072, PA2133, bifA, morA, and rocR that show PDE and DGC activity in the NO induced turnover of c-di-GMP. Genes were marked as present if sequence coverage was >80%.

In a similar fashion to the genes identified in Figure 22, Figure 23 shows that almost all genes are present in all isolates except for PA05, which does not possess the gene encoding for the protein

PA1390. All other genes are present in each isolate regardless of the observed NO dispersal response with a ≥99.95% coverage of all present genes.

		Gene												
Isolate	Dispersal Phenotpye	anr	dnr	fhp	narG	narH	narI	narL	narX	nirQ	nirS	norB	norC	nosZ
PA01	↓	■	■	■	■	■	■	■	■	■	■	■	■	■
PA05	↔	■	■	■	■	■	■	■	■	■	■	■	■	■
PA10	↑	■	■	■	■	■	■	■	■	■	■	■	■	■
PA15	↑	■	■	■	■	■	■	■	■	■	■	■	■	■
PA20	↓	■	■	■	■	■	■	■	■	■	■	■	■	■
PA21	↓	■	■	■	■	■	■	■	■	■	■	■	■	■
PA26	↓	■	■	■	■	■	■	■	■	■	■	■	■	■
PA30	↓	■	■	■	■	■	■	■	■	■	■	■	■	■
PA31	↔	■	■	■	■	■	■	■	■	■	■	■	■	■
PA37	↑	■	■	■	■	■	■	■	■	■	■	■	■	■
PA47	↑	■	■	■	■	■	■	■	■	■	■	■	■	■
PA49	↑	■	■	■	■	■	■	■	■	■	■	■	■	■
PA55	↓	■	■	■	■	■	■	■	■	■	■	■	■	■
PA57	↓	■	■	■	■	■	■	■	■	■	■	■	■	■
PA66	↑	■	■	■	■	■	■	■	■	■	■	■	■	■
PA68	↓	■	■	■	■	■	■	■	■	■	■	■	■	■

Figure 22. Presence/absence matrix for genes within the denitrification pathway of *P. aeruginosa*. Nucleotide sequences for *P. aeruginosa* clinical isolates were blasted against a custom database using ABRicate. Genes were identified as present if the sequences possessed ≥80% coverage of the gene sequence identity. Present genes are represented by a blue square, and those absent represented by white. All genes identified as present here have ≥99.7% coverage. The dispersal phenotype is denoted by arrows (↓ = dispersing, ↔ = no change, ↑ = growth promotion)

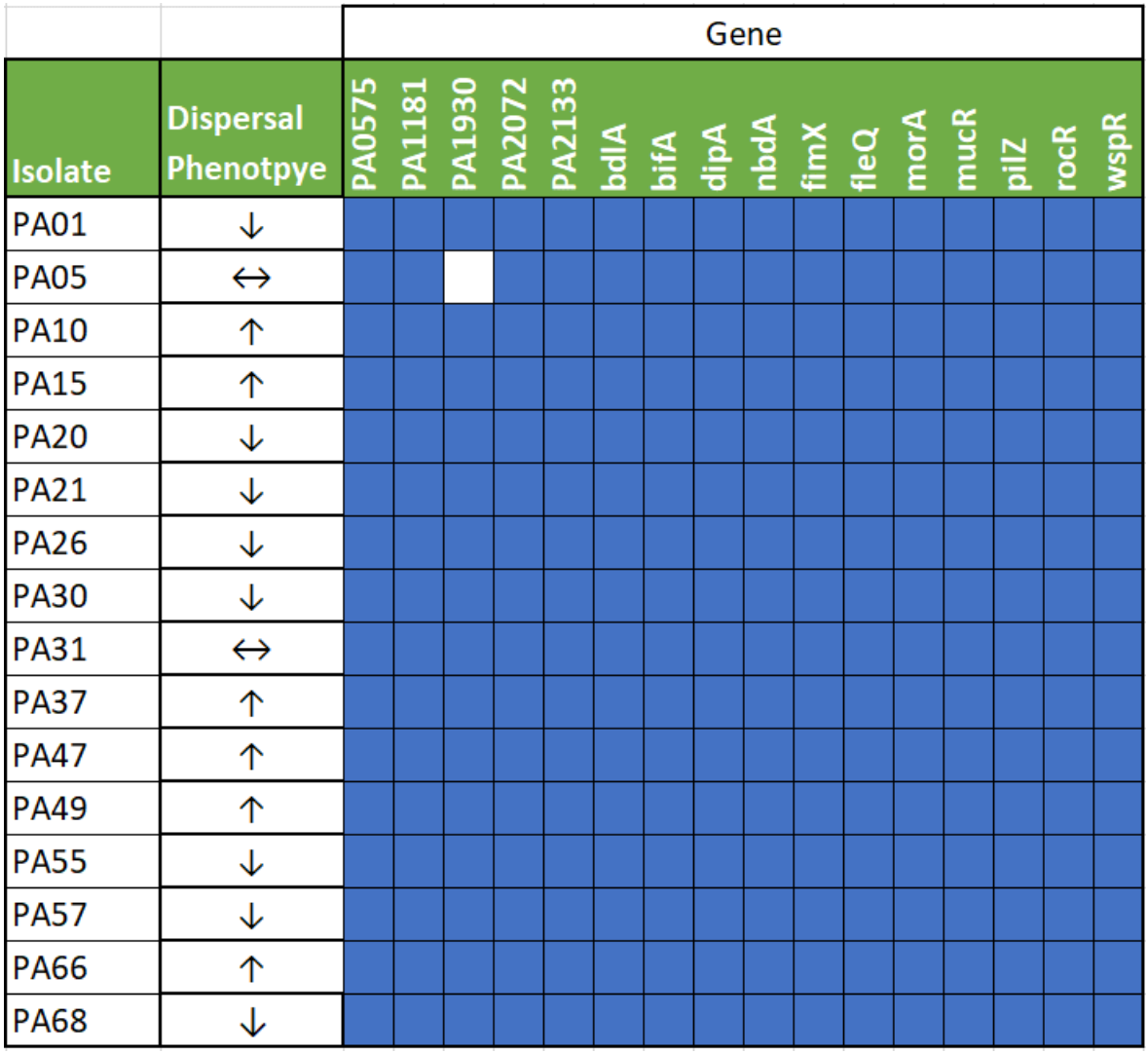

Figure 23. Presence/absence matrix for genes encoding for proteins that contain EAL domains, and genes identified to play a role within the induction pathway of *P. aeruginosa* nitric oxide dispersal. Nucleotide sequences for *P. aeruginosa* clinical isolates were blasted against a custom database using ABRicate. Genes were identified as present if the sequences possessed ≥80% coverage of the gene sequence identity. Present genes are represented by a blue square, and those absent represented by white. All genes identified as present here have ≥99.95% coverage. The dispersal phenotype is denoted by arrows (↓ = dispersing, ↔ = no change, ↑ = growth promotion)

5.3 Discussion

This chapter set out to identify if any genomic features in each of the isolates were responsible for the varied responses seen to the NO dispersal signal. Utilising a range of methods to analyse the whole genome sequence data, most isolates were as expected with genome sizes ranging between 6.3-6.8 Mbp as would typically be expected from *P. aeruginosa* (Klockgether et al. 2010). Sequencing was largely successful, however with some unexpected results and no markers found indicating an influence on the overall dispersal phenotype.

5.3.1 Metagenomic analysis reveals misidentification of bacterial species.

The results of the Kraken2 database to classify reads to a bacterial species showed that two isolates, PA44 and PA56, previously thought to be *P. aeruginosa* were in fact *A. xylosoxidans.* This bacterium is an emerging pathogen in CF patients and often the most prevalent isolation from patients when using molecular methods (Lambiase et al. 2011; Firmida et al. 2017). Patients infected with *A. xylosoxidans* often display similar markers of chronic infection, such as decline in FEV1, increased rate of exacerbations, and inflammation akin to that of a *P. aeruginosa* infection, with which they are typically co-colonised (Tetart et al.; Hansen et al. 2010; Lambiase et al. 2011).

This raises questions as to the initial isolation methods from CF sputum, and the use of selective media in bacterial identification within the clinic. The isolates in the culture collection used in this study were initially selected using traditional culture methods following guidance for the isolation of *P. aeruginosa* on selective cetrimide agar from the manufacture as it was believed to only select for this species. However as apparent, *A. xylosoxidans* also grows on cetrimide media (Holmes et al. 1977). Ideally, these isolates should have undergone further molecular testing to correctly identify the bacterial species.

Misidentification of *A. xylosoxidans* in CF has previously been reported, although rates are low. (Saiman et al. 2001; Kidd et al. 2009). The morphology of *A. xylosoxidans* colonies is similar in appearance *P. aeruginosa* and may be misidentified as such where traditional culture methods are used and facilities for molecular characterisation are not available. Correct species identification plays a vital role in understanding the CF pathogen epidemiology and tracking of emerging pathogens and epidemic strains (Saiman et al. 2001; De Baets et al. 2006).

5.3.2 Phylogeny and MLST analyses identify epidemic strains, but no clustering of isolates with similar NO dispersal response.

The relatedness and sequence type of the isolates in this study was assessed with the aim of observing clustered isolates with similar phenotypic responses to the NO dispersal signal. This observation was not apparent, with closely related isolates remaining to display varied responses. The isolates PA30 and PA66 were found to be closely related based on their core genome SNP analysis and relative 'age' but did not share either the ST or the NO dispersal phenotype.

The same can be said about the clade of five isolate that share the same age in comparison to the PA01 reference. Isolates PA31, PA47, PA15, PA55, and PA20 do not share similarities in their response to the NO dispersal trigger, but all belong to ST146. ST146 is also known as the Liverpool epidemic strain (LES), the most well-known and widely distributed *P. aeruginosa* clone. It is the most common clone identified in CF patients in the UK with evidence of intercontinental spread between CF clinics in Europe and North America (Dettman et al. 2013; Parkins et al. 2018). The LES is capable of superinfection (infection of patients already colonised by *P. aeruginosa*) and has crucial factors of concern including the increase in some virulence factors, patient morbidity, and resistance to antimicrobials (McCallum et al. 2001; Goodyear et al. 2022).

All other isolates that underwent MLST analysis in this study had an individually unique ST, regardless of the genome similarity and relatedness. Of note, PA49 (ST217) is a clone of the Manchester epidemic strain originally identified as the cause of cross infection in an adult CF clinic in Manchester. The surveillance study by Jones et al. (2001), 14% of patients had unusual phenotype belonging to this ST, isolates were non-pigmented, non-motile, and resistant to multiple antibiotics supporting the phenotypic characterisation in the study by Soren for the PA49 isolate (Jones et al. 2001)

ST253 (PA30) belongs to a lineage that is the most prevalent ExoU positive strains and occurs primarily as long-term chronic infection (Fischer et al. 2020). ExoU is an extracellular cytotoxin transported by T3SS that induces lung epithelial cell damage and increase inflammation in chronically infected patients (Rabin and Hauser 2003; Hardy et al. 2022).

ST532 (PA66), ST16 (PA68), and ST274 (PA57) are important multidrug resistant clones. Recently with an isolate of the ST532 clonal lineage was reported to have CrpP, a ciprofloxacin-modifying enzyme (Founou et al. 2020; Zhao et al. 2023). An ST16 isolate was identified as the causative agent in a recent amikacin resistant outbreak (Fernández-Cuenca et al. 2020), and ST274 labelled

as international extensively drug-resistant clone with a carbapenem non-susceptible phenotype (Mangoni et al. 2023) the latter two STs have been listed as high-risk lineages

Other clonal lineages are of lesser concern, ST433 (PA37), ST1858 (PA21), ST1716 (PA05), and ST399 (PA26) hove small numbers of isolates reported with these specific ST (1,4,1, and 4, respectively) in the *P. aeruginosa* PubMLST database (Jolley et al. 2018).

Whilst the clonal lineage and associated factors for patient health are of interest, the epidemiology of the isolates in this study is not a primary focus, and it can be determined that the phylogeny nor MLST can predict and explain the varies responses to NO for biofilm dispersal.

5.3.3 Gene loss is not responsible for the varied NO dispersal response.

A database of genes previously known to be involved in the *P. aeruginosa* denitrification, and NO biofilm dispersal induction pathways was created, and sequences blasted to highlight presence or absence of these genes. The rational being loss or minimal identity and coverage of these genes within the core genome may result in the breakdown of function of these specific pathways. Interestingly, most genes were present in all isolates. The exception is PA05, which lacks the gene encoding for the PA1390 (McpS) chemotaxis regulator that contains two PAS domains like that of BdlA that are involved in redox sensing as previously discussed in chapter 1 (D'Argenio et al. 2007; Hutchin et al. 2021).

However, it has been shown to have a contrasting effect on swimming motility to BdlA, with overexpression resulting in reduced swimming motility (Bardy 2005). The absence of BdlA in PA05, if anything, would suggest the isolate was able to induce swimming motility and dispersal rather than hinder it. The presence of McpS in the remaining isolates suggests other regulatory mechanisms are at play in the dispersal response as numerous isolates still possess the typical dispersal response.

Had an isolate with a non-dispersing phenotype i.e., PA10 been lacking all genes with PDE activity, it could have been said this specific isolate was unable to degrade intracellular levels of c-di-GMP. Maintaining a high intracellular c-di-GMP in this manner would favour that of the biofilm phenotype and could explain the tolerance to the NO signal.

5.3.4 Conclusion

The aim of this chapter was to explore the genomic features of the isolates within the culture collection and identify any relationships or genes that may explain the varied dispersal phenotype in response to NO. Whilst the genomes have been explored for the presence and absence of

genomic features, there appears to be no association between the genotype and dispersal phenotype, with all key genes present. This would suggest a greater role of the regulation of these genes that needs to be explored.

A takeaway from this chapter is the emphasis on the importance of molecular methods in accurate diagnosis of bacterial infection of specific pathogens in CF patients. Misidentification may lead to misdiagnosis and inappropriate treatment choice, with the ever-growing accessibility of molecular methods, modern day laboratories should now have the capability to accurately identify bacterial species.

Chapter 6 RNA sequencing of *P. aeruginosa* clinical CF isolates

6.1 Introduction

Understanding the basis on how organisms react to external stimuli massively relies on gene expression studies, and advances in next generation sequencing technologies have increased the accessibility of transcriptome profiling to many research teams trying to understand the complexities of the bacterial regulatory networks (Croucher and Thomson 2010)

Previous molecular methods utilised to study gene expression relied on low throughput methods, such as norther blots, and microarray analysis with hybridised fluorescent probes (Croucher and Thomson 2010; Kukurba and Montgomery 2015). Next generation sequencing allows the whole transcriptome to be profiled where other methods only allow the detection of transcripts/genes through hybridization (Rao 2019). This enables better depth and resolution by mapping read to a bacterial genome in an unbiased manner, allowing for differing isolates with high genome variability to be profiled (Wang et al. 2009; Croucher and Thomson 2010). The use of this methodology will be of great benefit in this study with clinical isolates of varying genomes.

As highlighted in the previous chapter, genes that are known to be involved in the denitrification and the NO dispersal induction pathways remain to be present in the core genomes of all the isolates tested. This leads to the assumption that it is not the loss of function of these genes, but rather their regulation that results in the varies responses of the clinical isolates to NO. Transcriptome profiling may also elucidate alternative pathways that have not previously been shown to be influenced by NO.

The current model used for culturing biofilms involves the use of multi-well plates in which the biofilms would be cultured with slow shaking before SNP treatment, the subsequent separation of biofilm and dispersed/ planktonic populations would be performed by aspirating the surrounding culture media and scraping the biofilm from the well. Issues with this culture system arise with the aspiration of surrounding media and can prove difficult not to disturb and aspirate the attached biofilm in the well. This could lead to issues with reproducibility and user error in separating the populations. This chapter focuses on the adaptation of a previously used biofilm culture method for proteomic studies to better replicate the growth of biofilm in a microfluidic chip vs a 96 well format used previously.

Varadarajan et al., 2020, reported an integrated microfluidic model under flow provides a more reproducible method of culturing biofilms for the broad application of better mechanistic understanding of biofilms. This previously described model will be adapted here to assess its suitability as a biofilm dispersal model offering treatment with SNP delivered over a sustained period with the goal of easy collection of biomasses with reduced handling time to reduce impact on RNA quality.

The aims of this chapter are to validate the dispersal model in the PDMS device and the processing of RNA-seq data set generated on both biofilm and 'dispersed' populations, in both the control strain mPA01 with the typical dispersal response, and PA10 with an atypical dispersal response to identify whether changes in gene regulation pathways can be attributed to the response seen.

6.2 Results

Prior to transcriptomic analysis the microfluidic biofilm model first had to be validated to ensure the same dispersal effect seen in a 96 well plate format was also observed in this microfluidic setup. Bacterial isolates mPA01 and PA10 were both assessed for their dispersal response within the microfluidic model with quantitative confocal imaging and CFU counts performed on the outflow from the system.

6.2.1 Confocal imaging and CFU counts validate the suitability of microfluidic biofilm culture as a dispersal model.

Table 11. Quantitative assessment of the dispersal response in a microfluidic biofilm culture system. The mean average live/dead cell volumes have been calculated from *n*=5 images. The bacterial numbers in the outflow of the system were assessed via CFU counts (*n*=3).

Strain	Treatment	Average live cell volume (μm^3)	Average dead cell volume (μm^3)	CFU/ml in outflow
mPA01	Control (M9)	4153.23	34349.65	6.67E+08
	8µm SNP	2098.15	35896.83	1.03E+10
PA10	Control (M9)	N/A	N/A	1.33E+09
	8µm SNP	N/A	N/A	1.07E+09

The average volume for both live and dead cells were calculated based on the mean average of 5 confocal images taken at various positions along the microfluidic channel. The following positions were imaged progressing down the channel; Inlet, 25%, 50%, 75%, and outlet.

Table 11 shows the average live cell volumes for both the control (M9 treated) and the SNP treated (4um SNP) 4153.23, and 2098.15 μm^3, respectively. This shows a 50.5% reduction in live cell biomass with the dispersal trigger of NO from SNP. An increase in the CFU/ml in the outflow of the microfluidic system in mPA01 with SNP treatment suggests the dispersal of cells from the biofilm and into the surrounding bulk fluid, ultimately caught in the continuous media flow and out of the system. Coupled with the decrease in live cell biofilm volume shows dispersal effect.

A visual representation of this reduction is show in Figure 24. The volume of dead cells in both treatment and non-treated samples appears unusually high (34349.65, and 35896.83 μm^3 respectively). This may be due to the image quality in the dead channel producing a lot of noise. PDMS imaging can prove difficult with the elastomer retaining some stain. Despite noise reduction steps in the image analysis software, this background noise may not have fully been filtered out and thus the noise here is accounted for as a biofilm aggregate or cell resulting in the unexpectedly high average volume.

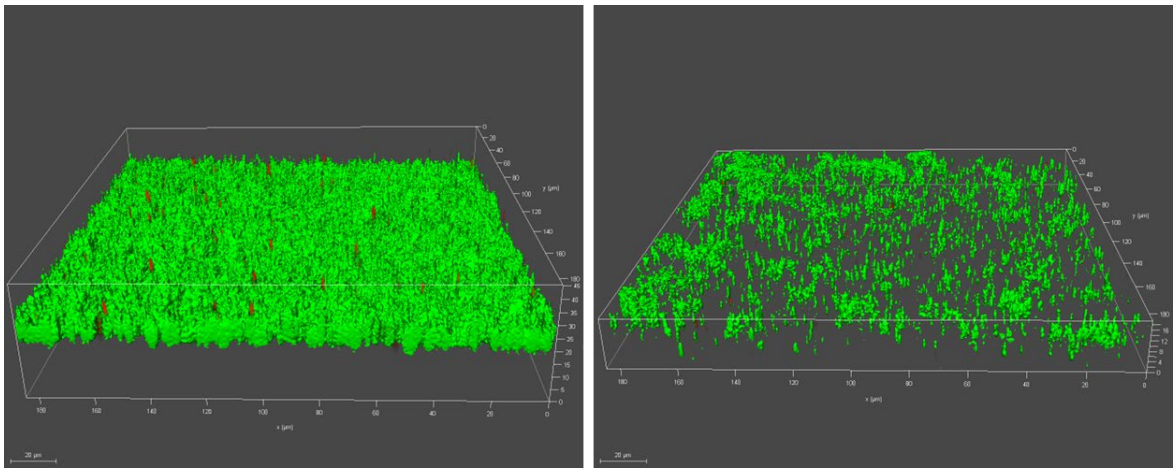

Figure 24. Representative 3D scanning confocal images of mPA01 biofilms without (Left) and with the NO dispersal signal from SNP in the microfluidic biofilm culture device.

The representative images for PA10 with and without the SNP (Figure 25), visually looks as though there is no biofilm dispersal effect in response to the NO signal, and potentially a slight increase in biofilm thickness from ~22µm in the z stack without SNP, to ~35µm with the SNP. It would also appear there is a higher proportion of dead cell clusters. However, Imaris batch analysis on the confocal image stacks was unable to produce quantitative measure on volume of live/dead cell counts.

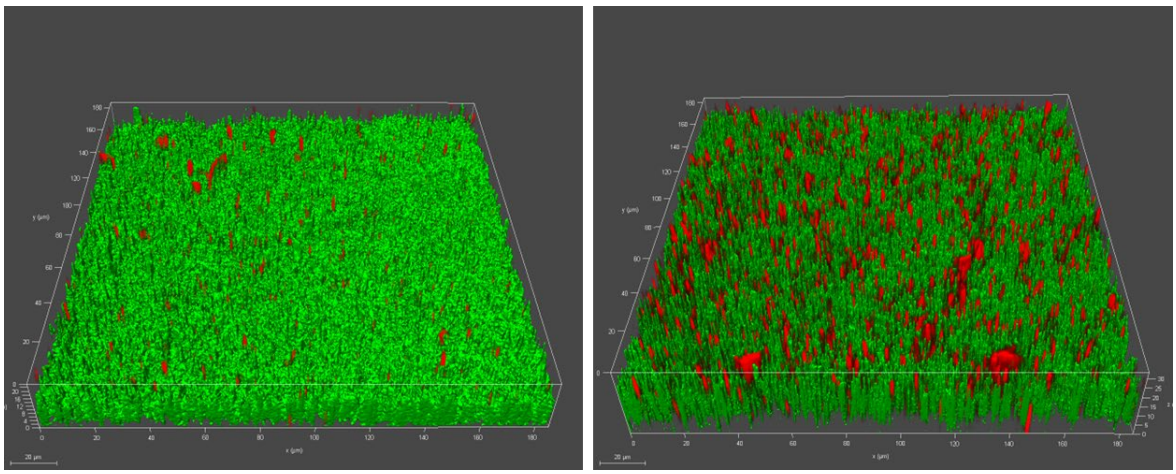

Figure 25. Representative 3D scanning confocal images of PA10 biofilms without (Left) and with the NO dispersal signal from SNP in the microfluidic biofilm culture device.

6.2.2 RNA Sequencing

Following on from the validation of the microfluidic biofilm dispersal model, an array of samples were collected via the methods previously described for RNA sequencing. With the aim to determine differential gene expression in the two isolates mPA01 and PA10 with distinctly

different biofilm dispersal responses when treated with the NO donor SNP. Biomass was collected and subsequent RNA extracted from mPA01 and PA10 biofilms and out flow, with and without 8μM SNP treatment. A total of 24 RNA samples were extracted (*n*=3 per condition). Unfortunately, only 13 of these samples could be processed for RNA sequencing.

6.2.3 Differential expression analysis of mPA01 biofilms with and without SNP treatment.

6.2.3.1 Hierarchical clustering and PCA analysis

Initially, to assess the quality of the overall experiment, hierarchical clustering, and a principal component analysis (PCA) was performed. The comparative samples of SNP treated and untreated biofilm can be seen here.

The hierarchical clustering analyses Figure 26 identifies any similarity between the samples in the dataset. It can be seen in Figure 26 that the untreated biofilm samples cluster together in the tree, and their correlation values remain >0.8 indicating similar gene expression profiles in the untreated sample group.

The same cannot be said about the treated biofilm, here there is only one replicate that we can draw a comparison to so no clustering can be seen. The correlation value, however, is calculated in comparison to the treatment group, and a deep blue colour represents a correlation value around >0.5 suggesting the gene expression profile to differ between the treatments, and the SNP treatment indeed influences the gene expression.

Further principal component analysis was performed to identify any additional variance between the samples. As can be seen in Figure 27, the largest variance (PC1) is between the treated and untreated samples as expected. There appears to be large variation between replicates (PC2) in the untreated sample set with no clustering observed, with the absence of additional replicates, it cannot be determined which of these may be an outlier.

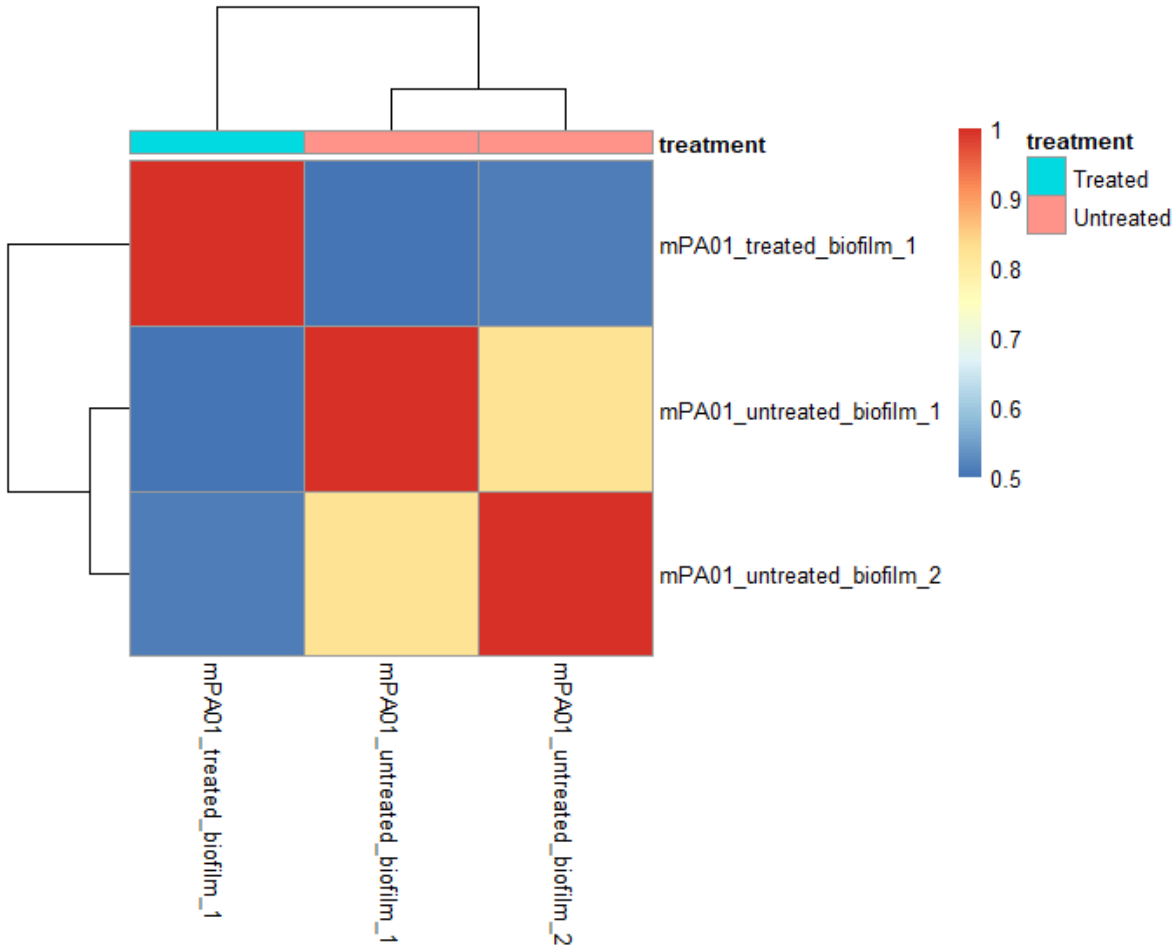

Figure 26. Hierarchical clustering analysis of gene counts comparing the 8µM SNP untreated and treated biofilm populations of the isolate, mPA01. Colour gradient scale represents the correlation value of each replicate in the dendrogram. A value of 1 is indicative of perfect correlation.

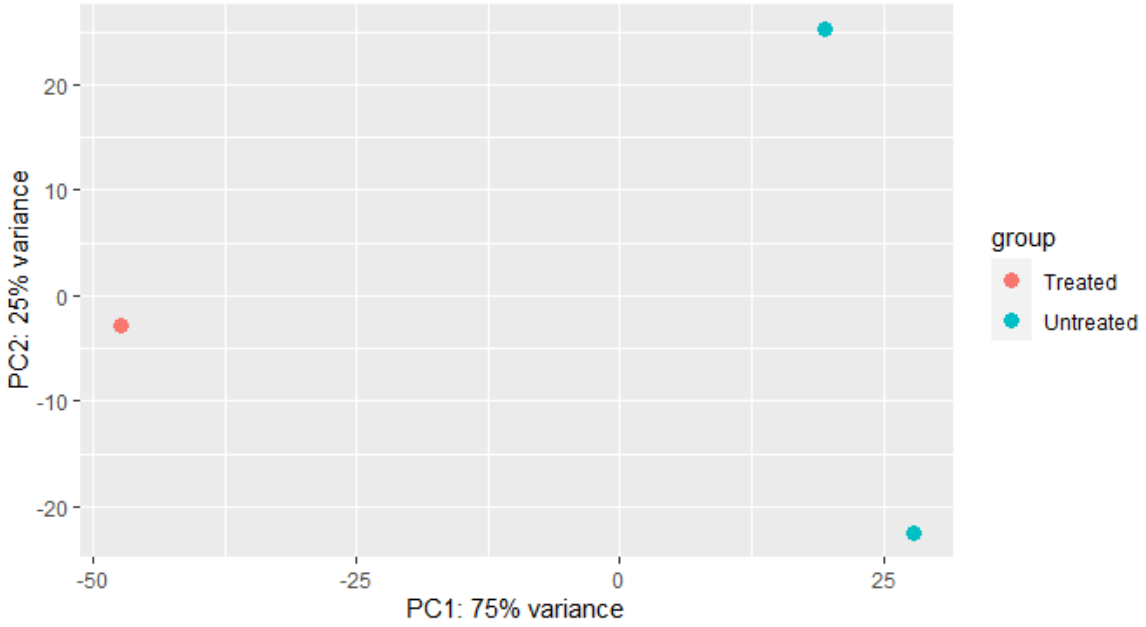

Figure 27. Principal component analysis displaying the between treatment groups, and the variance between experimental replicates. Here comparing the comparing the 8µM SNP untreated and treated biofilm populations of the isolate, mPA01.

6.2.3.2 Differential gene expression analysis

Analysis with DESeq2 for differential gene expression was carried out on the available count data, normalised to the estimated size factors for each column in the count matrix. Genes were determined as differentially expressed if they had a significant ($p < 0.05$) and a log2fold change of >1 or <-1. In this data set 2069 were found to be differentially expressed with SNP treatment. The total number of genes with differential expression are displayed in the volcano plot Figure 28. Results with a N/A or 0 value have been filtered out, those coloured blue are considered significant. The shift of data points towards the right suggests the majority of significant, differentially expressed genes are upregulated.

6.2.3.3 STRING Pathway analysis

Rather than look at individual genes and their log2fold change in expression, it is more beneficial to delve deeper into the cellular pathways in which they are involved. For this the top 100 differentially expressed genes (with $p<0.05$) were uploaded to STRING (string-db.org v12.0) using the *P. aeruginosa* PA01 reference database for further analysis. SRING network can be seen in Figure 29.

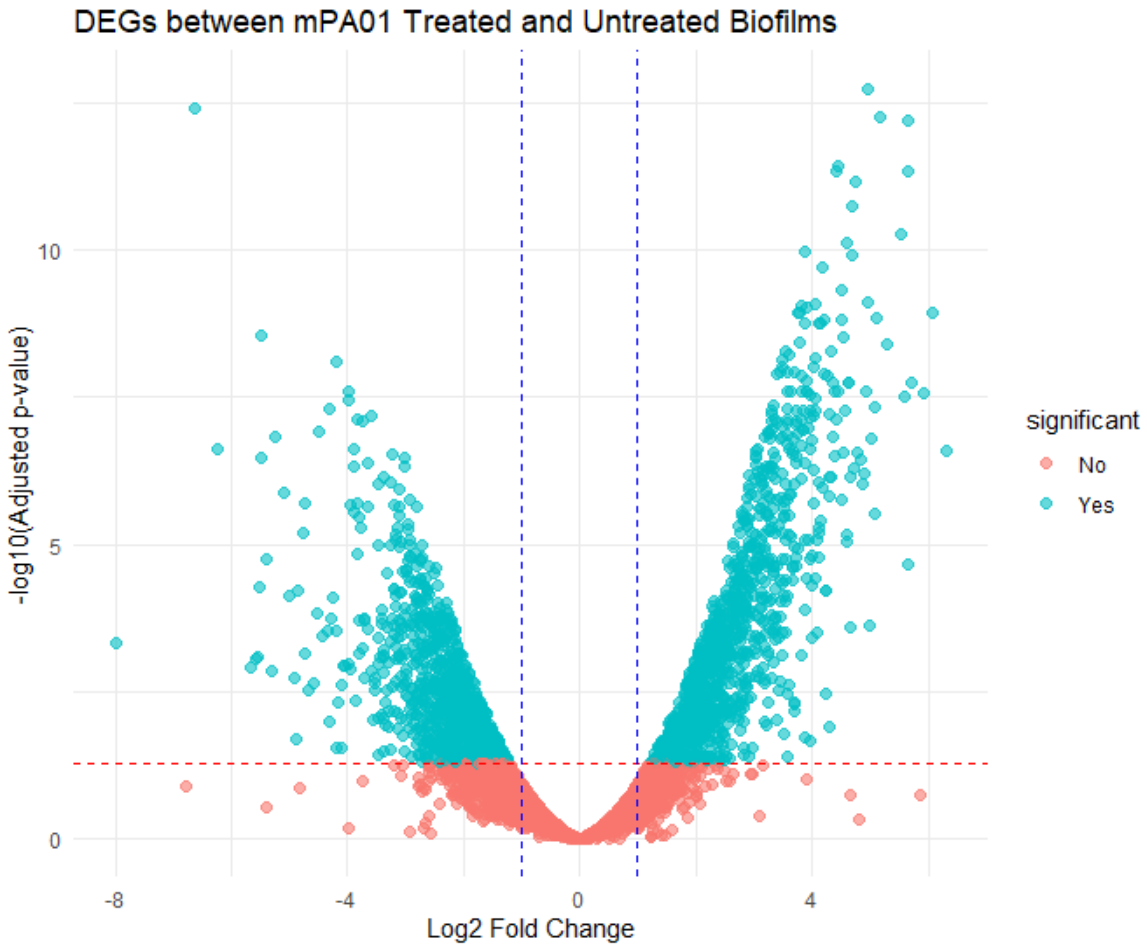

Figure 28. Differentially expressed genes between the 8µM SNP untreated and treated biofilm populations of the isolate, mPA01. Genes are determined as differentially expressed if they have significant ($p < 0.05$) log2fold change of >1 or <-1 and represented here by a blue dot. Values that contained N/A or 0 have been filtered and are not displayed.

As can be seen the STRING network analysis, related genes cluster into their functional protein sets, using k-means clustering, three local network clusters were identified and can be seen in Figure 29 and described below.

1. (Red) Responsible for cellular transport at the cell membrane and cell periphery including ABC transporters.

2. (Green) responsible for DNA replication, repair and nucleic acid metabolism, some genes responsible for bacterial chemotaxis.

3. (Blue) largely encode for hypothetical proteins involved in metabolic processes.

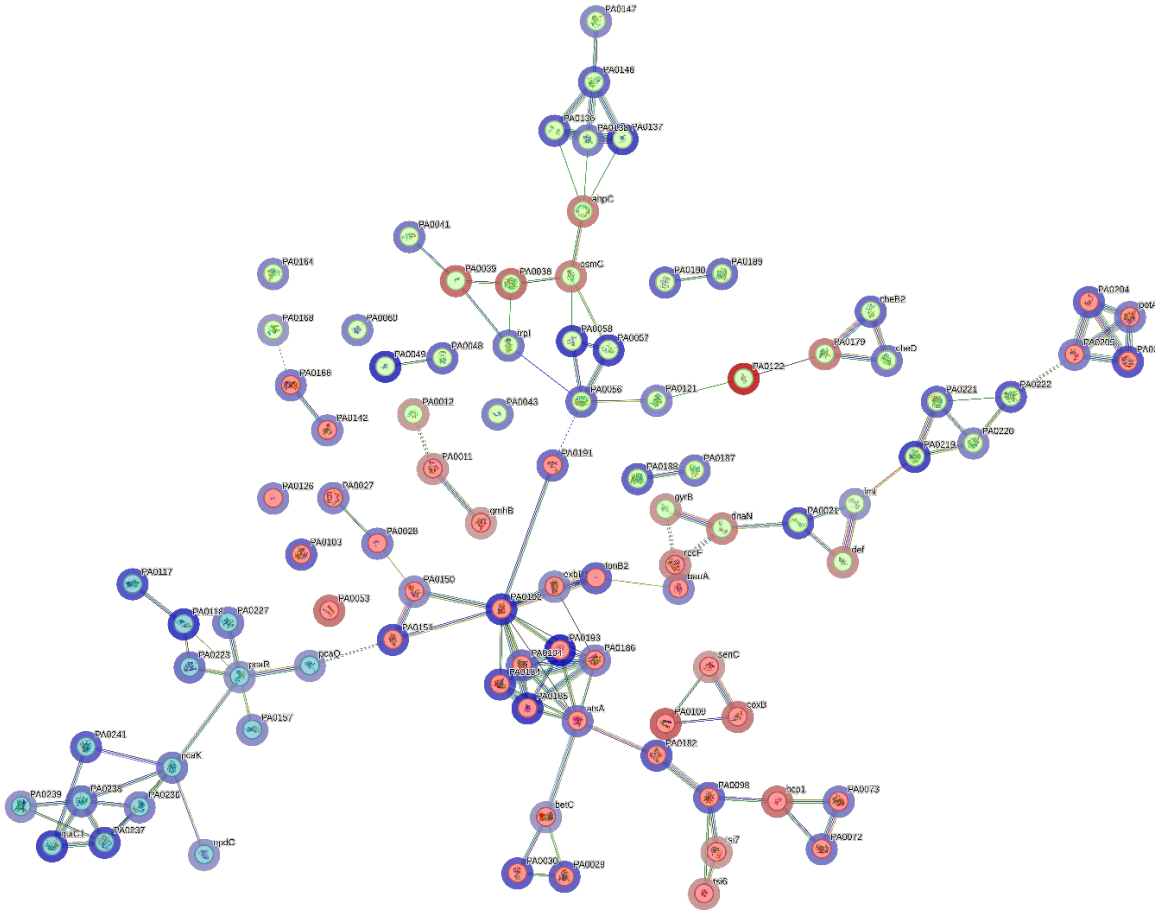

Figure 29. STRING network to identify gene associations in the top 100 differentially expressed genes in the 8µM SNP untreated and treated biofilm populations of the isolate, mPA01. Gene clusters are coloured in the centre of the ring (red, green, blue). Halos surround individual genes are colour coded to represent level of differential expression (blue = fold increase, red = fold decrease) a deeper shade depicts a greater fold change. Linkages between gene identifiers shows the potential interaction between different pathways.

6.2.4 Differential expression analysis of mPA01 outflow populations with and without SNP treatment.

6.2.4.1 Hierarchical clustering and PCA analysis

As with the other analyses above, hierarchical clustering, and PCA were performed. Initial analysis revealed high variation within one of the treated replicates, with clustering of gene profiles closer to that of the untreated sample set. This identified the replicate as an outlier and therefore removed and analysis repeated. The repeated hierarchical clustering (Figure 30) shows the two groups, treatment, and non-treatment groups cluster separately with high correlations between replicates. PCA analysis (Figure 31) shows separation of the treatment groups with variance in PC1 suggesting different gene expression profiles as would be expected. PC2 shows similar gene expression profiles between replicates.

6.2.4.2 Differential gene expression analysis

Differential expression was again analysed using the same methods as mentioned above. For the comparative counts between the mPA01 outflow bacterial populations with and without SNP treatment, 3043 genes were identified to have significant differential expression. The total number of genes with differential expression (log2fold change >1 or <-1) are displayed in the volcano plot Figure 32. Results with a N/A or 0 value have again been filtered out, those coloured blue are considered significant ($p < 0.05$). It can be said there are a large proportion of upregulated genes in cells in the outflow populations following SNP treatment.

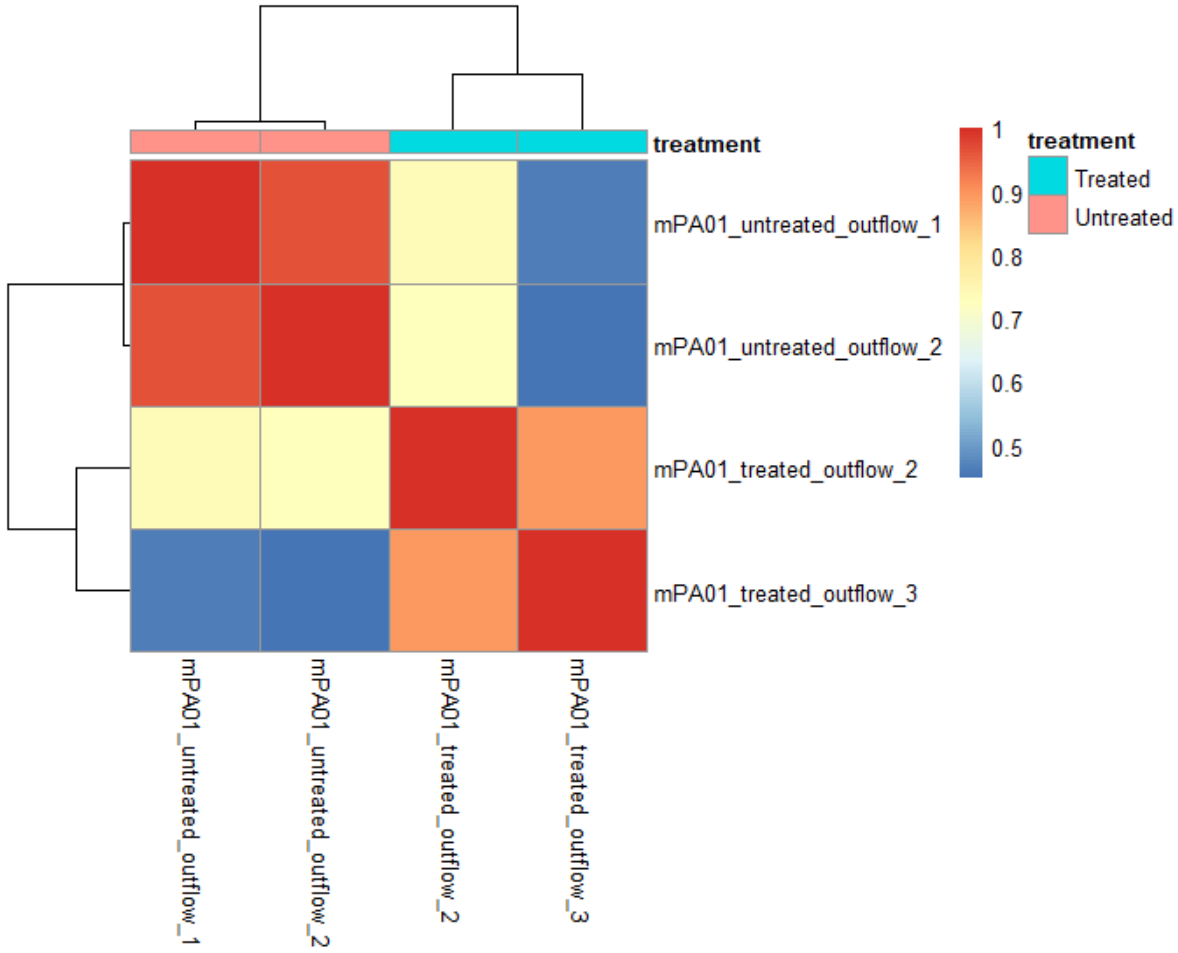

Figure 30. Hierarchical clustering analysis of gene counts comparing the 8µM SNP untreated and treated outflow populations of the isolate, mPA01. Colour gradient scale represents the correlation value of each replicate in the dendrogram. A value of 1 is indicative of perfect correlation.

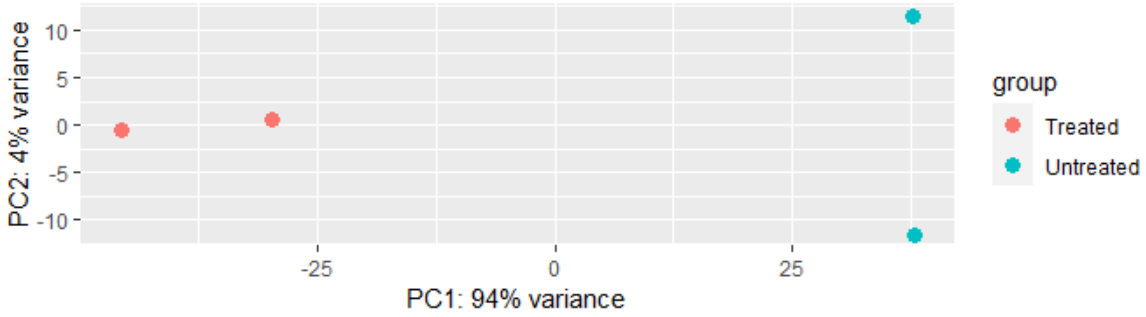

Figure 31. Principal component analysis displaying the between treatment groups, and the variance between experimental replicates. Here comparing the comparing the 8µM SNP untreated and treated outflow populations of the isolate, mPA01.

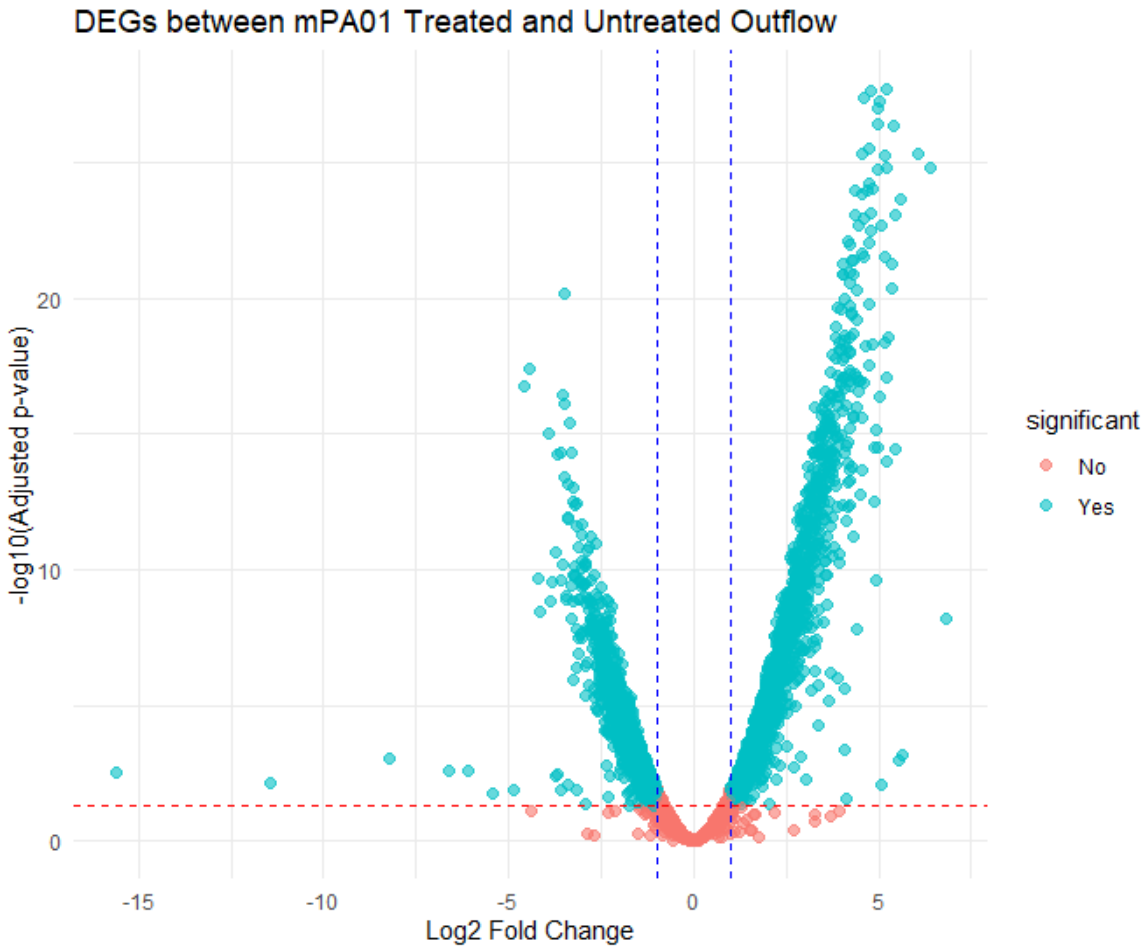

Figure 32. Differentially expressed genes between the 8µM SNP treated and untreated outflow populations of the isolate, mPA01. Genes are determined as differentially expressed if they have significant ($p < 0.05$) log2fold change of >1 or <-1 and represented here by a blue dot. Values that contained N/A or 0 have been filtered and are not displayed.

6.2.4.3 STRING Pathway analysis

As with the previous comparisons of the mPA01 biofilms, STRING pathway analysis was performed for the outflow. The top 100 genes were filtered for NA values for gene identity and uploaded to the STRING database to produce the network seen in Figure 33. K-means clustering was performed to highlight the three main clusters.

1. (Red) Biosynthesis of siderophores, oxidoreductase activity acting on nitrogenous compounds, and other mostly uncharacterised pathways. Of note there is significant downregulation of the pyochelin biosynthetic pathway, and Fe(III)-pyochelin outer membrane receptors. The nitrogenous oxidoreductase activity includes the 1.8 and 2.3 log2fold increase in expression of norC and nirQ.

2. (Green) Largely probably proteins, regulation of bacterial secretion systems, biofilm formation, and chemotaxis. Notably upregulated are ppkA and pppA (2.6, 2.2 log2fold respectively), clpV1 (1.75 log2fold), and cheB2, cheD (3.51, 2.99 log2fold increase).

3. (Blue) Predominantly mixed pathways including sulphur metabolism.

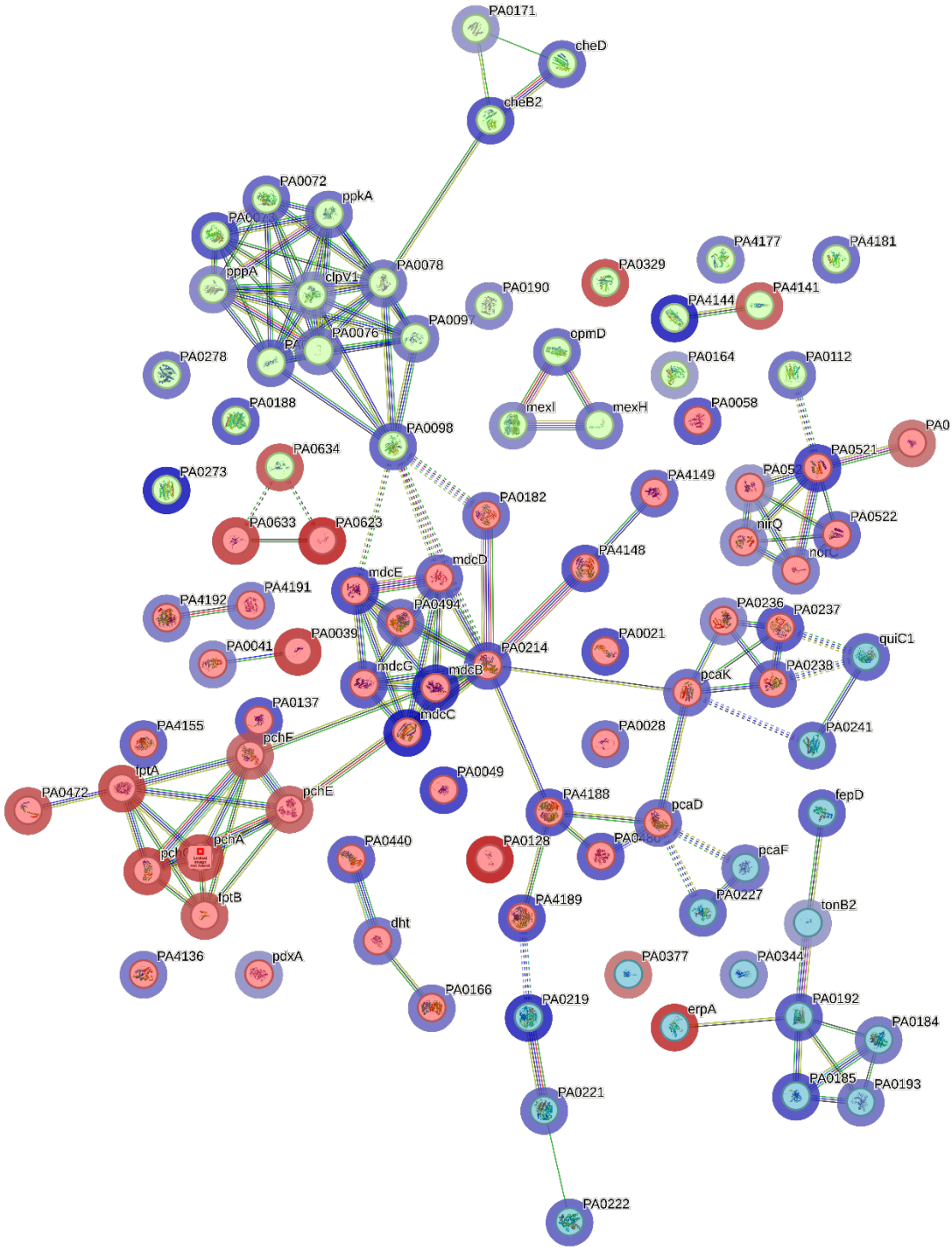

Figure 33. STRING network to identify gene associations in the top 100 differentially expressed genes in the 8µM SNP untreated and treated outflow populations of the isolate, mPA01. Gene

clusters are coloured in the centre of the ring (red, green, blue). Halos surround individual genes are colour coded to represent level of differential expression (blue = fold increase, red = fold decrease) a deeper shade depicts a greater fold change. Linkages between gene identifiers shows the potential interaction between different pathways.

6.2.5 Differential expression analysis between mPA01 biofilm and outflow populations with 8µM SNP treatment

6.2.5.1 Hierarchical clustering and PCA analysis

Large amounts of variation are seen in the data between the biofilm and outflow populations from the SNP treated flow cell. Hierarchical clustering (Figure 34) shows a high correlation between the biofilm sample and two of the outflow samples. PCA analysis confirms this (Figure 35) with no variance between the expected PC1 group (biofilm vs outflow) no clustering is observed between either replicates or conditions. Showing poor experimental conditions for further analysis.

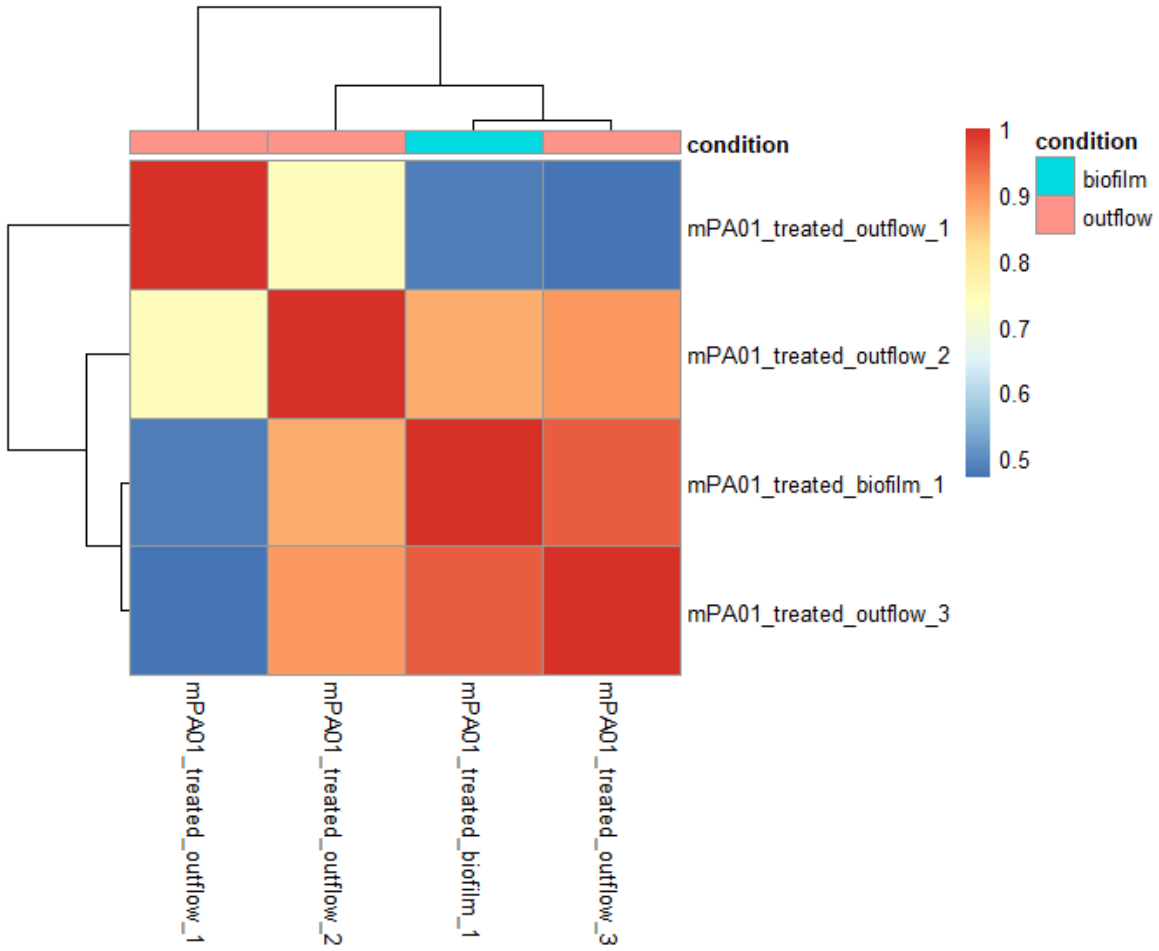

Figure 34. Hierarchical clustering analysis of gene counts comparing the 8µM SNP untreated and treated outflow populations of the isolate, mPA01. Colour gradient scale represents the correlation value of each replicate in the dendrogram. A value of 1 is indicative of perfect correlation.

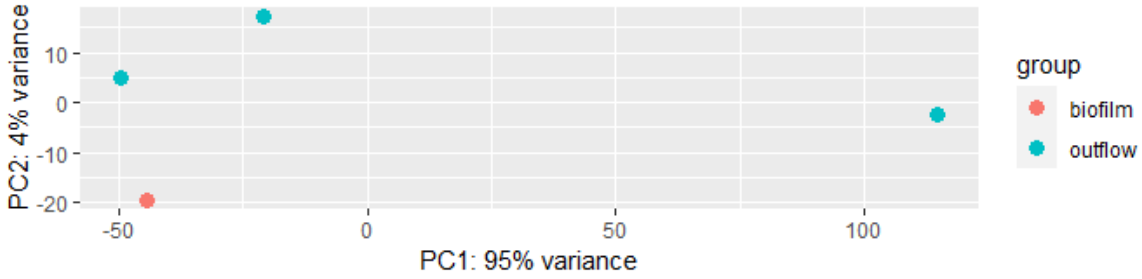

Figure 35. Principal component analysis displaying the difference between phenotype groups, and the variance between experimental replicates. Here comparing the comparing the 8µM SNP treated biofilm and outflow populations of the isolate, mPA01.

6.2.5.2 Differential gene expression analysis

Regardless of the analyses above, differential gene expression was carried out. As above differentially expressed genes were noted if they had a significant ($p < 0.05$) and a log2fold change of >1 or <-1. Unsurprisingly, only eight of the 5764 genes identified in the count matrix were counted as having a significant change in expression. The volcano plot of Figure 36 demonstrates these results with those coloured blue considered significant. No comparisons can be drawn from this analysis, and further pathway analysis was neither possible nor worthwhile.

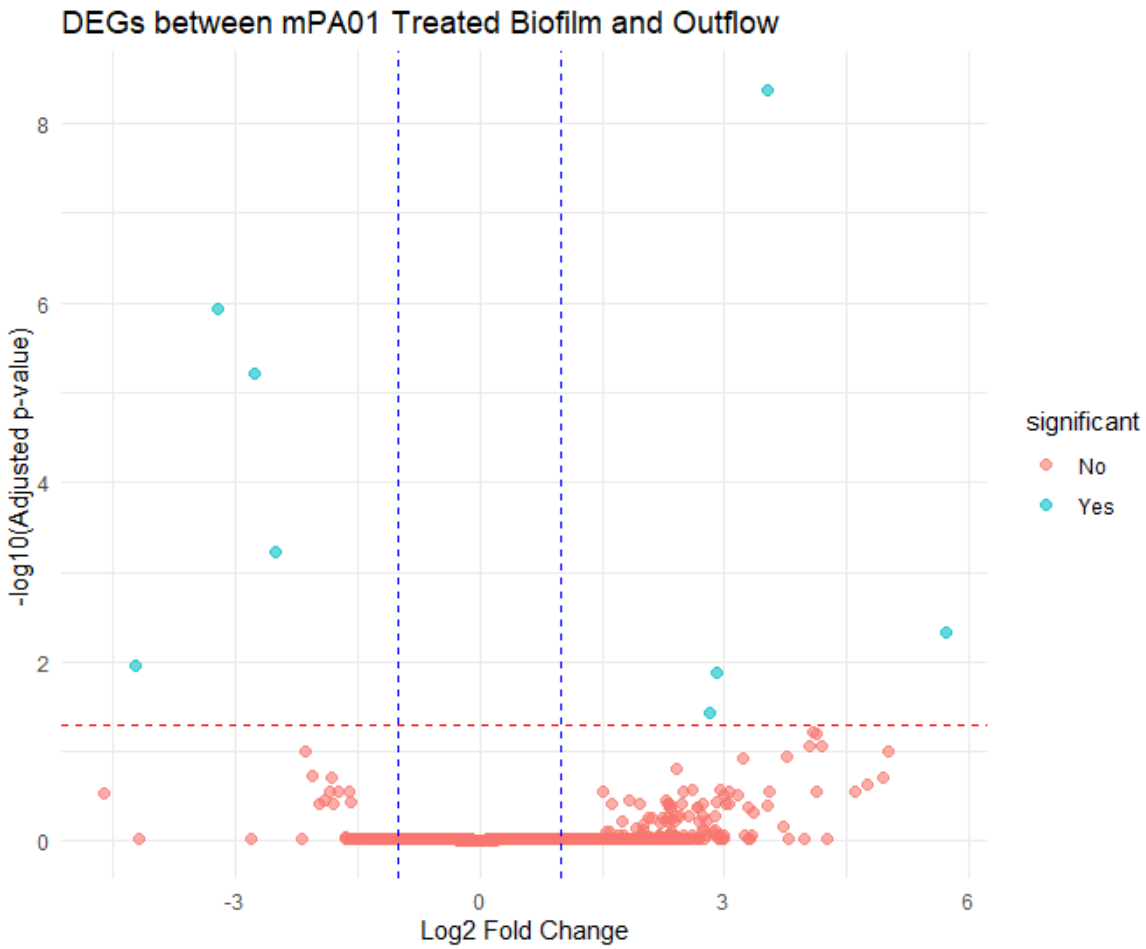

Figure 36. Differentially expressed genes between the 8µM SNP treated biofilm and outflow populations of the isolate, mPA01. Genes are determined as differentially expressed if they have significant ($p < 0.05$) log2fold change of >1 or <-1 and represented here by a blue dot. Values that contained N/A or 0 have been filtered and are not displayed.

6.2.6 Differential expression analysis between biofilm and outflow populations of the non-dispersing isolate PA10 with 8µM SNP treatment

6.2.6.1 Hierarchical clustering and PCA analysis

Here we again assessed the quality of the experimental conditions through hierarchical clustering, and PCA. Initial analysis revealed high correlation between two replicates, one biofilm sample, and one outflow sample both originating from the same flow cell experiment, suggesting similar gene expression profiles. These replicates were as outliers removed from the data set to improve the quality of our comparisons. The repeated hierarchical clustering (Figure 37) shows the two groups, biofilm, and outflow cluster separately with high correlations between replicates, and lower correlation between conditions. PCA analysis (Figure 38) shows separation of the treatment groups with variance in PC1 suggesting different gene expression profiles as would be expected. However, PC2 shows some variation between the replicates.

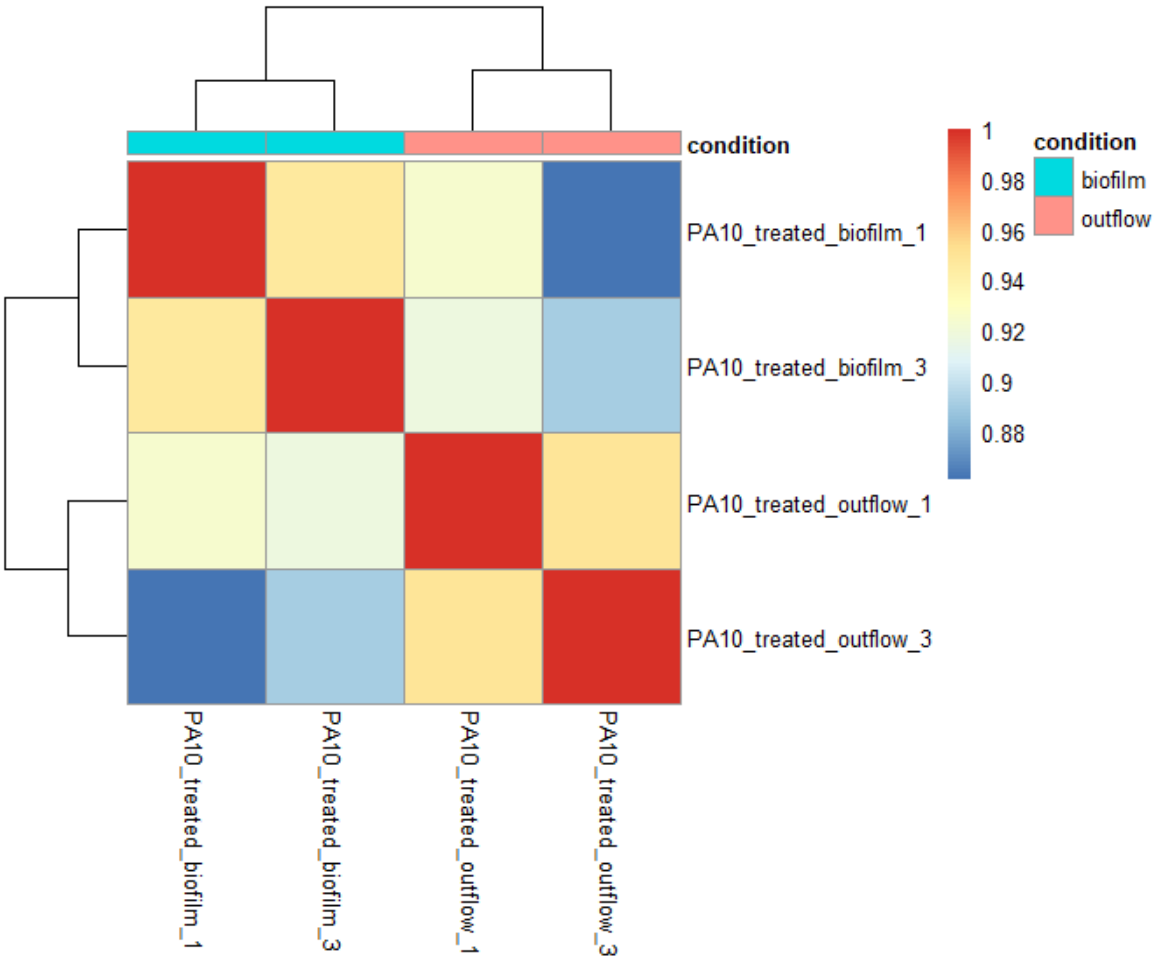

Figure 37. Hierarchical clustering analysis of gene counts comparing the 8µM SNP treated biofilm and outflow populations of the isolate, PA10. Colour gradient scale represents the correlation value of each replicate in the dendrogram. A value of 1 is indicative of perfect correlation.

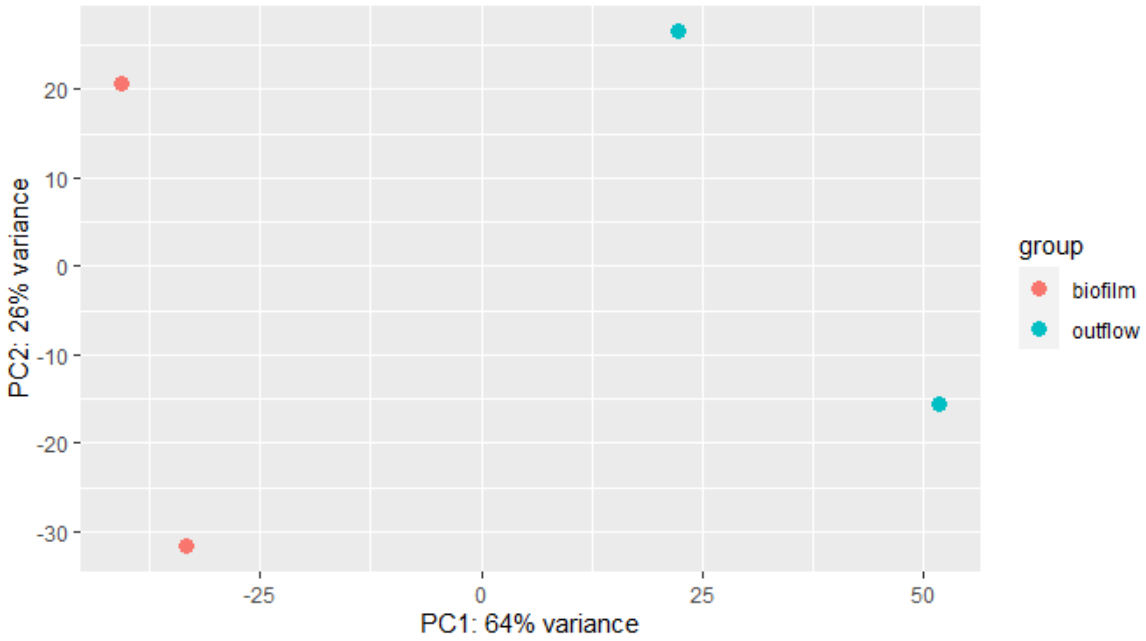

Figure 38. Principal component analysis displaying the variance between phenotype groups, and the between experimental replicates. This PCA compares the 8µM SNP treated biofilm and outflow populations of the non-dispersing isolate, mPA01.

6.2.6.2 Differential gene expression analysis

As before, DESeq2 was utilised to assess the DGE, when comparing the PA10 biofilms to the cellular population in the outflow, with SNP treatment, 475 genes were recognised to have significant differential expression. The total number of genes with differential expression (log2fold change >1 or <-1) are displayed in the volcano plot Figure 39. Results with a N/A or 0 value have been filtered out, those coloured blue are considered significant ($p < 0.05$) with a large proportion of the genes having positive upregulation.

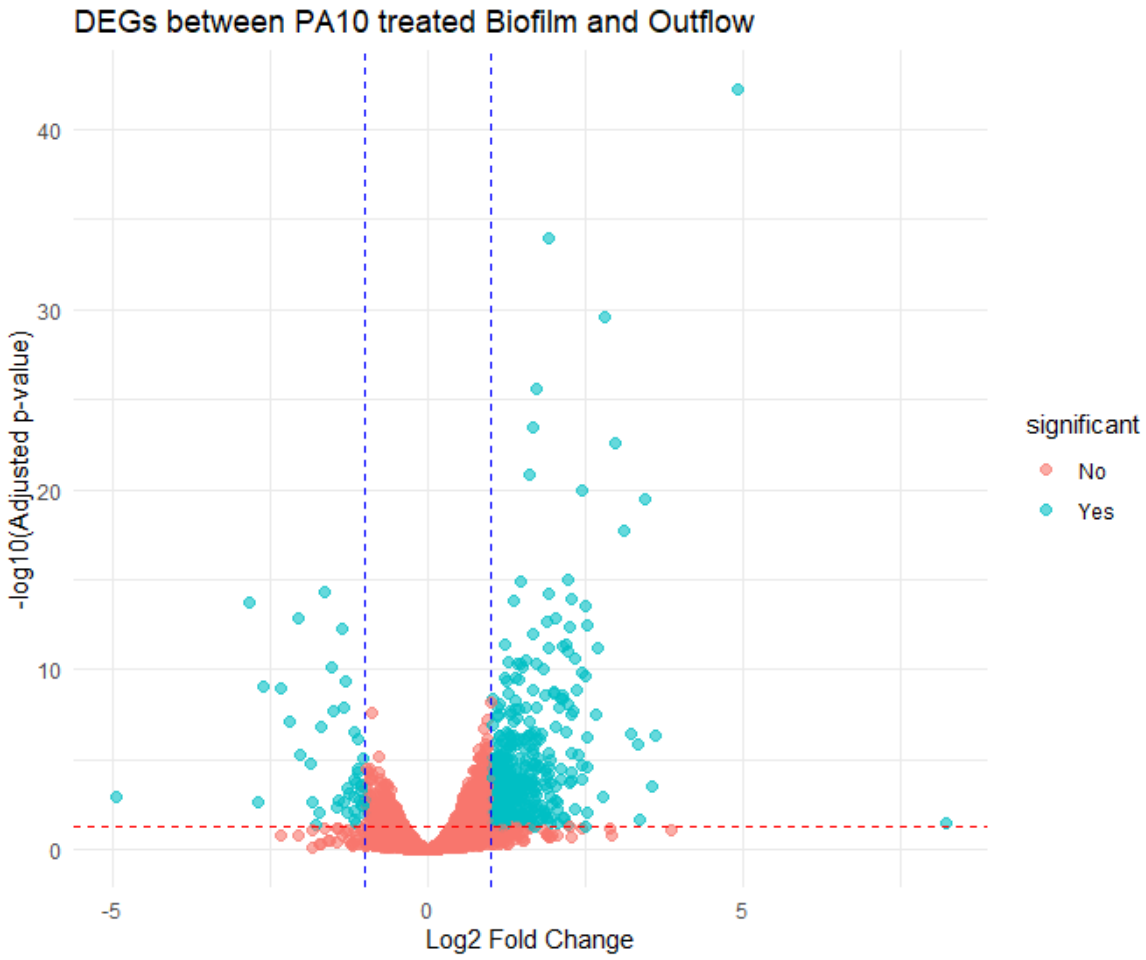

Figure 39. Differentially expressed genes between the 8µM SNP treated biofilm and outflow populations of the isolate, PA10. Genes are determined as differentially expressed if they have significant ($p < 0.05$) log2fold change of >1 or <-1 and represented here by a blue dot. Values that contained N/A or 0 have been filtered and are not displayed.

6.2.6.3 STRING Pathway analysis

In the same fashion as mPA01 comparisons, STRING pathway analysis was performed for the PA10 biofilm vs. outflow. Again, the top 100 genes were filtered for NA values and uploaded to the STING database to produce the network Figure 40. K-means clustering was performed to highlight three main clusters.

1. (Red) Predominantly genes involved with the upregulation of phospholipid transporter activity, and stress response, with upregulation of 1.94 and 2.06 log2fold groEL-groES complex genes.

2. (Green) Upregulation of genes responsible for flagella dependent motility, flagella biosynthesis and assembly (flg and fli gene clusters)

3. (Blue) Mixed network of hypothetical proteins some involved with sodium: proton exporter activity. Of interest, there is a significant upregulation in the two-component response regulator

curiously phoP, phoQ (2.5, 1.66 log2fold respectively), downstream of this there is a 2.77 log2fold increase of the PhoP/Q inducible and low Mg2+ inducible outer membrane protein gene oprH. A gene encoding the periplasmic nitrate reductase protein NapE was curiously downregulated by -1.28 log2fold.

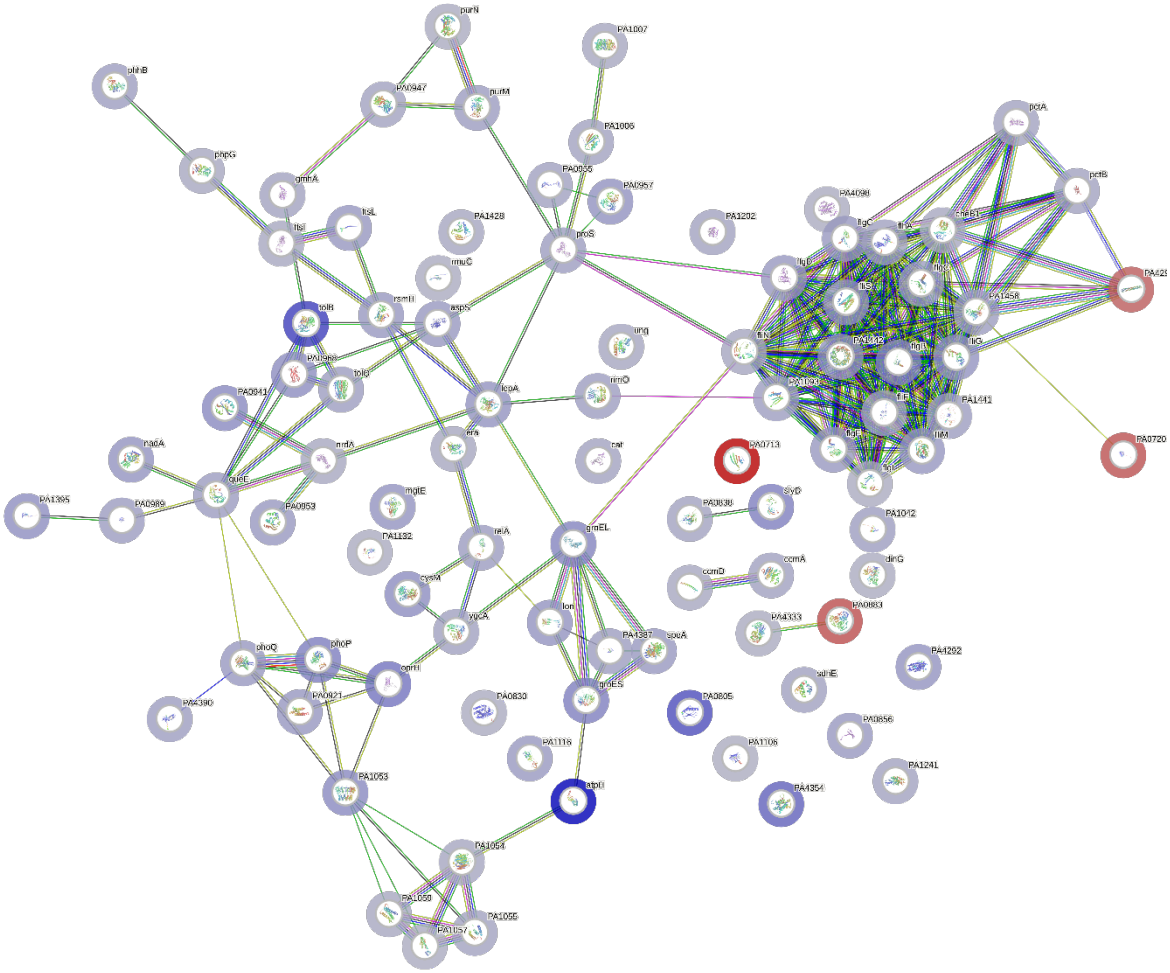

Figure 40. STRING network to identify gene associations in the top 100 differentially expressed genes in the 8µM SNP treated biofilm and outflow populations of the isolate, PA10. Gene clusters are coloured in the centre of the ring (red, green, blue). Halos surround individual genes are colour coded to represent level of differential expression (blue = fold increase, red = fold decrease) a deeper shade depicts a greater fold change. Linkages between gene identifiers shows the potential interaction between different pathways for the red, blue and green colours described in text.

6.3 Discussion

6.3.1 A biofilm dispersal assay was successfully validated in a microfluidic biofilm culture model.

This chapter firstly aimed to validate a microfluidic biofilm culture model as previously demonstrated by Varadarajan et al. 2020 to be used as a more reproducible biofilm dispersal model in order to gather sufficient biomass material for RNA extractions and to easily separate biofilm and surrounding bulk fluid cell populations. The experimental setup in this study has achieved both mentioned above.

Confocal imaging and CFU count data indicate the dispersal of biofilms formed by mPA01, and the retention of cells within the outflow of the system. The separation of surrounding fluid and biofilm cells is much easier compared to pipetting off in a standard 12 or 96w plate format with minimal human disruption of the biofilm leading to mix samples, the collected effluent/ outflow can easily be placed on ice as it exits the flow system to enable downstream processing.

A drawback of using the microfluidic cell is the potential of leaks where the PDMS does not properly adhere to the glass coverslip. Leaks may occur at any stage during the experimental process. If a leak occurs after the inoculation of the device, the PDMS chip may not be used again, and the experiment is abandoned/ restarted with a fresh PDMS device causing loss of experimental time and money. To avoid this issue, PDMS may be irreversibly bonded to the glass coverslip using an oxygen plasma treatment creating stronger silicon bonds at the glass: PDMS interface, forming a tight seal between the layers (Xiong et al. 2014). Using this method of plasma bonding would however require an alternate method for biofilm lysis from within the microfluidic channels since the glass would no longer be able to be removed and biofilm biomass scraped out. Sanfilippo et al., 2019, used a similar microfluidic device plasma bonded to a glass slide when investigating the effects of flow on gene regulation. For RNA extraction, the authors used a total lysis solution (TrisHCl, EDTA, lysozyme and SDS) flowed through the device. A subsequent citrate-saturated phenol chloroform RNA extraction was performed (Sanfilippo et al. 2019).

6.3.2 Complete analysis of differential expression between all conditions was not possible.

The use of an external company for RNA sequencing incurred significant delays in obtaining the sequencing data, and suspected degradation of RNA integrity. In-house QC of the extracted RNA indicated that the samples were of the companies specified quality and quantity required for sequencing, however significant delays in shipping resulted in the company QC showing sample degradation and low RNA quantity resulting in the complete loss of 11 samples to be sequenced.

Therefore, DEG comparisons may not be commented on confidently due to issues with the varied *n* numbers in each condition.

Further downstream analysis of the biological pathway associated with the differential gene expression between mPA01 and PA10 with contrasting dispersal responses was not possible. The annotated GTF files were parsed from GFF3 file created by annotation of the bacterial genome with PROKKA. The parsing and creation of the GTF files used in the RNA seq analysis pathway, produced 'gene_id' descriptors that were different between both mPA01 and PA10 and computation was not possible. For example, the gene ID for the flavohaemoprotein, fhp, was assigned the nbis-gene-id-4446 in PA10, whereas in mPA01 it was assigned nbis-gene-id-2320. This resulted in the two isolates being unable to be compared for differential gene expression as the count matrices loaded into DEseq2 would have conflicting gene names. For future analysis, the annotation files needed for gene count generation would need to be repeated and DESeq2 analysis rerun with matching gene IDs.

6.3.3 Upregulation of ABC transporter genes following SNP treatment to mPA01 biofilms

When subject to the NO donor SNP biofilms formed by mPA01 show an upregulation in genes encoding numerous hypothetical ABC transporter proteins. ABC transporters play a vital role in the uptake of nutrients into the bacterial cell and contain various ATP binding domains to enable their function (Higgins 2001). ABC transporters can uptake various metals and can contribute to the virulence of pathogenic bacteria, however this is rarely reported in *P. aeruginosa*. Due to the nature of uptake from the external environment ABC transporters can be prime targets for antimicrobial compounds and their delivery to the cytoplasmic space (Garmory and Titball 2004).

A study by Pletzer et al 2015 showed that the ABC transporter system Npp is involved in the active uptake of peptidyl nucleoside antibiotics opening the door for potential new therapies of pathogen specific antibiotics (Pletzer et al. 2015). Should the upregulation of these transporters be due to the NO signal, it has the potential for exploration of conjugate antimicrobial therapies. If NO can induce the increase in binding sites for targeted peptidyl nucleoside antibiotics this could be a valuable therapeutic target

The upregulation of these transporter systems could however just be indicative of adaptation to the low nutrient environment of the minimal media M9 used in this study with its upregulation necessary for the acquisition of nutrients to sustain viability. From the analysis of mPA01 biofilms

with and without SNP treatment, the is no indication of gene regulation that influences the dispersal response.

6.3.4 NO treatment induces a switch in iron uptake mechanism in dispersed cells.

The comparison of mPA01 outflow populations saw a significant downregulation in genes responsible for pyochelin synthesis. Pyochelin is a siderophore produced by *P. aeruginosa* in iron limited conditions, with metabolites produced during it biosynthesis also having the ability to bind and sequester iron and promote growth in a siderophore-like manner (Brandel et al. 2012; Kaplan et al. 2021) The downregulation seen here in response to NO is quite interesting.

Studies have suggested that *P. aeruginosa* may switch the siderophore used under extreme iron limitation (Dumas et al. 2013). The downregulation of pyochelin may indicate this switch to pyoverdine, this is more metabolically expensive but is more efficient with a higher binding affinity for iron. Evidence of this is switch in siderophore synthesis is supported by the upregulation of ppkA-pppA. (Goldová et al. 2011) showed that ppkA- pppA are involved with the regulation of pyoverdine biosynthesis with double mutants exhibiting reduced secretion of pyoverdine, and reduced growth rate. Upregulation of these regulatory serine/threonine kinases and simultaneous downregulation of the pyochelin biosynthetic pathway, strongly suggest the siderophore switching ability. This may be as a result of the NO dispersed cells entering a more iron limited environment and seeking additional metabolites to support their attachment and regrowth into the protective biofilm state.

However, it has been shown that NO can inhibit the expression of pyoverdine (Zhu et al. 2019). The study authors showed via transcriptomic profiling that NO treated cells had reduced expression of genes for the synthesis of both pyoverdine and pyochelin. This offers an alternative explanation for the downregulation of pyochelin. The level of expression of pyoverdine is not seen in this study but would be useful to explore further.

Zhu et al. went on to suggest that NO may induce dispersal by degrading the exopolysaccharide Psl and showed that iron limited biofilms are more sensitive to dispersal by NO suggesting combined treatments with iron chelators may be more effective. The use of minimal media in this study without iron supplementation predisposes the biofilms to iron limited environments. Given the findings mentioned above. It may suggest the non-dispersing isolate PA10 is better adapted to retaining and scavenging exogenous iron and may resist the NO inhibition of siderophore production. Future studies with PA10 and an iron chelator may provide more insight to this link.

6.3.5 NO dispersed mPA01 cells exhibit upregulation of key denitrification genes.

The treatment mPA01 cells in the outflow of the microfluid system also demonstrated an upregulation of the gene involved in the denitrification pathway of *P. aeruginosa*. Here we see increases in gene counts of both nirQ and norC, but not norB. The upregulation is somewhat expected in the treatment group by way of the cell reducing toxic endogenous NO concentrations if there is also an elevated level of NO in the environment and indicates the suitability of *P. aeruginosa* for growth in anoxic environments. This regulation indicates the denitrification regulation pathway is in action. Dnr, responsive to NO, NarL to upregulate the transcription of *nirQ,* in turn modulating the activity of NorCB (Arai 2003; Schreiber et al. 2007; Arat et al. 2015; Lichtenberg et al. 2021)

Despite genome analysis for mPA01 showing the presence of the norB gene (Appendix A. **Error! R eference source not found.**), this gene was not identified in the gene count matrix for RNA sequencing, presuming errors in the RNA reference creation as discussed previously we can infer that norB would also have been upregulated.

6.3.6 SNP treated PA10 shows upregulated flagella mediated motility in dispersed cells.

The sequencing data set for PA10 was by far the best quality from which comparisons can be confidently drawn, hierarchical clustering indicates that the reads from PA10 biofilm and outflow conditions are optimal representations for different gene expression profiles.

Following treatment with SNP, the outflow or 'dispersed' cells showed a significant upregulation of genes clusters for the flg operon and fli genes involved with flagella assembly and flagella dependent motility (Bouteiller et al. 2021). As these cells are in the outflow populations, it could be argued this increase in flagella mediate motility is expected as these cells have been dispersed from the biofilm, however this is intriguing since PA10 has been shown in this study and others, not to disperse with the NO signal. The intracellular levels of c-di-GMP are shown to regulate large networks within the cell including flagella synthesis, with low concentration favouring that of the planktonic lifestyle and thus typically increased motility (Hengge 2009b; Bouteiller et al. 2021).

It has previously been thought that flagella are only necessary and modulated in specific stages of the biofilm lifecycle; in young biofilms to aid the migration between microcolonies; or in the end stages of the biofilm lifecycle during active dispersal. With the mature stages existing in a sessile community (McDougald et al. 2012; Guttenplan and Kearns 2013)

However, through flagella bio-tracking with a GFP reporter, Ozer et al. explored spatialised tracking of flagella throughout mature biofilm structures. They discovered that even though resource intensive, flagella are constantly being produced throughout the biofilm lifecycle and contribute to the biofilms physical strength by creating scaffold like structures. The authors also noted flagellated cells are continually dispersed throughout the biofilm lifecycle and not just at distinct stages (Ozer et al. 2021).

Whilst PA10 has a slow planktonic growth rate, the moderate biofilm growth may result in reaching biofilm maturity more quickly than others and thus has greater number of these flagella created scaffolds, this could benefit the PA10 biofilms structurally and mechanically. The upregulation of these flagella with NO treatment could possibly be induced by c-di-GMP turnover and subsequent regulation of flagella mediated motility. This in turn could further enhance the growth and structural integrity of the biofilms formed by PA10. Unfortunately, we are not able to compare PA10 samples to the untreated control, hence we may only speculate the role of NO in the varied dispersal response. Further analysis of PA10 with flagella lacking mutants could confirm this theory.

6.3.7 PA10 outflow populations upregulate the two-component system PhoPQ in response to NO

STRING analysis also revealed there was significant upregulation in the PhoPQ two component system, the PhoPQ inducible oprH, and downregulation in napE a periplasmic nitrate reductase that is poorly characterised. The PhoPQ two component regulatory system is well known for its role in *P. aeruginosa* virulence. Under low Mg2+ conditions PhoPG regulates the overexpression of the outer membrane protein OprH which offers increased resistance to polymyxin B (Gooderham et al. 2009; Rouillard et al. 2021).

Whilst not well described in *P. aeruginosa,* in other bacterial species, namely *Pectobacterium versatile* it has been suggested via transcriptome profiling that a PhoPQ system may control the regulation of genes in the *nap* operon responsible for periplasmic nitrate reductases (Kravchenko, gogoleva 2021). This shares similarities to what we have seen in this study suggesting the PhoPQ role in denitrification regulation also exists in *P. aeruginosa* in response to exogenous NO. This is an intriguing area that may be further explored to explain if it plays any greater role in the varied NO dispersal response.

Network analysis on STRING suggests a functional link between the upregulation phoPQ, oprH and the downregulation of napE, but due to the little-known functionality this protein, significant

conclusions cannot be drawn. It has been suggested that the nitrate reductases similar to napE in the periplasm play a role in nitrate scavenging in certain bacteria (Potter et al. 2001).

6.3.8 Conclusions

Overall, in this chapter, the biological interpretation of the differential gene expression has little significance due to the absence of and appropriate number of replicates in each case. Direct comparisons between the two isolates with contrasting dispersal phenotypes cannot be made, limiting these findings to individual isolates. The statistical power is lost since it cannot be ruled out the effects seen are just the products of random variation between the individual samples. A larger *n* number would be required to enable any outliers and sources of variation to be corrected for an achieve a fully comparable transcriptome profile.

Nevertheless, the transcriptome profiling carried out with RNA sequencing has revealed some interesting channels for future exploration, in particular the roles of PhoPQ in the regulation of the denitrification pathway in *P. aeruginosa,* and the greater role of flagella in the integrity of biofilms formed by the non-dispersing isolate PA10.

This chapter set out to validate a microfluidic biofilm dispersal model which was largely successful. The chapter also aimed to determine the regulatory changes in two bacterial isolates with two distinct responses to the NO biofilm dispersal signal, these results will be important for future experimentations in understanding the varied NO response, however with the lack of replicates and the inability to compare the two, no confident conclusion in relation to the hypothesis can be made.

Chapter 7 Discussion

The colonisation of CF patients by *P. aeruginosa* is associated with persistent morbidity, and increased mortality. Aggressive antibiotic regimes aimed at eradicating or controlling the infection are the current treatment strategy. However, the airway mucus in CF patients hinders the delivery of antibiotics to the infection site, and prolonged treatments regimes reduce their effectiveness over time. Structured biofilm aggregates also offer an increased tolerance to antimicrobials, and treatments are often not effective at clearing the underlying chronic infection. Diagnosis of a biofilm infection is complex and relies mainly on the repeated culture of *P. aeruginosa.* As biofilms are largely unculturable, traditional culture cannot confirm the biofilm status and other patient factors are considered for diagnosis. With a lack of biomarkers escalating this issue.

Alternative biofilm treatment strategies, that utilise NO as biofilm dispersal signal have been trialled and shown success (Howlin et al. 2017). Previous studies explored the effects of NO donor prodrugs, C3D's, and observed varied responses in the dispersal of biofilms formed by clinical isolates of *P. aeruginosa* when treated in vitro (Rineh et al. 2020).

In this study we focused on the utilisation of a range of methods to; 1) determine the biofilm status of patients with cystic fibrosis undergoing antibiotic requiring exacerbation, 2) Identify potential biofilm biomarkers within CF patient sputum that may indicate the biofilm status, 3) explore the underlying mechanisms resulting in the varied response to NO.

7.1 FISH as a tool to determine the biofilm status in CF sputum.

Biofilm phenotyping was successful in all patients where samples, where available, and levels of total biomass able to be quantified and the number of biofilm aggregates calculated. When assessing the whole patient cohort, there is no apparent effect of the use of antibiotics to disrupt the *P. aeruginosa* biofilms. However, FISH imaging highlighted the patient-to-patient variability in the biofilm response to antibiotics, with some patients displaying a surprising increase in total biofilm biomass, whilst others behaved expectedly, and biomass was reduced. There have been previous reports that sublethal concentrations of antibiotics can in fact cause growth promotion of biofilms. This emphasises the need of personalised approaches to CF treatment and resistance profiling of *P. aeruginosa* isolates to proper direct treatment options.

Biofilm to planktonic ratios were calculated for the available patient data and again the cohort overall showed no difference between the proportions of biofilm or planktonic cell biomass in response to antibiotics. Like the above, individual patients showed interesting results. Patients

generally display an increase planktonic cell volume and a reduction in biofilm biomass. We can assume here this is due to the action of antibiotics disrupting, but not fully eradicating the biofilm. Where small biofilm aggregates remain, a combination therapy with a dispersal agent i.e., NO donor prodrugs (C3Ds) would be beneficial in this case to disperse the remaining biofilm aggregates with the aim of total eradication.

7.2 Histone H4 holds potential as a biofilm biomarker.

The biofilm imaging data were compared to proteomics data sets previously acquired as part of a larger multi-centre study with to identify potential biomarkers of biofilm infection. Of the proteins that were identified to be significant in their differential expression between treatment timepoints, histone h4 was carried forward for further analysis as it appeared to change in abundance with antibiotic therapy. Validation of this protein change was attempted with western blotting, however this assay proved to not be sensitive enough to detect the low levels of H4 expressed in CF sputum, and experimental design was somewhat flawed by the limited number of samples available compare.

As with the validation, linking these data sets had limitations in that not all patients provided samples at each timepoint, due to the unassisted nature of sputum expectoration, if the patient was not able to produce sputum at the specified time point, the sample did not exist. Of the time points that had imaging data, not all had corresponding proteomics data. This resulted in a low sample number for a powerful statistical comparison. Correlation data for the biofilm and H4 proportion showed no link between the biofilm biomass and the abundance of protein, this rejects the hypothesis that the lung sputum can be used for biomarker and predict CF biofilm status. However, other studies have shown that H4 elevated in CF patients known to be chronically infected with *P. aeruginosa*, this study may require a larger sample size and repeated H4 profiling of the CF sputum to fully classify the biofilm biomarker status.

7.3 Slow growing *P. aeruginosa* isolates display varied NO responses.

After identifying the biofilm is not fully eradicated in the CF sputum, and that dispersal treatments would be of benefit to some select patients. The NO biofilm dispersal phenotype was further explored following previous observations of a varied NO response. Understanding this variation is critical when deciding patient eligibility for NO therapy. Some clinical isolates have been observed to increase in biofilm biomass under the influence of the NO donor SNP, delivering a NO therapy

to a patient that harbours such an isolate could be detrimental to the CF lung disease state and potentially accelerate its progression.

Soren 2019 tested a subset of isolates available in the Southampton culture collection and hypothesised that slow growing isolates were more conducive to a non-dispersing NO response. Here we further tested the response from the remaining isolates in the culture collection that were predominantly classified as poor biofilm formers with slow growth rates. We again observed a differential response in the NO induced biofilm dispersal showing the findings of Soren not to be exclusive to slow growing isolates. Three distinct dispersal types were categorised: 1) dispersing, 2) no biomass change, 3) biofilm growth promotion. This suggests a greater role of multiple factors that cannot be determined these phenotyping methods.

7.4 Genomic analysis reveals a greater regulatory role in the NO dispersal response.

Given that the isolates remain to show varied responses to NO, it was hypothesised that the results of gene loss in key pathways relating to denitrification and NO dispersal induction may offer an explanation. Fifteen of the clinical isolates underwent whole genome sequencing, of these, thirteen were taxonomically classified as *P. aeruginosa* and the presence or absence of genes encoding for denitrification and known NO effectors and regulators was assessed. All isolates, regardless of their response contained all genes identified as part of the denitrification and NO induction pathways.

Two of the isolates in this study to were revealed not to be *P. aeruginosa* and were in fact identified as *A. xylosoxidans.* This bacterium shares similar morphology and phenotypic characteristics to *P. aeruginosa* and is a common CF pathogen that grows on media we previously believed to be selective for *P. aeruginosa* species only. Here we highlight the importance of additional molecular confirmation of any isolates obtained from CF sputum for accurate diagnosis and epidemiological reporting.

Phylogeny and MLST was employed to categorise the isolates in terms of relatedness. This hoped to show that isolates with a shared sequence types (ST) also shared the NO dispersal response. This was unsuccessful, with variation still observed within clades of isolates that shared the same ST. Interestingly this analysis revealed multiple different ST within the collection, some of which belong to the clonal lineages of concern including the Liverpool, and Manchester epidemic strains which can cross infect patients in CF clinics. Whilst of interest in future epidemiological studies, unfortunately, it reveals no information as to the varied NO dispersal mechanisms.

The genomic analysis performed in this study suggests that gene absence from the nitrate metabolism pathway, or the c-di-GMP turnover is not the governing factor in the differing responses of *P. aeruginosa* biofilms to NO, and rather a greater regulatory role in the expression of these or other genes. Further analysis and integration of the transcriptome data into future genomic studies of these isolates would be beneficial. This may help to identify if those that are differentially expressed in response to NO are present or absent in all of the isolates that share the same dispersal phenotype. For example, to assess the presence/ absence of flagella related genes as seen to be upregulated in the non-dispersing isolate PA10.

7.5 An alternative culture model for dispersal

To assess the differential gene expression in isolates subject to NO treatments, first a more reproducible biofilm culture model needed to be developed. Whilst 96 well based biofilm culture methods offer high throughput, the use for the isolation of biofilm and dispersed populations proved challenging, with biofilm material being easily disrupted and frequently resulting in mixed population samples. In this study we adapted a microfluid culture method previously used by colleagues at Southampton, this culture method allowed more reproducible biofilm growth and separation of the two bacterial populations required for the downstream experiments. The dispersal method was validated for as dispersal assay with SNP, with 50% reduction in live cell biofilm volume. Future dispersal works can continue to use this method in a bid to standardise biofilm culture.

7.6 Transcriptome analysis shows promise for elucidating the varied NO response.

To understand the regulatory mechanisms RNA sequencing performed on biomass and outflow of mPA01 and PA10 with and without NSP treatment. Due to poor sample quality on arrival to the sequencing facility, only 13 of the 24 samples were able to be sequenced. Of those sequenced, where possible the differential gene expression was analysed. Analysis was limited with some comparisons were drawn with only one replicate providing limited statistical power.

However, DGE analysis was performed and STRING network analysis with the top 100 differentially expressed revealing a network cluster of functional pathways to be explored. Of note the role of NO in the induction of flagella mediated motility is of significant interest with other studies demonstrating a greater structural role of flagella within the biofilm that may

explain the PA10 specific response to NO. Other mechanisms including the role of the two-component regulator PhoPQ in the modulation of the *P. aeruginosa* are to be explored further.

The results provide brief insights into the gene regulation induced by NO, but we cannot confidently draw conclusion around any specific genes. Further replicates, RNA extraction, sequencing and data manipulation would be required to enable this.

7.7 Future directions

In this study it has been shown that the biofilm phenotyping for expectorated sputum from CF patients has been successful with the employment of FISH, this allowed visualisation of the biofilm status and the behaviour of the biofilm aggregates in response to antibiotics. This revealed that patients vary and exhibit contrasting trends than would typically be expected. It is important to consider these findings when treating patients in the clinic and assess the patient suitability for certain therapies. The analysis of the biofilm: planktonic ratios demonstrated the tolerance of biofilms to antimicrobials and the difficulties in complete eradication of a chronic biofilm infection.

The suggestion of using dispersal therapies such as NO in these patients is to be further explored. The varied response to NO is an important point to consider, with some isolates not dispersing as well as others, and some exhibiting growth promotion it may not be suitable to apply a blanket therapy of NO to all patients as there is potential this may exacerbate the disease progression.

A deeper analysis of the bacterial genomes of the isolates used in this study, and potentially others from collaborators with extensive *P. aeruginosa* CF culture collections should be considered. Colleagues at Imperial College London has such collection with a large number of these isolates with associated whole genome sequence data. This may help to identify genetic markers on a larger scale than currently explored in this study and may predict how isolates will respond to the NO dispersal signal.

Taking this sequencing data even further, should genetic markers be identified, metagenomic analysis of patient sputum samples could be employed to identify suitability for a NO treatment. Leading a stratified and personal approaches to *P. aeruginosa* infections in CF.

It would be of great interest to explore the biofilm biomarker potential of histone H4 in an extended cohort of patients and sputum samples to solidify the findings of this study and others. The proven elevated abundance of H4 in the sputum of patients known to be chronically infected with *P. aeruginosa* more substantially linked to the biofilm phenotype in a full comparative data

would validate the use of H4 as a biomarker, with implications of improving the efficiency of chronic *P. aeruginosa* lung infection.

Whilst we were unable to fully elucidate the mechanisms behind the varied response of *P. aeruginosa* isolates to NO, further questions have been opened into the downstream effectors of the NO signal. Knockout mutant studies in PA10 for flagella related genes would be beneficial to properly characterise the role they play in relation to the biofilm structure and its tolerance to NO. Similarly, deeper understanding of apparent NO induced PhoPQ system regulator network for denitrification in *P. aeruginosa* could shed light on the different dispersal phenotypes characterised in this study.

This study identified the use of a modified microfluidic biofilm model for the assessment of dispersal. This model is well thought out and produces replicable results between laboratories, however, for the future research of CF specific biofilm dispersal we suggest the development of a model that more closely replicates that of the anoxic and microaerophilic environmental niches often experienced by these isolates within the CF lung.

References

Acosta N, Waddell B, Heirali A, et al (2020) Cystic Fibrosis Patients Infected With Epidemic *Pseudomonas aeruginosa* Strains Have Unique Microbial Communities. Front Cell Infect Microbiol 10:173. https://doi.org/10.3389/fcimb.2020.00173

Aeschlimann JR (2003) The Role of Multidrug Efflux Pumps in the Antibiotic Resistance of *Pseudomonas aeruginosa* and Other Gram-Negative Bacteria. Pharmacotherapy 23:916–924. https://doi.org/10.1592/phco.23.7.916.32722

Aghapour Z, Gholizadeh P, Ganbarov K, et al (2019) Molecular mechanisms related to colistin resistance in Enterobacteriaceae. Infect Drug Resist Volume 12:965–975. https://doi.org/10.2147/IDR.S199844

Alcorn JF, Wright JR (2004) Degradation of pulmonary surfactant protein D by *Pseudomonas aeruginosa* elastase abrogates innate immune function. J Biol Chem 279:30871–30879. https://doi.org/10.1074/jbc.M400796200

Alfonso-Sánchez MA, Pérez-Miranda AM, García-Obregón S, Peña JA (2010) An evolutionary approach to the high frequency of the Delta F508 CFTR mutation in European populations. Med Hypotheses 74:989–992. https://doi.org/10.1016/j.mehy.2009.12.018

Alhede M, Bjarnsholt T, Givskov M, Alhede M (2014) *Pseudomonas aeruginosa* Biofilms. In: Advances in Applied Microbiology. Academic Press Inc., pp 1–40

Alhede M, Kragh KN, Qvortrup K, et al (2011) Phenotypes of Non-Attached *Pseudomonas aeruginosa* Aggregates Resemble Surface Attached Biofilm. PLoS One 6:e27943. https://doi.org/10.1371/journal.pone.0027943

Allen L, Dockrell DH, Pattery T, et al (2005) Pyocyanin Production by *Pseudomonas aeruginosa* Induces Neutrophil Apoptosis and Impairs Neutrophil-Mediated Host Defenses In Vivo . J Immunol 174:3643–3649. https://doi.org/10.4049/jimmunol.174.6.3643

Allesen-Holm M, Barken KB, Yang L, et al (2006) A characterization of DNA release in *Pseudomonas aeruginosa* cultures and biofilms. Mol Microbiol 59:1114–1128. https://doi.org/10.1111/j.1365-2958.2005.05008.x

Alontaga AY, Rodriguez JC, Schönbrunn E, et al (2009) Structural characterization of the hemophore HasAp from *Pseudomonas aeruginosa*: NMR Spectroscopy reveals protein-protein interactions between holo-HasAp and hemoglobin. Biochemistry 48:96–109. https://doi.org/10.1021/bi801860g

Amann RI, Binder BJ, Olson RJ, et al (1990) Combination of 16S rRNA-targeted oligonucleotide probes with flow cytometry for analyzing mixed microbial populations. Appl Environ Microbiol 56:1919. https://doi.org/10.1128/AEM.56.6.1919-1925.1990

Amikam D, Galperin MY (2006) PilZ domain is part of the bacterial c-di-GMP binding protein. Bioinformatics 22:3–6. https://doi.org/10.1093/bioinformatics/bti739

An S, Wu J, Zhang L-H (2010) Modulation of *Pseudomonas aeruginosa* Biofilm Dispersal by a Cyclic-Di-GMP Phosphodiesterase with a Putative Hypoxia-Sensing Domain. Appl Environ Microbiol 76:8160–8173. https://doi.org/10.1128/AEM.01233-10

Andersen DH (1938) Cystic fibrosis of the pancreas and its relation to celiac disease. Am J Dis Child 56:344. https://doi.org/10.1001/archpedi.1938.01980140114013

Andersen SB, Ghoul M, Griffin AS, et al (2017) Diversity, Prevalence, and Longitudinal Occurrence of Type II Toxin-Antitoxin Systems of *Pseudomonas aeruginosa* Infecting Cystic Fibrosis

Lungs. Front Microbiol 8:1180. https://doi.org/10.3389/fmicb.2017.01180

Arai H (2011) Regulation and Function of Versatile Aerobic and Anaerobic Respiratory Metabolism in *Pseudomonas aeruginosa*. Front Microbiol 2:103. https://doi.org/10.3389/fmicb.2011.00103

Arai H (2003) Transcriptional regulation of the nos genes for nitrous oxide reductase in *Pseudomonas aeruginosa*. Microbiology 149:29–36. https://doi.org/10.1099/mic.0.25936-0

Arai H, Hayashi M, Kuroi A, et al (2005) Transcriptional Regulation of the Flavohemoglobin Gene for Aerobic Nitric Oxide Detoxification by the Second Nitric Oxide-Responsive Regulator of *Pseudomonas aeruginosa*. J Bacteriol 187:3960–3968. https://doi.org/10.1128/JB.187.12.3960-3968.2005

Arat S, Bullerjahn GS, Laubenbacher R (2015) A Network Biology Approach to Denitrification in *Pseudomonas aeruginosa*. PLoS One 10:e0118235. https://doi.org/10.1371/journal.pone.0118235

Aridgides D, Dessaint J, Atkins G, et al (2021) Safety of research bronchoscopy with BAL in stable adult patients with cystic fibrosis. PLoS One 16:. https://doi.org/10.1371/JOURNAL.PONE.0245696

Aujoulat F, Roger F, Bourdier A, et al (2012) From Environment to Man: Genome Evolution and Adaptation of Human Opportunistic Bacterial Pathogens. Genes (Basel) 3:191–232. https://doi.org/10.3390/genes3020191

Bahl CD, Morisseau C, Bomberger JM, et al (2010) Crystal Structure of the Cystic Fibrosis Transmembrane Conductance Regulator Inhibitory Factor Cif Reveals Novel Active-Site Features of an Epoxide Hydrolase Virulence Factor. J Bacteriol 192:1785. https://doi.org/10.1128/JB.01348-09

Balaban NQ, Merrin J, Chait R, et al (2004) Bacterial Persistence as a Phenotypic Switch. Science (80-) 305:1622–1625. https://doi.org/10.1126/science.1099390

Ballok AE, Filkins LM, Bomberger JM, et al (2014) Epoxide-mediated differential packaging of cif and other virulence factors into outer membrane vesicles. J Bacteriol 196:3633–3642. https://doi.org/10.1128/JB.01760-14

Ballok AE, O'Toole GA (2013) Pouring Salt on a Wound: *Pseudomonas aeruginosa* Virulence Factors Alter Na+ and Cl- Flux in the Lung. J Bacteriol 195:4013–4019. https://doi.org/10.1128/JB.00339-13

Baraquet C, Harwood CS (2013) Cyclic diguanosine monophosphate represses bacterial flagella synthesis by interacting with the Walker a motif of the enhancer-binding protein FleQ. Proc Natl Acad Sci U S A 110:18478–18483. https://doi.org/10.1073/pnas.1318972110

Barbieri JT, Sun J (2004) *Pseudomonas aeruginosa* ExoS and ExoT. Rev Physiol Biochem Pharmacol 152:79–92. https://doi.org/10.1007/s10254-004-0031-7

Bardoel BW, van Kessel KPM, van Strijp JAG, Milder FJ (2012) Inhibition of *Pseudomonas aeruginosa* Virulence: Characterization of the AprA–AprI Interface and Species Selectivity. J Mol Biol 415:573–583. https://doi.org/10.1016/j.jmb.2011.11.039

Barken KB, Pamp SJ, Yang L, et al (2008) Roles of type IV pili, flagellum-mediated motility and extracellular DNA in the formation of mature multicellular structures in *Pseudomonas aeruginosa* biofilms. Environ Microbiol 10:2331–2343. https://doi.org/10.1111/j.1462-2920.2008.01658.x

Barraud N, Hassett DJ, Hwang SH, et al (2006) Involvement of nitric oxide in biofilm dispersal of *Pseudomonas aeruginosa*. J Bacteriol 188:7344–7353. https://doi.org/10.1128/JB.00779-06

Barraud N, Schleheck D, Klebensberger J, et al (2009) Nitric oxide signaling in *Pseudomonas aeruginosa* biofilms mediates phosphodiesterase activity, decreased cyclic di-GMP levels, and enhanced dispersal. J Bacteriol 191:7333–7342. https://doi.org/10.1128/JB.00975-09

Bartell JA, Sommer LM, Haagensen JAJ, et al (2019) Evolutionary highways to persistent bacterial infection. Nat Commun 10:. https://doi.org/10.1038/s41467-019-08504-7

Batani G, Bayer K, Böge J, et al (2019) Fluorescence in situ hybridization (FISH) and cell sorting of living bacteria. Sci Reports 2019 91 9:1–13. https://doi.org/10.1038/s41598-019-55049-2

Bell SC, Mall MA, Gutierrez H, et al (2020) The future of cystic fibrosis care: a global perspective. Lancet Respir Med 8:65–124. https://doi.org/10.1016/S2213-2600(19)30337-6

Bennett PM (2008) Plasmid encoded antibiotic resistance: Acquisition and transfer of antibiotic resistance genes in bacteria. In: British Journal of Pharmacology. John Wiley & Sons, Ltd, pp S347–S357

Bernardy EE, Iii RAP, Raghuram V, et al (2020) Genotypic and Phenotypic Diversity of *Staphylococcus aureus* Isolates from Cystic Fibrosis Patient Lung Infections and Their Interactions with *Pseudomonas aeruginosa*. https://doi.org/10.1128/mBio.00735-20

Berne C, Ducret A, Hardy GG, Brun Y V (2015) Adhesins Involved in Attachment to Abiotic Surfaces by Gram-Negative Bacteria. Microbiol Spectr 3:. https://doi.org/10.1128/microbiolspec.MB-0018-2015

Berni B, Soscia C, Djermoun S, et al (2019) A Type VI Secretion System Trans-Kingdom Effector Is Required for the Delivery of a Novel Antibacterial Toxin in *Pseudomonas aeruginosa*. Front Microbiol 10:1218. https://doi.org/10.3389/fmicb.2019.01218

Berrazeg M, Jeannot K, Ntsogo Enguéné VY, et al (2015) Mutations in β-lactamase AmpC increase resistance of *Pseudomonas aeruginosa* isolates to antipseudomonal cephalosporins. Antimicrob Agents Chemother 59:6248–6255. https://doi.org/10.1128/AAC.00825-15

Bertranpetit J, Calafell F (1996) Genetic and geographical variability in cystic fibrosis: Evolutionary considerations. CIBA Found Symp 97–118. https://doi.org/10.1002/9780470514887.ch6

Bhagirath AY, Li Y, Somayajula D, et al (2016) Cystic fibrosis lung environment and *Pseudomonas aeruginosa* infection. BMC Pulm Med 16:. https://doi.org/10.1186/s12890-016-0339-5

Bittar F, Rolain J-M (2010) Detection and accurate identification of new or emerging bacteria in cystic fibrosis patients. Clin Microbiol Infect 16:809–820. https://doi.org/10.1111/j.1469-0691.2010.03236.x

Bjarnsholt T (2013) The role of bacterial biofilms in chronic infections. APMIS 121:1–58. https://doi.org/10.1111/apm.12099

Bjarnsholt T, Jensen PØ, Fiandaca MJ, et al (2009) *Pseudomonas aeruginosa* biofilms in the respiratory tract of cystic fibrosis patients. Pediatr Pulmonol 44:547–558. https://doi.org/10.1002/ppul.21011

Bjarnsholt T, Jensen PØ, Jakobsen TH, et al (2010) Quorum Sensing and Virulence of *Pseudomonas aeruginosa* during Lung Infection of Cystic Fibrosis Patients. PLoS One 5:e10115. https://doi.org/10.1371/journal.pone.0010115

Bleves S (2016) Game of Trans-Kingdom Effectors. Trends Microbiol 24:773–774. https://doi.org/10.1016/j.tim.2016.08.002

Bleves S, Viarre V, Salacha R, et al (2010) Protein secretion systems in *Pseudomonas aeruginosa*: A

wealth of pathogenic weapons. Int J Med Microbiol 300:534–543. https://doi.org/10.1016/j.ijmm.2010.08.005

Bobadilla JL, Macek M, Fine JP, Farrell PM (2002) Cystic fibrosis: A worldwide analysis ofCFTR mutations?correlation with incidence data and application to screening. Hum Mutat 19:575–606. https://doi.org/10.1002/humu.10041

Boles BR, Thoendel M, Singh PK (2005) Rhamnolipids mediate detachment of *Pseudomonas aeruginosa* from biofilms. Mol Microbiol 57:1210–1223. https://doi.org/10.1111/j.1365-2958.2005.04743.x

Bolger AM, Lohse M, Usadel B (2014) Trimmomatic: a flexible trimmer for Illumina sequence data. Bioinformatics 30:2114–2120. https://doi.org/10.1093/BIOINFORMATICS/BTU170

Boucher RC (2007) Airway Surface Dehydration in Cystic Fibrosis: Pathogenesis and Therapy. Annu Rev Med 58:157–170. https://doi.org/10.1146/annurev.med.58.071905.105316

Bouteiller M, Dupont C, Bourigault Y, et al (2021) *Pseudomonas* Flagella: Generalities and Specificities. Int J Mol Sci 22:3337. https://doi.org/10.3390/IJMS22073337

Boyd A, Chakrabarty AM (1994) Role of alginate lyase in cell detachment of *Pseudomonas aeruginosa*. Appl Environ Microbiol 60:2355–2359. https://doi.org/10.1128/aem.60.7.2355-2359.1994

Brandel J, Humbert N, Elhabiri M, et al (2012) Pyochelin, a siderophore of *Pseudomonas aeruginosa*: Physicochemical characterization of the iron(III), copper(II) and zinc(II) complexes. Dalt Trans 41:2820–2834. https://doi.org/10.1039/C1DT11804H

Bredt DS (1999) Endogenous nitric oxide synthesis: Biological functions and pathophysiology. Free Radic Res 31:577–596. https://doi.org/10.1080/10715769900301161

Breitwieser FP, Salzberg SL (2020) Pavian: interactive analysis of metagenomics data for microbiome studies and pathogen identification. Bioinformatics 36:1303–1304. https://doi.org/10.1093/BIOINFORMATICS/BTZ715

Briard B, Bomme P, Lechner BE, et al (2015) *Pseudomonas aeruginosa* manipulates redox and iron homeostasis of its microbiota partner Aspergillus fumigatus via phenazines. Sci Rep 5:1–13. https://doi.org/10.1038/srep08220

Bryan NS, Grisham MB (2007) Methods to detect nitric oxide and its metabolites in biological samples. Free Radic Biol Med 43:645–657. https://doi.org/10.1016/j.freeradbiomed.2007.04.026

Bryan R, Kube D, Perez A, et al (1998) Overproduction of the CFTR R domain leads to increased levels of asialoGM1 and increased *Pseudomonas aeruginosa* binding by epithelial cells. Am J Respir Cell Mol Biol 19:269–277. https://doi.org/10.1165/ajrcmb.19.2.2889

Burns JL, Rolain J-M (2014) Culture-based diagnostic microbiology in cystic fibrosis: Can we simplify the complexity? J Cyst Fibros 13:1–9. https://doi.org/10.1016/j.jcf.2013.09.004

Butterworth MB (2010) Regulation of the epithelial sodium channel (ENaC) by membrane trafficking. Biochim. Biophys. Acta - Mol. Basis Dis. 1802:1166–1177

Button B, Cai LH, Ehre C, et al (2012) A periciliary brush promotes the lung health by separating the mucus layer from airway epithelia. Science (80-) 337:937–941. https://doi.org/10.1126/science.1223012

Caballero JD, Clark ST, Coburn B, et al (2015) Selective Sweeps and Parallel Pathoadaptation Drive

Pseudomonas aeruginosa Evolution in the Cystic Fibrosis Lung. MBio 6:. https://doi.org/10.1128/MBIO.00981-15

Caiazza NC, Merritt JH, Brothers KM, O'Toole GA (2007) Inverse regulation of biofilm formation and swarming motility by *Pseudomonas aeruginosa* PA14. J Bacteriol 189:3603–3612. https://doi.org/10.1128/JB.01685-06

Caiazza NC, O'Toole GA (2004) SadB is required for the transition from reversible to irreversible attachment during biofilm formation by *Pseudomonas aeruginosa* PA14. J Bacteriol 186:4476–4485. https://doi.org/10.1128/JB.186.14.4476-4485.2004

Caldwell CC, Chen Y, Goetzmann HS, et al (2009) *Pseudomonas aeruginosa* exotoxin pyocyanin causes cystic fibrosis airway pathogenesis. Am J Pathol 175:2473–2488. https://doi.org/10.2353/ajpath.2009.090166

Carroll TP, Schwiebert EM, Guggino WB (1993) CFTR: Structure and Function. Cell Physiol Biochem 3:388–399. https://doi.org/10.1159/000154700

Caselli E, D'Accolti M, Soffritti I, et al (2018) Spread of mcr-1 –Driven Colistin Resistance on Hospital Surfaces, Italy. Emerg Infect Dis 24:1752–1753. https://doi.org/10.3201/eid2409.171386

Ceri H, Olson ME, Stremick C, et al (1999) The Calgary Biofilm Device: New Technology for Rapid Determination of Antibiotic Susceptibilities of Bacterial Biofilms. J Clin Microbiol 37:1771–1776. https://doi.org/10.1128/JCM.37.6.1771-1776.1999

Chakravarty S, Massé E (2019) RNA-Dependent Regulation of Virulence in Pathogenic Bacteria. Front. Cell. Infect. Microbiol. 9:337

Chang C-Y (2018) Surface Sensing for Biofilm Formation in *Pseudomonas aeruginosa*. Front Microbiol 8:2671. https://doi.org/10.3389/fmicb.2017.02671

Chen H, Wubbolts RW, Haagsman HP, Veldhuizen EJA (2018) Inhibition and Eradication of *Pseudomonas aeruginosa* Biofilms by Host Defence Peptides. Sci Rep 8:10446. https://doi.org/10.1038/s41598-018-28842-8

Chen J-H, Cai Z, Li H, Sheppard DN (2005) Function of CFTR Protein: Ion Transport. In: Cystic Fibrosis in the 21st Century. KARGER, Basel, pp 38–44

Chew SC, Kundukad B, Seviour T, et al (2014) Dynamic remodeling of microbial biofilms by functionally distinct exopolysaccharides. MBio 5:1–11. https://doi.org/10.1128/mBio.01536-14

Chmiel JF, Berger M, Konstan MW (2002) The Role of Inflammation in the Pathophysiology of CF Lung Disease. Clin Rev Allergy Immunol 23:005–028. https://doi.org/10.1385/CRIAI:23:1:005

Cholon DM, Esther CR, Gentzsch M (2016) Efficacy of lumacaftor-ivacaftor for the treatment of cystic fibrosis patients homozygous for the F508del-CFTR mutation. Expert Rev Precis Med Drug Dev 1:235–243. https://doi.org/10.1080/23808993.2016.1175299

Chrzanowska NM, Kowalewski J, Lewandowska MA (2020) Use of Fluorescence In Situ Hybridization (FISH) in Diagnosis and Tailored Therapies in Solid Tumors. Molecules 25:. https://doi.org/10.3390/MOLECULES25081864

Chrzanowski Ł, Ławniczak Ł, Czaczyk K (2012) Why do microorganisms produce rhamnolipids? World J Microbiol Biotechnol 28:401–419. https://doi.org/10.1007/s11274-011-0854-8

Ciofu O, Tolker-Nielsen T (2019) Tolerance and Resistance of *Pseudomonas aeruginosa* Biofilms to Antimicrobial Agents—How P. aeruginosa Can Escape Antibiotics. Front Microbiol 10:913. https://doi.org/10.3389/fmicb.2019.00913

Ciofu O, Tolker-Nielsen T, Jensen PØ, et al (2015) Antimicrobial resistance, respiratory tract infections and role of biofilms in lung infections in cystic fibrosis patients. Adv. Drug Deliv. Rev. 85:7–23

Ciornei CD, Novikov A, Beloin C, et al (2010) Biofilm-forming *Pseudomonas aeruginosa* bacteria undergo lipopolysaccharide structural modifications and induce enhanced inflammatory cytokine response in human monocytes. 288–301. https://doi.org/10.1177/1753425909341807

Clancy JP, Rowe SM, Accurso FJ, et al (2012) Results of a phase IIa study of VX-809, an investigational CFTR corrector compound, in subjects with cystic fibrosis homozygous for the F508del-CFTR mutation. Thorax 67:12–18. https://doi.org/10.1136/thoraxjnl-2011-200393

Clunes MT, Boucher RC (2007) Cystic fibrosis: the mechanisms of pathogenesis of an inherited lung disorder. Drug Discov Today Dis Mech 4:63–72. https://doi.org/10.1016/j.ddmec.2007.09.001

Cohen TS, Prince A (2012) Cystic fibrosis: a mucosal immunodeficiency syndrome. Nat Med 18:509–519. https://doi.org/10.1038/nm.2715

Colvin KM, Irie Y, Tart CS, et al (2012) The Pel and Psl polysaccharides provide *Pseudomonas aeruginosa* structural redundancy within the biofilm matrix. Environ Microbiol 14:1913–1928. https://doi.org/10.1111/j.1462-2920.2011.02657.x

Condren ME, Bradshaw MD (2013) Ivacaftor: A Novel Gene-Based Therapeutic Approach for Cystic Fibrosis. J Pediatr Pharmacol Ther 18:8–13. https://doi.org/10.5863/1551-6776-18.1.8

Costa SS, Guimarães LC, Silva A, et al (2020) First Steps in the Analysis of Prokaryotic Pan-Genomes. Bioinform Biol Insights 14:. https://doi.org/10.1177/1177932220938064

Croucher NJ, Thomson NR (2010) Studying bacterial transcriptomes using RNA-seq. Curr Opin Microbiol 13:619–624. https://doi.org/10.1016/J.MIB.2010.09.009

Cuthbertson L, Walker AW, Oliver AE, et al (2020) Lung function and microbiota diversity in cystic fibrosis. Microbiome 8:45. https://doi.org/10.1186/s40168-020-00810-3

Cystic Fibrosis Trust (2018) UK Cystic Fibrosis Registry Annual data report 2018

Cystic Fibrosis Trust (2011) Standards for the Clinical Care of Children and Adults with cystic fibrosis in the UK

D'Argenio DA, Wu M, Hoffman LR, et al (2007) Growth phenotypes of *Pseudomonas aeruginosa* lasR mutants adapted to the airways of cystic fibrosis patients. Mol Microbiol 64:512–533. https://doi.org/10.1111/j.1365-2958.2007.05678.x

Daims H, Lücker S, Wagner M (2006) daime, a novel image analysis program for microbial ecology and biofilm research. Environ Microbiol 8:200–213. https://doi.org/10.1111/J.1462-2920.2005.00880.X

Davies DG, Parsek MR, Pearson JP, et al (1998) The involvement of cell-to-cell signals in the development of a bacterial biofilm. Science (80-) 280:295–298. https://doi.org/10.1126/science.280.5361.295

Davies JC (2002) *Pseudomonas aeruginosa* in cystic fibrosis: Pathogenesis and persistence. Paediatr Respir Rev 3:128–134. https://doi.org/10.1016/S1526-0550(02)00003-3

Davies JC, Alton EWFW, Bush A (2007) Cystic fibrosis. BMJ 335:1255–1259. https://doi.org/10.1136/bmj.39391.713229.AD

Davies JC, Martin I (2018) New anti-pseudomonal agents for cystic fibrosis- still needed in the era of small molecule CFTR modulators? Expert Opin. Pharmacother. 19:1327–1336

De Baets F, Schelstraete P, Van Daele S, et al (2006) *Achromobacter xylosoxidans* in cystic fibrosis: Prevalence and clinical relevance. https://doi.org/10.1016/j.jcf.2006.05.011

De Bentzmann S, Polette M, Zahm JM, et al (2000) *Pseudomonas aeruginosa* virulence factors delay airway epithelial wound repair by altering the actin cytoskeleton and inducing overactivation of epithelial matrix metalloproteinase-2. Lab Investig 80:209–219. https://doi.org/10.1038/labinvest.3780024

De Oliveira DMP, Forde BM, Kidd TJ, et al (2020) Antimicrobial resistance in ESKAPE pathogens. Clin Microbiol Rev 33:. https://doi.org/10.1128/CMR.00181-19

Defraine V, Fauvart M, Michiels J (2018) Fighting bacterial persistence: Current and emerging anti-persister strategies and therapeutics. Drug Resist Updat 38:12–26. https://doi.org/10.1016/J.DRUP.2018.03.002

Delcour AH (2009) Outer membrane permeability and antibiotic resistance. Biochim Biophys Acta - Proteins Proteomics 1794:808–816. https://doi.org/10.1016/j.bbapap.2008.11.005

Dettman JR, Rodrigue N, Aaron SD, Kassen R (2013) Evolutionary genomics of epidemic and nonepidemic strains of *Pseudomonas aeruginosa*. Proc Natl Acad Sci U S A 110:21065–21070. https://doi.org/10.1073/PNAS.1307862110

Du K, Lukacs GL (2009) Cooperative assembly and misfolding of CFTR domains in vivo. Mol Biol Cell 20:1903–1915. https://doi.org/10.1091/mbc.E08-09-0950

Dumas Z, Ross-Gillespie A, Kümmerli R (2013) Switching between apparently redundant iron-uptake mechanisms benefits bacteria in changeable environments. Proc R Soc B Biol Sci 280:. https://doi.org/10.1098/RSPB.2013.1055

Ehsan Z, Clancy JP (2015) Management of *Pseudomonas aeruginosa* infection in cystic fibrosis patients using inhaled antibiotics with a focus on nebulized liposomal amikacin. Future Microbiol 10:1901–1912. https://doi.org/10.2217/fmb.15.117

Elborn JS (2016) Cystic fibrosis. Lancet 388:2519–2531. https://doi.org/10.1016/S0140-6736(16)00576-6

Equi AC, Pike SE, Davies J, Bush A (2001) Use of cough swabs in a cystic fibrosis clinic

Ernst RK, Moskowitz SM, Emerson JC, et al (2007) Unique lipid A modifications in *Pseudomonas aeruginosa* isolated from the airways of patients with cystic fibrosis. J Infect Dis 196:1088–1092. https://doi.org/10.1086/521367

Ernst RK, Yi EC, Guo L, et al (1999) Specific lipopolysaccharide found in cystic fibrosis airway *Pseudomonas aeruginosa*. Science (80-) 286:1561–1565. https://doi.org/10.1126/science.286.5444.1561

Fahy J V., Dickey BF (2010) Airway Mucus Function and Dysfunction. N Engl J Med 363:2233–2247. https://doi.org/10.1056/NEJMra0910061

Farrell PM, White TB, Ren CL, et al (2017) Diagnosis of Cystic Fibrosis: Consensus Guidelines from the Cystic Fibrosis Foundation. J Pediatr 181:S4-S15.e1. https://doi.org/10.1016/j.jpeds.2016.09.064

Feigelman R, Kahlert CR, Baty F, et al (2017) Sputum DNA sequencing in cystic fibrosis: Non-invasive access to the lung microbiome and to pathogen details. Microbiome 5:1–14. https://doi.org/10.1186/S40168-017-0234-1/FIGURES/5

Feldman M, Bryan R, Rajan S, et al (1998) Role of flagella in pathogenesis of *Pseudomonas*

aeruginosa pulmonary infection. Infect Immun 66:43–51. https://doi.org/10.1128/iai.66.1.43-51.1998

Feltman H, Schulert G, Khan S, et al (2001) Prevalence of type III secretion genes in clinical and environmental isolates of *Pseudomonas aeruginosa*. Microbiology 147:2659–2669. https://doi.org/10.1099/00221287-147-10-2659

Fernández-Cuenca F, Pérez-Palacios P, Galán-Sánchez F, et al (2020) First identification of blaNDM-1 carbapenemase in blaOXA-94-producing *Acinetobacter baumannii* ST85 in Spain. Enfermedades Infecc y Microbiol Clin (English ed) 38:11–15. https://doi.org/10.1016/j.eimce.2019.03.013

Firmida MC, Marques EA, Leão RS, et al (2017) *Achromobacter xylosoxidans* infection in cystic fibrosis siblings with different outcomes: Case reports. Respir Med case reports 20:98–103. https://doi.org/10.1016/j.rmcr.2017.01.005

Fischer S, Dethlefsen S, Klockgether J, Tümmler B (2020) Phenotypic and Genomic Comparison of the Two Most Common ExoU-Positive *Pseudomonas aeruginosa* Clones, PA14 and ST235. mSystems 5:. https://doi.org/10.1128/MSYSTEMS.01007-20

Flemming H-C, Wingender J (2010) The biofilm matrix. Nat Rev Microbiol 8:623–633. https://doi.org/10.1038/nrmicro2415

Flemming HC, Wuertz S (2019) Bacteria and archaea on Earth and their abundance in biofilms. Nat Rev Microbiol 2019 174 17:247–260. https://doi.org/10.1038/s41579-019-0158-9

Flume PA, Strange C, Ye X, et al (2005a) Pneumothorax in cystic fibrosis. Chest 128:720–728. https://doi.org/10.1378/chest.128.2.720

Flume PA, Yankaskas JR, Ebeling M, et al (2005b) Massive hemoptysis in cystic fibrosis. Chest 128:729–738. https://doi.org/10.1378/chest.128.2.729

Fodor AA, Klem ER, Gilpin DF, et al (2012) The Adult Cystic Fibrosis Airway Microbiota Is Stable over Time and Infection Type, and Highly Resilient to Antibiotic Treatment of Exacerbations. PLoS One 7:e45001. https://doi.org/10.1371/journal.pone.0045001

Founou RC, Founou LL, Allam M, et al (2020) First report of a clinical multidrug-resistant *Pseudomonas aeruginosa* ST532 isolate harbouring a ciprofloxacin-modifying enzyme (CrpP) in South Africa. J Glob Antimicrob Resist 22:145–146. https://doi.org/10.1016/J.JGAR.2020.05.012

Frimmersdorf E, Horatzek S, Pelnikevich A, et al (2010) How *Pseudomonas aeruginosa* adapts to various environments: A metabolomic approach. Environ Microbiol 12:1734–1747. https://doi.org/10.1111/j.1462-2920.2010.02253.x

Fuqua C, Winans SC, Greenberg EP (1996) CENSUS AND CONSENSUS IN BACTERIAL ECOSYSTEMS: The LuxR-LuxI Family of Quorum-Sensing Transcriptional Regulators. Annu Rev Microbiol 50:727–751. https://doi.org/10.1146/annurev.micro.50.1.727

Gadsby DC, Vergani P, Csanády L (2006) The ABC protein turned chloride channel whose failure causes cystic fibrosis. Nature 440:477–483. https://doi.org/10.1038/nature04712

Gallagher LA, Mcknight SL, Kuznetsova MS, et al (2002) Functions Required for Extracellular Quinolone Signaling by *Pseudomonas aeruginosa* Downloaded from. J Bacteriol 184:6472–6480. https://doi.org/10.1128/JB.184.23.6472-6480.2002

Galperin MY, Gaidenko TA, Mulkidjanian AY, et al (2001) MHYT, a new integral membrane sensor

domain. FEMS Microbiol Lett 205:17–23. https://doi.org/10.1111/j.1574-6968.2001.tb10919.x

Garmory HS, Titball RW (2004) ATP-Binding Cassette Transporters Are Targets for the Development of Antibacterial Vaccines and Therapies. Infect Immun 72:6757. https://doi.org/10.1128/IAI.72.12.6757-6763.2004

Gaston B, Ratjen F, Vaughan JW, et al (2002) Nitrogen redox balance in the cystic fibrosis airway: Effects of antipseudomonal therapy. Am J Respir Crit Care Med 165:387–390. https://doi.org/10.1164/ajrccm.165.3.2106006

Ghafoor A, Hay ID, Rehm BHA (2011) Role of exopolysaccharides in *Pseudomonas aeruginosa* biofilm formation and architecture. Appl Environ Microbiol 77:5238–5246. https://doi.org/10.1128/AEM.00637-11

Ghanbari A, Dehghany J, Schwebs T, et al (2016) Inoculation density and nutrient level determine the formation of mushroom-shaped structures in *Pseudomonas aeruginosa* biofilms. Sci Reports 2016 61 6:1–12. https://doi.org/10.1038/srep32097

Ghosh S, Erzurum SC (2011) Nitric oxide metabolism in asthma pathophysiology. Biochim Biophys Acta - Gen Subj 1810:1008–1016. https://doi.org/10.1016/j.bbagen.2011.06.009

Goldová J, Ulrych A, Hercík K, Branny P (2011) A eukaryotic-type signalling system of *Pseudomonas aeruginosa* contributes to oxidative stress resistance, intracellular survival and virulence. BMC Genomics 12:437. https://doi.org/10.1186/1471-2164-12-437

Gooderham WJ, Gellatly SL, Sanschagrin F, et al (2009) The sensor kinase PhoQ mediates virulence in *Pseudomonas aeruginosa*. Microbiology 155:699–711. https://doi.org/10.1099/MIC.0.024554-0/CITE/REFWORKS

Goodyear MC, Garnier NE, Levesque RC, Khursigara CM (2022) Liverpool Epidemic Strain Isolates of *Pseudomonas aeruginosa* Display High Levels of Antimicrobial Resistance during Both Planktonic and Biofilm Growth. Microbiol Spectr 10:. https://doi.org/10.1128/SPECTRUM.01024-22

Gordon CA, Hodges NA, Marriott C (1988) Antibiotic interaction and diffusion through alginate and exopolysaccharide of cystic fibrosis-derived *Pseudomonas aeruginosa*. J Antimicrob Chemother 22:667–674. https://doi.org/10.1093/jac/22.5.667

Goss CH, Burns JL (2007) Exacerbations in cystic fibrosis {middle dot} 1: Epidemiology and pathogenesis. Thorax 62:360–367. https://doi.org/10.1136/thx.2006.060889

Grasemann H, Grasemann C, Kurtz F, et al (2005) Oral L-arginine supplementation in cystic fibrosis patients: A placebo-controlled study. Eur Respir J 25:62–68. https://doi.org/10.1183/09031936.04.00086104

Grasemann H, Michler E, Wallot M, Ratjen F (1997) Decreased concentration of exhaled nitric oxide (NO) in patients with cystic fibrosis. Pediatr Pulmonol 24:173–177. https://doi.org/10.1002/(SICI)1099-0496(199709)24:3<173::AID-PPUL2>3.0.CO;2-O

GRUBB BR, BOUCHER RC (1999) Pathophysiology of Gene-Targeted Mouse Models for Cystic Fibrosis. Physiol Rev 79:S193–S214. https://doi.org/10.1152/physrev.1999.79.1.S193

Guillon A, Brea D, Morello E, et al (2017) *Pseudomonas aeruginosa* proteolytically alters the interleukin 22-dependent lung mucosal defense. Virulence 8:810–820. https://doi.org/10.1080/21505594.2016.1253658

Guo Y, Su M, McNutt MA, Gu J (2009) Expression and distribution of cystic fibrosis transmembrane conductance regulator in neurons of the human brain. J Histochem Cytochem 57:1113–1120. https://doi.org/10.1369/jhc.2009.953455

Gutiérrez O, Juan C, Cercenado E, et al (2007) Molecular epidemiology and mechanisms of carbapenem resistance in *Pseudomonas aeruginosa* isolates from Spanish hospitals. Antimicrob Agents Chemother 51:4329–4335. https://doi.org/10.1128/AAC.00810-07

Guttenplan SB, Kearns DB (2013) Regulation of flagellar motility during biofilm formation. FEMS Microbiol Rev 37:849–871. https://doi.org/10.1111/1574-6976.12018

Ha D-G, O'Toole GA (2015) c-di-GMP and its Effects on Biofilm Formation and Dispersion: a *Pseudomonas aeruginosa* Review. Microbiol Spectr 3:. https://doi.org/10.1128/microbiolspec.mb-0003-2014

Hajjar AM, Tsai JH, Wilson CB, Miller SI (2002) Human Toll-like receptor 4 recognizes host-specific LPS modifications. Nat Immunol 3:354–359. https://doi.org/10.1038/ni777

Hall-Stoodley L, Costerton JW, Stoodley P (2004) Bacterial biofilms: from the Natural environment to infectious diseases. Nat Rev Microbiol 2:95–108. https://doi.org/10.1038/nrmicro821

Hall CW, Mah T-F (2017) Molecular mechanisms of biofilm-based antibiotic resistance and tolerance in pathogenic bacteria. FEMS Microbiol Rev 41:276–301. https://doi.org/10.1093/femsre/fux010

Hancock REW, Speert DP (2000) Antibiotic resistance in *Pseudomonas aeruginosa*: Mechanisms and impact on treatment. Drug Resist Updat 3:247–255. https://doi.org/10.1054/drup.2000.0152

Hansen CR, Pressler T, Nielsen KG, et al (2010) Inflammation in *Achromobacter xylosoxidans* infected cystic fibrosis patients. J Cyst Fibros 9:51–58. https://doi.org/10.1016/J.JCF.2009.10.005

Hardy KS, Tuckey AN, Renema P, et al (2022) ExoU Induces Lung Endothelial Cell Damage and Activates Pro-Inflammatory Caspase-1 during *Pseudomonas aeruginosa* Infection. Toxins (Basel) 14:. https://doi.org/10.3390/TOXINS14020152/S1

Hauser AR (2009) The type III secretion system of *Pseudomonas aeruginosa*: infection by injection. Nat Rev Microbiol 7:654–665. https://doi.org/10.1038/nrmicro2199

Hay ID, Gatland K, Campisano A, et al (2009) Impact of alginate overproduction on attachment and biofilm architecture of a supermucoid *Pseudomonas aeruginosa* strain. Appl Environ Microbiol 75:6022–6025. https://doi.org/10.1128/AEM.01078-09

Heijerman HGM, McKone EF, Downey DG, et al (2019) Efficacy and safety of the elexacaftor plus tezacaftor plus ivacaftor combination regimen in people with cystic fibrosis homozygous for the F508del mutation: a double-blind, randomised, phase 3 trial. Lancet 394:1940–1948. https://doi.org/10.1016/S0140-6736(19)32597-8

Hengge R (2009a) Principles of c-di-GMP signalling in bacteria. Nat Rev Microbiol 7:263–273. https://doi.org/10.1038/nrmicro2109

Hengge R (2009b) Principles of c-di-GMP signalling in bacteria. Nat Rev Microbiol 7:263–273. https://doi.org/10.1038/NRMICRO2109

Hengzhuang W, Ciofu O, Yang L, et al (2013) High β-lactamase levels change the pharmacodynamics of β-lactam antibiotics in *Pseudomonas aeruginosa* biofilms. Antimicrob Agents Chemother 57:196–204. https://doi.org/10.1128/AAC.01393-12

Hickman JW, Harwood CS (2008) Identification of FleQ from *Pseudomonas aeruginosa* as a c-di-GMP-responsive transcription factor. Mol Microbiol 69:376–389.

https://doi.org/10.1111/j.1365-2958.2008.06281.x

Higgins CF (2001) ABC transporters: physiology, structure and mechanism – an overview. Res Microbiol 152:205–210. https://doi.org/10.1016/S0923-2508(01)01193-7

Hofer M, Mueller L, Rechsteiner T, et al (2009) Extended nitric oxide measurements in exhaled air of cystic fibrosis and healthy adults. Lung 187:307–313. https://doi.org/10.1007/s00408-009-9160-8

Hogardt M, Trebesius K, Geiger AM, et al (2000) Specific and rapid detection by fluorescent in situ hybridization of bacteria in clinical samples obtained from cystic fibrosis patients. J Clin Microbiol 38:818–825. https://doi.org/10.1128/JCM.38.2.818-825.2000

Hohmann S, Neidig A, Kühl B, et al (2017) A new data processing routine facilitating the identification of surface adhered proteins from bacterial conditioning films via QCM-D/MALDI-ToF/MS. Anal Bioanal Chem 409:5965–5974. https://doi.org/10.1007/s00216-017-0521-5

Høiby N, Bjarnsholt T, Moser C, et al (2017) Diagnosis of biofilm infections in cystic fibrosis patients. APMIS 125:339–343. https://doi.org/10.1111/apm.12689

Holmes B, Snell JJS, Lapage SP (1977) Strains of *Achromobacter xylosoxidans* from clinical material. J clin Path 30:595–601. https://doi.org/10.1136/jcp.30.7.595

Hossain S, Boon EM (2017) Discovery of a Novel Nitric Oxide Binding Protein and Nitric-Oxide-Responsive Signaling Pathway in *Pseudomonas aeruginosa*. ACS Infect Dis 3:454–461. https://doi.org/10.1021/acsinfecdis.7b00027

Hossain S, Nisbett LM, Boon EM (2017) Discovery of Two Bacterial Nitric Oxide-Responsive Proteins and Their Roles in Bacterial Biofilm Regulation. Acc Chem Res 50:1633–1639. https://doi.org/10.1021/acs.accounts.7b00095

Housseini B Issa K, Phan G, Broutin I (2018) Functional Mechanism of the Efflux Pumps Transcription Regulators From *Pseudomonas aeruginosa* Based on 3D Structures. Front Mol Biosci 5:57. https://doi.org/10.3389/fmolb.2018.00057

Howlin RP, Cathie K, Hall-Stoodley L, et al (2017) Low-Dose Nitric Oxide as Targeted Anti-biofilm Adjunctive Therapy to Treat Chronic *Pseudomonas aeruginosa* Infection in Cystic Fibrosis. Mol Ther 25:2104–2116. https://doi.org/10.1016/j.ymthe.2017.06.021

Hubert D, Aubourg F, Fauroux B, et al (2009) Exhaled nitric oxide in cystic fibrosis: Relationships with airway and lung vascular impairments. Eur Respir J 34:117–124. https://doi.org/10.1183/09031936.00164508

Hurley M, Bhatt J, Smyth A (2011) Treatment massive haemoptysis in cystic fibrosis with tranexamic acid. J R Soc Med Suppl 104:S49. https://doi.org/10.1258/jrsm.2011.s11109

Hutchin A, Cordery C, Walsh MA, et al (2021) Phylogenetic Analysis with Prediction of Cofactor or Ligand Binding for *Pseudomonas aeruginosa* PAS and Cache Domains

Hwang TC, Kirk KL (2013) The CFTR Ion channel: Gating, regulation, and anion permeation. Cold Spring Harb Perspect Med 3:. https://doi.org/10.1101/cshperspect.a009498

Iglewski BH (1996) *Pseudomonas*. Elsevier

Iiyama K, Takahashi E, Lee JM, et al (2017) Alkaline protease contributes to pyocyanin production in *Pseudomonas aeruginosa*. FEMS Microbiol Lett 364:51. https://doi.org/10.1093/femsle/fnx051

Jacobs MA, Alwood A, Thaipisuttikul I, et al (2003) Comprehensive transposon mutant library of *Pseudomonas aeruginosa*. Proc Natl Acad Sci 100:14339–14344.

https://doi.org/10.1073/PNAS.2036282100

Jayaseelan S, Ramaswamy D, Dharmaraj S (2014) Pyocyanin: production, applications, challenges and new insights. World J Microbiol Biotechnol 30:1159–1168. https://doi.org/10.1007/s11274-013-1552-5

Jenal U, Reinders A, Lori C (2017) Cyclic di-GMP: second messenger extraordinaire. Nat Rev Microbiol 15:271–284. https://doi.org/10.1038/nrmicro.2016.190

Jolley KA, Bray JE, Maiden MCJ (2018) Open-access bacterial population genomics: BIGSdb software, the PubMLST.org website and their applications [version 1; referees: 2 approved]. Wellcome Open Res 3:. https://doi.org/10.12688/WELLCOMEOPENRES.14826.1/DOI

Jones AM (2005) Eradication therapy for early *Pseudomonas aeruginosa* infection in CF: many questions still unanswered. Eur Respir J 26:373–375. https://doi.org/10.1183/09031936.05.00069705

Jones AM, Govan JRW, Doherty CJ, et al (2001) Spread of a multiresistant strain of *Pseudomonas aeruginosa* in an adult cystic fibrosis clinic. Lancet 358:557–558. https://doi.org/10.1016/S0140-6736(01)05714-2

Jørgensen KM, Wassermann T, Jensen PØ, et al (2013) Sublethal ciprofloxacin treatment leads to rapid development of high-level ciprofloxacin resistance during long-term experimental evolution of *Pseudomonas aeruginosa*. Antimicrob Agents Chemother 57:4215–4221. https://doi.org/10.1128/AAC.00493-13

Jorth P, Staudinger BJ, Wu X, et al (2015) Regional Isolation Drives Bacterial Diversification within Cystic Fibrosis Lungs. Cell Host Microbe 18:307–319. https://doi.org/10.1016/j.chom.2015.07.006

Kang D, Revtovich A V., Chen Q, et al (2019) Pyoverdine-Dependent Virulence of *Pseudomonas aeruginosa* Isolates From Cystic Fibrosis Patients. Front Microbiol 10:. https://doi.org/10.3389/fmicb.2019.02048

Kaplan AR, Musaev DG, Wuest WM (2021) Pyochelin Biosynthetic Metabolites Bind Iron and Promote Growth in Pseudomonads Demonstrating Siderophore-like Activity. ACS Infect Dis 7:544–551. https://doi.org/10.1021/ACSINFECDIS.0C00897/SUPPL_FILE/ID0C00897_SI_001.PDF

Karimi A, Karig D, Kumar A, Ardekani AM (2015) Interplay of physical mechanisms and biofilm processes: review of microfluidic methods. Lab Chip 15:23–42. https://doi.org/10.1039/C4LC01095G

Katusic ZS, Caplice NM, Nath KA (2003) Nitric Oxide Synthase Gene Transfer as a Tool to Study Biology of Endothelial Cells. Arterioscler Thromb Vasc Biol 23:1990–1994. https://doi.org/10.1161/01.ATV.0000078522.50981.55

Kerem BS, Rommens JM, Buchanan JA, et al (1989) Identification of the cystic fibrosis gene: Genetic analysis. Science (80-) 245:1073–1080. https://doi.org/10.1126/science.2570460

Kettle AJ, Turner R, Gangell CL, et al (2014) Oxidation contributes to low glutathione in the airways of children with cystic fibrosis. Eur Respir J 44:122–129. https://doi.org/10.1183/09031936.00170213

Kharitonov SA, Barnes PJ (2000) Clinical aspects of exhaled nitric oxide. Eur Respir J 16:781–792. https://doi.org/10.1183/09031936.00.16478100

Kida Y, Higashimoto Y, Inoue H, et al (2008) A novel secreted protease from *Pseudomonas aeruginosa* activates NF-κB through protease-activated receptors. Cell Microbiol 10:1491–1504. https://doi.org/10.1111/j.1462-5822.2008.01142.x

Kidd TJ, Ramsay KA, Hu H, et al (2009) Low Rates of *Pseudomonas aeruginosa* Misidentification in Isolates from Cystic Fibrosis Patients. J Clin Microbiol 47:1503. https://doi.org/10.1128/JCM.00014-09

Kim D, Paggi JM, Park C, et al (2019) Graph-based genome alignment and genotyping with HISAT2 and HISAT-genotype. Nat Biotechnol 2019 378 37:907–915. https://doi.org/10.1038/s41587-019-0201-4

Kim SJ, Skach WR (2012) Mechanisms of CFTR Folding at the Endoplasmic Reticulum. Front Pharmacol 3:. https://doi.org/10.3389/fphar.2012.00201

Kirk KL, Wang W (2011) A Unified View of Cystic Fibrosis Transmembrane Conductance Regulator (CFTR) Gating: Combining the Allosterism of a Ligand-gated Channel with the Enzymatic Activity of an ATP-binding Cassette (ABC) Transporter. J Biol Chem 286:12813–12819. https://doi.org/10.1074/jbc.R111.219634

Kirov SM, Webb JS, O'May CY, et al (2007) Biofilm differentiation and dispersal in mucoid *Pseudomonas aeruginosa* isolates from patients with cystic fibrosis. Microbiology 153:3264–3274. https://doi.org/10.1099/mic.0.2007/009092-0

Klausen M, Aaes-Jørgensen A, Molin S, Tolker-Nielsen T (2003) Involvement of bacterial migration in the development of complex multicellular structures in *Pseudomonas aeruginosa* biofilms. Mol Microbiol 50:61–68. https://doi.org/10.1046/j.1365-2958.2003.03677.x

Klockgether J, Munder A, Neugebauer J, et al (2010) Genome diversity of *Pseudomonas aeruginosa* PAO1 laboratory strains. J Bacteriol 192:1113–1121. https://doi.org/10.1128/JB.01515-09

Kloth C, Schirmer B, Munder A, et al (2018) The role of *Pseudomonas aeruginosa* exoy in an acute mouse lung infection model. Toxins (Basel) 10:. https://doi.org/10.3390/toxins10050185

Knowles MR, Boucher RC (2002) Mucus clearance as a primary innate defense mechanism for mammalian airways. J Clin Invest 109:571–577. https://doi.org/10.1172/jci15217

Kogan I, Ramjeesingh M, Li C, et al (2003) CFTR directly mediates nucleotide-regulated glutathione flux. EMBO J 22:1981–1989. https://doi.org/10.1093/emboj/cdg194

Kolmogorov M, Yuan J, Lin Y, Pevzner PA (2019) Assembly of long, error-prone reads using repeat graphs. Nat Biotechnol 2019 375 37:540–546. https://doi.org/10.1038/s41587-019-0072-8

Kordes A, Preusse M, Willger SD, et al (2019) Genetically diverse *Pseudomonas aeruginosa* populations display similar transcriptomic profiles in a cystic fibrosis explanted lung. Nat Commun 10:. https://doi.org/10.1038/s41467-019-11414-3

Koskenkorva-Frank TS, Kallio PT (2009) Induction of *Pseudomonas aeruginosa* fhp and fhpR by reactive oxygen species. Can J Microbiol 55:657–663. https://doi.org/10.1139/W09-024

Kuang Z, Hao Y, Walling BE, et al (2011) *Pseudomonas aeruginosa* Elastase Provides an Escape from Phagocytosis by Degrading the Pulmonary Surfactant Protein-A. PLoS One 6:e27091. https://doi.org/10.1371/journal.pone.0027091

Kukurba KR, Montgomery SB (2015) RNA Sequencing and Analysis. Cold Spring Harb Protoc 2015:951. https://doi.org/10.1101/PDB.TOP084970

Kulasakara H, Lee V, Brencic A, et al (2006) Analysis of *Pseudomonas aeruginosa* diguanylate cyclases and phosphodiesterases reveals a role for bis-(3'-5')-cyclic-GMP in virulence. Proc

Natl Acad Sci U S A 103:2839–2844. https://doi.org/10.1073/pnas.0511090103

Kurbatova P, Bessonov N, Volpert V, et al (2015) Model of mucociliary clearance in cystic fibrosis lungs. J Theor Biol 372:81–88. https://doi.org/10.1016/j.jtbi.2015.02.023

Laarman AJ, Bardoel BW, Ruyken M, et al (2012) *Pseudomonas aeruginosa* Alkaline Protease Blocks Complement Activation via the Classical and Lectin Pathways. J Immunol 188:386–393. https://doi.org/10.4049/jimmunol.1102162

Lam JS, Taylor VL, Islam ST, et al (2011) Genetic and Functional Diversity of *Pseudomonas aeruginosa* Lipopolysaccharide. Front Microbiol 2:118. https://doi.org/10.3389/fmicb.2011.00118

Lambiase A, Catania MR, Del Pezzo M, et al (2011) *Achromobacter xylosoxidans* respiratory tract infection in cystic fibrosis patients. Eur J Clin Microbiol Infect Dis 30:973–980. https://doi.org/10.1007/S10096-011-1182-5

Langton Hewer SC, Smyth AR (2017) Antibiotic strategies for eradicating *Pseudomonas aeruginosa* in people with cystic fibrosis. Cochrane Database Syst Rev 2020:. https://doi.org/10.1002/14651858.CD004197.pub5

Lau GW, Hassett DJ, Ran H, Kong F (2004a) The role of pyocyanin in *Pseudomonas aeruginosa* infection. Trends Mol. Med. 10:599–606

Lau GW, Ran H, Kong F, et al (2004b) *Pseudomonas aeruginosa* pyocyanin is critical for lung infection in mice. Infect Immun 72:4275–4278. https://doi.org/10.1128/IAI.72.7.4275-4278.2004

Lazdunski AM, Ventre I, Sturgis JN (2004) Regulatory circuits and communication in Gram-negative bacteria. Nat Rev Microbiol 2:581–592. https://doi.org/10.1038/nrmicro924

Lee J, Wu J, Deng Y, et al (2013) A cell-cell communication signal integrates quorum sensing and stress response. Nat Chem Biol 9:339–343. https://doi.org/10.1038/nchembio.1225

Lee J, Zhang L (2014) The hierarchy quorum sensing network in *Pseudomonas aeruginosa*. Protein Cell 6:26–41. https://doi.org/10.1007/s13238-014-0100-x

Letunic I, Bork P (2021) Interactive Tree Of Life (iTOL) v5: an online tool for phylogenetic tree display and annotation. Nucleic Acids Res 49:W293–W296. https://doi.org/10.1093/NAR/GKAB301

Lewis K (2007) Persister cells, dormancy and infectious disease. Nat Rev Microbiol 5:48–56. https://doi.org/10.1038/nrmicro1557

Lewis K (2010) Persister Cells. Annu Rev Microbiol 64:357–372. https://doi.org/10.1146/annurev.micro.112408.134306

Li Y, Heine S, Entian M, et al (2013) NO-induced biofilm dispersion in *Pseudomonas aeruginosa* is mediated by an MHYT domain-coupled phosphodiesterase. J Bacteriol 195:3531–3542. https://doi.org/10.1128/JB.01156-12

Liao Y, Smyth GK, Shi W (2014) featureCounts: an efficient general purpose program for assigning sequence reads to genomic features. Bioinformatics 30:923–930. https://doi.org/10.1093/BIOINFORMATICS/BTT656

Lichtenberg M, Line L, Schrameyer V, et al (2021) Nitric-oxide-driven oxygen release in anoxic *Pseudomonas aeruginosa*. iScience 24:103404. https://doi.org/10.1016/J.ISCI.2021.103404

Lin J, Cheng J, Wang Y, Shen X (2018) The *Pseudomonas* Quinolone Signal (PQS): Not Just for Quorum Sensing Anymore. Front Cell Infect Microbiol 8:230. https://doi.org/10.3389/fcimb.2018.00230

Line L, Alhede M, Kolpen M, et al (2014) Physiological levels of nitrate support anoxic growth by denitrification of *Pseudomonas aeruginosa* at growth rates reported in cystic fibrosis lungs and sputum. Front Microbiol 5:113236. https://doi.org/10.3389/FMICB.2014.00554/BIBTEX

Lipinksi JH, Ranjan P, Dickson RP, O'Dwyer DN (2024) The Lung Microbiome. J Immunol 212:1269–1275. https://doi.org/10.4049/JIMMUNOL.2300716

LiPuma JJ (2010) The Changing Microbial Epidemiology in Cystic Fibrosis. Clin Microbiol Rev 23:299–323. https://doi.org/10.1128/CMR.00068-09

Lister PD, Wolter DJ, Hanson ND (2009) Antibacterial-Resistant *Pseudomonas aeruginosa* : Clinical Impact and Complex Regulation of Chromosomally Encoded Resistance Mechanisms. Clin Microbiol Rev 22:582–610. https://doi.org/10.1128/CMR.00040-09

Liu F, Zhang Z, Szló Csaná L, et al (2017) Molecular Structure of the Human CFTR Ion Channel Article Molecular Structure of the Human CFTR Ion Channel. Cell 169:85-91.e8. https://doi.org/10.1016/j.cell.2017.02.024

Liu N, Xu Y, Hossain S, et al (2012) Nitric oxide regulation of cyclic di-GMP synthesis and hydrolysis in Shewanella woodyi. Biochemistry 51:2087–2099. https://doi.org/10.1021/bi201753f

Liu YY, Wang Y, Walsh TR, et al (2016) Emergence of plasmid-mediated colistin resistance mechanism MCR-1 in animals and human beings in China: A microbiological and molecular biological study. Lancet Infect Dis 16:161–168. https://doi.org/10.1016/S1473-3099(15)00424-7

Livermore DM (2001) Of *Pseudomonas*, porins, pumps and carbapenems. J Antimicrob Chemother 47:247–250. https://doi.org/10.1093/jac/47.3.247

Llanes C, Hocquet D, Vogne C, et al (2004) Clinical Strains of *Pseudomonas aeruginosa* Overproducing MexAB-OprM and MexXY Efflux Pumps Simultaneously. Antimicrob Agents Chemother 48:1797–1802. https://doi.org/10.1128/AAC.48.5.1797-1802.2004

Lopes-Pacheco M (2020) CFTR Modulators: The Changing Face of Cystic Fibrosis in the Era of Precision Medicine. Front Pharmacol 10:1662. https://doi.org/10.3389/fphar.2019.01662

López-Causapé C, Rojo-Molinero E, Macià MD, Oliver A (2015) The problems of antibiotic resistance in cystic fibrosis and solutions. Expert Rev Respir Med 9:73–88. https://doi.org/10.1586/17476348.2015.995640

Lorentzen D, Durairaj L, Pezzulo AA, et al (2011) Concentration of the antibacterial precursor thiocyanate in cystic fibrosis airway secretions. Free Radic Biol Med 50:1144–1150. https://doi.org/10.1016/j.freeradbiomed.2011.02.013

Lorite GS, Rodrigues CM, de Souza AA, et al (2011) The role of conditioning film formation and surface chemical changes on Xylella fastidiosa adhesion and biofilm evolution. J Colloid Interface Sci 359:289–295. https://doi.org/10.1016/J.JCIS.2011.03.066

Lyczak JB, Cannon CL, Pier GB (2002) Lung Infections Associated with Cystic Fibrosis. Clin Microbiol Rev 15:194–222. https://doi.org/10.1128/CMR.15.2.194-222.2002

Ma L, Conover M, Lu H, et al (2009) Assembly and development of the *Pseudomonas aeruginosa* biofilm matrix. PLoS Pathog 5:1000354. https://doi.org/10.1371/journal.ppat.1000354

Ma L, Jackson KD, Landry RM, et al (2006) Analysis of *Pseudomonas aeruginosa* conditional psl variants reveals roles for the psl polysaccharide in adhesion and maintaining biofilm

structure postattachment. J Bacteriol 188:8213–21. https://doi.org/10.1128/JB.01202-06

Ma L, Lu H, Sprinkle A, et al (2007) *Pseudomonas aeruginosa* Psl Is a Galactose- and Mannose-Rich Exopolysaccharide. J Bacteriol 189:8353–8356. https://doi.org/10.1128/JB.00620-07

MacGregor G, Gray RD, Hilliard TN, et al (2008) Biomarkers for cystic fibrosis lung disease: Application of SELDI-TOF mass spectrometry to BAL fluid. J Cyst Fibros 7:352–358. https://doi.org/10.1016/j.jcf.2007.12.005

MacLeod DL, Nelson LE, Shawar RM, et al (2000) Aminoglycoside-Resistance Mechanisms for Cystic Fibrosis *Pseudomonas aeruginosa* Isolates Are Unchanged by Long-Term, Intermittent, Inhaled Tobramycin Treatment. J Infect Dis 181:1180–1184. https://doi.org/10.1086/315312

Madsen JS, Burmølle M, Hansen LH, Sørensen SJ (2012) The interconnection between biofilm formation and horizontal gene transfer. FEMS Immunol Med Microbiol 65:183–195. https://doi.org/10.1111/J.1574-695X.2012.00960.X

Makarova KS, Wolf YI, Koonin E V (2009) Comprehensive comparative-genomic analysis of Type 2 toxin-antitoxin systems and related mobile stress response systems in prokaryotes. Biol Direct 4:19. https://doi.org/10.1186/1745-6150-4-19

Malloy JL, Veldhuizen RAW, Thibodeaux BA, et al (2005) *Pseudomonas aeruginosa* protease IV degrades surfactant proteins and inhibits surfactant host defense and biophysical functions. Am J Physiol - Lung Cell Mol Physiol 288:409–418. https://doi.org/10.1152/ajplung.00322.2004

Mangoni L, Chichón G, López M, et al (2023) Spread of *Pseudomonas aeruginosa* ST274 Clone in Different Niches: Resistome, Virulome, and Phylogenetic Relationship. Antibiot 2023, Vol 12, Page 1561 12:1561. https://doi.org/10.3390/ANTIBIOTICS12111561

Mann EE, Wozniak DJ (2012) *Pseudomonas* biofilm matrix composition and niche biology. FEMS Microbiol Rev 36:893–916. https://doi.org/10.1111/j.1574-6976.2011.00322.x

Marturano JE, Lowery TJ (2019) ESKAPE pathogens in bloodstream infections are associated with higher cost and mortality but can be predicted using diagnoses upon admission. Open Forum Infect Dis 6:. https://doi.org/10.1093/ofid/ofz503

May KL, Grabowicz M (2018) The bacterial outer membrane is an evolving antibiotic barrier. Proc Natl Acad Sci 115:8852–8854. https://doi.org/10.1073/pnas.1812779115

Mayer-Hamblett N, Aitken ML, Accurso FJ, et al (2007) Association between Pulmonary Function and Sputum Biomarkers in Cystic Fibrosis. Am J Respir Crit Care Med 175:822. https://doi.org/10.1164/RCCM.200609-1354OC

McCallum SJ, Corkill J, Gallagher M, et al (2001) Superinfection with a transmissible strain of *Pseudomonas aeruginosa* in adults with cystic fibrosis chronically colonised by P aeruginosa. Lancet 358:558–560. https://doi.org/10.1016/S0140-6736(01)05715-4

McDougald D, Rice SA, Barraud N, et al (2012) Should we stay or should we go: mechanisms and ecological consequences for biofilm dispersal. Nat Rev Microbiol 10:39–50. https://doi.org/10.1038/nrmicro2695

McElroy KE, Hui JGK, Woo JKK, et al (2014) Strain-specific parallel evolution drives short-term diversification during *Pseudomonas aeruginosa* biofilm formation. Proc Natl Acad Sci U S A 111:E1419–E1427. https://doi.org/10.1073/pnas.1314340111

Meachery G, De Soyza A, Nicholson A, et al (2008) Outcomes of lung transplantation for cystic

fibrosis in a large UK cohort. Thorax 63:725–731. https://doi.org/10.1136/thx.2007.092056

Mendoza JL, Schmidt A, Li Q, et al (2012) Requirements for efficient correction of Δf508 CFTR revealed by analyses of evolved sequences. Cell 148:164–174. https://doi.org/10.1016/j.cell.2011.11.023

Meskini M, Siadat SD, Seifi S, et al (2021) An Overview on the Upper and Lower Airway Microbiome in Cystic Fibrosis Patients. Tanaffos 20:86–98

Michalska M, Wolf P (2015) *Pseudomonas* Exotoxin A: optimized by evolution for effective killing. Front Microbiol 6:15. https://doi.org/10.3389/fmicb.2015.00963

Michl RK, Hentschel J, Fischer C, et al (2013) Reduced nasal nitric oxide production in cystic fibrosis patients with elevated systemic inflammation markers. PLoS One 8:. https://doi.org/10.1371/journal.pone.0079141

Middleton PG, Mall MA, Dřevínek P, et al (2019) Elexacaftor-tezacaftor-ivacaftor for cystic fibrosis with a single Phe508del allele. N Engl J Med 381:1809–1819. https://doi.org/10.1056/NEJMoa1908639

Miller HK, Auerbuch V (2015) Bacterial iron-sulfur cluster sensors in mammalian pathogens. Metallomics 7:943–956. https://doi.org/10.1039/c5mt00012b

Minandri F, Imperi F, Frangipani E, et al (2016) Role of iron uptake systems in *Pseudomonas aeruginosa* virulence and airway infection. Infect Immun 84:2324–2335. https://doi.org/10.1128/IAI.00098-16

Mogayzel PJ, Naureckas ET, Robinson KA, et al (2013) Cystic Fibrosis Pulmonary Guidelines. Am J Respir Crit Care Med 187:680–689. https://doi.org/10.1164/rccm.201207-1160OE

Moradali MF, Ghods S, Rehm BHA (2017) *Pseudomonas aeruginosa* Lifestyle: A Paradigm for Adaptation, Survival, and Persistence. Front Cell Infect Microbiol 7:39. https://doi.org/10.3389/fcimb.2017.00039

Morgan R, Kohn S, Hwang S-H, et al (2006) BdlA, a Chemotaxis Regulator Essential for Biofilm Dispersion in *Pseudomonas aeruginosa*. J Bacteriol 188:7335–7343. https://doi.org/10.1128/JB.00599-06

Morita Y, Tomida J, Kawamura Y (2012) MexXY multidrug efflux system of *Pseudomonas aeruginosa*. Front Microbiol 3:. https://doi.org/10.3389/fmicb.2012.00408

Morlon-Guyot J, Méré J, Bonhoure A, Beaumelle B (2009) Processing of *Pseudomonas aeruginosa* exotoxin A is dispensable for cell intoxication. Infect Immun 77:3090–3099. https://doi.org/10.1128/IAI.01390-08

Morrell MR, Pilewski JM (2016) Lung Transplantation for Cystic Fibrosis. Clin Chest Med 37:127–138. https://doi.org/10.1016/j.ccm.2015.11.008

Morrissey BM, Schilling K, Weil J V., et al (2002) Nitric oxide and protein nitration in the cystic fibrosis airway. Arch Biochem Biophys 406:33–39. https://doi.org/10.1016/S0003-9861(02)00427-7

Moskwa P, Lorentzen D, Excoffon KJDA, et al (2007) A novel host defense system of airways is defective in cystic fibrosis. Am J Respir Crit Care Med 175:174–183. https://doi.org/10.1164/rccm.200607-1029OC

Moter A, Göbel UB (2000) Fluorescence in situ hybridization (FISH) for direct visualization of microorganisms. J Microbiol Methods 41:85–112. https://doi.org/10.1016/S0167-7012(00)00152-4

Mulcahy H, Charron-Mazenod L, Lewenza S (2008) Extracellular DNA chelates cations and induces

antibiotic resistance in *Pseudomonas aeruginosa* biofilms. PLoS Pathog 4:e1000213. https://doi.org/10.1371/journal.ppat.1000213

Mulcahy LR, Isabella VM, Lewis K (2014) *Pseudomonas aeruginosa* biofilms in disease. Microb Ecol 68:1–12. https://doi.org/10.1007/s00248-013-0297-x

Munder A, Rothschuh J, Schirmer B, et al (2018) The *Pseudomonas aeruginosa* ExoY phenotype of high-copy-number recombinants is not detectable in natural isolates. Open Biol 8:. https://doi.org/10.1098/rsob.170250

Nadal Jimenez P, Koch G, Thompson JA, et al (2012) The Multiple Signaling Systems Regulating Virulence in *Pseudomonas aeruginosa*. Microbiol Mol Biol Rev 76:46–65. https://doi.org/10.1128/mmbr.05007-11

National Institute for Health and Care Excellence (2017) Cystic Fibrosis: Diagnosis and management NICE guideline [NG78]. https://www.nice.org.uk/guidance/ng78. Accessed 7 Jul 2020

Nguyen D, Joshi-Datar A, Lepine F, et al (2011) Active starvation responses mediate antibiotic tolerance in biofilms and nutrient-limited bacteria. Science (80-) 334:982–986. https://doi.org/10.1126/science.1211037

NHS England (2020) NHS patients among first in Europe to benefit from landmark deal for cystic fibrosis treatment. https://www.england.nhs.uk/2020/06/nhs-patients-among-first-in-europe-to-benefit-from-landmark-deal-for-cystic-fibrosis-treatment/. Accessed 4 Jul 2020

Nicas TI, Frank DW, Stenzel P, et al (1985) Role of exoenzyme S in chronic *Pseudomonas aeruginosa* lung infections. Eur J Clin Microbiol 4:175–179. https://doi.org/10.1007/BF02013593

Nikaido H (2003) Molecular Basis of Bacterial Outer Membrane Permeability Revisited. Microbiol Mol Biol Rev 67:593–656. https://doi.org/10.1128/mmbr.67.4.593-656.2003

O'Toole GA, Kolter R (1998) Flagellar and twitching motility are necessary for *Pseudomonas aeruginosa* biofilm development. Mol Microbiol 30:295–304. https://doi.org/10.1046/j.1365-2958.1998.01062.x

Okiyoneda T, Veit G, Dekkers JF, et al (2013) Mechanism-based corrector combination restores ΔF508-CFTR folding and function. Nat Chem Biol 9:444–454. https://doi.org/10.1038/nchembio.1253

Okshevsky M, Meyer RL (2015) The role of extracellular DNA in the establishment, maintenance and perpetuation of bacterial biofilms. Crit Rev Microbiol 41:341–352. https://doi.org/10.3109/1040841X.2013.841639

Olivares E, Badel-Berchoux S, Provot C, et al (2020) Clinical Impact of Antibiotics for the Treatment of *Pseudomonas aeruginosa* Biofilm Infections. Front Microbiol 0:2894. https://doi.org/10.3389/FMICB.2019.02894

Oliver A, Mulet X, López-Causapé C, Juan C (2015) The increasing threat of *Pseudomonas aeruginosa* high-risk clones. Drug Resist Updat 21–22:41–59. https://doi.org/10.1016/j.drup.2015.08.002

Oppezzo OJ, Forte Giacobone AF (2018) Lethal Effect of Photodynamic Treatment on Persister Bacteria. Photochem Photobiol 94:186–189. https://doi.org/10.1111/php.12843

Orman MA, Henry TC, DeCoste CJ, Brynildsen MP (2016) Analyzing Persister Physiology with

Fluorescence-Activated Cell Sorting. In: Methods in Molecular Biology. pp 83–100

Ozer E, Yaniv K, Chetrit E, et al (2021) An inside look at a biofilm: *Pseudomonas aeruginosa* flagella biotracking. Sci Adv 7:8581–8592. https://doi.org/10.1126/SCIADV.ABG8581/SUPPL_FILE/SCIADV.ABG8581_SM.PDF

Pachori P, Gothalwal R, Gandhi P (2019) Emergence of antibiotic resistance *Pseudomonas aeruginosa* in intensive care unit; a critical review. Genes Dis 6:109–119. https://doi.org/10.1016/j.gendis.2019.04.001

Palleroni NJ (2015) *Pseudomonas*. Bergey's Man Syst Archaea Bact 1–1. https://doi.org/10.1002/9781118960608.GBM01210

Pang Z, Raudonis R, Glick BR, et al (2019) Antibiotic resistance in *Pseudomonas aeruginosa*: mechanisms and alternative therapeutic strategies. Biotechnol Adv 37:177–192. https://doi.org/10.1016/j.biotechadv.2018.11.013

Parkins MD, Somayaji R, Waters VJ (2018) Epidemiology, Biology, and Impact of Clonal *Pseudomonas aeruginosa* Infections in Cystic Fibrosis. Clin Microbiol Rev 31:. https://doi.org/10.1128/CMR.00019-18

Patrick AE, Thomas PJ (2012) Development of CFTR structure. Front Pharmacol 3 SEP: https://doi.org/10.3389/fphar.2012.00162

Pattison SH, Gibson DS, Johnston E, et al (2017) Proteomic profile of cystic fibrosis sputum cells in adults chronically infected with *Pseudomonas aeruginosa*. Eur Respir J 50:. https://doi.org/10.1183/13993003.01569-2016

Pesci EC, Milbank JBJ, Pearson JP, et al (1999) Quinolone signaling in the cell-to-cell communication system of *Pseudomonas aeruginosa*. Proc Natl Acad Sci 96:11229–11234. https://doi.org/10.1073/pnas.96.20.11229

Pestrak MJ, Wozniak DJ (2020) Regulation of Cyclic di-GMP Signaling in *Pseudomonas aeruginosa*. In: Microbial Cyclic Di-Nucleotide Signaling. Springer International Publishing, Cham, pp 471–486

Petrova OE, Sauer K (2012) Dispersion by *Pseudomonas aeruginosa* requires an unusual posttranslational modification of BdlA. Proc Natl Acad Sci U S A 109:16690–16695. https://doi.org/10.1073/pnas.1207832109

Pezzulo AA, Tang XX, Hoegger MJ, et al (2012) Reduced airway surface pH impairs bacterial killing in the porcine cystic fibrosis lung. Nature 487:109–113. https://doi.org/10.1038/nature11130

Pier G (2002) CFTR mutations and host susceptibility to *Pseudomonas aeruginosa* lung infection. Curr Opin Microbiol 5:81–86. https://doi.org/10.1016/S1369-5274(02)00290-4

Pier GB, Grout M, Zaidi TS, et al (1996) Role of mutant CFTR in hypersusceptibility of cystic fibrosis patients to lung infections. Science (80-) 271:64–67. https://doi.org/10.1126/science.271.5245.64

Plate L, Marletta MA (2012) Nitric Oxide Modulates Bacterial Biofilm Formation through a Multicomponent Cyclic-di-GMP Signaling Network. Mol Cell 46:449–460. https://doi.org/10.1016/j.molcel.2012.03.023

Pletzer D, Braun Y, Dubiley S, et al (2015) The *Pseudomonas aeruginosa* PA14 ABC Transporter NppA1A2BCD Is Required for Uptake of Peptidyl Nucleoside Antibiotics. J Bacteriol 197:2217. https://doi.org/10.1128/JB.00234-15

Poole K (2005) Aminoglycoside Resistance in *Pseudomonas aeruginosa*. Antimicrob Agents

Chemother 49:479–487. https://doi.org/10.1128/AAC.49.2.479-487.2005

Poolman EM, Galvani AP (2007) Evaluating candidate agents of selective pressure for cystic fibrosis. J R Soc Interface 4:91–98. https://doi.org/10.1098/rsif.2006.0154

Potter L, Angove H, Richardson D, Cole J (2001) Nitrate reduction in the periplasm of gram-negative bacteria. Adv Microb Physiol 45:51–112. https://doi.org/10.1016/S0065-2911(01)45002-8

Prior A-R, Gunaratnam C, Humphreys H (2017) *Ralstonia* species – do these bacteria matter in cystic fibrosis? Paediatr Respir Rev 23:78–83. https://doi.org/10.1016/j.prrv.2016.09.005

Privett BJ, Shin JH, Schoenfisch MH (2010) Electrochemical nitric oxide sensors for physiological measurements. Chem Soc Rev 39:1925–1935. https://doi.org/10.1039/b701906h

Proesmans M, Vermeulen F, De Boeck K (2008) What's new in cystic fibrosis? From treating symptoms to correction of the basic defect. Eur J Pediatr 167:839–849. https://doi.org/10.1007/s00431-008-0693-2

Purevdorj-Gage B, Costerton WJ, Stoodley P (2005) Phenotypic differentiation and seeding dispersal in non-mucoid and mucoid *Pseudomonas aeruginosa* biofilms. Microbiology 151:1569–1576. https://doi.org/10.1099/mic.0.27536-0

Rabin SDP, Hauser AR (2003) *Pseudomonas aeruginosa* ExoU, a Toxin Transported by the Type III Secretion System, Kills Saccharomyces cerevisiae. Infect Immun 71:4144. https://doi.org/10.1128/IAI.71.7.4144-4150.2003

Rada B, Leto TL (2013) Pyocyanin effects on respiratory epithelium: relevance in *Pseudomonas aeruginosa* airway infections. Trends Microbiol 21:73–81. https://doi.org/10.1016/j.tim.2012.10.004

Ramos KJ, Smith PJ, McKone EF, et al (2019) Lung transplant referral for individuals with cystic fibrosis: Cystic Fibrosis Foundation consensus guidelines. J Cyst Fibros 18:321–333. https://doi.org/10.1016/j.jcf.2019.03.002

Ramsey BW, Davies J, McElvaney NG, et al (2011) A CFTR potentiator in patients with cystic fibrosis and the G551D mutation. N Engl J Med 365:1663–1672. https://doi.org/10.1056/NEJMoa1105185

Ratjen F, Bell SC, Rowe SM, et al (2015) Cystic fibrosis. Nat Rev Dis Prim 1:15010. https://doi.org/10.1038/nrdp.2015.10

Ratjen F, Döring G (2003) Cystic fibrosis. Lancet 361:681–689. https://doi.org/10.1016/S0140-6736(03)12567-6

Reid DEW, Carroll V, O'May C, et al (2007) Increased airway iron as a potential factor in the persistence of *Pseudomonas aeruginosa* infection in cystic fibrosis. Eur Respir J 30:286–292. https://doi.org/10.1183/09031936.00154006

Renelli M, Matias V, Lo RY, Beveridge TJ (2004) DNA-containing membrane vesicles of *Pseudomonas aeruginosa* PAO1 and their genetic transformation potential. Microbiology 150:2161–2169. https://doi.org/10.1099/mic.0.26841-0

Ridley K, Condren M (2020) Elexacaftor-tezacaftor-ivacaftor: The first triple-combination cystic fibrosis transmembrane conductance regulator modulating therapy. J Pediatr Pharmacol Ther 25:192–197. https://doi.org/10.5863/1551-6776-25.3.192

Rinaldo S, Giardina G, Mantoni F, et al (2018) Beyond nitrogen metabolism: nitric oxide, cyclic-di-

GMP and bacterial biofilms. FEMS Microbiol Lett 365:. https://doi.org/10.1093/femsle/fny029

Rineh A, Soren O, McEwan T, et al (2020) Discovery of Cephalosporin-3'-Diazeniumdiolates That Show Dual Antibacterial and Antibiofilm Effects against *Pseudomonas aeruginosa* Clinical Cystic Fibrosis Isolates and Efficacy in a Murine Respiratory Infection Model. ACS Infect Dis 6:1460–1479. https://doi.org/10.1021/acsinfecdis.0c00070

Riordan JR (2008) CFTR Function and Prospects for Therapy. Annu Rev Biochem 77:701–726. https://doi.org/10.1146/annurev.biochem.75.103004.142532

Riordan JR, Rommens JM, Kerem BS, et al (1989) Identification of the cystic fibrosis gene: Cloning and characterization of complementary DNA. Science (80-) 245:1066–1073. https://doi.org/10.1126/science.2475911

Rogers CS, Stoltz DA, Meyerholz DK, et al (2008) Disruption of the CFTR gene produces a model of cystic fibrosis in newborn pigs. Science (80-) 321:1837–1841. https://doi.org/10.1126/science.1163600

Romling U, Galperin MY, Gomelsky M (2013) Cyclic di-GMP: the First 25 Years of a Universal Bacterial Second Messenger. Microbiol Mol Biol Rev 77:1–52. https://doi.org/10.1128/mmbr.00043-12

Rommens JM, Iannuzzi MC, Kerem BS, et al (1989) Identification of the cystic fibrosis gene: Chromosome walking and jumping. Science (80-) 245:1059–1065. https://doi.org/10.1126/science.2772657

Rosenfeld M, Emerson J, Williams-Warren J, et al (2001) Defining a pulmonary exacerbation in cystic fibrosis. J Pediatr 139:359–365. https://doi.org/10.1067/mpd.2001.117288

Rouillard KR, Novak OP, Pistiolis AM, et al (2021) Exogenous Nitric Oxide Improves Antibiotic Susceptibility in Resistant Bacteria. ACS Infect Dis 7:23–33. https://doi.org/10.1021/acsinfecdis.0c00337

Rowe SM, Heltshe SL, Gonska T, et al (2014) Clinical mechanism of the cystic fibrosis transmembrane conductance regulator potentiator ivacaftor in G551D-mediated cystic fibrosis. Am J Respir Crit Care Med 190:175–184. https://doi.org/10.1164/rccm.201404-0703OC

Roxo-Rosa M, Da Costa G, Luider TM, et al (2006) Proteomic analysis of nasal cells from cystic fibrosis patients and non-cystic fibrosis control individuals: Search for novel biomarkers of cystic fibrosis lung disease. Proteomics 6:2314–2325. https://doi.org/10.1002/PMIC.200500273

Roy AB, Petrova OE, Sauer K (2012) The phosphodiesterase DipA (PA5017) is essential for *Pseudomonas aeruginosa* biofilm dispersion. J Bacteriol 194:2904–2915. https://doi.org/10.1128/JB.05346-11

Rozanova S, Barkovits K, Nikolov M, et al (2021) Quantitative Mass Spectrometry-Based Proteomics: An Overview. Methods Mol Biol 2228:85–116. https://doi.org/10.1007/978-1-0716-1024-4_8/TABLES/1

Ruan K, Yamamoto TG, Asakawa H, et al (2015) Histone H4 acetylation required for chromatin decompaction during DNA replication. Sci Rep 5:1–10. https://doi.org/10.1038/srep12720

Rybtke M, Hultqvist LD, Givskov M, Tolker-Nielsen T (2015) *Pseudomonas aeruginosa* Biofilm Infections: Community Structure, Antimicrobial Tolerance and Immune Response. J Mol Biol 427:3628–3645. https://doi.org/10.1016/j.jmb.2015.08.016

Ryder C, Byrd M, Wozniak DJ (2007) Role of polysaccharides in *Pseudomonas aeruginosa* biofilm

development. Curr Opin Microbiol 10:644–648. https://doi.org/10.1016/j.mib.2007.09.010

Ryjenkov DA, Simm R, Römling U, Gomelsky M (2006) The PilZ domain is a receptor for the second messenger c-di-GMP: The PilZ domain protein YcgR controls motility in enterobacteria. J Biol Chem 281:30310–30314. https://doi.org/10.1074/jbc.C600179200

Sabtcheva S, Galimand M, Gerbaud G, et al (2003) Aminoglycoside resistance gene ant(4')-IIb of *Pseudomonas aeruginosa* BM4492, a clinical isolate from Bulgaria. Antimicrob Agents Chemother 47:1584–1588. https://doi.org/10.1128/AAC.47.5.1584-1588.2003

Sadikot RT, Blackwell TS, Christman JW, Prince AS (2005) Pathogen–Host Interactions in *Pseudomonas aeruginosa* Pneumonia. Am J Respir Crit Care Med 171:1209–1223. https://doi.org/10.1164/rccm.200408-1044SO

Saiman L, Chen Y, Tabibi S, et al (2001) Identification and Antimicrobial Susceptibility of *Alcaligenes xylosoxidans* Isolated from Patients with Cystic Fibrosis. J Clin Microbiol 39:3942. https://doi.org/10.1128/JCM.39.11.3942-3945.2001

Saiman L, Prince A (1993) *Pseudomonas aeruginosa* pili bind to asialoGM1 which is increased on the surface of cystic fibrosis epithelial cells. J Clin Invest 92:1875–1880. https://doi.org/10.1172/JCI116779

Saint-Criq V, Gray MA (2017) Role of CFTR in epithelial physiology. Cell Mol Life Sci 74:93–115. https://doi.org/10.1007/s00018-016-2391-y

Salipante SJ, Sengupta DJ, Rosenthal C, et al (2013) Rapid 16S rRNA Next-Generation Sequencing of Polymicrobial Clinical Samples for Diagnosis of Complex Bacterial Infections. PLoS One 8:e65226. https://doi.org/10.1371/journal.pone.0065226

Sanders DB, Bittner RCL, Rosenfeld M, et al (2010) Failure to recover to baseline pulmonary function after cystic fibrosis pulmonary exacerbation. Am J Respir Crit Care Med 182:627–632. https://doi.org/10.1164/rccm.200909-1421OC

Sanfilippo JE, Lorestani A, Koch MD, et al (2019) Microfluidic-based transcriptomics reveal force-independent bacterial rheosensing. Nat Microbiol 2019 48 4:1274–1281. https://doi.org/10.1038/s41564-019-0455-0

Sauer K, Camper AK, Ehrlich GD, et al (2002) *Pseudomonas aeruginosa* displays multiple phenotypes during development as a biofilm. J Bacteriol 184:1140–1154. https://doi.org/10.1128/jb.184.4.1140-1154.2002

Schreiber K, Krieger R, Benkert B, et al (2007) The anaerobic regulatory network required for *Pseudomonas aeruginosa* nitrate respiration. J Bacteriol 189:4310–4314. https://doi.org/10.1128/JB.00240-07

Schrijver I (2011) Mutation Distribution in Expanded Screening for Cystic Fibrosis: Making Up the Balance in a Context of Ethnic Diversity. Clin Chem 57:799–801. https://doi.org/10.1373/clinchem.2011.164673

Seemann T (2014) Prokka: rapid prokaryotic genome annotation. Bioinformatics 30:2068–2069. https://doi.org/10.1093/BIOINFORMATICS/BTU153

Sermet-Gaudelus I (2013) Ivacaftor treatment in patients with cystic fibrosis and the G551D-CFTR mutation. Eur Respir Rev 22:66–71. https://doi.org/10.1183/09059180.00008512

Shakya M, Ahmed SA, Davenport KW, et al (2020) Standardized phylogenetic and molecular evolutionary analysis applied to species across the microbial tree of life. Sci Reports 2020

101 10:1–15. https://doi.org/10.1038/s41598-020-58356-1

Shaver CM, Hauser AR (2004) Relative contributions of *Pseudomonas aeruginosa* ExoU, ExoS, and ExoT to virulence in the lung. Infect Immun 72:6969–6977. https://doi.org/10.1128/IAI.72.12.6969-6977.2004

SHEPPARD DN, WELSH MJ (1999) Structure and Function of the CFTR Chloride Channel. Physiol Rev 79:S23–S45. https://doi.org/10.1152/physrev.1999.79.1.S23

Shih PC, Huang CT (2002) Effects of quorum-sensing deficiency on *Pseudomonas aeruginosa* biofilm formation and antibiotic resistance. J Antimicrob Chemother 49:309–314. https://doi.org/10.1093/jac/49.2.309

Simmonds NJ (2019) Is it cystic fibrosis? The challenges of diagnosing cystic fibrosis. Paediatr Respir Rev 31:6–8. https://doi.org/10.1016/j.prrv.2019.02.004

Soren O (2018) Investigation into Novel Nitric Oxide Based Anti-Biofilm Strategies to Target *Pseudomonas aeruginosa* Infection in Cystic Fibrosis

Soren O, Rineh A, Silva DG, et al (2020) Cephalosporin nitric oxide-donor prodrug DEA-C3D disperses biofilms formed by clinical cystic fibrosis isolates of *Pseudomonas aeruginosa*. J Antimicrob Chemother 75:117–125. https://doi.org/10.1093/jac/dkz378

Spoering AL, Lewis K (2001) Biofilms and planktonic cells of *Pseudomonas aeruginosa* have similar resistance to killing by antimicrobials. J Bacteriol 183:6746–6751. https://doi.org/10.1128/JB.183.23.6746-6751.2001

Stern M, Bertrand DP, Bignamini E, et al (2014) European Cystic Fibrosis Society Standards of Care: Quality Management in cystic fibrosis. J Cyst Fibros 13:S43–S59. https://doi.org/10.1016/j.jcf.2014.03.011

Stewart PS (2003) Diffusion in Biofilms. J Bacteriol 185:1485–1491. https://doi.org/10.1128/JB.185.5.1485-1491.2003

Stewart PS, Franklin MJ (2008) Physiological heterogeneity in biofilms. Nat Rev Microbiol 6:199–210. https://doi.org/10.1038/nrmicro1838

Stewart PS, William Costerton J (2001) Antibiotic resistance of bacteria in biofilms. Lancet 358:135–138. https://doi.org/10.1016/S0140-6736(01)05321-1

Stewart PS, Zhang T, Xu R, et al (2016) Reaction–diffusion theory explains hypoxia and heterogeneous growth within microbial biofilms associated with chronic infections. npj Biofilms Microbiomes 2:16012. https://doi.org/10.1038/npjbiofilms.2016.12

Stoltz DA, Meyerholz DK, Pezzulo AA, et al (2010) Cystic fibrosis pigs develop lung disease and exhibit defective bacterial eradication at birth. Sci Transl Med 2:29ra31-29ra31. https://doi.org/10.1126/scitranslmed.3000928

Stoltz DA, Meyerholz DK, Welsh MJ (2015) Origins of Cystic Fibrosis Lung Disease. N Engl J Med 372:351–362. https://doi.org/10.1056/NEJMra1300109

Stoodley P, Cargo R, Rupp CJ, et al (2002a) Biofilm material properties as related to shear-induced deformation and detachment phenomena. J Ind Microbiol Biotechnol 29:361–367. https://doi.org/10.1038/sj.jim.7000282

Stoodley P, Sauer K, Davies DG, Costerton JW (2002b) Biofilms as Complex Differentiated Communities. Annu Rev Microbiol 56:187–209. https://doi.org/10.1146/annurev.micro.56.012302.160705

Stover CK, Pham XQ, Erwin AL, et al (2000) Complete genome sequence of *Pseudomonas aeruginosa* PAO1, an opportunistic pathogen. Nature 406:959–964.

https://doi.org/10.1038/35023079

Strateva T, Mitov I (2011) Contribution of an arsenal of virulence factors to pathogenesis of *Pseudomonas aeruginosa* infections. Ann Microbiol 61:717–732. https://doi.org/10.1007/s13213-011-0273-y

Sultana ST, Call DR, Beyenal H (2016) Eradication of *Pseudomonas aeruginosa* biofilms and persister cells using an electrochemical scaffold and enhanced antibiotic susceptibility /692/700 /631/1647 article. npj Biofilms Microbiomes 2:2. https://doi.org/10.1038/s41522-016-0003-0

Sundar IK, Nevid MZ, Friedman AE, Rahman I (2014) Cigarette smoke induces distinct chromatin histone modifications in lung cells: implication in pathogenesis of COPD and lung cancer. J Proteome Res 13:982. https://doi.org/10.1021/PR400998N

Szczesniak R, Heltshe SL, Stanojevic S, Mayer-Hamblett N (2017) Use of FEV1 in cystic fibrosis epidemiologic studies and clinical trials: A statistical perspective for the clinical researcher. J Cyst Fibros 16:318–326. https://doi.org/10.1016/j.jcf.2017.01.002

Taccetti G, Campana S, Festini F, et al (2005) Early eradication therapy against *Pseudomonas aeruginosa* in cystic fibrosis patients. Eur Respir J 26:458–461. https://doi.org/10.1183/09031936.05.00009605

Tajbakhsh S, Hogardt M, Heesemann J, et al (2008) Detection of *Pseudomonas aeruginosa* in sputum samples by modified fluorescent in situ hybridization. African J Biotechnol 7:553–556. https://doi.org/10.5897/AJB07.918

Takase H, Nitanai H, Hoshino K, Otani T (2000) Impact of siderophore production on *Pseudomonas aeruginosa* infections in immunosuppressed mice. Infect Immun 68:1834–1839. https://doi.org/10.1128/IAI.68.4.1834-1839.2000

Tetart M, Wallet F, Kyheng M, et al Impact of *Achromobacter xylosoxidans* isolation on the respiratory function of adult patients with cystic fibrosis. https://doi.org/10.1183/23120541.00051-2019

Texereau J, Marullo S, Hubert D, et al (2004) Nitric oxide synthase 1 as a potential modifier gene of decline in lung function in patients with cystic fibrosis. Thorax 59:156–158. https://doi.org/10.1136/thorax.2003.006718

Tolker-Nielsen T (2014) *Pseudomonas aeruginosa* biofilm infections: From molecular biofilm biology to new treatment possibilities. APMIS 122:1–51. https://doi.org/10.1111/apm.12335

Tolker-Nielsen T, Brinch UC, Ragas PC, et al (2000) Development and dynamics of *Pseudomonas* sp. biofilms. J Bacteriol 182:6482–6489. https://doi.org/10.1128/JB.182.22.6482-6489.2000

Toyofuku M, Yoon S-S (2018) Nitric Oxide, an Old Molecule With Noble Functions in *Pseudomonas aeruginosa* Biology. In: Advances in Microbial Physiology. Academic Press, pp 117–145

Travis SM, Singh PK, Welsh MJ (2001) Antimicrobial peptides and proteins in the innate defense of the airway surface. Curr Opin Immunol 13:89–95. https://doi.org/10.1016/S0952-7915(00)00187-4

Treangen TJ, Ondov BD, Koren S, Phillippy AM (2014) The Harvest suite for rapid core-genome alignment and visualization of thousands of intraspecific microbial genomes. Genome Biol 15:524. https://doi.org/10.1186/s13059-014-0524-x

Trottmann F, Franke J, Ishida K, et al (2019) A Pair of Bacterial Siderophores Releases and Traps an

Intercellular Signal Molecule: An Unusual Case of Natural Nitrone Bioconjugation. Angew Chemie Int Ed 58:200–204. https://doi.org/10.1002/anie.201811131

Tseng BS, Zhang W, Harrison JJ, et al (2013) The extracellular matrix protects *Pseudomonas aeruginosa* biofilms by limiting the penetration of tobramycin. Environ Microbiol 15:2865–2878. https://doi.org/10.1111/1462-2920.12155

Turcios NL (2020) Cystic Fibrosis Lung Disease: An Overview. Respir Care 65:233–251. https://doi.org/10.4187/respcare.06697

UniProt (2019) Proteomes - Homo sapiens (Human). https://www.uniprot.org/proteomes/UP000005640

Valentini M, Filloux A (2016) Biofilms and Cyclic di-GMP (c-di-GMP) Signaling: Lessons from *Pseudomonas aeruginosa* and Other Bacteria. J Biol Chem 291:12547–12555. https://doi.org/10.1074/jbc.R115.711507

Valentini M, Filloux A (2019) Multiple roles of c-di-GMP signaling in bacterial pathogenesis. Annu. Rev. Microbiol. 73:387–406

Van Goor F, Hadida S, Grootenhuis PDJ, et al (2009) Rescue of CF airway epithelial cell function in vitro by a CFTR potentiator, VX-770. Proc Natl Acad Sci U S A 106:18825–18830. https://doi.org/10.1073/pnas.0904709106

Vankeerberghen A, Cuppens H, Cassiman JJ (2002) The cystic fibrosis transmembrane conductance regulator: An intriguing protein with pleiotropic functions. J Cyst Fibros 1:13–29. https://doi.org/10.1016/S1569-1993(01)00003-0

Varadarajan AR, Allan RN, Valentin JDP, et al (2020) An integrated model system to gain mechanistic insights into biofilm-associated antimicrobial resistance in *Pseudomonas aeruginosa* MPAO1. npj Biofilms Microbiomes 6:1–17. https://doi.org/10.1038/s41522-020-00154-8

Venturi V (2006) Regulation of quorum sensing in *Pseudomonas*. FEMS Microbiol Rev 30:274–291. https://doi.org/10.1111/j.1574-6976.2005.00012.x

Venzac B, Deng S, Mahmoud Z, et al (2021) PDMS Curing Inhibition on 3D-Printed Molds: Why? Also, How to Avoid It? Anal Chem 93:7180–7187. https://doi.org/10.1021/ACS.ANALCHEM.0C04944/ASSET/IMAGES/LARGE/AC0C04944_0006.JPEG

Verhaeghe C, Delbecque K, de Leval L, et al (2007) Early inflammation in the airways of a cystic fibrosis foetus. J Cyst Fibros 6:304–308. https://doi.org/10.1016/j.jcf.2006.12.001

Walters MC, Roe F, Bugnicourt A, et al (2003) Contributions of antibiotic penetration, oxygen limitation, and low metabolic activity to tolerance of *Pseudomonas aeruginosa* biofilms to ciprofloxacin and tobramycin. Antimicrob Agents Chemother 47:317–323. https://doi.org/10.1128/AAC.47.1.317-323.2003

Wang J, Chen K, Ren Q, et al (2021) Systematic Comparison of the Performances of De Novo Genome Assemblers for Oxford Nanopore Technology Reads From Piroplasm. Front Cell Infect Microbiol 11:696669. https://doi.org/10.3389/fcimb.2021.696669

Wang J, Wang C, Yu H, et al (2019) Bacterial quorum-sensing signal IQS induces host cell apoptosis by targeting POT1–p53 signalling pathway. Cell Microbiol 21:. https://doi.org/10.1111/cmi.13076

Wang S, Liu X, Liu H, et al (2015) The exopolysaccharide Psl-eDNA interaction enables the formation of a biofilm skeleton in *Pseudomonas aeruginosa*. Environ Microbiol Rep 7:330–340. https://doi.org/10.1111/1758-2229.12252

Wang Z, Gerstein M, Snyder M (2009) RNA-Seq: a revolutionary tool for transcriptomics. Nat Rev Genet 10:57. https://doi.org/10.1038/NRG2484

Wassermann T, Jørgensen KM, Ivanyshyn K, et al (2016) The phenotypic evolution of *Pseudomonas aeruginosa* populations changes in the presence of subinhibitory concentrations of ciprofloxacin. Microbiology 162:865–875. https://doi.org/10.1099/MIC.0.000273

Waters CM, Goldberg JB (2019) *Pseudomonas aeruginosa* in cystic fibrosis: A chronic cheater. Proc Natl Acad Sci 116:6525–6527. https://doi.org/10.1073/pnas.1902734116

Webb JS, Thompson LS, James S, et al (2003) Cell death in *Pseudomonas aeruginosa* biofilm development. J Bacteriol 185:4585–4592. https://doi.org/10.1128/JB.185.15.4585-4592.2003

Wettstadt S, Wood TE, Fecht S, Filloux A (2019) Delivery of the *Pseudomonas aeruginosa* Phospholipase Effectors PldA and PldB in a VgrG- and H2-T6SS-Dependent Manner. Front Microbiol 10:1718. https://doi.org/10.3389/fmicb.2019.01718

Whitchurch CB, Tolker-Nielsen T, Ragas PC, Mattick JS (2002) Extracellular DNA required for bacterial biofilm formation. Science (80-) 295:1487. https://doi.org/10.1126/science.295.5559.1487

Whiteley M, Greenberg EP (2001) Promoter Specificity Elements in *Pseudomonas aeruginosa* Quorum-Sensing-Controlled Genes Downloaded from. J Bacteriol 183:5529–5534. https://doi.org/10.1128/JB.183.19.5529-5534.2001

Wilhelm S, Gdynia A, Tielen P, et al (2007) The autotransporter esterase EstA of *Pseudomonas aeruginosa* is required for rhamnolipid production, cell motility, and biofilm formation. J Bacteriol 189:6695–6703. https://doi.org/10.1128/JB.00023-07

Williams P, Cámara M (2009) Quorum sensing and environmental adaptation in *Pseudomonas aeruginosa*: a tale of regulatory networks and multifunctional signal molecules. Curr Opin Microbiol 12:182–191. https://doi.org/10.1016/j.mib.2009.01.005

Wilton M, Charron-Mazenod L, Moore R, Lewenza S (2016) Extracellular DNA acidifies biofilms and induces aminoglycoside resistance in *Pseudomonas aeruginosa*. Antimicrob Agents Chemother 60:544–553. https://doi.org/10.1128/AAC.01650-15

Winstanley C, Fothergill JL (2009) The role of quorum sensing in chronic cystic fibrosis *Pseudomonas aeruginosa* infections. FEMS Microbiol Lett 290:1–9. https://doi.org/10.1111/j.1574-6968.2008.01394.x

Winter-de Groot KM de, Ent CK va. der (2005) Nitric oxide in cystic fibrosis. J Cyst Fibros 4:25–29. https://doi.org/10.1016/j.jcf.2005.05.008

Wolska KI, Grudniak AM, Rudnicka Z, Markowska K (2016) Genetic control of bacterial biofilms. J Appl Genet 57:225–238. https://doi.org/10.1007/s13353-015-0309-2

Wood DE, Lu J, Langmead B (2019) Improved metagenomic analysis with Kraken 2. Genome Biol 20:1–13. https://doi.org/10.1186/S13059-019-1891-0/FIGURES/2

Worlitzsch D, Tarran R, Ulrich M, et al (2002) Effects of reduced mucus oxygen concentration in airway *Pseudomonas* infections of cystic fibrosis patients. J Clin Invest 109:317–325. https://doi.org/10.1172/JCI0213870

Xiong L, Chen P, Zhou Q (2014) Adhesion promotion between PDMS and glass by oxygen plasma

pre-treatment. http://dx.doi.org/101080/016942432014883774 28:1046–1054. https://doi.org/10.1080/01694243.2014.883774

Yang S, Cheng X, Jin Z, et al (2018) Differential production of Psl in planktonic cells leads to two distinctive attachment phenotypes in *Pseudomonas aeruginosa*. Appl Environ Microbiol 84:e00700-18. https://doi.org/10.1128/AEM.00700-18

Yang Y, Qi PK, Yang ZL, Huang N (2015) Nitric oxide based strategies for applications of biomedical devices. Biosurface and Biotribology 1:177–201. https://doi.org/10.1016/j.bsbt.2015.08.003

Yepuri NR, Barraud N, Mohammadi NS, et al (2013) Synthesis of cephalosporin-3'-diazeniumdiolates: Biofilm dispersing NO-donor prodrugs activated by β-lactamase. Chem Commun 49:4791–4793. https://doi.org/10.1039/c3cc40869h

Yoon SS, Hennigan RF, Hilliard GM, et al (2002) *Pseudomonas aeruginosa* anaerobic respiration in biofilms: Relationships to cystic fibrosis pathogenesis. Dev Cell 3:593–603. https://doi.org/10.1016/S1534-5807(02)00295-2

Yordanov D, Strateva T (2009) *Pseudomonas aeruginosa* – a phenomenon of bacterial resistance. J Med Microbiol 58:1133–1148. https://doi.org/10.1099/jmm.0.009142-0

Yu B, Ichinose F, Bloch DB, Zapol WM (2019) Inhaled nitric oxide. Br J Pharmacol 176:246–255. https://doi.org/10.1111/bph.14512

Zemanick ET, Hoffman LR (2016) Cystic Fibrosis: Microbiology and Host Response. Pediatr Clin North Am 63:617–36. https://doi.org/10.1016/j.pcl.2016.04.003

Zhao K, Tseng BS, Beckerman B, et al (2013) Psl trails guide exploration and microcolony formation in *Pseudomonas aeruginosa* biofilms. Nature 497:388–391. https://doi.org/10.1038/nature12155

Zhao Y, Chen D, Ji B, et al (2023) Whole-genome sequencing reveals high-risk clones of *Pseudomonas aeruginosa* in Guangdong, China. Front Microbiol 14:. https://doi.org/10.3389/FMICB.2023.1117017/FULL

Zheng S, Xu W, Bose S, et al (2004) Impaired nitric oxide synthase-2 signaling pathway in cystic fibrosis airway epithelium. Am J Physiol - Lung Cell Mol Physiol 287:. https://doi.org/10.1152/ajplung.00039.2004

Zhu X, Rice SA, Barraud N (2019) Nitric Oxide and Iron Signaling Cues Have Opposing Effects on Biofilm Development in *Pseudomonas aeruginosa*. Appl Environ Microbiol 85:. https://doi.org/10.1128/AEM.02175-18

Zielenski J, Rozmahel R, Bozon D, et al (1991) Genomic DNA sequence of the cystic fibrosis transmembrane conductance regulator (CFTR) gene. Genomics 10:214–228. https://doi.org/10.1016/0888-7543(91)90503-7

Appendix A

A.1 Protocol for processing of sputum samples obtained in the Pacify Study

PACIFY – Sputum Protein Processing 01-Mar-2017

Day 1

Bligh-Dyer extraction

- Prepare glass test tubes and lids by rinsing with distilled water, then 100% methanol, and then 1 mL dichloromethane.
- Invert glass test tubes to dry
- Add 200 µL sputum to 600 µL 0.9% saline solution
- Add 2 mL methanol and mix
- Add 1 mL dichloromethane and mix
- Centrifuge at 1,000 *xg* for 10 min at 10 °C to pellet
- Solvent and aqueous phases removed and pellets stored at -80 °C

Day 2

Prepare the following:

- 0.1 M ammonium bicarbonate (Ambic) to required volume
- 50% trifluoroethanol (TFE) in 0.1 M Ambic to required volume
- 0.1 M Dithiothreitol (DTT) and keep on ice
- 0.2 M Iodoacetic acid (IDA) and keep on ice in dark

Processing:

- Working in laminar flow, invert test tubes containing pellets for 2 min, and then upright for 2 min to allow volatiles to escape
- Record pellet appearance (score 1-10 based on pellet size, and note any other differences)
- Dissolve pellet in 150 µL 50% TFE with intermittent vortexing
- Transfer to microcentrifuge tube and heat at 60 °C for 30 min
- Vortex and pulse spin
- Add 5 µL 0.1 M DTT to each sample and heat at 60 °C for 45 min
- Vortex and pulse spin
- Add 5 µL 0.2 M IDA to each sample and incubate at room temperature in dark for 45 min
- During IDA treatment step prepare 1 mg/mL trypsin in 0.1 M Ambic and leave at room temperature for 30 min
- Add 1 mL 0.1 M Ambic to each sample
- Add 1.5 µL trypsin to each sample and incubate overnight at 37 °C in dark

Day 3

- Add a further 0.5 µL of 1 mg/mL trypsin to each sample and incubate for 1 h at 37 °C in dark
- Wash 10 K molecular weight cut-off Amicon ultrafiltration devices twice with 0.1 M Ambic at 8,000 *xg* for 15 min
- Filter 425 µL of sputum digests through Amicon ultrafiltration devices at 8,000 *xg* for 15 min
- Transfer filtrate to new microcentrifuge tube
- Repeat filtration step until all of digest samples have been filtered and transferred into respective sample microcentrifuge tubes
- Dry samples in vacuum concentrator
- Store at -80 oC

Day 4

- Record pellet appearance (score 1-10 based on pellet size, and note any other differences)
- Resuspend pellets in 100 µL rinse buffer (3% acetonitrile + 0.1% Trifluoroacetic acid in 0.1 M Ambic)
- Seal unused wells in Empore C18 plate
- Place waste plate in manifold base
- Insert C18 extraction plate
- Add 100 µL methanol to each well and wait 30 seconds until passed through to waste plate
- Add 200 µL MQ water to each well and vacuum until drained
- Replace waste plate with collection plate in manifold base
- Add 100 µL sample to each well and centrifuge at 250 *xg* for 2 min
- Store collection plate at -20 °C (flow-through sample)
- Place waste plate in manifold base
- Wash 3x with 200 µL 0.5% acetic acid (in MQ water) using vacuum
- Replace waste plate with collection plate in manifold base
- Add 150 µL eluting solvent (65% acetonitrile + 0.1% trifluoroacetic acid in 0.1 M Ambic) and wait 30 seconds
- Centrifuge at 100 *xg* for 2 min
- Vacuum concentrate samples

Day 5

- Samples resuspended in 50 µL 3% acetonitrile + 0.1% trifluoroacetic acid (in 0.1 M Ambic)
- 2 µL of each sample measured using Direct Detect system and low peptide quantification performed (2 µL buffer added to each card as control)
- Direct Detect cards retained for future reference

A.2 Gene presence/absence analysis of denitrification genes in mPA01

#FILE	anr	dnr	fhp	narG	narH	narI	narL	narX	nirQ	nirS	norB	norC	nosZ
mPAO1.fasta	100	100	100	100	100	100	100	100	100	100	100	100	100